ROLE OF INTERLEUKIN-6 IN CELLULAR AND SYSTEMIC RESPONSES TO IONIZING RADIATION

THESIS

Submitted to Delhi Technological University
for the award of the degree of

DOCTOR OF PHILOSOPHY

in

BIOTECHNOLOGY

By

NEERAJ KUMARI

DEPARTMENT OF BIOTECHNOLOGY
DELHI TECHNOLOGICAL UNIVERSITY
DELHI, 110042

MAY 2020

Copyright © Delhi Technological University- 2019

All rights reserved

Dedicated

to

My Parents

DECLARATION

I, **Neeraj Kumari**, certify that the work embodied in this thesis entitled "**Role of Interleukin-6 in cellular and systemic responses to ionizing radiation**" to be submitted for the Degree of Doctor of Philosophy is my own bonafied work carried out under the joint supervision of **Dr Anant Narayan Bhatt** (Scientist' E', Institute of Nuclear Medicine and Allied Sciences, DRDO, Delhi) and **Dr Asmita Das** (Assistant Professor, Department of Biotechnology, Delhi Technological University) for a period of July 2014 to May 2020 at INMAS and DTU. The matter embodied in this thesis has not been submitted for the award of any degree/diploma.

I declare that I have faithfully acknowledged, given credit and referred to the research workers wherever their works have been cited in the text and the body of the thesis.

Date: 29.05.2020

Place: Delhi

Neeraj Kumari

(Reg. No: 2K14/Ph.D/BT/06)

DELHI TECHNOLOGICAL UNIVERSITY

CERTIFICATE

This is to certify that the Ph.D. thesis entitled "**Role of Interleukin-6 in cellular and systemic responses to ionizing radiation**" submitted by Neeraj Kumari (Reg. No: 2K14/PhD/BT/06) to the Delhi Technological University, Delhi for the award of the degree of **Doctor of philosophy** is based on the original work carried out under our supervision. It is further certified that the work embodied in this thesis has neither partially nor fully submitted to any other University or Institution for the award of any degree or diploma.

Dr Anant Narayan Bhatt
(Supervisor)
Scientist 'E'
Institute of Nuclear Medicine and
Allied Sciences, DRDO

Dr Asmita Das
(Supervisor)
Assistant professor
Department of Biotechnology,
Delhi Technological University

Prof Jai Gopal Sharma
Head of Department
Department of Biotechnology
Delhi Technological University

ACKNOWLEDGEMENTS

Undertaking PhD has been a truly life changing experience for me, and it would not have been possible to do without the support and guidance of several people. I would like to express my sincere gratitude to all of them.

First of all, I want to thank my mentor and supervisors, ***Dr Anant Narayan Bhatt****, and* ***Dr Asmita Das****, who allowed me to work under their guidance. Their constant support and motivation carried this day in my life. Words will not be enough to show my gratitude to Sir, a person with an amicable and positive disposition who made me not only a good researcher but cultivated a passion for research. His guidance helped me in all the time of research and writing of this thesis. Sir has always made himself available to clarify our doubts despite his busy schedules and never got bothered with our untimely calls or messages. I consider it as an excellent opportunity to do my PhD degree under his guidance and to learn from his immense knowledge, research expertise, and the passion towards science. Sir has been very gentle and understanding towards his students that genuinely helped me to work stress-free and smooth accomplishment of this work. Sir's critical thinking and analysis really helped me to get positive from my failures, and inspired me to do best. I could not have imagined having a better supervisor for my PhD. Thank you, Sir, for all your help and support.*

I found myself fortunate to work with ***Dwarakanath Sir*** *whose timely motivation, encouragement, friendly behaviour of teaching science and valuable suggestions always helped me in my research.*

I am incredibly grateful to ***Dr Ajay Kumar Singh*** *ex-Director INMAS, and* ***Dr Tarun Sekhari,*** *Director INMAS for providing me with the opportunity to work as a researcher in the institute. I feel privileged to be part of INMAS and express my thankfulness to them for getting the best infrastructure and research facility.*

I want to express my sincere gratitude to ***Prof. Yogesh Singh****, Vice-Chancellor DTU for providing me with a privilege to be part of this esteemed University as a research scholar. I*

*take this opportunity to acknowledge **Prof. Jai Gopal Sharma**, Head, Dept. of Biotechnology DTU for his kind support.*

*I thank my lab mates for the stimulating discussions and for all the fun and snacks parties☺ we have had in the last five years. I heartily thank **Yogesh** who was after Sir to encourage me to do the best out of me, with whom I completed my basic training in the lab. His criticism and suggestions helped me to work focused. He used to be involved directly or indirectly in most of my experiments which helped me in smooth completion of this work and is truly a good friend. I thank **Dhananjay** who take care of routine use plastic ware to animal demands and other things. He also used to be actively involved in my experiments, especially animal studies and extended his helping hands when needed. We have good lifelong memories of trips for attending conferences☺ I heartily thank **Ankit Sir**, my senior com friend com brother, his technical and experimental help in many ways proved very fruitful. We have a lot of good memories, especially over Tea made by him☺ I thank **Anita Ma'am**, who always helped me and shared a senior com friendly bond with me. I genuinely thank **Abhishek** who was taking care of daily use lab requirements from tissue paper to blotting sheet for last two year and also helped me in the final thesis check. I deeply thank **Manju** for sincerely helping me in final thesis corrections. I am highly grateful to **Dinesh bhaiya** and **Tarun** for maintaining basic necessities in the lab from washing to autoclaving and helped in smooth running of work. Even Dinesh bhaiya helped me more than a lab attendant. The memories I made with my team, will cherish forever.*

*I thank my seniors, especially **Sanjay sir**, his easy to go behaviour was always fascinating for me. His practical approaches, and the main thing flow antibodies☺ helped me a lot. I bothered him a lot by making calls in abrupt timings, and he used to clarify my doubts in sleeping mode also☺. I sincerely thank **Suchit Sir** and **Poorani Ma'am** for teaching me some basic experiments in my initial days. I also thank **Saurav Sir** and **Aastha Ma'am** for helping me when needed.*

I thank my colleagues in DTU, ***Richa ma'am, Divya, Sunil*** *for their cordial behaviour and support throughout my tenure. Also, I thank my friend* ***Shine*** *in DTU for her help regarding college notices and all.*

Some faculty members of the institute have been very kind enough to extend their help at various phases of this research, whenever I approached them, I do hereby acknowledge all of them. I am grateful to ***Chaudhury Sir*** *and his team, and sincerely thank him for facilitating microscopic and comet assay facilities. I acknowledge* ***Chandana Sir*** *and his lab, especially* ***Bincy, Shwetanjali*** *and* ***Kanu Ma'am*** *for extending their help. I sincerely acknowledge* ***Prem Sir*** *for PCR and blood cell counting facility. I wholeheartedly thank* ***Ravi Sir*** *for providing smooth running of radiation facility, and he seriously helped me so many times out of the way, when radiation needed for any experiment. I am also grateful to* ***Paban Sir*** *for his kind help when needed.*

I am also thankful to the technical staff from DTU ***Mr C. B. Singh, Mr Jitendra*** *and* ***Ms Soumya Maurice*** *for providing the professional help and information well before deadlines.*

I appreciate the technical staff of INMAS ***Mrs Namita Kalra, Mrs Anjali,*** *and* ***Mr Nitin Kumar*** *for the smooth running of the machinery in a central facility and helping me in achieving my research objectives.*

I also thank my friends in INMAS, ***Akanchha, Madhuri*** *and* ***Simran*** *with whom I enjoyed a lot in experiment free time, and shared many memories of trips and parties. Akanchha helped me several times in her lab. I learnt a lot of things from them. I am also very thankful to* ***Anoushka*** *who helped me so many times when needed and mainly in carrying my laptop on campus premises in the time of security.*

I thank my friend ***Vandana*** *in DU for helping out of the way mainly for chemidoc-system☺ I also thank* ***Anuranjani*** *for the same.*

I am also feeling great to express my thankfulness to my besties ***Goldy*** *and* ***Lizu*** *for their support either scientifically, mentally or personally, they shared my all good and tough times. Goldy being a statistician, also helped in data analysis.*

I also thank my close friends ***Nidhi*** *and* ***Nupur****, with whom I enjoyed my stay in Delhi and never feel alone and found myself refreshed after meeting with them.*

I also wanted to acknowledge ***Sarika Ma'am*** *for all the get togethers, Tea parties and Trips that is a kind of familial support shown by Sir and Ma'am outside the home.*

I feel in debt to my Parents, who showed immense faith in me and their struggle and sacrifice brought me here today that I can withstand in the society. They helped me at every stage of my personal and academic life and longed to see this achievement come true. I am highly thankful to my brothers ***Harikesh*** *and* ***Lokesh****, who were staying with me that never made me feel homesick. They always encouraged me to do best out of me. Loving phone calls from my younger brother* ***Sachin*** *and sister* ***Poonam*** *used to make my stressed day happy.*

I gratefully acknowledge to DRDO and ICMR for providing me financial support to commence this research.

Above all, I owe it all to Almighty God for granting me the wisdom, health and strength to undertake this research task and enabling me to its completion.

I appreciate each and everyone whom I mentioned here or forgot to mention, who were directly or indirectly supported me during this journey.

Neeraj Kumari

CONTENTS

LIST OF FIGURES

LIST OF TABLES

ABBREVIATIONS

2-NBDG	:	2-(*N*-(7-Nitrobenz-2-oxa-1,3-diazol-4-yl)Amino)-2-Deoxyglucose
2-DG	:	2-deoxy-D-glucose
4-HNE	:	4-hydroxynonenal
53BP 1	:	53 Binding protein1
8-OHdG	:	8-Hydroxyguanine
ADAM	:	A disintegrin and metalloproteinase
AF	:	Acentric fragments
AMP	:	Adenosine monophosphate
AO	:	Acridine orange
AP-1	:	Activator Protein 1
ARS	:	Acute Radiation Syndrome
ATM	:	Ataxia telangiectasia mutated
ATP	:	Adenosine triphosphate
ATR	:	Ataxia telangiectasia and Rad3 related
BCA	:	Bicinchoninic acid
BCl_2	:	B-cell lymphoma 2
Bcl-xL	:	B-cell lymphoma-extra large
BER	:	Base excision repair
BrdU	:	5- Bomo-2'-deoxyuridine
BRIT	:	Board of radiation and isotope technology
BSA	:	Bovine serum albumin
BSF-2	:	B cell differentiation factor -2
Cdc 25	:	Cell division cycle 25
cDNA	:	Complementary deoxyribonuleic acid
CFSE	:	Carboxyfluorescein succinimidyl ester
CHK	:	Checkpoint kinases
CNS	:	Central Nervous System
CRS	:	Cutaneous Radiation Syndrome

CSF	:	Colony stimulating factor
CV	:	Cardiovascular
CXCL	:	C-X-C Motif Chemokine Ligand
DDR	:	DNA Damage Response
DMEM	:	Dulbecco's Modified Eagle's Medium
DMSO	:	Dimethyl sulfoxide
DNA	:	Deoxyribonucleic acid
DPX	:	Dibutylphthalate Polystyrene Xylene
DSBs	:	Double strand breaks
DTNB	:	5, 5'-dithiobis-(2-nitrobenzoic acid)
EDTA	:	Ethylenediaminetetraacetic acid
ELISA	:	Enzyme-linked Immune Sorbent Assay
EPO	:	Erythropoietin
EtBr	:	Ethidium Bromide
FACS	:	Fluorescence activated cell sorting
FBS	:	Fetal Bovine Serum
FDA	:	Food and Drug Administration
FITC	:	Fluorescein isothiocyanate
Flt-3	:	FMS-like receptor tyrosine kinase-*3*
GAA	:	Glacial acetic Acid
G-CSF	:	Granulocyte - colony stimulating factor
GFP	:	Green Fluorescent protein
GI	:	Gastrointestinal
GI-ARS	:	Gastrointestinal-Acute radiation syndrome
GLUT4	:	Glucose transporter type 4
GM-CSF	:	Granulocyte Macrophage-colony stimulating factor
GSH	:	Reduced Glutathione
Gy	:	Gray
H&E	:	Haematoxylin and eosin
H_2DCFH-DA	:	Dichlorodihydrofluorescein diacetate
H-ARS	:	Hematopoietic syndrome

Hb	:	Hemoglobin
HBSS	:	Hank's Balanced Salt Solution
HEPES	:	4-(2-Hydroxyethyl)-1-piperazineethanesulfonic acid
HK	:	Hexokinase
HRP	:	Horseradish peroxidase
HRR	:	Homologous Recombination Repair
hrs	:	Hours
HSC	:	Hematopoietic stem cells
i.p	:	Intraperitoneal
i.m.	:	Inramuscular
IAEA	:	International Atomic Energy Agency
ICRP	:	International Commission on Radiological Protection
Igf1/2	:	Insulin Like Growth Factor ½
IHC	:	Immunohistochemistry
IL-6	:	Interleukin-6
IL-6 R	:	Interleukin-6 receptor
IR	:	Ionizing radiation
JAK	:	Janus kinase
LD	:	Lethal dose
LDI	:	Low dose irradiator
LET	:	Linear energy transfer
LMP	:	Low melting point
LT- HSC	:	Long term- Hematopoietic stem cells
MAPK	:	Mitogen activated protein kinase
mbIL-6R	:	Membrane bound IL-6R
Mcl-1	:	Myeloid cell leukemia 1
MCM	:	Medical countermeasures
M-CSF	:	Macrophage- colony stimulating factor
MDA	:	Malondialdehyde
MDSC	:	Myeloid derived suppressor cells

MF	:	Micronuclei-Fraction (M-fraction)
Mfn	:	Mitofusin
MI	:	Micronuclei Induction
MMP	:	Mitochondrial membrane potential
MMR	:	Mis-match repair
MN	:	Micronuclei
MnSOD	:	Manganese superoxide dismutase
MTT	:	3- (4, 5-dimethylthiazol-2-yl)- 2,5-diphenyltetrazolium bromide
NBS 1	:	Nijmegen breakage syndrome protein 1
NCCS	:	National Centre for Cell Science
NCRP	:	National Council on Radiation Protection and Measurements
NER	:	Nucleotide Excision repair
NFkB	:	nuclear factor kappa-light-chain-enhancer of activated B cells
NHEJ	:	Non-Homologous End Joining
NMP	:	Normal melting point
PARP	:	Poly ADP ribose polymerase
PBMCs	:	Peripheral blood mononuclear cells
PBS	:	Phosphate-buffered saline
PD	:	Petri dish
PE	:	Plating efficiency
PFA	:	Paraformadehyde
PARP1	:	PolyADP-ribose polymerase 1
PFK-1	:	Phosphofrutokinase
PI	:	Propidium Iodide
PI3K	:	Phosphoinositide 3-kinase
PIKKs	:	Phosphatidylinositol 3-kinase-related kinases
PKM2	:	Pyruvate kinase isozyme type M2
PS	:	Phosphatidylserine
PVDF	:	Polyvinylidene difluoride
RBC	:	Red blood cells
RNA	:	Ribonucleic acid

RNase-A	:	Ribonuclease-A
RNS	:	Reactive nitrogen species
ROS	:	Reactive oxygen species
SDH	:	Succinate dehygrogenase
SDS	:	Sodium Dodecyl Sulphate
SDS-PAGE	:	Sodium dodecyl sulfate–polyacrylamide gel electrophoresis
SF	:	Surviving Fraction
sIL-6R	:	Soluble receptor IL-6R
siRNA	:	Small interfering RNA
SLS	:	S-Lauryl Sodium Sarcosinate
SOCS3	:	The suppressor of cytokine signalling
SOD	:	Superoxide dismutase
SRB	:	Sulforhodamine B
SSBs	:	Single strand breaks
ST- HSC	:	Short term- Hematopoietic stem cells
STAT-3	:	Signal transducer and activator of transcription-3
TAMs	:	Tumour associated macrophages
TBA	:	Thiobarbituric acid
TBARS	:	Thiobarbituric acid reactive substances
TBST	:	Tris-buffered saline tween
TMRM	:	Tetramethylrhodamine methyl ester
TNF	:	Tumour necrosis factor
TP53	:	Tumour protein *p53*
TTBS	:	Tris-Tween Buffered Saline
TUNEL	:	Terminal Deoxynucleotidyl Transferase dUTP Nick End Labeling
UV rays	:	Ultra-violet rays
VDAC	:	Voltage-dependent anion-selective channel
WBC	:	White blood cells
WBI	:	Whole-body irradiation

LIST OF PUBLICATIONS

Publications

1) **Kumari N,** Dwarakanath BS, Das A, Bhatt AN (2016) Role of interleukin-6 in cancer progression and therapeutic resistance. ***Tumor biology.***2016 Sep;37(9):11553-11572.

2) **Kumari N**, Das A, Bhatt AN (2019). Interleukin-6 confers radio-resistance by inducing Akt mediated glycolysis and reducing mitochondrial damage in cells. ***The Journal of Biochemistry***. 2020;167(3):303–314,

3) **Kumari N,** Dwarakanath BS, Das A, Bhatt AN IL-6 mediated STAT-3 pathway activation enhances hematopoietic reconstitution and protects from lethal radiation. Manuscript in submission

4) Rai Y, Yadav P, **Kumari N,** Kalra N, Bhatt AN. (2019). Hexokinase II inhibition by 3-Bromopyruvate sensitizes myeloid leukemic cells K-562 to anti leukemic drug Daunorubicin. ***Bioscience reports*** 2019, 39 (9).

5) Rai Y, Pathak, R, **Kumari, N**, Sah, D. K, Pandey S, Kalra N, Bhatt, A. N. (2018). Mitochondrial biogenesis and metabolic hyperactivation limits the application of MTT assay in the estimation of radiation induced growth inhibition. ***Scientific Reports***, 8, 1531.

Conference Attended

1. The 65th annual meeting of Radiation Research Society **(RRS 2019)** 'IL-6 protects from radiation induced cell death and injury by activating stat-3 signalling' **Neeraj Kumari**, Asmita Das, Anant Narayan Bhatt. **(**received **Travel Award)**

2. International conference on radiation biology **(ICRB 2018).** 'IL-6 protects from radiation induced cell death by preventing oxidative stress and DNA damage' **Neeraj Kumari**, Asmita Das, Anant Narayan Bhatt. (received **Young Scientist Award**)

3. International Conference on **Cell Death in Cancer and Toxicology (CDCT 2018) '**IL-6 protects the cells from radiation induced cell death by switching metabolism and activating STAT-3 mediated pro-survival signalling' **Neeraj Kumari**, Asmita Das, Anant Narayan Bhatt. Abstract published in ***Cancer medicine*** (2018) vol 7 (1) 1-58.

4. 43rd Meeting of European Radiation Research Society **(ERRS-GBS 2017) '**IL-6 protects cells from radiation induced cell death by activating antioxidant defence and STAT-3 mediated pro-survival signalling' **Neeraj Kumari**, Asmita Das, Anant Narayan Bhatt. **(**received **Travel Award)**

OUTLINE OF THE THESIS

The contents of the thesis have been organized into 5 independent chapters, as outlined below:

- The introductory chapter, **Chapter-1**, which gives a brief overview of the study including relevant facts about the topic of research, statement of the problem, scope and significance of the study and lastly, the objectives designed to address the issue.
- **Chapter-2** provides the scientific background pertaining to the studies undertaken in this thesis.
- **Chapter-3** embodies the details of the materials used and methodologies employed to perform these studies.
- Results are presented in **Chapter-4**, which is further subdivided into 4 sections according to the objectives.

Section 4.1: **IL-6 induced STAT-3 signalling protects cells from radiation-induced cell death and confers radio-resistance**

In this objective, we studied the effect of IL-6 on radiation-induced cell death in multiple cell lines. We primarily focused on IL-6-STAT-3, which is known to involve directly in cell survival and proliferation. Apart from preliminary experiments, most of the study was done in RAW264.7 cells (murine monocyte cells) to check the potential of IL-6-STAT-3 in radioprotection. The parameters studied are cell proliferation, cell cycle, oxidative stress, macromolecular damage, and apoptosis.

Section 4.2: **Interleukin-6 confers radio-resistance by inducing Akt mediated glycolysis and reducing mitochondrial damage in cells**

In this study, we investigated the mechanism of IL-6-induced glycolysis in RAW264.7 cells and tested, if IL-6 can protect healthy cells from ionizing radiation (IR) by inducing glycolysis-mediated radio-resistance. IL-6-Akt signalling modulates the radiation response by metabolic modification through enhancing glycolysis that leads to radio-resistance. The main parameters studied are glycolysis, Akt pathway, and mitochondrial protection.

Section 4.3: **To investigate the role of IL-6 in cellular responses to radiation-induced DNA damage**

In this objective, we evaluated the effect of IL-6 on radiation-induced DNA damage and repair *in-vitro*. Since radiation triggers substantial DNA damage which may lead to cell death, we, therefore, performed multiple assays to study the impact of IL-6 on single/double-strand breaks, the extent of DNA damage and the activation repair pathways after irradiation.

Section 4.4: Evaluation of radio-protective efficacy of IL-6 *in-vivo* (mice) models

This section highlights the role of IL-6 on *in-vivo* radiation response. Here we focused mainly on hematopoietic and gastrointestinal recovery in the presence of IL-6 after irradiation. C57B/L6 mice were injected with IL-6 via intramuscular route, one dose 2hr before radiation and three doses post-irradiation at 24, 48, and 72 hrs. The study includes peripheral blood count, survival analysis, stem cell enumeration, splenocytes analysis, bone marrow analysis, antioxidant potential in GI, apoptosis and proliferation in GI tissues.

- **Chapter 5** comprises of discussion of results and conclusions.

Chapter 1
Introduction

CHAPTER 1

INTRODUCTION

One cannot imagine the medical practices of the modern world without acknowledging the discovery of X-rays by German physicist Wilhelm Conrad Roentgen. The X-rays can pass through different solid materials except for bone and metals. Later this property of x-rays was exploited to create an impression of bones on a gelatin-coated polymer-based film (X-ray film). He first captured his wife Bertha's hand impression on a film in 1895 (Fig;1.1). Later many researchers followed this extraordinary discovery worldwide. After a few months of invention, the radiographs were being created in many places, including the United States and Europe. They were using this technique on battlefields to locate the bullets in injured soldiers. Due to the high voltage required to create X-ray images, the source tube would often get collapsed by high energy. This problem was resolved only after the creation of a Coolidge tube (a large vacuum x-ray tube) in 1913 that later served as a reliable and robust source to generate X-rays. This invention provided a useful tool for the medical industry to image soft tissues and bones having fractures, dislocation, swelling and any alien bodies in the human body can be identified.

Image Source: R.VanTiggelen, 2001

Figure 1.1: First X-ray image on film

Soon after the discovery of X-rays, a French scientist Henri Becquerel discovered the phenomenon of natural phosphorescence or radioactivity, another form of rays having similar penetrating power. He observed, when some minerals are exposed to sunlight, they eventually irradiate or fluoresce. He captured this radiation or fluorescence on photographic plates or films. He mainly worked with uranium, and his continued research validated that uranium was the chief source of radiation. At the same time, Polish-French physicist Marie Curie was also working with her husband Pierre Curie, to discover other sources of radiation in the uranium ore. In 1898, the Curies unearthed polonium and (named after Marie's native Poland) and Radium. Both were highly radioactive than uranium. Later on, Ernest Rutherford identified alpha and beta particles while working on atoms. J. Chadwick discovered the neutron in 1932, and in 1934, F. Joliot and I. Curie were able to prove the production of an artificial radionuclide (^{30}P). George Charles de Hevesy, developed ^{32}P, a radioactive tracer to study chemical reactions and metabolism in animals. These radionuclides; ^{32}P, ^{24}Na and ^{131}I were then commonly used for diagnosis and therapy. Phosphorus and iodine are still being used in radionuclide therapy; where ^{131}I is very important in diagnostic nuclear medicine. It has not only been used as radionuclide for multiple examinations of the thyroid but also employed as a tracer to label various pharmaceuticals. It was immediately implemented in humans after its discovery and first reported in excised thyroid gland following the uptake of the radionuclide. Presently, the ^{99}Tc^{m} radionuclide is most extensively used in diagnostic nuclear medicine imaging.

In the late 19th and early 20th centuries, after the discoveries of radioactivity and x-rays, various health care industries were allowed to set up x-rays machines. Through these years, there was no concern of unintended consequences of the follow-up usage of these

rays. Nobody was aware that these rays could be detrimental, in part, because of the slow onset of symptoms. Some investigators noticed changes in the skin due to much exposure to the X-rays. These changes were mostly evidenced in the hands of radiographers, who commonly used their hands to fix the source in the tube. The first radiation burnt hand was reported in Germany on July 9, 1896. In general, the early investigators would not even suspect a problem with the rays similar to light because they could neither see, smell, hear, nor feel. Furthermore, the effects were delayed and often attributed to some other cause. However, continuous exposure leads to substantial damage in the skin and even resulted in deaths of radiation workers. There were many martyrs to radiology in those early days. Later, in 1936 the "Deutsche Röntgen Gesellschaft", upon the suggestion of Hans Meyer (1877-1964), a radiotherapist from Bremen, erected a monument to the martyrs of X-ray and Radium from all nations.

1.1 Casualties of radiation exposure

Pierre Curie, during his Nobel Prize lecture, highlighted the primary complications of radiation exposure for the first time and speculated that radiation could be abused by criminal hands and would be more dangerous. Thus, questioned whether humanity would benefit at all after knowing this aspect of radiation, particularly concerning about the use of radiation in war.

The two times Nobel Prize winner (physics and chemistry), Marie Currie died of aplastic anaemia an illness characterized by depletion of bone marrow ability to produce new blood cells. She used to carry radium vials in her lab coat or stored them in her writing desk. Unfortunately, this habit exposed her to such a high amount of ionizing radiation that her personal belongings are still radioactive and having

radiation that will last for an additional 1500 years. Any scientist who wants to visit Curie's possessions is obligatory to sign a disclaimer and wear personal protective gears. Later the incidence of Radium girls came in picture in 1916. The United States Radium Corporation started a factory and hired 70 young women to paint digits on watches with a radiant paint, and routinely handled Radium with their bare hands or sometimes pull the brush between their lips to make excellent points. These factory workers also branded as "the radium girls" – began showing signs of radiation sickness and bone decay and all died within five years,

The two Atomic bombs used in the Second World War were dropped over Hiroshima and Nagasaki in 1945. The casualties were dreadful, about a half-million in both cities, including deaths in few days due to severe burns and radiation sickness. The radiation aftermaths were depressing until decades.

In 1986, the Chernobyl nuclear power plant disaster in Ukraine, then the Soviet Union, is the first and only accident of commercial atomic power known to cause fatalities. It was the outcome of a faulty reactor design, combined with human error. Operators ran the plant at the very low power supply, with inadequate safety precautions, the reactors were extremely unstable at low power hence the uncontrolled power flow led to Chernobyl destruction, exposing tons of reactor uranium core to the environment. This led to many deaths within a few weeks of the accident due to thermal burns and cardiac arrest followed by mass evacuation. After that, a circle-shaped exclusion zone of radius ~30km was created on the nuclear power plant, which was expanded later. Though no one lives in the exclusion zone, however scientists and others need permission to enter the area for a limited amount of time. In

2018, the United Nations Scientific Committee on the Effects of Atomic Radiation (UNSCEAR) reported nearly 20,000 documented cases of thyroid cancer among individuals who were under 18 years of age at the time of the accident.

Another unfortunate accident occurred in 1990 at a clinic in Spain, where cancer patients receiving radiation therapy were boomed with a high dose of radiation approx. Seven times higher than the applicable dose. A total of 27 patients were irradiated, out of them, 20 developed radiation sickness and died within five years.

One nuclear power plant based accident occurred on March 11, 2011, in Japan where a major earthquake resulting in 15-metre high tsunami waves caused the loss of power to Fukushima Daiichi reactors leading to the incident. The entire site got flooded with water, and most of the reactor units were disabled, including back-up generators. This resulted in the loss of proper maintenance of reactor cooling; thus, the hot water circulation function caused the melting of reactor core and leakage in water. Although there was no reported death due to radiation sickness, but over 100,000 people were displaced from their homes, and around 1000 deaths cases were reported due to evacuation stress and transfer trauma. Apart from this, there was a long-lasting, heavy radio-contamination to water and air that is still not decontaminated.

Sometimes such radiation accidents are not due to any natural mishappening or planned attacks but maybe because of unawareness of radiation hazards. In this context, Mayapuri incidence is very famous. Mayapuri is the junk metal capital of India where giant containers of scrap are imported from across the world. In 2010, a scrap dealer bought an unused gamma irradiator from a department of the university, which was left to scrap for the last 25 years. The radiological accident occurred at a scrap market in New Delhi,

where the source got mixed with the scrap and triggered radiation poisoning to seven people, one of them died due to radiation exposure, and several other were hospitalized after the onset of symptoms of radiation sickness. Later, the source was confirmed as Cobalt-60 pencils, one of the parts of irradiator. Thereafter, a case was registered against six professors of the University for such an irresponsible act.

It seems that the destruction caused by atomic bombs or radiation accidents were one of the most frightening events in the past century. Radiation is a compelling force that can kill and save lives (by radiotherapy). Radiation causalities can be disastrous, but these disasters taught us to be very careful with this high-powered phenomenon. It's a hard-earned lesson indeed. Such devastating events create more interest and enthusiasm towards the research in the field of radiation and its detrimental biological effects.

1.2 Radiation

Thinking of the term 'Radiation' bring so many thoughts to our mind. According to a physicist, radiation is a form of particle/waves which requires some medium or can travel in space. In contrast, for a chemist, radiation means its interaction with the surrounding, which might lead to bond breakage. Still, when it comes to a biologist, the first notion that arises is whether it can damage life forms. Thus, radiation can be defined as a form of energy having both particle and wave nature, can travel in the medium as well as in space, can break the bonds and also can damage or affect the living beings. Basically, radiation is of two types; ionizing (alpha, beta, gamma, X rays, etc.) and nonionizing (UV, IR waves). Non-ionizing radiation has sufficient energy to raise electrons in atoms or molecules to a higher energy level (excitation), but not enough to cause ionization.

1.2.1 Ionizing Radiation:

Ionizing radiation (IR) consists of high energy that can break bonds, while non-ionizing radiation can only move or vibrate the bonds. Ionizing radiation has adequate strength in its photons to remove orbital electrons from molecules or atoms resulting in the production of free radicals, consisting of unpaired electrons. The Free radicals generated are highly reactive having extremely short half-life (nanoseconds to a few seconds) and are characterized by the localized release of a large amount of energy, examples are Alpha, Beta particles, electrons, protons, neutrons or heavy particles (particulate) and X-ray or gamma-ray photons (electromagnetic radiation). Ionizing radiation is further classified into two categories- High LET radiation (Neutrons, alpha particle) and Low LET radiation (X rays, Gamma rays). High LET radiation is a form of radiation that deposits a large amount of energy in a short distance. In contrast, Low LET radiation deposits less energy along the track and travel a long distance. High LET radiation ionizes water into H and OH over a short path, two events befall in a single cell so as to make a pair of two adjacent OH radical that combine to form peroxide, H_2O_2 that causes oxidative injury to cell (Fig;1.2). Low LET radiation also ionizes water, but over a long distance, two events occur in two distinct cells, such that adjacent radicals are of the opposite type; hence H and OH radical unite to form H_2O (Fig;1.2).

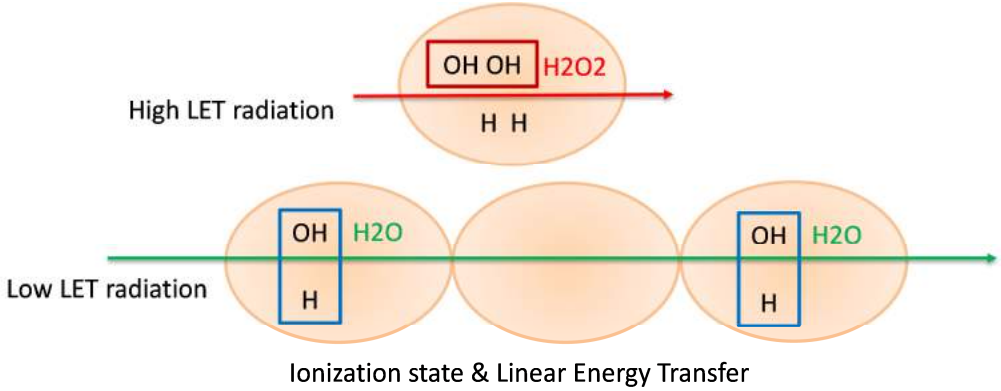

Figure 1.2: High LET versus Low LET radiation

Radiation affects the life forms by mainly two methods - direct and indirect. The direct effect is observed in the case of radiation with high energy where direct cleavage of bonds occurs, which lead to DNA damage and protein denaturation. Immediate effects can be prevented by using radiation shielding materials such as lead.

In the indirect method, the radiation interacts with other atoms/ molecules in a cell that are not direct targets (mainly water), to produce highly oxidizing free radicals which then diffuse and damage the crucial sites. The indirect effect involves the formation of intermediates like ROS (reactive oxygen species), which will further lead to macromolecular (DNA, lipid, protein) damage. As cytoplasm of most cell contains 80% water, when radiation acts on cytoplasm, water gets hydrolyzed to hydroxide radical (OH, H, HO_2, H_3O^+ etc.). These free radicals encounter cellular macromolecules, such as DNA, RNA, proteins, membrane, which leads to cell dysfunction and mortality (Fig;1.3). Electromagnetic radiations both high and low LET are ionizing.

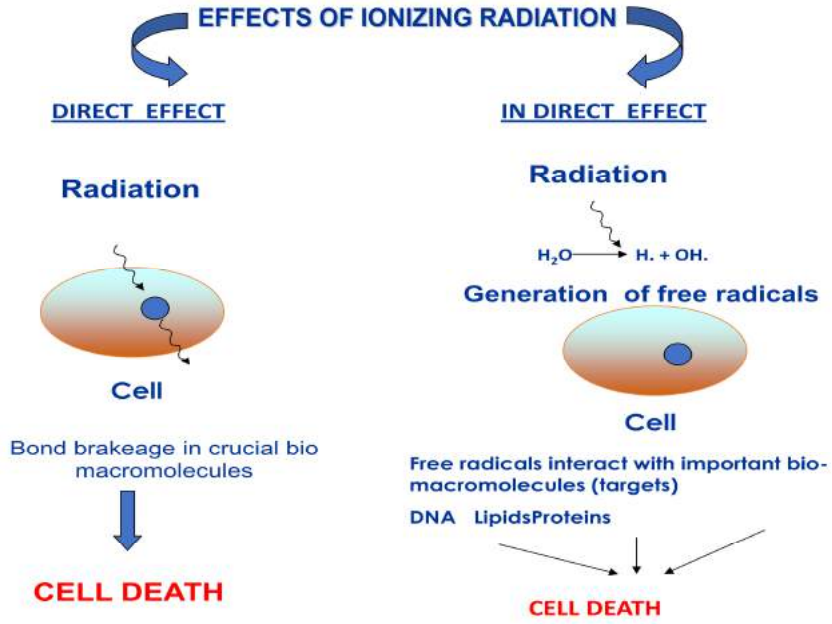

Figure 1.3: Effects of ionizing radiation on cellular systems

The extent of radiation-induced damage is determined by the total amount of energy absorbed, the time duration of exposure, the dose rate of exposure and particularly which organ has been exposed (Akleyev, 2016). The radio-sensitivity of the cells of tissue is directly related to the speed of cell proliferation and inversely proportional to the extent of cell differentiation (Packard, 1930). It means that aggressively dividing cells or immature type of undifferentiated cells are most vulnerable to radiation. Therefore, the cells having a high division rate, high metabolic rate, well-nourished and of un-specialized type are most radio-sensitive. Cells/tissues undergoing rapid proliferation have high sensitivity to radiation, for example, cells of the hematopoietic and gastrointestinal (GI) system, spermatogenic cells and the vascular system (Akleyev, 2016).

Table 1.1: Levels of radio-sensitivity in different tissues

Radiosensitivity of various type of Tissue/Cells	
Radiosensitivity	**Tissue/ Cells**
High	Lymphoid organs, bone marrow, blood, testes, ovaries, intestines
Fairly high	Skin and other organs with epithelial cell lining
Moderate	Optic lens, stomach, growing cartilage, fine vasculature, growing bone
Fairly Low	Mature cartilage or bones, salivary glands, respiratory organs, kidneys, liver, pancreas, thyroid, adrenal and pituitary glands
Low	Muscle, brain, spinal cord

Aggressively dividing cells are more radio-sensitive than non-dividing cells (Packard, 1930). Out of four phases of Mitosis (G1, S, G2, M), M phase in which condensation of chromosomes takes place is the most radio-sensitive phase. Here,

complete DNA is present at this stage of the cell cycle, hence results in being the most radio-sensitive stage. Another instance of a highly radio-sensitive cell system is a malignant tumour, where, the outer layer of tumour cells rapidly generate, and have a good supply of blood and oxygen. Since the reproducing cells are more sensitive to radiation, the presence of oxygen in quickly dividing cells increase sensitivity towards radiation. Anoxic cells (cells having insufficient oxygen), such as the cells that reside in the heart of a tumour tend to be dormant. Therefore, when a tumour is opened up to radiation, the outer layer of fast proliferating cells is destroyed, causing it to shrink in size. A tumour cannot be given a massive dose of radiation to destroy it in one go, as the patient may suffer radiation-based morbid complications. Instead, a fraction of radiation doses are given each day that causes gradual shrinking of tumour, and this also gives a chance to the healthy tissue for self-recovery. Similarly, the growing embryo also comprises of fast-dividing cells and having a regular blood supply and plenty of oxygen makes them more sensitive to radiation like tumours but with different consequences.

Biological effects of radiation are typically divided into two categories. The first category is of deterministic effect, in which high dose radiation exposure occurring for short duration causes short term or acute effects. The second category includes exposure to low dose radiation for an extended period leading to long term, or chronic effects are known as stochastic effects. Low doses did not cause any immediate effect, but they damage slowly over time and remain only at a cellular level, the results are often seen after years of exposure, e.g., mutations. However, high dose radiation causes extensive damage to tissues and organs and may cause a rapid whole-body response called the Acute Radiation Syndrome (ARS). Acute radiation syndrome or

acute radiation sickness is generally referred to describe the multiple sign and symptoms observed after whole-body or significant partial body irradiation with a certain dose of radiation (>0.5 Gy) delivered at a high rate. In general, these signs and symptoms are necessarily the consequences of severe radiation injury to particular tissues of specific organs. ARS is further categorised into three sub syndromes: hematopoietic, gastrointestinal and neurovascular syndrome.

Hematopoietic syndrome: Bone marrow is home to the hematopoietic stem cells and progenitors, which undergo rapid proliferation and produce all type of blood cell. Therefore, these rapidly dividing cells are susceptible to ionizing radiation. Hence, the hematopoietic syndrome can be observed at radiation doses exceeding 1 Gy, below this the surviving cells will be able to replenish the whole blood cells, and only an insignificant diminution can be noted in blood cell count. The extent of damage depends on the absorbed dose of radiation, higher the absorbed dose, more damage will occur to hematopoietic stem and precursors cells. In turn, the bone marrow may be left with no stem cell to regenerate the lost blood cells and causes the development of hypoplasia or aplasia of bone marrow. In such cases, mortality may occur due to infection or bleeding. At doses between 4.5–6 Gy without any supportive care, Lymphopenia may occur before the onset of any other cytopenias, due to the radiation-induced apoptosis in lymphocytes within 24 hour of a moderate to high dose exposure.

Gastrointestinal syndrome: It generally occurs at a radiation dose between 6 to 15 Gy. The clinical symptoms appear due to the damage to stem cells located in the crypts that are required to regenerate the villi. Thus, the denudation of intestinal mucosa initiated within 7 to 10 days post-radiation exposure, causes diarrhoea,

dehydration, loss of electrolytes, intestinal bleeding, perforation, and translocation of gut microbiota. The immunosuppression accompanied by the hematopoietic syndrome favours the opportunistic infections and death prevails due to sepsis, dehydration and multi-organ failure.

Neurovascular syndrome: occurs at a radiation dose higher than 20 Gy and is characterized by very short prodromal and latent phases followed by neurological symptoms such as headache, abnormal cognition, neurological deficits and finally somnolent state, loss of consciousness and death.

Exposure to radiation is not an assurance of harm. There is no threshold model, thus more the exposure the higher will be the risk, and no radiation dose is small enough to produce no effect. Therefore recovery needs the intervention of some molecules for the stimulation and proliferation of stem cells after irradiation. Thus to overcome such situations and to reduce life-threatening events, the role of radio-protectors and mitigators comes in play. These are compounds given before or after the radiation exposure and have the ability to protect the cells from radiation-induced damages.

1.3 Radio-protector and Radio-Mitigators

The research and development of radio-protective agents have been conducting for many years. A radio-protector is the compound given prior or at the time of radiation exposure which reduces the side effects of radiation on the healthy tissues. Radio-mitigator is the compound given at the time or after radiation exposure. They could be either artificially synthetic compounds or isolated from natural resources. These are mainly intended to protect the normal and healthy cells of an organism against acute

and late effects of ionizing radiation. They can effectively reduce morbidity or mortality if given pre or post-radiation exposure. Radio-protectors should prevent the detrimental effects of radiation and protect patients during treatment to offer therapeutic advantage and enhance the overall quality of life (Citrin et al., 2010). Radio-protective agents could counteract radiation effects either from accidental or intended exposures hence are also called as radiation countermeasures.

The need for radio-protectors is mainly for the benefit of radiotherapy and applications in the nuclear industry, outer space, military and accidental exposures. The worldwide increase in cancer disease demands radiotherapy for effective treatment and safe radio-protectors to maximise benefits of radiation by minimizing normal tissue toxicity during radiotherapy of tumours. In the patients having inoperable tumours, radiotherapy is sometimes the only choice, though accompanied by the adverse effects on healthy tissues. The cases of death as a consequence of therapeutic radiation exposure are rare; however, the accidental radiation exposure brings severe early and late effects sequel such as cancer (I, Board, Studies, & Council, 2012). Therefore, research of the radio-protective agents is needed to furnish protection to human being against detrimental health consequences from radiation exposure, particularly in the present-day medical fields as well as to conquer nuclear warfare.

Ionizing radiation (IR) induced biological damage mainly arises after the interaction of IR generated free radicals with cellular biomolecules. Implementation of scavengers for free radicals could subsequently reduce the manifestation of loss. Thus, the antioxidant compounds hold the potential to minimize the damage caused by the indirect mechanism through free radical. The compound containing sulfhydryl

group are excellent scavengers, retain the tendency to donate a hydrogen atom requisite to chemically reduce the free radical species (C. K. Nair, Parida, & Nomura, 2001). To date, Amifostine (WR-2721) is the only FDA approved radio-protector. It is a synthetic aminothiol (*S*-2-(3-aminopropylamino) ethyl phosphorothioate) sulfhydryl containing compound normally used in clinics for protecting the normal healthy tissue via scavenging of free radicals(Citrin et al., 2010). So far, amifostine has been used as a cytoprotective adjuvant in clinics against xerostomia during radiotherapy of head and neck cancer (Hensley et al., 2009). Amifostine is highly specific and does not protect the tumour tissue because of differential microenvironments like higher pH, higher alkaline phosphatase activity and vascular permeation of healthy tissues as compared to tumour tissue(Kouvaris, Kouloulias, & Vlahos, 2007). Despite its approval as a radio-protective drug, the use of amifostine is limited due to its cumulative toxicity that is expressed as nausea, vomiting, hypotension, and allergic reactions. These allergic responses may be localized or widespread and indicated by skin rashes, erythema, urticaria, diarrhoea, multiforme, and few reports of anaphylactoid reactions (Kouvaris et al., 2007). The inherent systemic toxicity, high cost, and a narrow therapeutic window make it unsuitable for applications in the non-clinical setting. Moreover, other non-sulfhydryl-containing compounds that can inhibit the generation of free radicals or destroy them by chemical reactions could also function as a radio-protective drug (Citrin et al., 2010).

To date, numerous medicinal plants, either as in pure form or in the herbal preparations, fractionated extracts or as isolated components have been assessed for their radio-protective potential against IR induced damage(Weiss & Landauer, 2009). Most of them showed an anti-inflammatory, immunomodulatory, antimicrobial,

antioxidant, or anti-stress properties, but none of them has been approved as a potential radio-protective agent (Arora et al., 2005). Albeit herbs and medicinal plants are in practice since ages and generally considered as safe, natural and human friendly, but their usage in particular conditions still needs scientific approval and validation, these might have side effects too.

Therefore the present demand is for developing new, safer and effective radio-protector, with higher success and no/less biological consequences. Thinking of the body's immune system cytokines comes first as action molecules after radiation exposure. Cytokines are highly influential molecules that generally express transiently in response to any stimuli. The reactions are highly organised within a network of units that perform collaborative and overlapping functions accordingly to meet the challenges (Schaue, Kachikwu, & McBride, 2012). Cytokines also impact the modifications in cell adhesion molecules, immune recognition, cell cycle arrest/proliferation, cell death or survival, and metabolism to harmonize cell and tissue responses. Cytokines also affect inherent cellular radio-sensitivity, the prevalence and type of tissue complications, radiation bystander effects, genomic instabilities and cancer (Schaue et al., 2012). In cancer, cytokine pathways are often dysregulated, and several inflammatory cytokines are found to modulate therapeutic gain that results in tumour relapse, invasion and angiogenesis.

1.3.1 Interleukin-6 (IL-6); a promising radio-protector

A variety of cytokines have been upregulated in response to anticancer therapies including IL-6, IL-8 and TNFα (Landskron, De La Fuente, Thuwajit, Thuwajit, & Hermoso, 2014). Amongst these, IL-6 is known to contribute to poor therapeutic

gain, tumour relapse and aggressive tumour growth (Kumari, Dwarakanath, Das, & Bhatt, 2016). Interleukin-6 (IL-6) is a ubiquitous cytokine, pleiotropic with both pro- and anti-inflammatory properties, produced and secreted by various types of cells, including the tumour cells. IL-6 is also recognised as a critical regulator of immunosuppression in patients with advanced cancer. IL-6 protects cells from radiation cytotoxicity, though it affects radiation response differently in different cancers. IL-6 plays an important role in cancer growth and progression by influencing nearly all hallmarks of cancer such as resisting cell death, anti-oxidant defence system, DNA damage repair, metabolic remodelling etc. (Kumari et al., 2016).

Radiation either directly causes DNA damage or indirectly produces the reactive oxygen species (ROS) that damage the cells. Manganese superoxide dismutase (MnSOD) is the principal antioxidant enzyme, which catalyses the protonation of superoxide anion radicals and protects the cells from ROS-mediated damage. Moreover, MnSOD regulates the radiation response of cells, tissues, and organs, which is very critical for the mitochondrial and cellular protection from oxidative stress. It is evidenced that increase in MnSOD expression mediate IL-6-induced resistance to radiation in myeloma cells (Brown et al., 2012). Hydrogen peroxide (H_2O_2) is a potent reactive oxygen species that cause mitochondrial dysfunction and cell death. The preconditioning of cells with IL-6 decreases H_2O_2-mediated cell death by increasing the expression of prohibitin, which is involved in mitochondrial biogenesis and metabolism, apoptosis and replicative senescence (Jia et al., 2012). This not only alleviates oxidative stress but also modulate the activation of cell death. The potential growth stimulatory effect of IL-6 in tumour cells is due to the activation of several signalling pathways. IL-6 stimulates tumour cell proliferation and survival by activating

the Ras/Raf/MEK/MAPK, PI3K/AKT and JAK/STAT pathways via gp130 tyrosine phosphorylation. IL-6 regulates the process of apoptosis by mainly activating the STAT-3 signalling, which transactivates the expression of anti-apoptotic proteins and downregulates pro-apoptotic proteins in many cancers (Kumari et al., 2016).

Moreover, enhanced aerobic glycolysis is one of the prominent phenotypes of a majority of cancer cells which facilitate proliferation and confer protection against death, besides energy production (Bhatt et al., 2015; Warburg, 1956). This induced glycolysis is one of the significant factors that contribute to IL-6-induced therapeutic resistance in cancer. Further, IL-6 has also been found to mediate its multi-lineage haematopoietic effects by shifting stem cells from the G0 to the G1 stage of the cell cycle, thereby inducing the proliferation and making stem cells more responsive to additional haematopoietic growth factors such as IL-3, IL-4, G-CSF, M-CSF or GM-CSF (Patchen, MacVittie, Williams, Schwartz, & Souza, 1991). Therefore, it appears that IL-6 facilitates tumour growth primarily by inhibiting apoptosis and enhancing cell proliferation. Since, IL-6 regulates nearly all hallmarks of cancer, such as inhibition of apoptosis, promotion of survival, proliferation, angiogenesis, invasiveness and metastasis, and importantly cancer cell metabolism, many of these properties of IL-6 make it a suitable candidate for radioprotection and convince us to check its radio-protective potential in normal and healthy cells as it protects the cancer cells from radiotherapy.

This study took the most radio-sensitive cells of hematopoietic and gastrointestinal (GI) system for *in-vitro* studies and focused mainly on the hematopoietic and GI systems *in-vivo.* In these tissues, whole-body irradiation causes decrease in cell

proliferation resulting in severe symptoms of radiation sickness, demonstrated by GI disorder, bacterial infection, loss of body fluids, anaemia, bleeding, electrolyte imbalance and death. A radiation dose of 1 Gy or above in humans is sufficient to cause the hematopoietic syndrome, leading to a decrease in leukocyte count and increased susceptibility to infection. At doses above 8 Gy, injury to the GI system are prominent and contributes to mortality. Therefore, a molecule that inhibits radiation-induced cell death, particularly in these two organs can be promising in the development of radio-protectors.

Aim and Objectives

In light of the above rationale, the thesis is aimed at evaluating the **Role of Interleukin-6 in cellular and systemic responses to ionizing radiation**. The objectives designed to achieve the above-mentioned Aim are as follows**:**

1) To study the cytoprotective potential of IL-6 against ionizing radiation using *in-vitro* models.
2) To investigate the role of IL-6 in cellular responses to radiation-induced DNA damage
3) Evaluation of radio-protective efficacy of IL-6 *in-vivo* (mice) models.

Chapter 2
Review of Literature

CHAPTER 2

REVIEW OF LITERATURE

2.1 Radiation

Introduction

Radiation is the energy given off by matter in the form of rays or high-speed particle energy that travels through space. To gain steady-state, unstable nuclei of atoms discharge excess atomic energy, and these spontaneous emissions of energy are called radiation. Radiation exists in two basic physical forms-

One form of radiation is pure energy with no mass known as electromagnetic radiation like waves of electrical and magnetic energy. Common types of electromagnetic radiation comprise sunlight (cosmic radiation), gamma rays, radar, x-rays, and radio waves. A different form of radiation is known as particle radiations consist of tiny fast-moving particles that have both energy and mass (weight). This form of radiation includes alpha particles, beta particles, and neutrons.

2.2 Types of radiation

Radiation is mainly divided into categories based on the interaction with matter.

Ionizing radiation	Non-ionizing radiation
• It has adequate energy in its photons to remove orbital electrons from molecules or atoms • Induces the production of free radicals, consisting of unpaired electrons • Resulting free radicals are very reactive with a very small half-life (nanoseconds to few seconds) • Characterized by the localized release of large amounts of energy • Examples: Alpha, Beta particles, electrons, protons, neutrons or heavy particles (particulate) and X-ray or gamma-ray photons (electromagnetic radiation)	• It has plenty of energy to raise electrons in atoms or molecules to an upper energy level (excitation), but not enough to cause ionization • Examples:- radio waves, visible light, microwaves.

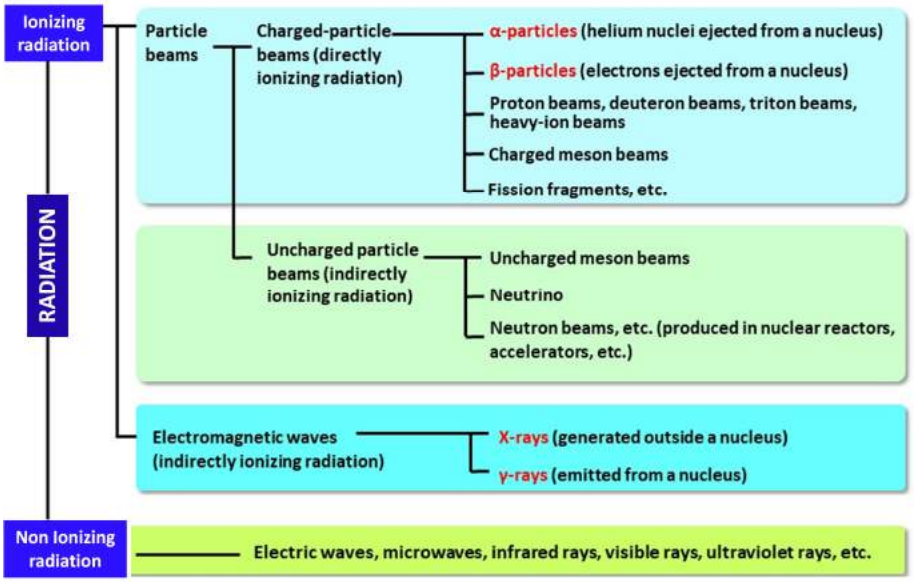

Figure 2.1: Types of radiation, ionizing vs non-ionizing

Types of ionizing radiation

Type of radiation	Nature/ identity	Properties
Alpha (α)	Positively charged Helium nucleus consisting of two neutrons and two protons	• Possess high ionizing power • The concise range of penetration (~ 1-2 inches) • Lose their kinetic energy quickly • Cannot enter human skin and can be prevented by a sheet of paper • Toxic only if internalized • Examples: Uranium, Thorium, Radium
Beta (β)	High-velocity electron ejected from a disintegrating nucleus (Negatron or Positron)	• Released from a neutron- excess radionuclide • Higher penetrating power than alpha particles (~ 30 feet) • Some beta particles can penetrate the skin; and can be prevented by a thin sheet of metal like aluminium, plastic or a block of wood • Hazardous if internalized • Examples: Strontium- 90, Tritium, Carbon-14, and Sulfur-35
Gamma (γ) and X- rays	Neutral, highly energetic electromagnetic radiation	• Highly penetrating; can only stop by several feet of a concrete wall or a few inches of solid material (lead) • Gamma rays are intranuclear, X- rays are extranuclear in origin • X-Rays are of longer wavelength and lower energy than gamma radiation • Examples of gamma emitters: iodine-131, cobalt-60, cesium-137, and radium-226
Neutrons	Small, Neutral particles with a mass very close to a proton	• Produced as a consequence of spontaneous or induced nuclear fission • Highly penetrating • Prevented by very dense hydrogen-containing materials (like concrete or water) • Found in nuclear reactors where steel, concrete and several feet of water offer effective shielding

Mode of action of ionizing radiation

Based on its interaction with the medium, IR is further categorized into two types:

Directly ionizing	Indirectly ionizing
• Radiation directly causes ionization/ excitation of atoms of the critical targets inside the cell, like DNA, producing chemical and biological damage themselves • High linear energy transfer (LET) radiations, such as neutrons or α-particles predominantly act through this mechanism • Direct effects can be prevented by using radiation shielding materials such as lead	• Radiation reacts with other atoms/ molecules in a cell that are not primary targets (particularly water), to generate highly oxidizing free radicals which then diffuse and damage the critical targets • Electromagnetic radiations (X- and γ-rays) are predominantly indirectly ionizing

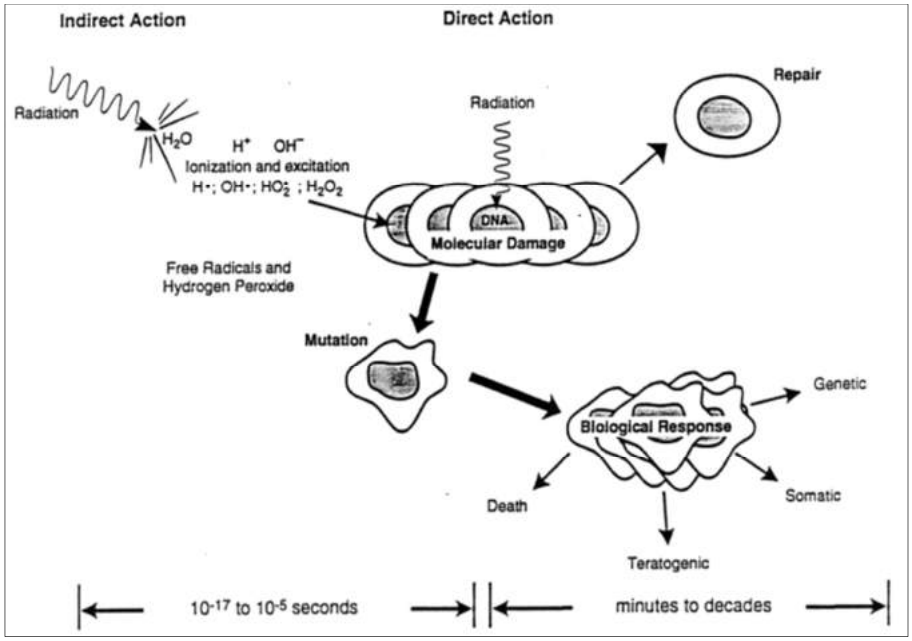

Source: https://www.slideshare.net/confitom/chap1-physics-and-chemistry-of-radiation-absorption

Figure 2.2: Different modes of action of ionizing radiation

2.3 Chemistry of Ionizing Radiation

Generation of reactive oxygen species (ROS)

The indirect mechanism accounts for approximately 60-70% of the biological damage produced by IR. Since water comprises 60-80% of the human tissues, most of the

ionizing events will take place in the water molecules as a result of radiolysis (Riley, 1994). The first event of the interaction of IR with matter involves the deposition of energy into the medium, which further generates secondary electrons, leading to secondary ionizations (Riley, 1994). The radiolysis or decomposition of water following exposure to IR results in the formation of highly reactive radicals and molecules (OH^o, $O_2^{\bullet-}$, H_2O_2 and H_2^+) and can be represented as:

$$H_2O \rightarrow H^o + OH^o + e_{aq}^- + H_2O_2 + H_3O^+ + H_2 + HO_2^o, OH^-$$

The radiolytic events occur in three main stages, taking place on different time scales, which is described in figure 2.3 (Le Caër, 2011).

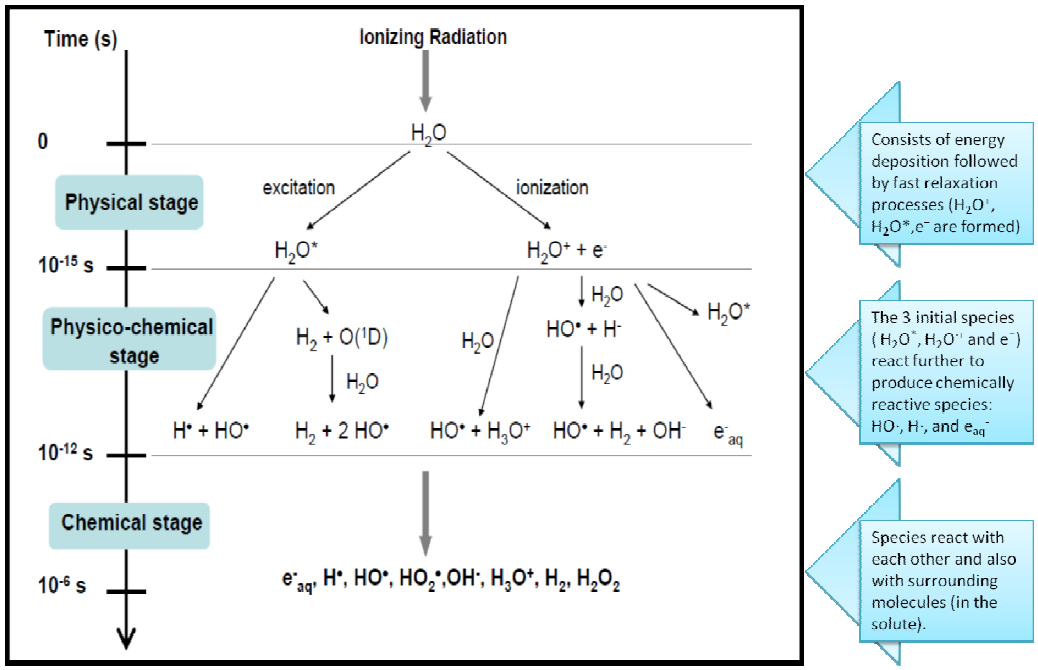

Source:(Le Caër, 2011)

Figure 2.3: Main reactions taking place during the three stages of water radiolysis

The free radicals generated as a result of radiolysis are incredibly short-lived (10^{-6}-10^{-10} second); however, they immediately react with any biomolecules present in their

vicinity to produce highly specific site-specific oxidative damage. The hydroxyl radical (•OH) is the most reactive of all the oxygen-derived free radicals, and an estimated 60-70% of the cellular DNA damage caused by IR is believed to be triggered by hydroxyl radical (•OH) (J. F. Ward, 1994). In the presence of oxygen, the primary ROS species can give rise to the secondary species ($O_2^{\bullet-}$, H_2O_2) within one picosecond. The superoxide radical ($O_2^{\bullet-}$) and hydrogen peroxide (H_2O_2) are moderately stable and can persist in the cellular milieu for more extended periods. Although $O_2^{\bullet-}$ is relatively unreactive than other ROS, it can lead to the formation of more reactive species such as peroxyl (ROO•), alkoxyl (RO•) and •OH radicals by reacting with biological materials. H_2O_2, on the other hand, is a weaker oxidant than $O_2^{\bullet-}$, but can aid in the formation of more reactive ROS molecules including hypochlorous acid (HOCl) by acting as an intermediate radical as follows:

$$H^+ + Cl^- + H_2O_2 \longrightarrow HOCl + H_2O$$

Additionally, in the presence of divalent metal catalysts (ferrous or cuprous ions), H_2O_2 can give rise to additional amounts of •OH by the Fenton reaction(Fridovich, 1997).

$$H_2O_2 + Cu^+/Fe^{2+} \longrightarrow OH^- + \bullet OH + Cu^{2+}/\ Fe^{3+}$$

Production of reactive nitrogen species (RNS)

The nitric oxide ($NO^{\bullet}$) are generated as a consequence of radiation mediated activation of nitric oxide synthase (NOS) activity in cells (Freeman & MacNaughton, 2000). $NO^{\bullet}$ arises in NOS dependent oxidation of L-arginine to L-citrulline, in the presence of NADPH, O_2, heme, flavin nucleotides, tetrahydrobiopterin, and

Ca^{2+}calmodulin as cofactors. The reaction of $O2^{\bullet-}$ with $NO^{\bullet}$ causes the formation of a membrane-permeable, reactive nitrogen oxide species peroxynitrite ($O=NOO^{-}$). While $NO^{\bullet}$ is chemically inert to most of the cell components, peroxynitrite can directly react with various biomolecules. Other potential RNS comprise nitrogen dioxide (NO_2), nitroxyl (HNO), and nitrosonium cation (NO^{+}) (Wink & Mitchell, 1998). Therefore, the radiolysis of water and timely stimulation of NOS are the significant causes of ROS/RNS production in irradiated cells under ambient oxygen.

The chemical change induced by the free radicals may be repaired before it becomes irreversible by recombination of free radicals and dissipation of energy or may be modified by the presence of agents such as molecular oxygen or radio-protective compounds. The presence of oxygen at the time of irradiation, or within microseconds of the radiation has been shown to enhance the damage (called *oxygen effect*) by chemically reacting with the newly formed DNA radical and ”fixing” (permanent) the damage (GRAY, CONGER, EBERT, HORNSEY, & SCOTT, 1953). Although the time required for the entire chain of physical and chemical events (from interaction with cells till damage induction) is of the order of microseconds or less, the subsequent development of biochemical or physiological changes may take hours, days or even years (as in cancer) to become visible.

2.4 Biological effects of ionizing radiation:

Radiation exposure can lead to many serious health effects, and these have been classified as deterministic and stochastic effects by the International Commission on Radiological Protection (ICRP, 1990).

2.4.1 Deterministic effects (non-stochastic effects)

These effects, also called non-stochastic effects, arise when a large population of cells in a tissue are inactivated by radiation, thus giving rise to anatomical or functional tissue damage. Non-stochastic effects generally detected when a minimum dose of radiation, the so-called *threshold dose*, has delivered. Examples of includes nausea, vomiting, skin redness, hair loss etc. Radiological protection intents at eluding the deterministic effects by fixing the dose limit, less than thresholds. Deterministic effects occur when many cells die, due to a high radiation dose, that cannot be replaced, and the equilibrium between proliferation and death shifted towards the latter. In turn, the targeted tissues and organs stopped working appropriately, which ultimately leads to biological alterations at the serious note. These effects are usually not fatal but can cause impairment of some body parts, and other non-malignant changes may arise. It may cause significant impairment in the form of necrosis and functional damage of tissues. The best example is cataract characterized by the opacity of eye lens and skin damage mostly seen as thinning and ulceration of the skin. High absorbed doses of several Gray are usually required to cause these conditions (ICRP 1991; IAEA Vienna 1996). The clinical severity of damage increases with increasing doses. The damage can appear at variable times ranging from a few hours or days to several years post-exposure, which depends upon the type or physiognomies of a particular tissue.

Effect	Organ/tissue	Time to develop effect	Absorbed dose (Gy)[e]
Morbidity:			*1% Incidence*
Temporary sterility	Testes	3–9 weeks	~0.1[a,b]
Permanent sterility	Testes	3 weeks	~6[a,b]
Permanent sterility	Ovaries	< 1week	~3[a,b]
Depression of blood-forming process	Bone marrow	3–7 days	~0.5[a,b]
Main phase of skin reddening	Skin (large areas)	1–4 weeks	<3–6[b]
Skin burns	Skin (large areas)	2–3 weeks	5–10[b]
Temporary hair loss	Skin	2–3 weeks	~4[b]
Cataract (visual impairment)	Eye	Several years	~1.5[a,c]
Mortality:			
Bone marrow syndrome:			
– without medical care	Bone marrow	30–60 days	~1[b]
– with good medical care	Bone marrow	30–60 days	2–3[b,d]
Gastro-intestinal syndrome:			
– without medical care	Small intestine	6–9 days	~6[d]
– with good medical care	Small intestine	6–9 days	>6[b,c,d]
Pneumonitis	Lung	1–7 months	6[b,c,d]

[a] ICRP (1984).
[b] UNSCEAR (1988).
[c] Edwards and Lloyd (1996).
[d] Scott and Hahn (1989), Scott (1993).
[e] Most values rounded to the nearest Gy; ranges indicate area dependence for skin and differing medical support for bone marrow.

Source: ICRP, 2007. The 2007 Recommendations of the International Commission on Radiological Protection. ICRP Publication 103. Ann. ICRP 37 (2-4))

Figure 2.4: Projected thresholds for tissue reactions (radiation doses that cause a 1% reaction) after whole-body gamma-ray exposures

2.4.2 Stochastic Effects

These are the effects that occur by chance, without any threshold level of dose, and whose possibility of occurrence is proportional to the received dose and its severity independent of the absorbed dose. Non-lethal mutations mainly cause stochastic effects in cells (particularly cancer). It is of important concern that IR can induce cancer, which normally does not evident up to several years of the initial exposure. Radiation-induced carcinogenesis and hereditary effects are two classic examples of stochastic effects of radiation. If a low dose of radiation is delivered slowly over a long period, then the cells have the opportunity to repair themselves without showing any signs or symptoms of injury. The damaging effects of radiation may appear much late in life (sometimes

decades), or even in the progenies of the irradiated person. Such type of effects are called stochastic effects, which are not certain to arise, but the probability increases as the radiation dose increases. Since the causes of the disease or syndrome are multi-factorial, it is normally difficult to discern clinically that which effect is primarily because of radiation exposure(Hall, Eric J. Giaccia, 2006) (ICRP 1991; IAEA Austria, 2004).

Determinants of biological effects:

1) Rate of Absorption

The rate of radiation absorbed dose is very critical in the determination of the type of effect going to arise. Since, a substantial recovery occurs from the radiation damage, as a given low dose rate will produce less impact than if a hefty dose of radiation given as a single dose in minimal time because this will not allow the repair to occur.

2) Area Exposed

The portion of the body irradiated is an essential parameter because the more significant the area exposed, the higher will be the overall damage to an organism. It is for the reason that more cells have been affected; as a result, there will be a high possibility of impacting significant portions of tissues or organs. For example, 20 Gy fractionated focal irradiation to the tumour regresses tumour and causes some side effects to the nearby healthy tissues. However, if the same dose is given as whole-body exposure, it will be lethal.

2.5 I R induced macromolecular damage

The ionizing events and free radicals production by radiation cause damage to vital cellular components. Because of their high reactivity, ROS can react with bio-molecules and set off chain reactions, which can cross-link proteins, cause peroxidation of lipids or

mutations in DNA by introducing single or double-strand breaks or modifying bases (Fig;2.5). The time between the breaking of chemical bonds and the manifestation of biological effect may vary from hours, days, months or years.

2.5.1 Lipid Peroxidation

In general, lipids are oxidized when a hydroxyl radical extract an electron from an unsaturated fatty acid. This generates a highly reactive lipid radical, which may react with oxygen and forms a fatty acid peroxyl radical. This peroxyl radical reacts with another unsaturated fatty acid to make a new lipid radical and peroxyl radical, hence propagating the damage. The continuous cycles of lipid peroxidation cause severe injuries to cell membranes. Radiation-induced ROS (mainly •OH radicals) is also harmful to membrane lipid. The oxidation of membrane phospholipids of the bilayer of plasma membrane and organelles such as the mitochondria disrupt membrane and organelle function, which can further cause cell death. Oxidation of membrane lipids leads to enhanced membrane rigidity, reduced the activity of membrane-bound enzymes, and also causes alterations in membrane permeability and the movement of membrane receptors. Lipid peroxidation also produces some other reactive species like 4-hydroxynonenal (4-HNE), and malondialdehyde (MDA) which further add into the cytotoxicity of a cell and have been used as biomarkers for evaluation of acute and chronic oxidative stress after irradiation (Awasthi et al., 2004).

2.5.2 Protein Oxidation

The reactive oxygen species generated by γ irradiation (mainly, but not only •OH) in the presence of oxygen causes covalent modification of proteins, resulted in protein

oxidation or damage. This includes oxidation of amino acid side chains, protein cross-links, protein aggregation, breakage of the peptide bond, and creation of protein carbonyls, etc. Out of several amino acids, some are most susceptible to oxidation such as Cys, Tyr, Val, His, Met, Try, Phe, Pro, Leu, Thr, Glu, Arg and Lys. Estimation of Protein carbonyl content has been used as a marker for the evaluation of radiation-induced oxidation of proteins (Manda, Anzai, Kumari, & Bhatia, 2007). The destruction of the inherent protein structure consequently leads to loss or gain of enzymatic activities, protein functions, increased/reduced susceptibility to proteolysis, abnormal cellular uptake, altered gene transcription, and augmented immunogenicity, etc.

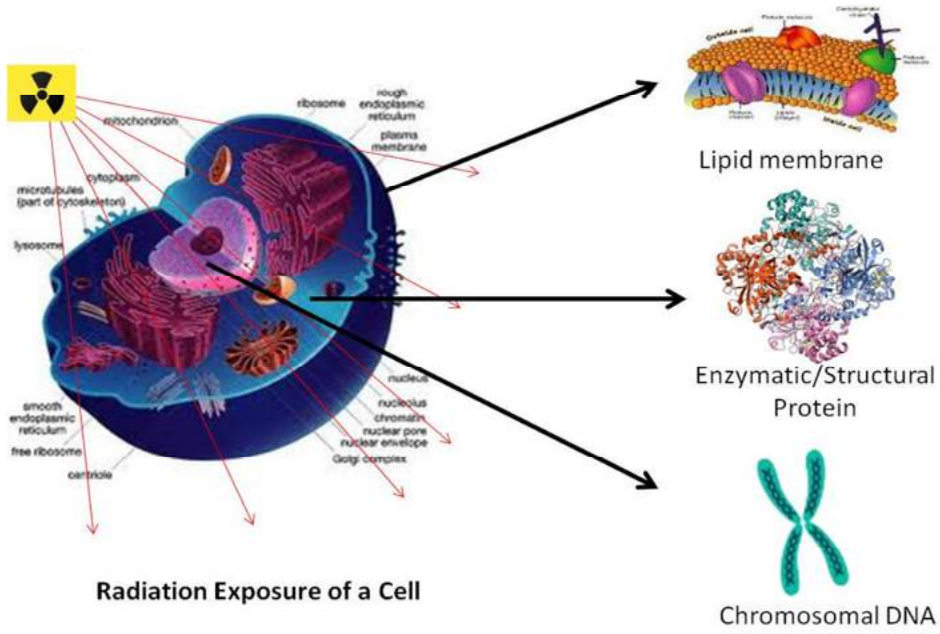

Figure 2.5: Radiation-induced macromolecular damage in cells, the picture shows the major target (membrane lipid, enzymatic and structural proteins and DNA) of radiation.

2.5.3 DNA damage

IR is a harsh DNA damaging agent, produces a variety of lesions including base modifications, alkali-labile sites, DNA–protein crosslinks, DNA–DNA intra- and

inter-strand crosslinks, single-strand breaks (SSBs), and double-strand breaks (DSBs). Interaction of •OH with the deoxyribose moiety leads to the release of free bases from DNA, various sugar modifications and simple abasic sites. 8-Hydroxyguanine (8-OHdG), hydroxyl uracil, thymine glycol and several other types of base modifications have been reported following exposure to ionizing radiations (Hagen, 1994; Santivasi & Xia, 2014). Out of these, 8-OHdG has been frequently studied as a biomarker for DNA oxidation (Gao et al., 2019). SSBs or DSBs are formed because of the disruption of the sugar-phosphate backbone by IR. One time exposure of cells to IR typically causes around 1000 SSBs, 40 DSBs and 3000 modified bases per Gray (Gy) (J. F. Ward, 1994). However, at 1 Gy radiation dose only 20 to 30% of mammalian cells die due to the high efficiency of DNA repair machinery- predominantly for non-DSB lesions. Generally, most of the damaged DNA is repaired within a few hours of exposure in a normal cell (Iliakis, 1991). DNA DSBs are regarded as the most lethal lesion produced by IR. Unlike SSBs, DSBs are highly toxic, irreparable, and lead to the extensive loss or reshuffling of genetic material at the time of replication and mitosis. DSBs can be observed cytogenetically at the first mitosis after exposure as translocations, dicentrics, ring chromosomes, micronuclei and double minutes. If the cells failed to mount this damage or there is unrepairable damage, they may decide to enter into senescence or may initiate programmed cell death (apoptosis) to evade the transmission of mutations to the daughter cells. The number of dicentrics per cell per Gray (Gy) of ionizing radiation is consistent in blood cells, which is exploited presently to assess the absorbed dose of radiation in exposed individuals as biological radiation dosimetry. Radiation induced micronuclei and gamma H2AX assay in blood cells are also popular methods in biological radiation dosimetry.

2.6 Cellular Response to Radiation

The biological effects and impact of IR depend on the radiation absorbed dose in cells or tissue which are at risk and is a complex function of several other biophysical factors, such as the radiation type, radiation dose, dose rate, the relative biological effectiveness, distribution of the energy, or the number of cells exposed. The magnitude of radiation damage also depends on the cellular radio-sensitivity, whereby cells with a high rate of proliferation or reduced degree of differentiation are more sensitive at a low dose of radiation than the slow dividing or more differentiated cells (Bolus, 2017; Packard, 1930)

In general, a cell exposed to IR can respond in one of the following ways:

- The cell may remain unharmed if IR causes alterations that generally occur in the cell
- The cell may revert to a healthy state if the damage is repaired by the cell
- Reproductive death of the cell may follow if the radiation-induced damage cannot be fixed by the cell or is mis-repaired
- Finally, if a cell is damaged extensively at such level where it stops responding to any other signal that controls cellular growth, it will permanently die.

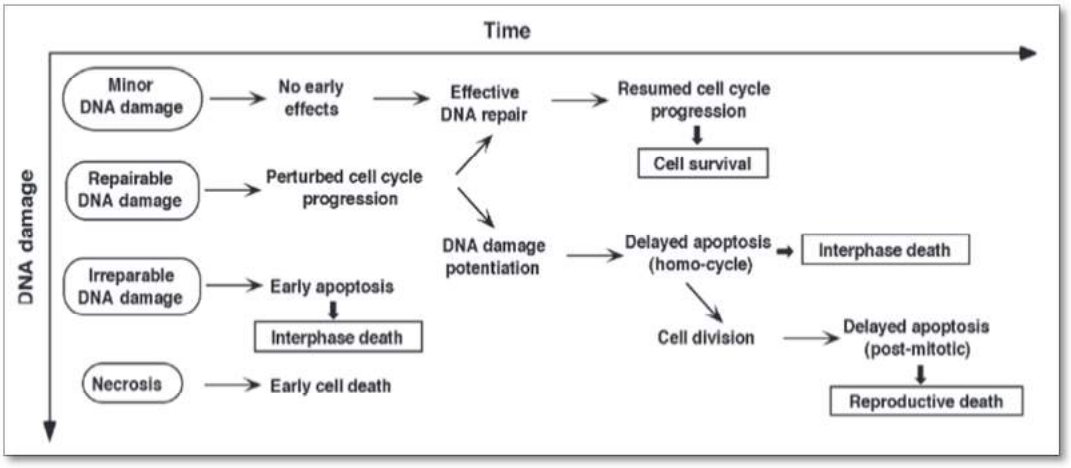

Source:(Shinomiya, 2001)

Figure 2.6: Fate of irradiated cells. Schematic representation of the relationship between initial DNA damage and the fate of the cell concerning cell cycle

The outcomes of these manifestations depend upon the nature of lesions, the capacity of cells to repair the damage, physiological, nutritional and environmental state of the cells. Since DNA is the prime target of radiation, DNA damage and repair, particularly DSBs, may influence the different fates of a cell, e.g. cell death, mutation and transformation (Surova & Zhivotovsky, 2013). The most accepted mechanism of action of IR on mammalian cells is the production of mutagenic and clastogenic effects and inhibition of mitosis (Brenner & Ward, 1992; Hagen, 1994). Many cellular and molecular determinants as well as mechanisms that profoundly influence the cellular radiation response have been identified over the last few decades through experimental studies. These include the induction and repair of DNA damage, cell cycle perturbation, apoptosis, gene induction and signal transduction (I. Ward & Chen, 2004).

2.6.1 DNA Damage Response (DDR)

IR induced DNA damage may elicit responses in the form of various biological endpoints viz. cell cycle delay, apoptosis, loss of reproductive potential, genomic instability, mutation and neoplastic transformation (Murray et al. 1999, Huang, Snyder, and Morgan 2003; Surova and Zhivotovsky 2013; Suzuki et al. 2003). The DDR signalling network works in this regards. It is indispensable for maintaining the genomic integrity, acting via the initiation and coordination of DNA repair mechanisms with the activation of appropriate cell cycle checkpoints. Within minutes of damage induction, the histone variant H2A-X is phosphorylated at Ser139 at sites of DNA damage by ATM or autophosphorylation. These local chromatin modifications provoke the further recruitment of a multitude of DNA-damage response proteins, including MDC1, NBS1, RAD50, MRE11, 53BP1, and BRCA1,

which amplify chromatin modifications over distances ranging in megabases of DNA leading to the generation of microscopic structures called DNA damage foci (Abraham, 2001; Bian, Meng, Zhang, & Li, 2019; Samstein & Riaz, 2018; Willers, Dahm-Daphi, & Powell, 2004). The mammalian cell systems possess several repair systems to cope up with various types of DNA damage and maintain genomic integrity. These are Homologous Recombination Repair (HRR), NHEJ, Nucleotide Excision Repair (NER), Base excision repair (BER) and Mis-match repair (MMR). Out of these, the NHEJ and HR pathways are involved in the restoration of DNA DSBs. The choice between these two mechanisms is determined by the chemical complexity of the breaks, conformational state of the chromatin, position of the cell in cell cycle and fidelity of repair required (Bhattacharya et al., 2017; Friedberg, 2003).

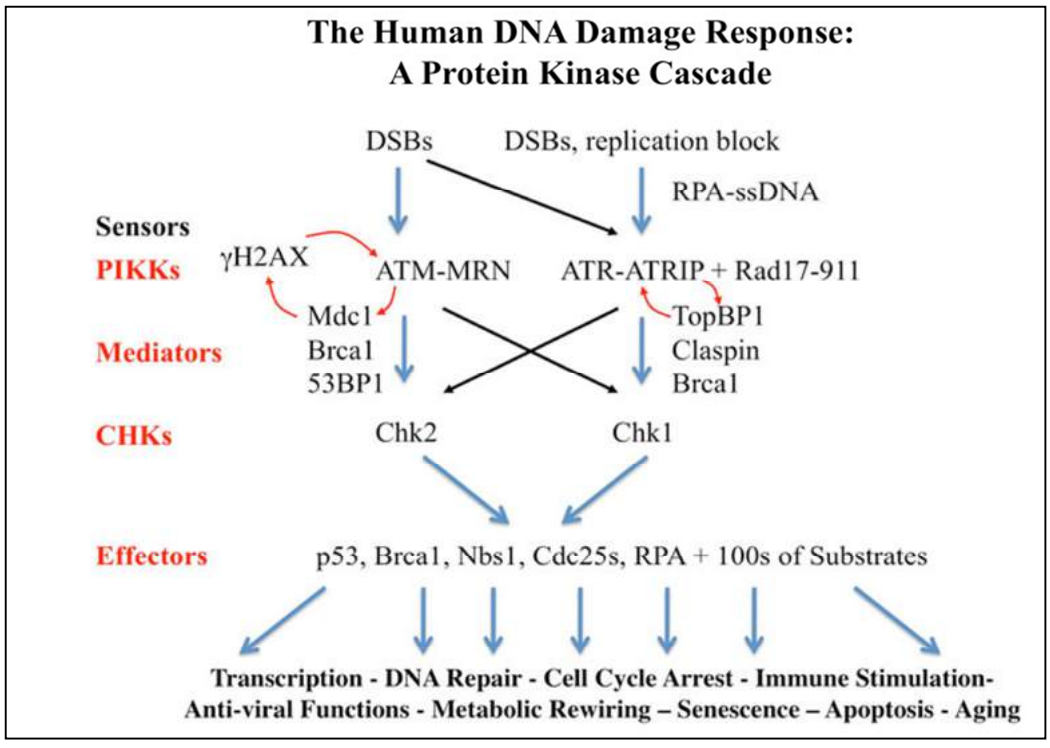

Source: http://elledgelab.med.harvard.edu/?page_id=264

Figure 2.7: The DNA damage response pathway

2.6.2 Induction of Cytogenetic damage (Micronuclei formation)

After exposure of cells to a DNA damaging agent such as high or low LET radiation, fragmented chromosomal material lacking spindle attachment organelles (kinetochores, centromeres), called "acentric fragments" (AF), may not be appropriately segregated into daughter cells during cell division and form small extranuclear bodies within the cytoplasm. Such cytoplasmic bodies called "micronuclei" (MN) can appear in the cytoplasm of the irradiated cell or maybe randomly segregated into either or both of the daughter cells. Cell division is a prerequisite for the appearance of MN, and the MN frequency will be expected to increase after the second and further post-irradiation divisions as more and more aberration-bearing cells pass through mitosis (Müller et al., 1996; Streffer, Müller, & Wuttke, 1994). The occurrence of MN indicates that the cells may suffer from loss of reproductive ability due to the loss of genetic material and in most cases, is doomed to die. This has been established from studies carried out to relate micronuclei frequencies and cell survival (Midander & Révész, 1980; Vral, Fenech, & Thierens, 2011).

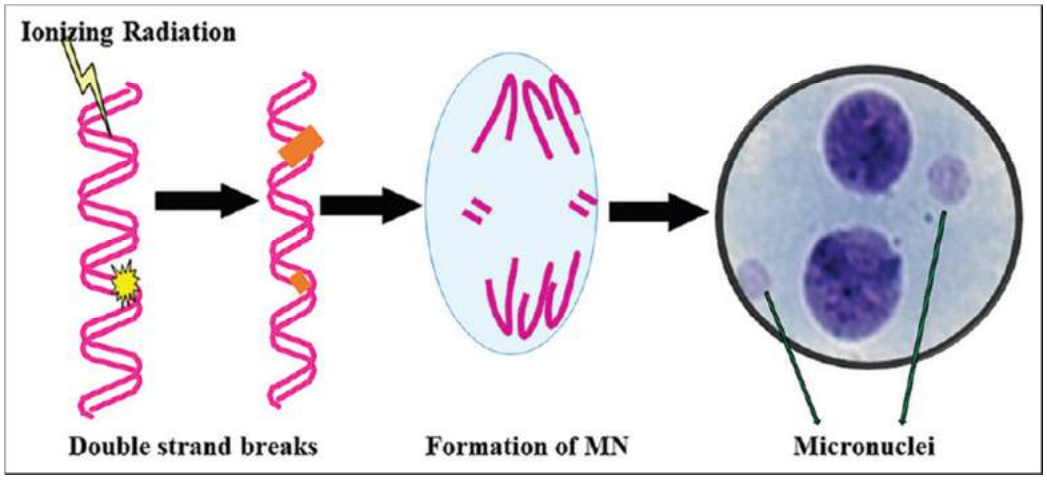

Source: Kanagaraj et al., 2017

Figure 2.8: Diagrammatic representation of micronuclei formation after chromosomal damage

2.6.3 Cell death

Cell death can be the ultimate result of cellular and tissue radiation injury. Radiation-induced cell death can occur through several distinct pathways depending upon the time course and cell-cycle position. That apoptotic cell death plays a crucial role in almost every mode of cell death (Surova & Zhivotovsky, 2013). IR-induced cellular death has been mainly categorized into two groups, based on the timing of cell death after irradiation, *interphase death*, and *reproductive or mitotic death*. Interphase death is defined as an irreversible breakdown of cellular structure and metabolism before undergoing the first mitotic division after irradiation. In contrast, reproductive or mitotic death occurs during one or even several divisions after the radiation. It is defined as a failure to undergo further cell division despite metabolic survival (Shinohara & Nakano, 1993). Both types of cell death can be manifested as apoptosis or necrosis. Interphase death is characterized by pyknosis, cell shrinkage and inter-nucleosomal DNA fragmentation, all of which are hallmarks of apoptotic cell death (Saraste & Pulkki, 2000). On the other hand, reproductive or mitotic cell death is characterized by the loss of clonogenic cell survival, and this mode of cell death is usually evaluated by colony-forming assay (Méry et al., 2017).

Radiation hazards can vary from acute mortality to chronic pathologies. The dose and time of radiation exposure decide the severity or nature of the health effect. The health effects of radiation exposure can be divided into two categories: ***acute* and *late* effects.**

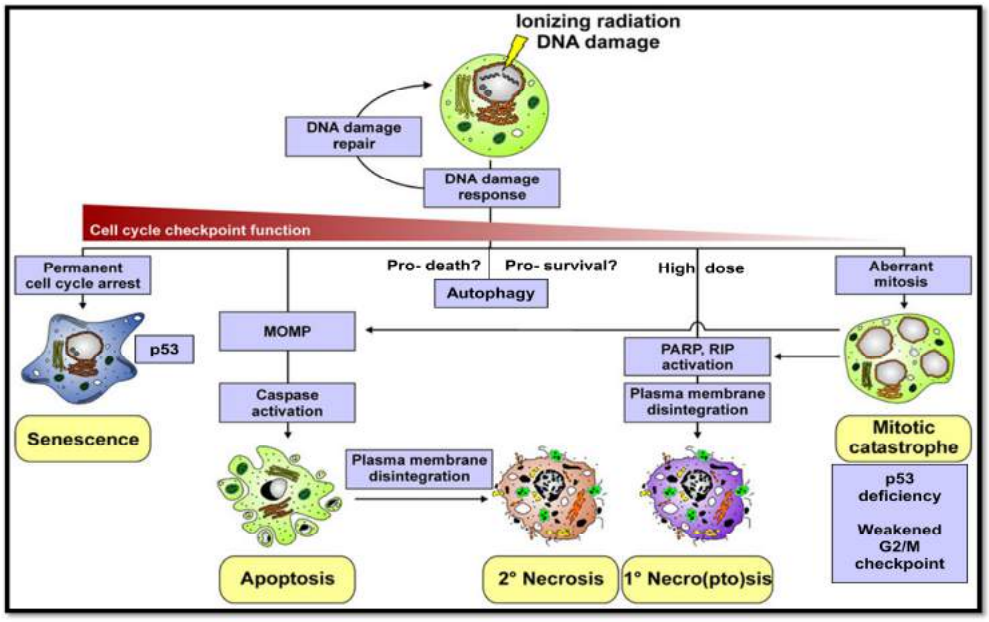

Source:(Lauber, Ernst, Orth, Herrmann, & Belka, 2012)

Figure 2.9: Different modes of cell death induced by IR

2.7 Acute Radiation Syndrome

When any subject is exposed to a high dose of radiation in a small period and shows symptoms like nausea, vomiting, headache and diarrhoea within few hours to few days and can sometimes result in mortality within few days or weeks. Shortly after radiation exposure, early symptoms develop which last for a limited time; this is generally referred as the prodromal radiation syndrome and popularly known as "Acute Radiation Syndrome" (ARS) or "Radiation Sickness". The minimum radiation dose to cause ARS is not below than 0.75 to 1 Gy delivered in a few minutes. The rate of radiation exposure is also very crucial besides the dose of radiation exposure (López & Martín, 2011). Large radiation dose in a small time scale can be more harmful and damaging than the same treatment offered in a long period (hours to days). A large amount of radiation can be delivered to individuals in very less time duration only in the scenarios like a nuclear

bomb explosion or nuclear reactor accident, casual handling of radioactive material or breaching of a highly radioactive source. Therefore, the Acute Radiation Syndrome is rare and can occur only in such unusual events where high radiation dose exposure occurs in a short time (Macià i Garau, Lucas Calduch, & López, 2011). The four factors which are responsible for ARS are:

1. It can occur only at high radiation dose (> 0.75 Gy to 1 Gy), which also depends on age, gender, health condition and individual's radiation sensitivity.
2. The individual has received the radiation dose in a small-time, generally within minutes.
3. The radiation had a high penetrating ability and reached internal organs. The absorbed dose should be > 0.75 Gy to 1 Gy.
4. Whole-body exposure, the person's entire body or most of it should receive the dose.

Acute whole-body exposure to dose >4.5Gy may result in a statistical probability that 50% of the exposed population will die within 60 days without medical intervention (Waselenko et al., 2004).

Since it was discussed earlier that fast-dividing cells are most sensitive to radiation and may die after nearly 1Gy ionizing radiation exposure, the highly radio-sensitive organs include the hematopoietic, gastrointestinal (GI), skin, spermatogenic, and vascular systems while the less sensitive is the nervous system (Hall, Eric J. Giaccia, 2006). This also conveyed that a growing embryo is utmost sensitive to radiation exposure in the *first* trimester than in later trimesters. The ARS further classified in different categories.

2.7.1 Hematopoietic syndrome (H-ARS)

The blood circulating leukocytes (white blood cells) and its stem cells, which are actively dividing in the bone marrow to supply newer leukocytes, are most radiation-sensitive cells and tissues of the human body. The full syndrome will typically occur at a dose between 0.7 to 10 Gy though mild symptoms may arise as low as 0.3 Gy. A sudden fall of lymphocytes in blood has been observed after 24 hr of radiation exposure, in individuals. The radiation-induced loss of haematopoietic cells and tissues is known as haematopoietic syndrome (Fig;2.10). The acute exposure of a high dose of ionizing radiation exerts both direct and indirect effect of radiation, causing haematopoietic cell death (Leibowitz et al., 2014).

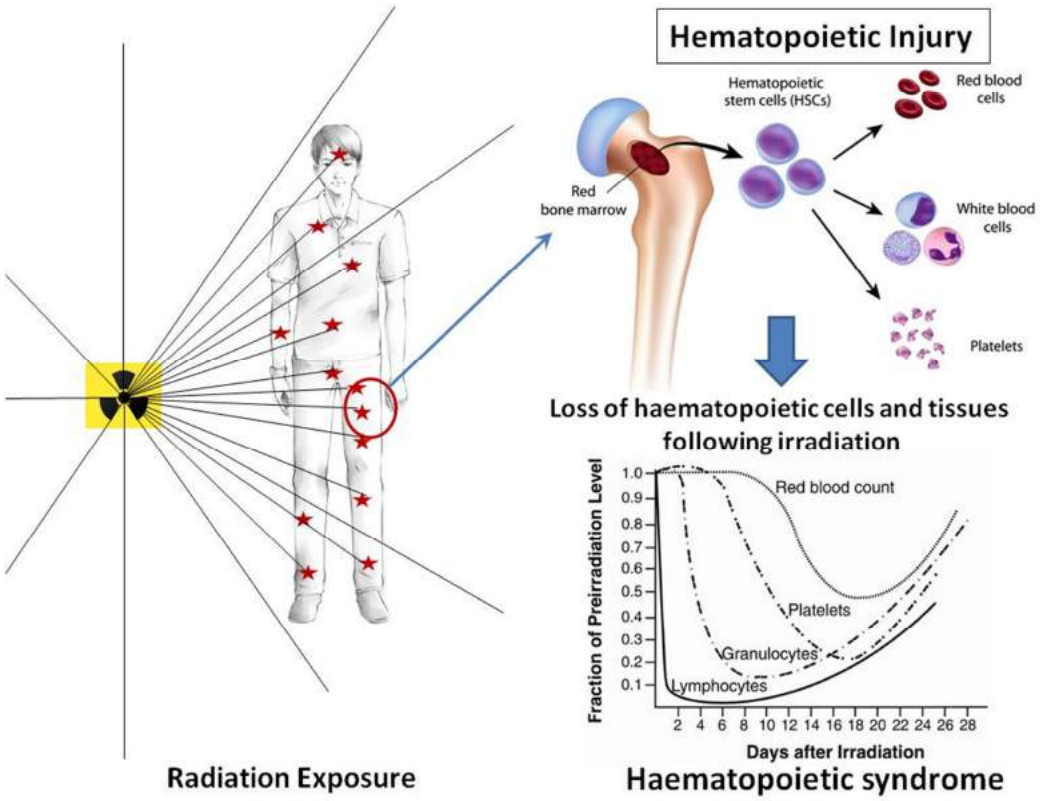

Figure 2.10: Radiation-induced Hematopoietic syndrome, shown by changes in peripheral blood indices following exposure to an intermediate dose of whole-body irradiation.

The symptoms of radiation sickness that develop after acute whole-body irradiation (WBI) are majorly due to the expression of hematopoietic syndrome. The prime cause of H-ARS induced death is radiation-induced destruction of the bone marrow, causing microbial infection (sepsis) and haemorrhage. The severity of H-ARS increases with an increase in radiation absorbed dose; therefore, the survival ratio of patients with H-ARS reduces with increasing dose. The therapeutic procedure includes bone marrow transplantation and supplementation with cytokines like GM-CSF, G-CSF, and stem cell factors help in recovering the proliferating potential of bone marrow. The recovery takes place only when the radiation dose (<6Gy) is not too high, which can otherwise be lethal. Acute bone marrow toxicity can be measured by granulocytopenia, thrombocytopenia, and, also, anaemia. However, peripheral blood cell counts often fail to demonstrate the actual level of damage to the hematopoietic stem cells or microenvironment and do not reflect the reserve capacity of the bone marrow.

All hematopoietic cells are differentially sensitive to ionizing radiation with the likelihood of stem-cells being most vulnerable, followed by lymphocytes and then other cells (Fig;2.10). This syndrome is identified by a substantial drop in lymphocyte and platelet count, and this depletion could be attributed to the mitotic catastrophe of the proliferating stem cells. The loss of cells from peripheral blood is not replenished by the bone marrow, which results in significantly low peripheral blood count leads the body into trouble. Mature granulocytes have a life span of one day; therefore, a radiation-induced decrease in the supply of granulocytes (Hypoplasia/ Leukopenia/granulocytopenia) occurs primarily followed by a reduction in platelets. Leukopenia continues till day 12, then further development of hematopoietic syndrome depends on the number of bone marrow cell survived the radiation insult. After day 12, the concentration of granulocytes reaches a plateau (~1000/μL). It is considered a favourable prognostic sign that still sufficient

numbers of stem cells are present that can regenerate bone marrow and peripheral blood cells. But if the count of granulocytes falls further beyond 1000/μL, there is a high risk of fatal consequences of leukopenia and thrombopenia (Bolus, 2017). In such cases, therapeutic options like stem cell transfusion and cytokine therapy are given. In experimental studies, after an acute dose of 8.5 Gy the animals (rodents) die of septicemia caused by severe leucopenia and diffuse interstitial haemorrhage and death takes place at the time of nadir of granulocyte depletion which is generally at the 3rd-week post-irradiation (Goans et al. 2001; Hall, Eric J. Giaccia 2006). Infection is a significant cause of death; however, that can be improved by the intervention of antibiotics, cytokines and growth factors (Chao, 2007; Hérodin & Drouet, 2005). Humans recover much slowly from H-ARS, death are on the peak at around 30 days and continued till day 60; however, in case of mice, most of the mortality occurs within 10 to 15 days followed by total death by day 30 after radiation exposure (Hall, Eric J. Giaccia, 2006).

2.7.2 Gastrointestinal (GI) syndrome (GI-ARS)

The actively dividing cells of crypts of the gastrointestinal wall are also very susceptible to ionizing radiation exposure. Therefore, the proliferating cells of the intestinal crypts are majorly affected, and the overall length of intestinal villi shortens (Fig;2.11). The full GI syndrome will occur at 10 Gy absorbed dose even though some symptoms may arise at as low as 6 Gy. The survival of persons suffering from GI Syndrome is highly unlikely, and death typically occurs within two weeks. Radiation-induced damage at such a high dose is critical and irreparable in both the GI tract and bone marrow, causing dehydration, electrolyte imbalance and infection (Dubois & Walker, 1989; Leibowitz et al., 2014). Since the mucosal lining is severely damaged, there is a high risk of disease from opportunistic microorganisms. The

treatment includes the administration of antibiotics, fluids and electrolyte (Booth, Tudor, Tudor, Katz, & MacVittie, 2012; Chao, 2007).

Radiation causes a highly toxic effect on cells or structures in the GI tract leading to inflammation and loss of physiological functions resulted in symptoms like vomiting and poor digestion. Intestine harbours stem cells at the base of the crypt which maintains the population of intestinal cells, being regularly lost from the villi tip (Fig; 2.11). Irradiation with a dose of 8 Gy (in mice and nearly 4.5 Gy in human) or more causes stem cell apoptosis leading to short supply of cells required to maintain mucosal lining and villi regeneration. Thus formed mucosal lesions lead to the breakdown of the GI mucosal barrier, fluid & electrolytes imbalance, impaired absorptive function, GI haemorrhage, bacterial infection, inflammation and septic shock, organ failure, and ultimately death by GI syndrome (Booth et al., 2012; Dubois & Walker, 1989).

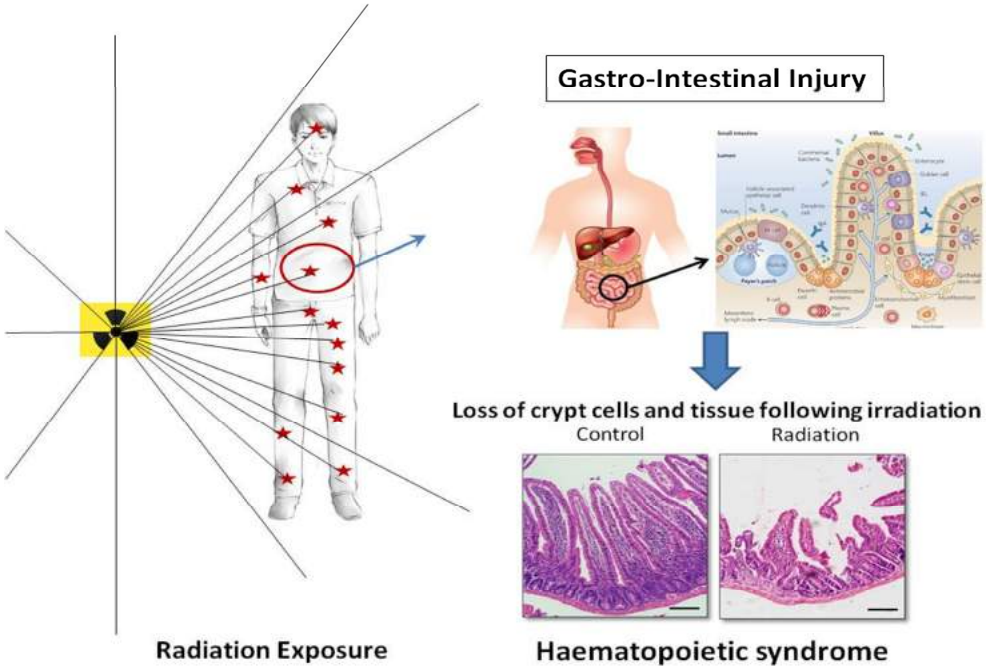

Figure 2.11: Radiation-induced gastrointestinal syndrome, diagrammatic representation of histological changes in the proximal jejunum from non-human primates

2.7.3 Central Nervous System (CNS) Syndrome/ Cardiovascular (CV) Syndrome

The CNS/CV syndrome will typically appear at a dose higher than 50 Gy while some symptoms of CNS/CV syndrome may seem at a low dose as 20 Gy. Mortality is observed within 2-3 days due to CNS/CV syndrome in persons exposed to such a higher dose. In such cases, death occurs due to collapse of the circulatory system and enhanced pressure in the cranial vault as the rise in fluid content triggered by edema, meningitis, and vasculitis. Symptoms include loss of coordination, jumbling, coma, seizures, shock, along with the symptoms of bone marrow and GI syndromes.

2.7.4 Cutaneous Radiation Syndrome (CRS)

The radiation exposure to skin results in skin damage and complex pathological syndrome, which is known as Cutaneous Radiation Syndrome (CRS) and now in recent years considered as ARS. The first symptom which appears in a few hours of irradiation is transient and irregular erythema with itching. Further, the radiation-induced skin damage reaches to the basal cell layer results in inflammation, redness, and skin exfoliations, also, damaged hair follicles causes hair loss. During the latent phase of CRS, intense redness, scorching, and ulceration at the irradiated site which last from few days up to several weeks. In the majority of the cases of CRS, the remedy is by regeneration; however, high doses of radiation cause permanent hair loss, impaired sweat and sebaceous glands, fibrosis, altered skin colouration, and ulceration of the exposed site (Dörr, Baier, & Meineke, 2013; Peter, Steinert, & Gottlöber, 2001).

Acute Radiation Syndrome is manifested in 4 stages:

- **Prodromal stage (N-V-D stage)***:* The early symptoms appear including nausea, vomiting, and diarrhoea, which arises from minutes to days after exposure, depending upon the dose of radiation. The symptoms may sustain (intermittently) for minutes up to several days.
- **Latent stage***:* The patients in this stage looks healthy and normal for a few hours to a few weeks.
- **Manifest illness stage***:* reflects the clinical symptoms related to radiation injury and can end from hours to several months.
- **Recovery or death***:* The recovery phase takes several weeks to two years. The patients who failed to recover from ARS will die within a few months.

Table 2.1: Summary of dose-response relationship during radiation exposure

Effect	Dose (Gy)
Blood count changes	0.5
Vomiting (threshold)	1
Mortality (threshold)	1.5
$LD_{50/60}$* (with minimal supportive care)	3.2- 3.6
$LD_{50/60}$ (with supportive medical treatment)	4.8- 5.4
100% mortality (with best available treatment)	8

Adapted from NCRP Report No. 98 "Guidance on Radiation Received in Space Activities, NCRP, Bethesda, MD (1989)

2.8 Late Effects of Radiation

Long-term effects of radiation generally appear after several years of initial exposure. The latent period is considerably more extended than that of the acute radiation

syndrome. Radiation-induced delayed effects comprise cancer and other health effects like fibrosis, cataracts, benign tumours, and genetic changes.

2.8.1 Radiation-induced Carcinogenesis

If the radiation-induced damage to cells is not repaired correctly, it may inhibit the cell from survival or reproduction or incur mutation. Radiation can produce carcinogenic changes by the following mechanisms: (1) induction of variations, including modifications in single gene or chromosome; (2) alterations in gene expression, without mutations; Studies have shown that radiation-induced carcinogenesis is a multiple-step process in which healthy cells acquire cancer cells characteristic of cellular immortality and tumorigenicity. Development of radiation-induced carcinogenesis is a stochastic multifactorial process involving many signalling pathways, and none of them attributed to the process of cancer development. The short latency period is 5-7 years for leukaemia, and solid tumours latency period may extend up to 30-40 years.

2.9 Radiation Countermeasures

In the present world, the increasing acts of terrorism, deadly nuclear accidents at nuclear power plants or atomic machinery, and expanding use of radiation in medical fields poses a severe threat from radiation. Hence, there is a crisis to develop potential countermeasures and interventions to encounter the lethal consequences of ionizing radiation.

Generally, the chemical or biological agents utilized to modify the normal tissue toxicity following radiation can be classified into three categories depending upon the time of delivery concerning irradiation (Citrin et al., 2010):

- *Radio-protectors*: are given before or at the time of irradiation to prevent or minimize radiation damage. Multiple events take place after exposure that could be normalized, or the body may be prepared to avoid the upcoming radiation insults by the intervention radio-protectors.
- *Mitigators*: are given at the time of radiation or after the irradiation, but before the manifestation of injury.
- *Therapeutics*: are the agents delivered after the development of radiation injury.

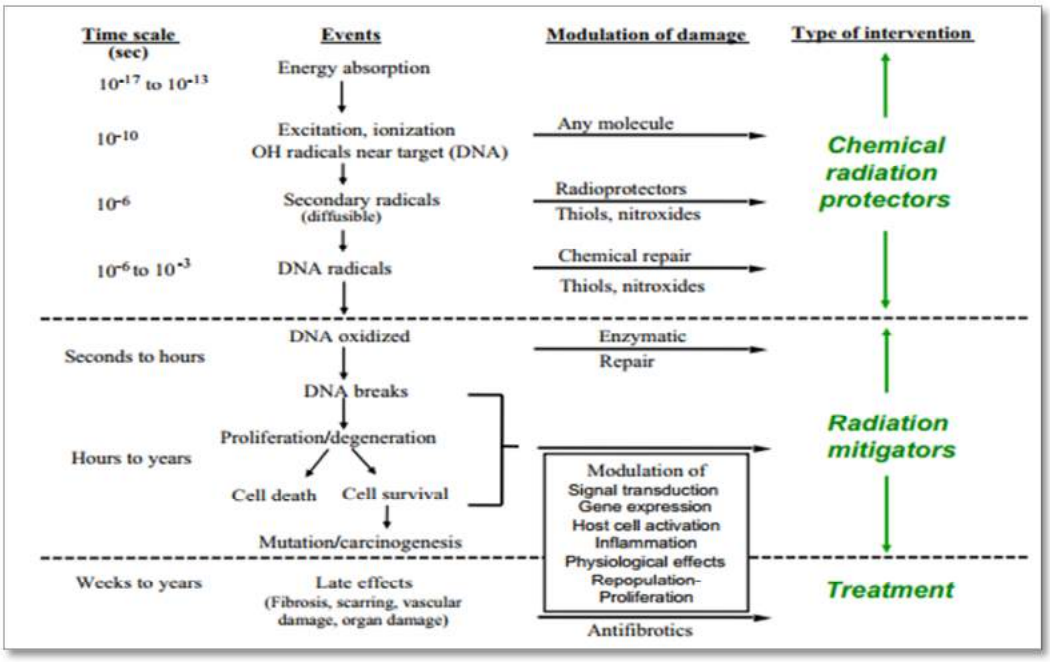

Source:(Citrin et al., 2010).

Figure 2.12: Series of events after radiation exposure and their modification by various damage modifying agents

2.9.1 Radio-protectors

Radio-protective agents may be any synthetic compound or natural extracts that reduce injuries caused by IR and must be taken before or at the time of irradiation for greater efficiency. The two major goals of developing radio-protectors are as follows:

- To overcome the detrimental effects on healthy tissues/ organs uncovered to radiation during radiotherapy
- To protect individuals from the acute effects of total body irradiation during nuclear accidents or occupational workers working in nuclear industries

Radio-protectors can act in the following ways: Free radical scavenging, up-regulation of the antioxidant defence system, hydrogen atom donation, metal chelation, repair stimulation, induction of hypoxia, modulation of signal transduction pathways involved in damage induction or they could be anti-inflammatory agents or growth factors (C. K. Nair et al., 2001).

An ideal radio-protective agent should justify the following criteria (Citrin et al., 2010; C. K. Nair et al., 2001):

i. It should be specific for healthy tissues, should not protect tumour tissue when used during radiotherapy.
ii. Must provide a broad spectrum of protection, i.e., protect multiple organs
iii. It should have a rapid mode of action
iv. Route of administration must be acceptable (first oral, or otherwise intramuscular)
v. It should not have self-toxicity and must have acceptable protective time-window.
vi. It must be stable within the system
vii. It must be compatible with other drugs administered to the patient (during cancer therapy)
viii. It should be safe if given at repeated doses
ix. It should be cost-effective and readily available

To develop an effective radio-protector, and further extrapolation to humans, it must be tested for protection to different species like rodents, canines and non-human primates. The routes of administration also obviously affect the mechanism of action and its toxicity.

Almost 70 years have passed since the radio-protective effects of cysteine, a sulfur-containing amino acid, against X- rays were first demonstrated by Patt and his co-workers in 1949 (Patt, Tyree, Straube, & Smith, 1949). Since then, several natural and chemical compounds, including analogues of cysteine and mercaptoethanolamine, have been screened for their radio-protective potential; however, their toxicity at optimum protective doses precluded their clinical use. Unfortunately, there is no radio-protector available to date that fulfils all of the abovementioned criteria. The development of Amifostine (WR-2721 or ethiofos; one of the 4000 compounds of the WR series) at the Walter Reed Army Institute of Research, during the anti-radiation Drug Development Program of the US Army in 1959, marked the arrival of the prototype radio-protective drug. Though it has been approved by the Food and Drug Administration (FDA) for clinical use, the US army has not approved it for use in military settings since it produced undesirable side effects, has poor bioavailability via the oral route and exhibits a narrow therapeutic window (Capizzi & Oster, 1995). Since then, numerous compounds from both synthetic and biological source have been tested for radioprotection globally in the last few decades (Table 2.2). Combined modalities have also been tested with some degree of success; for instance, prophylactic administration of phosphorothioates, with post-irradiation administration of immunomodulators has been reported to synergistically reduce radiation damage (Ruth Neta, 1988b).

Table 2.2: Different classes of radio-protectors

Sulphur containing compounds (Aminothiols)	N-acetylcysteine, glutathione, Thiourea, Amifostine
Antioxidants/ Free radical scavengers	Tempol, Vit A, C, E, Melatonin, SOD mimetics, Nitroxides, etc
DNA binding ligands	Hoechst, ellagic acid, WR- 1065
Hypoxia inducers	Carbon monoxide, ethanol, reserpine, histamine
Calcium antagonist	Dilitiazam
Chelating agents	EDTA, Defferoxiamine
Immunomodulators or anti- inflammatory agents	5-AED, misoprostol, prostaglandins
Cytokines	GM-CSF, IL-6, G-CSF, Flt-3 ligand, thrombopoeitin, EPO, interleukins
ACE inhibitors	Captopril, penicillamine
Metallothionins	Manganese chloride, Tungstate, Molybdate

Source: (Coleman et al., 2003; C. K. Nair et al., 2001; Varanda & Tavares, 1998)

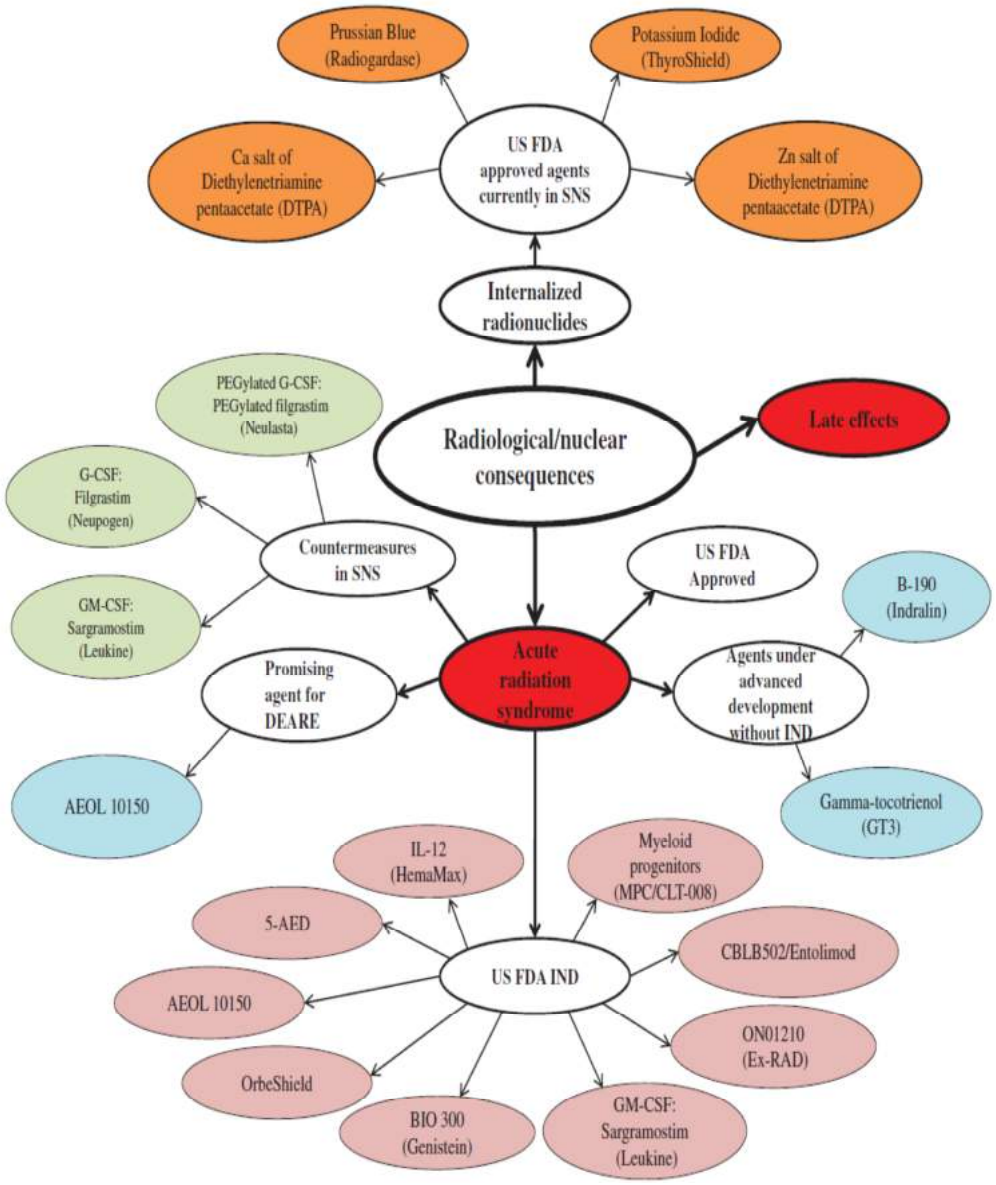

Source :(V. K. Singh & Seed, 2017)

Figure 2.13: Current status of radiation countermeasures for radiological and nuclear threats. Colour coding: red -acute and late-appearing injuries; light pink- medical countermeasure (MCM) under FDA investigation (IND status); baby blue - new countermeasures under development without IND status; burnt orange- FDA approved drugs for internalising radionuclides; light green- FDA approved drugs for ARS within nation. IND : investigational new drug, SNS : strategic national stockpile.

2.9.2 Cytokines in radioprotection

The cytokine system is a complex network with crosstalk between different pathways. A fascinating feature of this system is the reduction in the number of effectors from extracellular ligand binding to the localization in nucleus till transcription activation. At least around 100 different types of cytokines and growth factors are known, but limited receptors and surprisingly only fewer signalling molecules. Nearly 50 cytokines such as interleukins, interferons, and growth factors signals via hematopoietic growth factor receptor family, intracellular Janus kinases (Jak) and Seven Signal Transducer and Activators of Transcription (STAT) (Dörthe Schaue, Evelyn L. Kachikwu, 2012). This fact endures great significance for therapeutic inventions. The most extensively studied radio-protective cytokines are Interleukin-1 (IL-1), tumour necrosis factor-alpha (TNFα), granulocyte-colony stimulating factor (G-CSF), and granulocyte macrophage-CSF (GM- CSF) (Kalechman, Zuloff, Albeck, Strassmann, & Sredni, 1995). IL-1 and IL-6, are known to control cellular proliferation and differentiation. Earlier, Neta et al. showed the possible role of cytokines in radiation modulation (Ruth Neta, 1988a). Later, one more study from Neta et al. showed that injection of anti-IL-6 antibody to irradiated animals sensitized them to lethal irradiation and discussed the interaction of IL-6, IL-1 and TNF, and does not show any effects when given alone to mice (R Neta, Perlstein, Vogel, Ledney, & Abrams, 1992). However, a different study showed that subcutaneous injection of IL-6, 3–6 days after irradiation could exert radio-protective properties following sub lethal gamma irradiation (Patchen et al., 1991). There were some other studies as well, but none could clearly dissect the role of IL-6 in radioprotection and the underlying mechanism. Knowledge gained from previous studies of IL-6 mediated

radioprotection and its role in resistance to therapies, we aimed to test its radio-protective potential in normal scenario *in-vitro* and *in-vivo*.

2.9.3 Interleukin-6 (IL-6)

IL-6 is a glycosylated polypeptide of nearly 25 kDa, depending on the glycosylation and the species. It has a characteristic structure made up of four long α-helices arranged in an up–up–down–down topology (Scheller, Chalaris, Schmidt-Arras, & Rose-John, 2011). The primary structures of human and murine IL-6 consist of 184 and 187 amino acids, respectively, and shares 42% amino acid sequence similarity. IL-6 belongs to the class of hematopoietins; it has a characteristic structure made up of four long α-helices arranged in an up–up–down–down topology. It was first discovered as a B cell differentiation factor (BSF-2) which induces the maturation of B cells into antibody-producing cells (Simpson, Hammacher, Smith, Hews, & Ward, 1997).

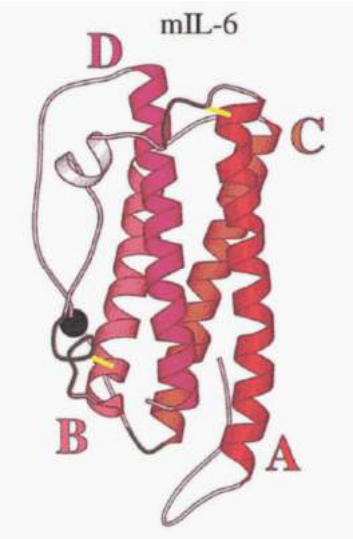

Figure 2.14: Helical structure of murine interleukin-6 made up of 4 alpha-helix, arranged in up-up-down-down topology.

Although human IL-6 (hIL-6) and mouse IL-6 (mIL-6) shares 42% sequence identity, hIL-6 is active in both human and murine cells; however, mIL-6 is only keen on

murine cell lines (Hammacher,' et al., 1994). It is a critical cytokine in immune regulation, plays a vital role in the maintenance of hepatocytes, haematopoietic progenitor cells, the skeleton, the placenta, the cardiovascular system, the endocrine and nervous systems. In the murine haematopoietic system, IL-6 induces the expansion of progenitor cells by stimulating cells from the resting stage to enter the G1 phase (Mihara, Hashizume, Yoshida, Suzuki, & Shiina, 2012). IL-6 also supports various physiological functions by acting as a hepatocyte stimulatory factor and by inducing the acute-phase protein synthesis. It is also known to stimulate osteoclast formation, cause bone resorption and is responsible for neural differentiation (Hirano et al., 1985). IL-6 supports the survival of cholinergic neurons, induces adrenocorticotropic hormone synthesis, and, in the placenta, causes the secretion of chorionic gonadotropin from trophoblasts (Mihara et al., 2012). IL-6 also plays a crucial role in metabolism. For example, in the absence of IL-6, mice develop glucose intolerance and insulin resistance, while IL-6−/− mice exhibit signs of liver inflammation (Kishimoto, Akira, Narazaki, & Taga, 1995).

2.9.3.1 IL6 expression and secretion

The common characteristic of many of the stimuli that activate IL-6 is that they are associated with tissue damage or stress (e.g., Ionizing radiation, UV, reactive oxygen species, viruses, microbial products and other pro-inflammatory cytokines). IL-6 production is predominantly regulated by changes in the gene expression of various transcription factors like NF-kB, CCAAT/enhancer-binding protein a (C/EBPa) and AP-1 (Activator Protein 1), the primary transcriptional regulator; although post-transcriptional mechanisms have also been identified (Akira & Kishimoto+, 1992).

Regulation of IL-6 expression by these transcription factors leads to the overexpression of this cytokine during inflammation.

The normal blood circulating level of IL-6 is nearly 1 pg/ml, but its increased levels are found in several conditions like acute hyperglycemia, after a high-fat meal, physical activity, and during/after surgery (Narbutt et al., 2008). Inconsistent levels of IL-6 have also been observed during pregnancy with median values of 129 pg/ml registered at delivery, decreasing to 58 pg/ml immediately afterwards (Keski-Nisula, Hirvonen, Roponen, Heinonen, & Pekkanen, 2004). Moreover, during sepsis, IL-6 levels may increase to very high in serum.

There are many physiological factors like diet, exercise, and stress which regulate the secretion of IL-6. It has been reported that exercise is an important stimulus for increased gene expression and production of IL-6 in skeletal muscle, and the majority of circulating IL-6 during exercise originates from contracting muscle, which can go as high as 100-fold of normal physiological level (Muñoz-Cánoves, Scheele, Pedersen, & Serrano, 2013). IL-6 produced in the working muscle during physical activity act as an energy sensor that activates AMP-activated kinase and enhances glucose uptake and metabolism, lipolysis and fat oxidation (Reihmane & Dela, 2014). IL-6 is also known to sensitize myotubes to insulin and enhances glucose uptake in muscles for high glycogen synthesis. Moreover, the reduced level of muscle glycogen also augments IL-6 production and secretion from muscle cells (Muñoz-Cánoves et al., 2013). In addition, to exercise, the expression of IL-6 increases in skeletal muscles under other conditions as well such as denervation of muscle and muscle dystrophy are other conditions, where up-regulated expression of muscle IL-6 has been noted

(Steensberg et al., 2001). The adipose tissue produces nearly 30% of circulating systemic IL-6, where it is closely associated with obesity, impaired glucose tolerance and insulin resistance (Bastard et al., 2002). Plasma IL-6 concentration is a predictor of the development of type 2 diabetes, and peripheral administration of IL-6 results in insulin resistance in rodents and humans by causing hyperlipidemia, and hyperglycemia (Bastard et al., 2002). Besides muscle cells, the cells of the immune system, e.g., macrophages, mast cells, dendritic cells, B cells, CD4 effector T helper (Th) cells are major sources of IL-6 production (Tanaka, Narazaki, & Kishimoto, 2014) (Fig; 2.15). In addition, IL-6 is also secreted by a variety of non-leukocytes cells such as fibroblasts, endothelial cells, epithelial cells, astrocytes and several malignant cells. During an inflammatory response, IL-6 is highly expressed, and circulating levels of this cytokine can rise dramatically from pg/ml range to several μg/ml in certain extreme cases (Tanaka, Narazaki, & Kishimoto, 2016). Enhanced levels of IL-6 have been found in many cancers, with an inverse relationship between IL- 6 level and response to chemotherapy and hormone therapy (Nolen et al., 2008). Further, the expression of IL-6 is known to be regulated epigenetically in breast cancer, hepatocellular carcinoma, colon cancer, prostate cancer and lung cancer through miRNAs (Lin28 and Let-7)(Iliopoulos, Hirsch, & Struhl, 2009). Moreover, IL-6 expression has been found to be higher in the recurrent tumours as compared to the primary tumours, as well as in the recurrent metastatic lesion as compared to the primary metastasis (Guo, Xu, Lu, Duan, & Zhang, 2012). The primary sources of IL-6 in the tumour microenvironment are tumour cells as well as tumour associated macrophages (TAMs), $CD4^+$ T cells, myeloid-derived suppressor cells MDSC, and fibroblasts. Basically, tumour cells produce IL-6 for promoting their survival and

progression and do not depend on the paracrine release of IL-6 by stromal cells. However, both autocrine and paracrine mechanisms of IL-6 are known to influence tumour progression and metastasis through IL-6 trans-signalling (Kumari et al., 2016).

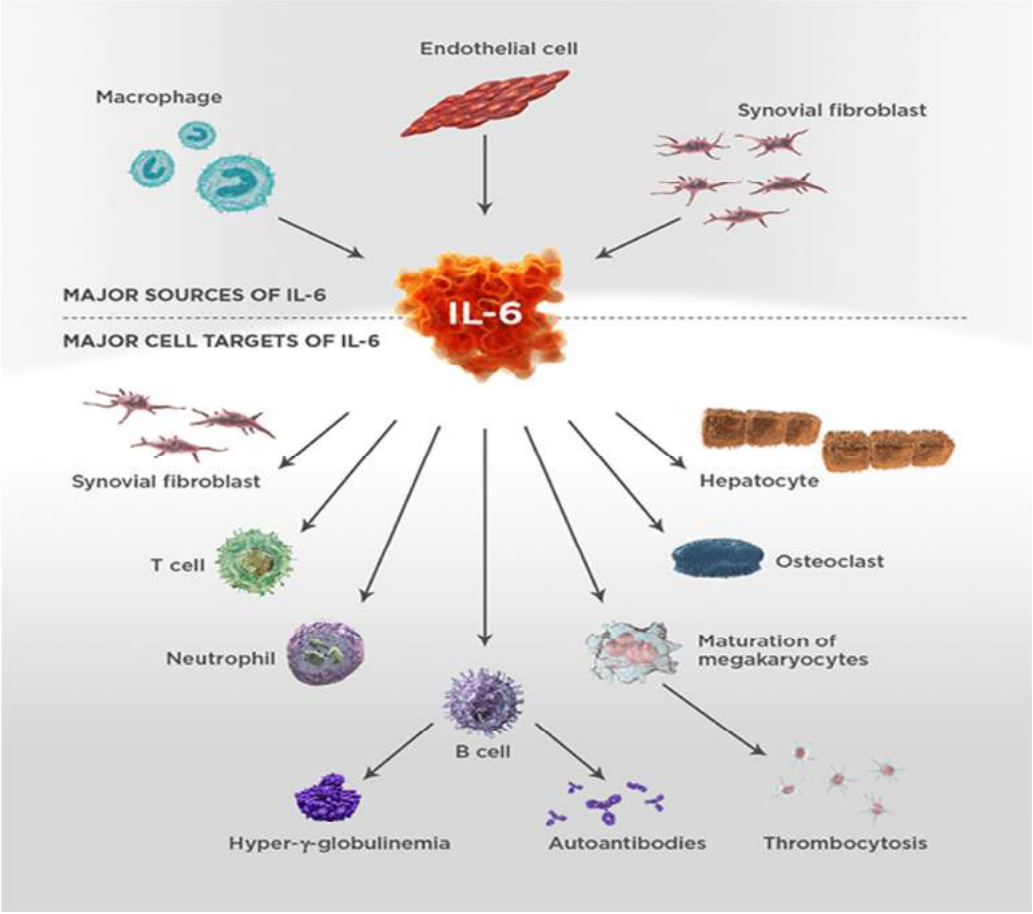

Figure 2.15: Major sources of IL-6 production and its target cells

2.9.3.2 IL-6 Signalling

The secretion and availability of IL-6 are ubiquitous, and it can bind to various types of cells in different tissues. IL-6 binding on different cell types may differ and result in two different types of IL-6-dependent cell signalling (Fig;2.16). IL-6 binds to the IL-6

receptor (IL-6R) on the plasma membrane, and the resultant IL-6/IL-6R complex associates with gp130 and causes gp130 homodimerization to form an activated IL-6 receptor complex, which is a hexameric structure consisting of two molecules each of IL-6, IL-6R and gp130. IL-6 triggers signal transduction via two forms of IL-6R: one a transmembrane 80-kDa receptor with a short cytoplasmic domain (mbIL-6R, also known as IL-6Rα, gp80or CD126) and the other a small, extracellular, secretory soluble receptor (sIL-6R) (Jones, Scheller, & Rose-John, 2011). Classical IL-6 signalling, which is the predominant form of IL-6 signalling, requires membrane-bound IL-6R (mbIL-6R) and is restricted to hepatocytes, some epithelial cells and certain leukocytes (Fig;2.16). IL-6R contains a very short cytosolic domain that lacks the major potential motifs for transduction of intracellular cell signalling. However, gp130 (also known as IL-6Rβ or CD130) in the same hexameric complex is rich in all these potential motifs required for intracellular signallings, such as SHP-2 domain and YXXQ motif for JAK/STAT signalling. Upon binding with IL-6/IL-6R, the dimerization of gp130 leads to the activation of associated cytoplasmic tyrosine kinases, resulting in the phosphorylation of various transcription factors (Hirano et al., 1985). gp130 is expressed in almost all organs, including the brain, heart, lung, liver, kidney, spleen and placenta, where it plays an indispensable role in their development, cell survival, growth and tissue homeostasis (Chalaris, Garbers, Rabe, Rose-John, & Scheller, 2011). gp130 is a common signal-transducing receptor and is also used by other members of the IL-6 family cytokines, such as IL-11, IL-12, IL-27, leukaemia inhibitory factor, oncostatin M, etc. Although the expression of transmembrane IL-6R is limited to the hepatocytes and subsets of leukocytes, gp130 is expressed ubiquitously. Therefore, the IL-6/sIL-6R complex can transduce the IL-6 signal in various cells, which do not express transmembrane IL-6R but express gp130, through a trans-signalling mechanism. sIL-6R is generated by alternative

splicing of IL-6R mRNA or by limited proteolysis of mbIL-6R by Zn dependent metalloproteinase (ADAM10 and ADAM17, a disintegrin and metalloproteinases 10 and 17 (Fig;2.16). sIL-6R is devoid of the cytoplasmic and transmembrane domains and binds to IL-6 with comparable affinity as the membrane-bound form, thereby mediating gp130 activation in an autocrine or paracrine manner (Scheller et al., 2011). Consequently, by binding to sIL-6R, IL-6 increases its reach to a wide variety of cells. There is enough evidence to suggest that neural cell, neural stem cells, haematopoietic stem cells, liver progenitor cells and embryonic stem cells depend on sIL-6R in their response to IL-6.

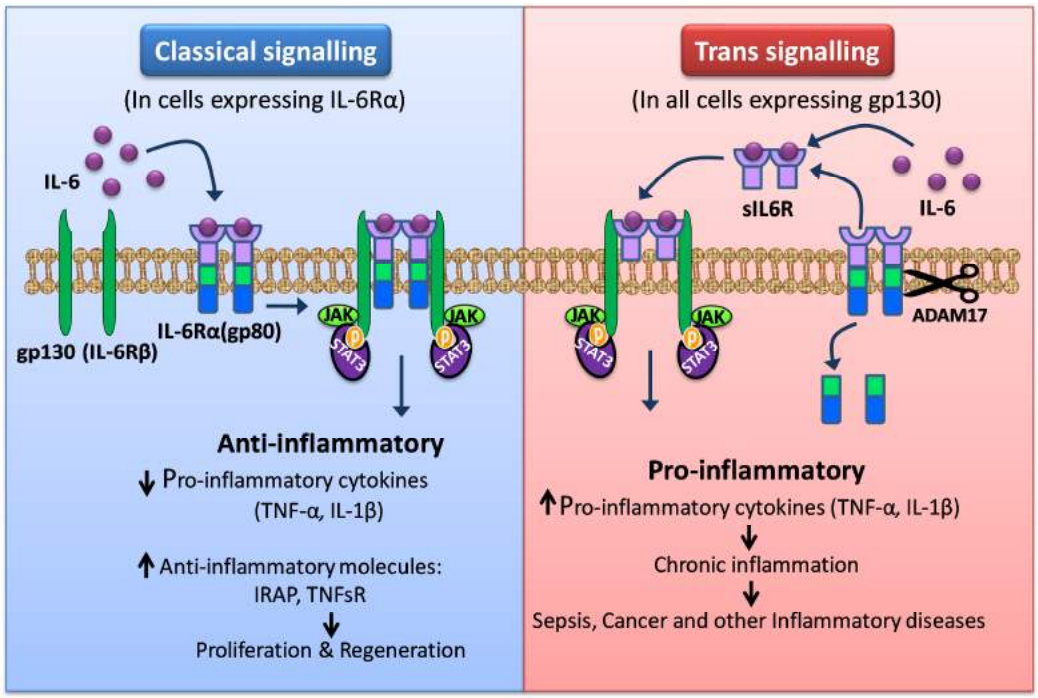

Figure 2.16: Classical and trans-signalling of IL-6. In classical signalling, IL-6 binds to the membrane-bound receptor mbIL-6Rα, which then forms a complex with the ubiquitously present cell receptor gp130 (IL-6Rβ). Trans signalling can occur in any cell expressing gp130.

2.9.3.3 Pleiotropic role of IL-6

Cytokines are important soluble factors that regulate cellular and systemic communication during inflammatory and immune responses. Different cytokines play a

different role in the onset and resolution of inflammation. However, the ubiquitous and functionally diverse cytokine, IL-6 is a pleiotropic cytokine with pro- and anti-inflammatory properties (Fig;2.16). It is an important cytokine regulating acute-phase response of inflammation. During inflammatory response, TNFα induces the expression of IL-6 together with other inflammatory alarm cytokines like IL-1β, which are involved in the elicitation of acute-phase inflammatory reactions/response (Fig;2.16) (Tanaka et al., 2014). Further, the IL-6 controls the level of acute inflammatory responses by downregulating the expression of pro-inflammatory cytokines and up-regulating anti-inflammatory molecules including IL-1 receptor antagonist protein (IRAP), TNF soluble receptor (TNFsR), and extra-hepatic protease inhibitors (Fig; 2.16). IL-6 has also been found to counter inflammation by inhibiting TNF*α* release in experimental endotoxemia (Schulte, Bernhagen, & Bucala, 2013). Moreover, IL-6 is involved in the development of specific cellular and humoral immune responses, including B cell differentiation, immunoglobulin secretion and T cell activation (Sebina et al., 2017). This pleiotropic nature of IL-6 maintains the host homeostasis.

In chronic inflammatory diseases, like collagen-induced arthritis (similar to rheumatoid arthritis), experimental autoimmune encephalomyelitis in rodents, and murine colitis, IL-6 acts as a pro-inflammatory molecule while, in acute inflammation, it exhibits an anti-inflammatory profile (Gabay, 2006). During the switch between pro- and anti-inflammatory roles, IL-6 signal transduction is controlled by SOCS3 (the suppressor of cytokine signalling) (Croker et al., 2003). TNFα and IL-1β negatively regulate IL-6 signalling at different levels, by enhancing the IL-6 induced expression of the SOCS3 (feedback inhibitor) and/or targeting IL-6 induced gene expression via its action on target gene promoters (Bode et al., 1999).

IL-1β also counteracts IL-6 mediated STAT-3 activation independent of SOCS3 expression (Ahmed, Mayer, Ji, & Ivashkiv, 2002). IL-1β is the major regulator of pro and anti-inflammatory nature of IL-6; on the one hand, it reduces the pro-inflammatory activity of IL-6 that results in the inhibition of overshooting immunological reactivity, like in inflammatory bowel disease or autoimmune arthritis. On the other hand, it delays the anti-inflammatory effects of IL-6 to reinforce the pro-inflammatory processes in the initial phase of inflammation (Radtke et al., 2010).

Emerging evidence suggest that IL-6 plays key roles in acute as well as transition (resolution) phase of inflammation (Xing et al., 1998). Recruitment of neutrophils activates IL-6 trans-signalling in local tissues, which suppresses neutrophil attracting chemokines and simultaneously enhances monocyte attracting chemokines, causing a switch from neutrophil to monocyte recruitment (Kaplanski, Marin, Montero-Julian, Mantovani, & Farnarier, 2003). Besides recruiting the monocytes for the clearance of neutrophil, IL-6 also induces apoptosis in neutrophils, supporting the notion that IL-6 controls acute inflammation (Romano et al., 1997). Further, IL-6 trans-signalling recruits the T cells at the site of inflammation by triggering the expression of T-cell attracting chemokines (CCL4, CCL5, CCL17, and CXCL10) (McLoughlin et al., 2005). Moreover, IL-6 also rescue T cells from entering apoptosis by STAT-3-dependent upregulation of anti-apoptotic regulators (Bcl-2, Bcl-xL) and modulation of Fas surface expression (Curnow et al., 2004).

Further, IL-6 regulates the differentiation of recruited T cells towards TH2 by inducing the expression of IL-4. Thus, IL-6 regulates some of the key steps in controlling the inflammation and sets the anti-inflammatory environment by promoting TH2 response

(Krishnamoorthy, oriss, Paglia, Ray, & Ray, 2007). Collectively, these evidence suggest that endogenous IL-6 play the vital anti-inflammatory role in both local and systemic acute inflammatory responses by controlling the level of pro-inflammatory cytokines, mainly. Interestingly, these anti-inflammatory activities lead by IL-6 cannot be recompensed by IL-10 or other members of the IL-6 cytokine family. The trans-signalling of IL-6 regulates mainly the pro-inflammatory response; however, IL-6 classical signalling imparts its anti-inflammatory or regenerative activity (Fig; 2.16) like inhibition of apoptosis and regeneration of cells of the intestinal epithelium and the initiation of the hepatic acute phase response.

2.9.3.4 Cytoprotective nature of IL-6

Earlier, IL-6 was solely known as a pro-inflammatory cytokine but now recognized as a multifunctional cytokine, basically pleiotropic, can elicit both pro- and anti-inflammatory reactions in a context-dependent manner. There is innumerable evidence which suggests that inflammatory signals from the tumour cells and surrounding microenvironment facilitate the tumour growth. Many cytokines are alleged to play an important role in therapeutic resistance and lead to tumour progression, invasion, and angiogenesis. Among these, IL-6 is known to contribute to poor therapeutic gain, tumour relapse and aggressive tumour growth. Tumour cells express and produce IL-6 as a protective mechanism against drug and radiation-induced death. Therefore, like the link between cancer and inflammation, a strong link exists between IL-6 and cancer. Majority of the phenotypes or hallmarks of cancer which are influenced by IL-6 comprise of many biological capabilities that are acquired during tumour development. Over-expression of IL-6 in many types of tumours like colorectal cancer, prostate cancer, breast cancer, ovarian carcinoma, pancreatic cancer, lung cancer, renal cell carcinoma, cervical cancer, multiple

myeloma and lymphomas established a strong link between IL-6 and cancer. IL-6 regulates nearly all hallmarks of cancer like inhibition of apoptosis, promotion of survival, proliferation, angiogenesis, invasiveness and metastasis and known to regulate cancer cell metabolism. Therefore, inhibiting IL-6 signalling or minimizing the level of IL-6, can be a potential therapeutic strategy for those cancers, which are characterized by pathological IL-6 overproduction. Cancer cells evolve a variety of cytoprotective approaches to limit or circumvent cell death programmes, mainly apoptosis. Besides evading growth suppression signalling, by loss ofTP53 function, tumours are also associated with an increase in the expression of anti-apoptotic regulators (Bcl-2, Bcl-xL and Mcl-1) and survival signals (Igf1/2) or down-regulated pro-apoptotic factors (Bax, Bim and Puma)(Borhani et al., 2014; Zhuang et al., 2007). In tumours, IL-6regulates the process of apoptosis by activating STAT-3 and NF-kB signalling, which transactivates the expression of many anti-apoptotic proteins such as Bcl-2, Bcl-xL, Mcl-1 (Wei et al., 2001). Besides this, IL-6-induced Bcl-2 regulates Bak interactions with mitofusins via inhibition of Bak dissociation from Mfn2 and also inhibits the interaction of Bak with Mfn1. These two mitochondrial events are the significant determinants of cell death pathways as they prevent mitochondrial fragmentation during apoptosis. Therefore, Bcl-2 appears to be an essential mediator of IL-6-induced cytoprotection (Waxman & Kolliputi, 2009). Besides Bcl-2 and Bcl-xL, IL-6 also supports tumour cell survival by inducing the expression of survivin through direct binding of STAT-3 to the survivin promoter (Gritsko et al., 2006). Collectively, it appears that IL-6 facilitates tumour growth primarily by inhibiting apoptosis and enhancing cell proliferation.

Interleukin-6 not only protects tumour cells but also showed a similar impact on healthy cells. The protective effects of IL-6 in infections were portrayed nearly three decades ago.

Leaving behind some controversial interpretations such as; it is still questionable whether in sepsis IL-6 signifies an inflammatory marker or a moderator of immune defence mechanism. Despite conflicting results, in neonatal mouse, IL-6 reduces TNF alpha secretion and expression of TNF receptor in macrophages to salvage streptococcal infection (Fisman & Tenenbaum, 2010). Moreover, exogenous administration of IL-6 enhanced survival and inhibiting IL-6 signalling ensured a high rate of mortality (Fisman & Tenenbaum, 2010). IL-6 pre-injection protects the mice severely infected with an intracellular pathogen, Listeria monocytogenes, in a dose-dependent fashion and lessen bacterial colonies in the liver and spleen. IL-6 has a significant role in priming the immune response against infection (Liu, Simpson, & Cheers, 1992).

The second physiological aspect of IL-6 is that it functions like **myokine** (Fig; 2.17). IL-6 signalling is found to be linked with several benefits like improved blood flow, reduced chronic inflammation, increased lipid metabolism, and regeneration of peripheral nerve fibres. During exercise, IL-6 is synthesized and secreted by skeletal muscle resulted in a rise in plasma IL-6 levels simultaneously with the increase in intensity and duration of the exercise. The expansion of IL-6 levels in response to physical activity boost up the insulin-stimulated glucose removal in the body (Reihmane & Dela, 2014). Exercise-induced IL-6 secretion improves insulin sensitivity. At the time of exercise, IL-6 is possibly the most prominent myokine having cardioprotective potential and also associated with triggering of ischemic preconditioning (McGinnis et al., 2015). The delayed phase of ischemic preconditioning increases the tolerance of myocardium to a later ischemic insult at 24–72 hours. A study conducted on Diabetic Peripheral Neuropathy (DPN) suggested that a low dose IL-6 delivered in a fraction which mimics the body's natural self-

response to exercise proved as an effective cure for protection and refurbishment of normal functions of peripheral nerve in DPN (Cox et al., 2017).

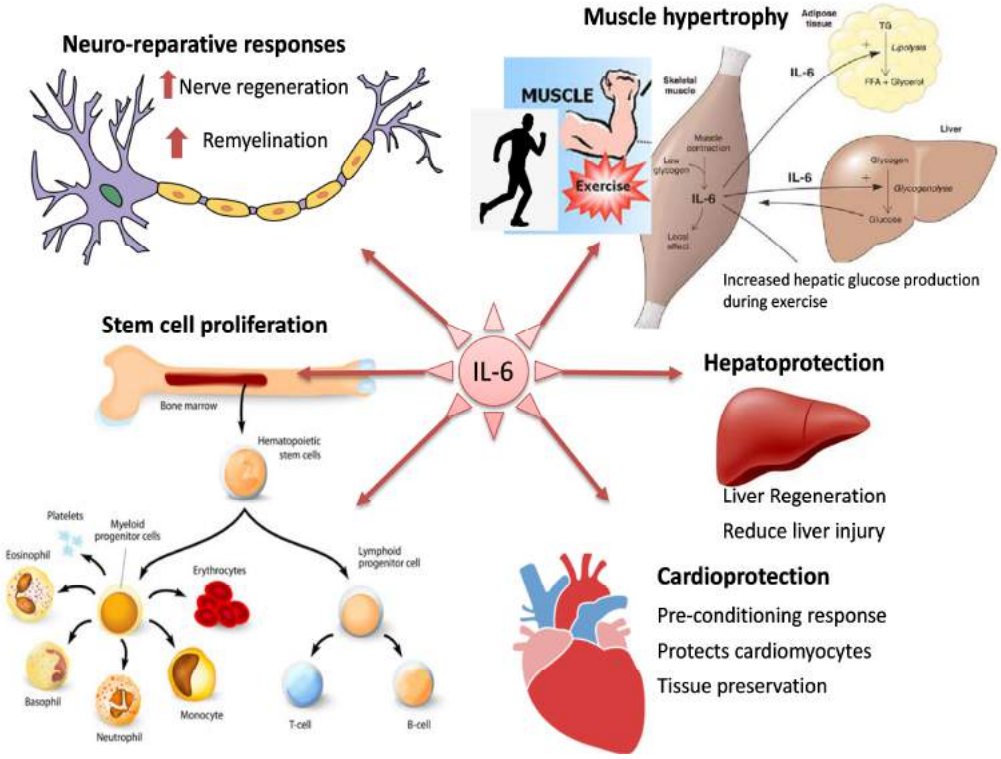

Figure 2.17: Biological effects of IL-6. IL-6 has a widespread reach to multiple organs where it mainly stimulates cell proliferation and regeneration.

Studies on IL-6 mediated cardioprotection have done both *in-vivo* and *in-vitro*. IL-6 induced preconditioning signalling via the Janus kinase and signal transducer and activator of transcription (JAK/ STAT) pathway, which reduces necrosis after 30 minutes of regional ischemia. These effects were abolished in IL-6-/-mice. IL-6 stimulates those signalling pathways that could delay the ischemic preconditioning. IL-6 protects cardiomyocytes by inducing PI 3-kinase which is involved in alterations of mitochondrial Ca^{2+} and inhibits reperfusion mediated mitochondrial depolarization, loss of mitochondrial structure and function, and leads to Ca^{2+} accumulation in mitochondria (Smart et al., 2006).

The directed disruption of the IL-6 receptor, specifically, gp130 in developing embryos displayed hypoplastic ventricular myocardium, decrease number of pluripotent cells, hematopoietic progenitors, blood loss and some other complications. This study revealed the vital role of gp130 in myocardial expansion and hematopoiesis throughout embryogenesis (Yoshida et al., 1996). IL-6 defends against hyperoxic and oxidative injuries (which are similar to IR injuries) both *in-vivo* and *in-vitro.* IL-6 preconditioning also prevents H_2O_2-induced oxidative injuries to cardiomyocytes through activation of STAT-3 pathway (Jia et al., 2012). Thus, IL-6/JAK/STAT-3 appears to be the primary pathway through which IL-6 regulates the majority of functions.

All these studies suggest that IL-6 can protect the cells from following deleterious factors, oxidative stress, disturbed Ca^{2+} homeostasis, altered mitochondrial metabolism and DNA damage, which are also caused by ionizing radiation. Therefore, we hypothesized that IL-6 may protect the cells from radiation-induced cell death and may be developed as a potential radio-protector.

Aim and Objectives of the study

In light of the above rationale, the thesis is aimed at evaluating the **Role of Interleukin-6 in cellular and systemic responses to ionizing radiation**. The objectives designed to achieve the above-mentioned aim are as follows**:**

1. To study the cytoprotective potential of IL-6 against ionizing radiation using *in-vitro* models.
2. To investigate the role of IL-6 in cellular responses to radiation-induced DNA damage
3. Evaluation of radio-protective efficacy of IL-6 in *in-vivo* (mice) models.

Chapter 3
Material and Method

CHAPTER 3
MATERIAL AND METHODS

3.1 Materials Required

Introduction

3.1.1 Cell lines

In vitro studies were carried out in multiple cell lines RAW264.7 (murine monocytic), INT407 (Human Intestinal epithelial cells), IEC-6 (Mouse intestinal epithelial cell), NIH-3T3 (murine embryonic fibroblast), HEK293 (human embryonic kidney cell). All the cell lines were purchased from the National Centre for Cell Science (NCCS), Pune, India.

3.1.2 Chemicals and Bio-chemicals

3.1.2.1 Drugs and Inhibitors

Mouse recombinant IL-6 was bought from Biolegend (San Diego, USA). JSI124 and MK2206 were procured from Sigma (Saint Louis, MO, USA) and Selleckchem (Texas, USA) respectively.

3.1.2.2 Cell culture reagents

High glucose DMEM (Dulbecco's Modified Eagle's Medium), Streptomycin, Penicillin, Nystatin, Trypsin, HEPES were procured from Sigma- Aldrich, USA. Hank's Balanced Salt Solution (HBSS) were procured from HiMedia, India. Fetal Bovine Serum (FBS) was procured from Gibco/BRL, MD, USA.

3.1.2.3 General Chemicals and Bio-chemicals

All the chemicals and bio-chemicals were of either analytical grade or molecular biological grade. Phosphate-buffered saline (PBS), propidium Iodide (PI), Citric Acid, Tween-20, 4, 6 diamidino 2-phenyl indole (DAPI), Methanol, Xylene, Glycerol, Ethanol,

Monobasic Potassium phosphate (KH_2PO4), Dibasic Potassium phosphate (K_2HPO4), Sodium phosphate dibasic (Na_2HPO4), Sodium phosphate monobasic (NaH_2PO4), Glacial acetic Acid (GAA), sodium bicarbonate, Sodium chloride, Potassium chloride were obtained from HiMedia chemicals. Dichlorodihydrofluorescein diacetate (H_2DCFH-DA), Low melting point (LMP) agarose, Ponceau S, PMSF, Protease inhibitor cocktail, bovine serum albumin (BSA), 2- mercaptoethanol, Ammonium persulfate, Hydrochloric acid, Trichloroacetic acid (TCA), glutathione, Thiobarbituric acid (TBA), TEMED, DPX mountant, Acetone, Bromophenol Blue, Sodium Dodecyl Sulphate (SDS), S-Lauryl Sodium Sarcosinate (SLS), Ethylene di-amine tetra acetic acid (EDTA), Na_2EDTA, 3- (4, 5-dimethylthiazol-2-yl)- 2,5-diphenyl tetrazolium bromide (MTT), Tris Base, Paraformadehyde (PFA), Bovine serum albumin (BSA), Ribonuclease-A (RNase-A), Collagenase Type IV were procured from Sigma-Aldrich, USA.

3.1.2.4 Antibodies

Antibodies against pSTAT-3, STAT-3, Bcl-2, Bax, cleaved caspase 3, PARP, pAkt, Akt, γ- H2AX, ATM, NBS1, RAD51, VDAC, and β-actin were procured from Cell Signalling Technology, USA. FITC conjugated anti-rabbit and mouse secondary antibody were purchased from Sigma-Aldrich, USA. Survivin, cyclin D, PKM2, GLUT-4, HK-2, HK-1 and HRP conjugated secondary antibodies were acquired from Santa Cruz Biotechnology, CA.

3.1.2.5 Biochemical and Molecular Biology Kits

Bicinchoninic acid (BCA) kit, Annexin V-Alexa flour Apoptosis Detection Kit, In Situ Cell Death Detection Kit, were purchased from Sigma-Aldrich, Saint Louis, MO, USA. IHC kit was purchased from Abcam, MA, USA. SOD assay kit and Total antioxidant assay kit were procured from Cell Biolabs, San Diego, USA. IL-6 ELISA

kit was bought from Affymetrix Biosciences. All DNA and RNA isolation kits were obtained from Qiagen, Germany. cDNA synthesis kit and Sybr green were purchased from Fermetas and Bio-Rad, USA, respectively.

3.1.3 Glassware and Plasticware

Tissue culture flasks, cell culture dishes, 96- well plates, scrapers and serological pipettes were obtained from Corning (USA) and BD Falcon (USA). The 0.22μm PVDF membrane, syringe filters and media filter membrane were obtained from MDI Membrane Technologies, India.

Table 3.1: Composition of various reagents/buffers used in the study

Buffer	**Composition**
Radioimmunoprecipitation assay (RIPA) Buffer for cell lysis	150mM sodium chloride, 1.0 % Triton X-100, 0.5 % (w/v) sodium deoxycholate, 0.1 % SDS (w/v), 50mM Tris HCl (pH 8.0), 1mM PMSF, 5mM sodium orthovanadate and protease inhibitor cocktail (1μL/100μL of RIPA buffer)
Laemmli buffer (2X)	0.125M Tris HCl (pH 6.8), 10% (v/v) 2-mercaptoethanol, 4% (w/v) SDS, 20% (v/v) glycerol and 0.004% (w/v) bromophenol blue
SDS- PAGE running buffer (1X)	25mM Tris base, 250 mM glycine (electrophoresis grade), 0.1% SDS
Transfer Buffer (1X)	25mM Tris base; 192mM Glycine; Methanol 20 %
10 % neutral buffered formalin	10% (w/v) formaldehyde in 1X PBS.
4 % PFA (fixative)	4% paraformaldehyde (w/v) in 1X PBS
Ponceau- S staining solution	0.1% Ponceau S in 5% GAA
PBST	0.1% Tween-20 in PBS
TBST	20mM Tris,150mM NaCl, 0.2% Tween-20
Blocking Buffer	5 % (w/v) dry non- fat milk or 5% (w/v) BSA in 1X PBST
10X Red Blood Cell (RBC) lysis buffer	8.02g Ammonium chloride, 0.84g Sodium bicarbonate, 0.37g Disodium EDTA, 100ml milli-Q water
Bouin's fixative	Saturated aqueous picric acid: 37-40% formaldehyde: GAA in 15:5:1 (v/v/v) ratio
Lysis buffer for Comet assay	2.5% SDS, 1% N- laurylsarcosine and 25mM EDTA, pH 9.5
Electrophoresis buffer for Comet assay	90mM Tris base, 90mM boric acid, 2.5mM disodium EDTA, pH 8.4

3.2 Methods

3.2.1 Sterilization

Sterilization of all the glass-wares and plastic-wares, wherever required, was performed by autoclaving at the pressure of 15lbs, 121^{o}C for 20min. Culture medium, heat-labile solutions and buffers were sterilized by filter sterilization wherever needed. Other buffers and solutions were sterilized by autoclaving.

3.2.2 Maintenance of cell lines

All the cell lines were maintained as monolayers at 37^{o}C in a humidified incubator with 5% CO_2 in 60mm Petri dishes. NIH- 3T3, IEC-6, INT407 and HEK293 cells were grown in high glucose (4.5g/ litre) DMEM supplemented with 10% FBS and RAW264.7 cells were maintained in high glucose DMEM supplemented with 10% heat-inactivated FBS. The growth media contained HEPES (10mM) as the buffering agent and antibiotics (Penicillin 50 IU/ml, Streptomycin 35µg/ml, and Nystatin 2.5 µg/ml). Cells were cultured routinely to maintain them in the exponential growth phase using either scraping for RAW264.7 cells or trypsinization with 0.05% trypsin solution (Himedia) for NIH-3T3, IEC-6, HEK293, and INT407. Cells growing in exponential growth phase were used for all experiments.

3.2.3 Drug treatment and irradiation

Monolayer cells were grown at varying densities (depending upon the assay) in 35mm/60mm Petri-dishes or 96-well plates for 24 hrs before treatment to ensure attachment. Lyophilized IL-6 was dissolved in autoclaved filtered milli-Q water to prepare stock solutions and then aliquoted as minimal volume to avoid repeated

freeze-thaw. A working concentration was ready at the time of the experiment by diluting the aliquoted stock in culture medium and added to the final volume in respective dishes. After 2 hrs of incubation with the IL-6, cells were gamma-irradiated using ^{60}Cobalt-Teletherapy Unit (Bhabhatron-II, Panacea Medical Technologies, Bangalore, India) at a source to sample distance of 80cm and a field size of 35x35cm^2. The dose rate during the entire course was kept 1 Gy/min. All the radiation treatments were done at room temperature. Cells were further incubated for studying different cellular responses at different time intervals.

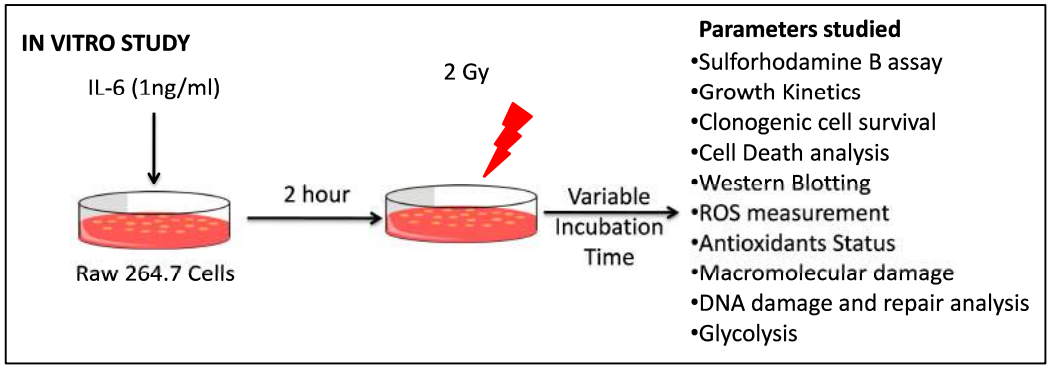

Figure 3.1: Experimental layout for *in vitro* studies. Cells treated with IL-6 before irradiation, and multiple parameters were studied.

3.2.4 Sulforhodamine B assay

The SRB assay is used to determine the cell density by measuring the cellular protein content. This assay is well established for cytotoxicity screening of any compound in adherent cells (Vichai & Kirtikara, 2006). For this assay, cells were seeded (3000/well) in 96-well plate a day before treatment. Next day cells were irradiated after treating with IL-6 for 2 hrs. After irradiation cells were incubated in CO_2 incubator till further time points. At particular time point cell monolayers were fixed with 10% (w/v) Trichloroacetic acid (TCA) followed by staining with 100µl of SRB (0.057% w/v) for 30 min. Thereafter, the excess stain was removed by multiple

washings with 1% (w/v) Acetic acid. Next, the dye bound to protein is dissolved in 10mM Tris-base solution on a shaker. OD read at 510nm wavelength on the micro-plate reader (Biotek Instruments, USA).

3.2.5 Clonogenic Cell Survival

The clonogenic cell survival assay utilizes the reproductive potential of a cell to divide indefinitely and forms colonies and is a gold-standard method for assessing the survival of cells following irradiation. A varying number of exponentially growing cells (100-3200, varied for different radiation doses and cell lines) were seeded in triplicates in 60mm Petri dishes 18-24hrs before any treatments, to facilitate the attachment of cells. After completion of treatment, cells were allowed to grow at 37°C in CO_2 (5%) incubator for 7-14 days (varied for cell lines). Colonies having at least 50 cells (5 to 6 doublings) were recorded as survivors. After the appearance of colonies, washed once with PBS to remove media, followed by fixation and staining with 1% crystal violet dye (dissolved in 7% methanol in PBS). Plating efficiency was calculated as:

PE = (Number of colonies counted / Number of cells plated) X 100

The Surviving Fraction (S.F.) was calculated as:

$SF = PE_T / PE_C$

Where PE_T is the plating efficiency of the treated group and PE_C is the value of the control group.

3.2.6 Cell proliferation/Growth Kinetics/Cell number

Healthy and growing cells were seeded with a density of 75000 to 100000 cells/Petri plate depending upon the cell line and allowed to grow for 24hrs. After IL-6 and radiation treatment cells were kept at 37°C in 5% CO_2 incubator for doublings for

different time (0-72hrs). Cells were harvested every 24 hrs by scraping, or trypsinization and the viable cells were counted using a Neubauer's improved counting chamber (Paul Marienfeld GmbH & Co. KG, Germany) under 10X objective, and 10X eyepiece magnification with a compound light microscope (Olympus CH30, Japan). The number of viable cells was calculated as follows:

Viable cells =Average cell count X Volume of cell suspension X Dilution factor

3.2.7 Analysis of cell proliferation using CFSE dye

Cell proliferation assay was executed using CFSE (Carboxyfluorescein succinimidyl ester) dye (Sigma), according to manufacturer's protocol. Cells were incubated with CFSE (5μM) in incomplete growth medium supplemented with 2% serum for 20 minutes at room temperature with constant rolling. Next, the unbound dye was washed off with respective complete growth medium two times and seeded in fresh medium with the density of $0.25X10^6$ and kept at 37°C in CO_2 incubator. After overnight incubation, cells were treated with IL-6 and radiation and incubated until further time points. Cells were terminated at 48 hrs post-treatment, and fluorescence was measured using flow cytometry (FACSAria III cell sorter, Becton Dickinson, USA).

3.2.8 Cell cycle distribution

Exponentially growing cells were seeded at a density of 6000 to 8000 cells/cm^2 and grown overnight. Following treatment, cells were incubated for varying intervals of time (0-48hrs). Both floating and attached cells were harvested at particular time intervals by scraping and fixed in chilled 80% ethanol (in PBS). The ethanol fixed cells were stained with the intercalating DNA fluorochrome, Propidium Iodide as

described by Zolzer et al. (Zölzer, Speer, Pelzer, & Streffer, 1995). Accordingly, 0.5 million cells were fixed in ethanol, washed with PBS to remove ethanol and incubated with RNase-A (200 µg/ml) for 30 minutes at 37^{o}C. Next, the cells were stained with PI (50 µg/ml) in PBS for 10 minutes. Measurements were made on a flow cytometer (FACSAria III cell sorter, Becton Dickinson, USA) using 488nm laser and analyzed using FACSDiva software (Version 3.0.1, Becton Dickinson, USA)

3.2.9 Cell Death analysis by Acridine orange ethidium bromide staining

RAW 264.7 cells were seeded in 96-well plates and stained with acridine orange-ethidium bromide according to Deborah Ribble protocol (Deborah Ribble, Nathaniel B Goldstein & Shellman, 2005) with minimal modifications. Briefly, the cultured cells in 96-well plates were centrifuged at indicated time points and incubated in 1:1 Acridine Orange and EtBr (Sigma-Aldrich) solution (10µg/ml each) at room temperature for 5-10 minutes. Images were captured under a fluorescence microscope using 10X objective, and 10X eyepiece magnification with a fluorescence microscope (Olympus IX51 Fluorescence Microscope, Japan).

3.2.10 Caspase-3/7 activity assay

Activation of caspases was assessed by Cell Event™ Caspase-3/7 (5 µM) activity probe (Invitrogen,) following manufacturer's protocol, briefly cells grown in 96-well plates followed by all the treatments, was replaced with a fluorescent probe and incubated for 30min. After washing with PBS, fluorescent cells were captured under a fluorescence microscope at 10x10 magnification. The stained cells showing green dots represented active caspase-3/7.

3.2.11 Cell Death analysis by Annexin-V-PI assay

Induction of apoptosis was studied by detecting externalized phosphatidylserine (PS) on the outer surface of the cell membrane in unfixed cells using Annexin-V-Alexa Fluor, which specifically binds to negatively charged PS (Vermes, Haanen, Steffens-Nakken, & Reutelingsperger, 1995). Annexin-V-Alexa Fluor/ PI staining is used to detect non-apoptotic live cells (both negative), early apoptotic cells (only Annexin positive), late apoptotic (both positive) and necrotic cells (only PI-positive). Exponentially growing cells were treated with IL-6, followed by irradiation. At particular time points, cells were collected by gentle scraping in the medium along with floaters. Cells were pelleted and re-suspended in binding buffer (provided in the kit) at a density of 1.0 x 10^6cells/ml in 100µl buffer. Next, 5µl of Annexin-V-Alexa Fluor and 10µl of PI (10 µg/ml) was mixed with cells in a tube, followed by incubation in the dark at room temperature for 15 minutes. The measurements were performed on FACSAria III cell sorter (Becton Dickinson, USA) and analyzed using FACSDiva software (Becton Dickinson, USA). The percent population of Annexin-V +ve/-ve and PI +ve/-ve cells were estimated by appropriate gating.

3.2.12 Measurement of intracellular ROS

The intracellular ROS levels of irradiated RAW264.7 cells were estimated by using the fluorescent probe CM-H_2DCFHDA. The cells after treatment (0 to 48hrs) were washed twice with PBS and held in PBS containing 1mM $CaCl_2$, 1mM $MgCl_2$, 5mM glucose and 10µg/ml CM-H_2DCFDA for 30 minutes in the dark at 37°C. After incubation, cells were washed with PBS, scraped and re-suspended in 500µl PBS, and 200µl of suspension transferred to 96-well dark bottom plate, and fluorescence was read at Excitation/Emission of 490/530nm. Rest of the cells were counted to

normalize the fluorescence read per cell. Alternatively, cells suspended in PBS were analyzed by flow cytometry (Becton Dickinson, USA) using 488nm laser.

3.2.13 Estimation of total cellular antioxidant capacity

Total antioxidant capacity was measured in the RAW264.7 cells using the OxiSelect™ Total Antioxidant Capacity Assay kit (San Diego, USA) at 4 &24 hrs post-irradiation. Briefly, 1-5x 10^6 cells were homogenized in 200 µL of cold PBS by sonication for 30 seconds twice and incubated on ice for 10 minutes. Cell supernatant was collected after centrifugation at 12000xg for 10 minutes. Samples were prepared in 96-well plate having all the components and incubated for 1hr at room temperature. Standard curve of Uric acid was generated by serially diluting 1mM uric acid. In a 96 well plate, 20 µL of sample/stand was taken, followed by the addition of 1x reaction buffer and initial reading was measured at 490nm. Then, the reaction was initiated by adding 50 µL of 1x copper ion and kept on an orbital shaker for 5 minutes. Further, the reaction was stopped by adding 1x stop solution, and final absorbance was read at 490nm on a 96 well-plate spectrophotometer. The results were represented as relative fold change in antioxidant capacity of each group.

3.2.14 Measurement of lipid peroxidation

Levels of lipid peroxidation were assayed by measuring the malondialdehyde (MDA) levels in thiobarbituric acid reactive substances (TBARS) assay (Buege & Aust, 1978). At 4 &24 hrs post-irradiation, cells were harvested and homogenized in ice-cold Tris-KCl buffer (10 mM Tris-HCl, 150 mM KCl, at pH 7.4). One volume of homogenate (without centrifugation) was mixed with two volumes of 0.37% w/v Thiobarbituric Acid and 15% w/v Trichloroacetic acid in Eppendorf and heated for 45 minutes in boiling water bath. Next, the solution was allowed to cool at room

temperature, centrifuged, and the absorbance of the clear supernatant was read at 532nm on a 96 well-plate spectrophotometer. Data quantified by using the molar extinction coefficient of MDA-TBA adduct (155 $mM^{-1}cm^{-1}$), normalized with protein content and calculated as nanomoles of MDA per milligram of protein.

3.2.15 Measurement of SOD activity

The activity of the antioxidant enzyme Superoxide dismutase (SOD) was measured in the RAW264.7 cells using the OxiSelect™ Superoxide Dismutase Activity Assay kit (San Diego, USA) at 4 &24 hrs post-irradiation. Briefly, 1-5 x 10^6 cells were lysed in 1mL of cold 1X Lysis Buffer (10mM Tris, pH 7.5, 150mM NaCl, 0.1 mM EDTA, 0.5% Triton-100) and incubated on ice for 10 minutes. Cell supernatant was collected after centrifugation at 12000xg for 10 minutes. Samples were prepared in 96-well plate, having all the reaction components and incubated for 1hr at room temperature. Absorbance was read at 490nm on a microplate reader. The results were represented as relative fold change in SOD activity of each group.

3.2.16 Estimation of Reduced Glutathione (GSH) levels

The level of reduced glutathione (GSH) was measured by its reaction with 5, 5'-dithiobis-(2-nitrobenzoic acid) (DTNB or Ellman's reagent) according to the method of Moron et al. (Moron, Depierre, & Mannervik, 1979). Briefly, 100µL of 20% Trichloroacetic acid (TCA) was added to 100µL of cell lysate to precipitate the protein on ice. Then, the tubes were centrifuged at 10,000 rpm for 10 minutes at 4^oC. Next, 100µl of the supernatant was mixed with 900µL of 0.2M phosphate buffer (pH 8.0) and 2.0ml of freshly prepared Ellman's reagent (0.6mM in 0.2M phosphate buffer pH 8.0). The absorbance of the yellow-coloured product formed [5-thio-2-nitrobenzoic acid (TNB)] was measured at 412nm in a microplate reader after 10 minutes against the reagent blank (containing 5%

TCA instead of homogenate). Standard curve of GSH was generated using concentrations ranging from 2 to 50 nanomoles of GSH in 5% TCA, and the amount of glutathione was expressed as nanomoles/mg protein.

3.2.17 Glucose uptake and lactate production assay

RAW264.7 cells were incubated in HGD before IL-6 treatment and irradiation. Cells were treated with IL-6, 1 hr prior to irradiation. Subsequently, cell medium was removed, and cells were incubated with 2NBDG (50uM, 2-(*N*-(7-Nitrobenz-2-oxa-1,3-diazol-4-yl)Amino)-2-Deoxyglucose) prepared in Phosphate Buffered Saline (PBS) for 30 minutes. Further, the cells were harvested and washed twice with cold PBS to analyze on the flow cytometer. Lactate production was estimated in the growth medium using enzymatic assays. Lactate was estimated using a lactate oxidase method using a kit (Randox; Cat. No.-LC2389). Glucose uptake and lactate production were normalized with the number of viable cell in respected wells.

3.2.18 Analysis of Protein levels using Western blot technique

The protein level of pSTAT-3, STAT-3, hexokinase 2, PFK-1, PKM2, GLUT4, Bcl-2, Bax, Bcl-xl, Mcl-1, cleaved caspase 3, PARP, phospho Akt, Akt, γ- H2AX, VDAC, ATM, RAD51, NBS1, Survivin, Cyclin D, and loading control β-Actin were determined in control and irradiated cells (RAW264.7) by immunoblot analysis. Cells were cultured in PD60 incubated in CO_2 incubator before treatment. Further, cells were harvested post-irradiation at various time points and lysed in ice-cold RIPA lysis buffer (Tris–HCl: 50mM, pH 7.4, NP-40: 1%, NaCl: 150mM, EDTA: 1mM, PMSF: 2mM, Na3VO4: 1mM, NaF: 1mM protease and phosphatase inhibitor cocktail). The protein concentration in cell lysates was determined using the BCA protein assay kit. Protein (30-40μg) was resolved on 10, 12 or 15% SDS–PAGE (depending on the

molecular weight) and electroblotted onto PVDF membrane (MDI). The membrane was then incubated in 5% BSA for 1 hr followed by primary antibody incubation HK-2 (1:1000), PKM2 (1:500), PFK-1 (1:500), GLUT4 (1:500) and β-Actin (1:3000), pAkt (1:1000), Akt (1:1000), SDH (1:1000), pSTAT-3 (1:1000), STAT-3 (1:1000), cleaved caspase 3 (1:1000), PARP (1:1000), Mcl-1 (1:1000), Bcl2 (1:1000), Bax (1:1000), Bcl-xl (1:1000), ATM (1:1000), RAD51 (1:1000), NBS1 (1:1000), at 4 ℃ for overnight. The membrane was washed 3 times (each for 10 minutes) followed by incubation with the appropriate HRP conjugated secondary antibody (1:5000) for 2 hrs. After washing for 3 times (each for 10 minutes), the blots were developed using Luminata Forte western HRP substrate (Millipore). The signal was captured by Chemidoc system (Bio-Rad, CA, USA) or ImageQuant LAS 500 (GE Lifesciences, USA) and band intensities for each protein were quantified by densitometry, corrected for background staining, and normalized to the signal for β-Actin. Densitometry analysis was done using ImageJ 1.52K (NIH, USA).

3.2.19 Gene expression analysis

Total RNA was isolated from cells by Qiagen RNA isolation kit according to the manufacturer's instructions (Qiagen RNeasy mini kit). Further, RNA was dissolved in nuclease-free water (Thermo Scientific, USA) and quantified with Nanodrop (Thermo Scientific, USA). 1ug of RNA was used for cDNA synthesis via First-strand cDNA synthesis kit (Thermo Scientific, USA) in a thermal cycler (Applied Biosystems, CA, USA). Kick start ready to use primers were purchased from Sigma Aldrich (St. Louis, USA). For real-time PCR, 25ng of cDNA was added to 100nM gene-specific primers and 1x Sybr Green supermix (Bio-Rad, CA, USA). The amplification program consisted of a hot start at 95℃ for 3 minutes, followed by 40 cycles of denaturation at

95°C for 15 seconds, annealing at 60°C for 30 seconds, and extension at 72°C for 15seconds. The amount of the target gene was normalized by β-Actin.

3.2.20 ATP measurement

ATP was measured using the ATP bioluminescent assay kit (Sigma Aldrich (St. Louis, USA)) following the manufacturer's protocol. Briefly, cells were treated with IL-6, followed by irradiation at 2 hrs. At 4 and 24 hrs, post-irradiation cells were washed and scraped in cold PBS and pelleted at 1000 rpm for 10 minutes. Cells were lysed in 350 μL of lysis buffer (4mM EDTA and 0.2% Triton X-100). 100 μL of this lysate was loaded per well in triplicates with 100 μL of ATP mix in a 96-well white luminescence measuring plate. Luminescence of samples along with standards was read at 562 nm and normalized with the cell number. ATP concentration is depicted as pg/cell.

3.2.21 Formazan quantification

The cells were plated in 24 well culture plates (40,000 cells/well) and incubated in a CO_2 incubator. Next day, treatment was given according to the experimental requirement. Further, at respective time points, 50 μL MTT solutions from the stock (5 mg/ml) was added and cells were incubated in CO_2 incubator in the dark for 2 hrs. The medium was removed, and Formazan crystals formed by the cells were dissolved using 500 μL of DMSO followed by transfer in 96-well plate. The absorbance was read at 570nm using 630nm as reference wavelength on a Multiwell plate reader (Biotech Instruments, USA). Reduced formazan quantification was done with Formazan standard. At each respective time points cell numbers were counted with a Neubauer's-improved counting chamber (Paul Marienfeld GmbH & Co. KG,

Germany) under 10X objective, and 10X eyepiece magnification with a compound light microscope (Olympus CH30, Japan).

3.2.22 Measurement of mitochondrial Mass and mitochondrial Calcium

Quantitative analysis of mitochondrial content was carried out using Mitotracker Green (at respective time points, post-irradiation), Cells were incubated with Mitotracker green (100 nM; 15 min; 37 °C), in PBS, then washed with PBS and resuspended in PBS before analysis. The signals were recorded using BD FACSAria™ III cell sorter. (BD Biosciences, USA). Images of Calcium loaded mitochondria were captured by staining cells with A23187 (6uM, 20min). Briefly, RAW264.7 cells were grown in PD-35 having coverslip. At 4 hrs post-irradiation medium was removed and stained for 20 minutes in the dark. The stain was removed, and cells washed with cold PBS. Images were captured under a fluorescence microscope with 40X objective.

3.2.23 Measurement of Mitochondrial membrane potential

Quantitative and qualitative analysis of mitochondrial membrane potential (MMP) was carried out using TMRM and JC-1 dyes respectively; Cells were incubated with TMRM (50 nM; 30 min; 37ºC) in PBS, then washed and resuspended in PBS for analysis. Fluorescence signals were measured by flow cytometer (BD FACSAria III cell sorter). For microscopy, cells were stained with JC-1 dye (10 mg/ml; 30 min; 37ºC). After staining, cells were washed with PBS and observed at 40X magnification under a fluorescence microscope (Olympus IX51 Fluorescence Microscope, Japan). JC-1 accumulates in mitochondria as monomer or J-aggregates depending on the membrane

potential. The monomeric form is predominately present in depolarized mitochondria and emits green fluorescence (~530 nm), whereas the oligomeric (J-aggregate) form in mitochondria has more potentials and emits red fluorescence (~590 nm).

3.2.24 Gene knockdown study using siRNA transfection

The control siRNA and Mouse Akt1/2 siRNA pool were purchased from Santacruz Biotechnology (Dallas, Texas, USA) to knock down gene expression. siRNA transfection was performed using Lipofectamine 2000 (Invitrogen, Carlsbad, USA), according to the manufacturer's instructions, briefly, 0.1 $x10^6$ cells were seeded in 6-well plate a day before transfection. Next day transfection was done in Opti-MEM (serum and antibiotic-free medium) for 4 hrs followed by 24 hrs recovery in 2x serum-containing medium. Pilot experiments were performed to optimize the amount and time of maximal protein knockdown.

3.2.25 γ- H2AX foci detection assay

Assessment of radiation-induced DNA damage and repair was done by microscopic evaluation of γ- H2AX foci in RAW264.7 cells. For measuring γ- H2AX by microscopy, cells were plated in 35mm Petri plates on a coverslip and allowed to grow overnight before treatment. The cells, following IL-6 treatment and irradiation, were gently washed once with PBS, fixed and permeabilized in acetone: methanol (1:1) at -20^oC for 20 minutes. Thereafter, the cells were gently washed twice with TBS, non-specific sites blocked by 5% goat serum (in TTBS) for 30 minutes at room temperature before incubation with rabbit monoclonal anti-γ-H2AX antibody diluted 1:1000 in TTBS containing 1% BSA. After primary antibody incubation for 1hr at

room temperature, cells were washed thrice with TTBS and incubated with goat anti-rabbit FITC conjugated IgG (dilution 1:1500 in 1% BSA in TBST) in the dark for 1 hr at room temperature. After completion of incubation, cells were washed thrice with TTBS; coverslip mounted over slide using SlowFade™ Gold Antifade Mountant (Thermo Fisher Scientific, USA) containing DAPI as the DNA-specific counterstain. Each slide was pre-scanned under 10X objective followed by γ-H2AX foci counting at 63X magnification in an automated Metafer microscope (MetaSystems, Germany) using the MetaCyte γ- H2AX foci scan software. About 500 nuclei were scanned per slide to calculate the frequency of γ- H2AX foci per cell.

3.2.26 Assessment of cytogenetic damage by Micronuclei formation

Exponentially growing cells were seeded at a density of 75000 cells/cm^2 and allowed to grow overnight. Following treatment, cells were incubated for varying intervals of time (0-72 hrs). Both floating and attached cells were harvested at every 12 hrs interval by scrapping and fixed in chilled Carnoy's fixative (3:1 V/V, Methanol: GAA), and stored at 4^oC for 2-4 hrs or at -20 ^oC long time (Fenech et al., 2003). The fixed cell was dropped over clean, chilled glass slides, then air-dried overnight and stained with DNA specific fluorochrome, Hoechst (1µg/ml) in phosphate buffer (0.45M Na_2HPO_4. $2H_2O$ and 0.01M citric acid in the ratio of 9:1, final pH: 7.4) containing 0.05%, Tween-20 for 10 minutes in the dark at room temperature. The excess stain washed off with distilled water followed by PBS; then slides were mounted with PBS-glycerol (1:1) and observed under fluorescence microscope at 40X magnification (Olympus IX51, Japan) using UV excitation filter. A total of 1000 cells

were analyzed for counting the number of cells containing micronuclei. The frequency of cells with micronuclei called the M-fraction (MF) was calculated as:

$MF\ (\%) = N_m/N_t \times 100$

where N_m is the number of cells with micronuclei, and N_t is the total number of cells analyzed.

3.2.27 Analysis of 53BP1-GFP foci formation

53BP-1 foci formation in response to radiation was assessed in stably transfected HEK cells. The 53BP1-GFP plasmid was a kind gift from Dr Deepak Saini's laboratory, Indian Institute of Science (IISC) Bangalore, India. The 53BP1-GFP plasmid was transfected in HEK cells and established a permanently transfected cell line. For microscopic evaluation, 0.075 $X10^6$ cells were seeded in 35mm Petri plates over coverslips containing 2ml growth medium/. Next day, cells were treated with IL-6, followed by radiation treatment and kept in a cell incubator. At 48 hrs post-treatment, images (GFP fluorescence) were captured using a fluorescence microscope (Olympus IX 51 fluorescence microscope, Japan) under 40X magnification. The foci formed were counted from at least 20 images per group and the percentage of cells with foci was plotted.

3.2.28 Alkaline Comet Assay

The quantification of damaged DNA was done by performing alkaline comet assay adopting the protocol of Singh et al. (N. P. Singh, McCoy, Tice, & Schneider, 1988) with minimal modifications. Briefly, one-end frosted slides were precoated with 700 μL of 1% normal melting point (NMP) agarose, 1 day before the experiment. After IL-6 treatment and irradiation, cells were scrapped in PBS; the single suspension was

prepared and counted. At least $5x10^4$ cells were taken in 50 μL volume and mixed with 650 μL of low melting point (LMP) agarose and layered over the properly labelled pre-coated slides on ice. When the agarose gets solidified, slides were engrossed in freshly prepared cold lysis buffer for 1 hr at 4°C. After lysis, slides were gently removed from lysis buffer and transferred to unwinding solution for 20 minutes to unwind DNA strands. Then slides were positioned in a comet electrophoretic unit (specialized for comet assay), freshly prepared electrophoresis buffer (PH>13.1) was poured into the electrophoretic tank. The electrophoretic run was then carried out at 14 volts (0.7 V/cm) 300 mA for 20 minutes. After the run, slides were neutralised with 0.4 M Tris base buffer (pH 7.4) for at least 5 minutes then washed with water to wipe out excess salts. Then slides were stained with propidium iodide (25 μg/ml) at room temperature for 10 minutes, washed with water and a coverslip was placed over it and DNA migration was visualised at 20X magnification using automated scoring fluorescence microscope Metafer 4 (Zeiss, Germany). The slides were scanned, and automated analysis was performed by the MetaCyte Comet Scan system of Metafer 4 microscope. One thousand nuclei per group were analyzed to determine tail length, % DNA in tail, tail movement, and olive tail movement.

In vivo studies

3.2.29 Experimental animals

C57BL/6 mice, 8-10 weeks old and with an average weight of 22–25 grams were obtained from the Institutional Animal Facility of INMAS, DRDO, Delhi, India. All the mice were accommodated in well-ventilated polypropylene cages (22±2˚C temperature and 12h/light- dark cycle) provided with standard rodent feed (Golden

Feeds, India) and water *ad libitum*. The mice were always acclimatized for at least one week before the execution of an experiment. All the experimental protocols were reviewed and approved by the Institute's Committee on the Ethics of Animal Experiments before the beginning of tests (Institutional Animal Ethical Committee number:-INM/IAEC/2017/20 and INM/IAEC/2018/21).

3.2.30 Drug preparation and administration

Freshly prepared IL-6 in sterile water was administered by intramuscular (i.m.) injection, 2 hrs prior to whole-body irradiation (WBI). The injectable volume was 10ng/50µL/mouse. JSI-124 was administered by intraperitoneal (i.p.) injection of 1mg/kg body weight dose in 50µL volume.

3.2.31 Irradiation of Animals

Un-anaesthetized mice (not more than 4) were kept in sample chamber using a wired mesh on top and irradiated in a Lose Dose Irradiator (LDI 2000) (BRIT, India) having ^{60}Cobalt as a radiation source. The dose rate during the entire course of study varied between 1.67-1.57 Gy/min. All irradiations were carried out at room temperature. After irradiation, all the experimental mice were kept in the institute's central animal facility and fed on standard diet and water throughout the study period.

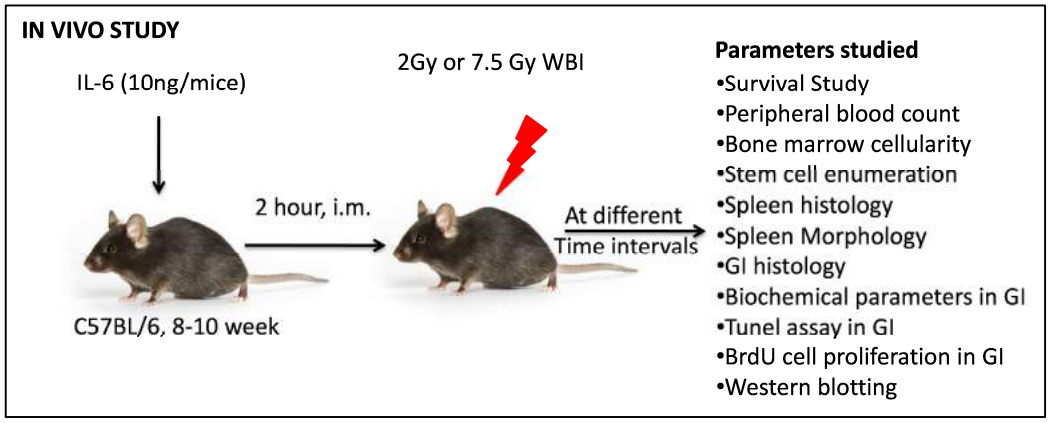

Figure 3.2: Treatment and Irradiation protocol for mice; parameters studied after irradiation

3.2.32 Animal survival

C57BL/6 mice were administered IL-6 (10ng/mice) with a single (pre) or multiple doses (1 pre 3 post till 72 hrs) for dose optimization before being exposed to $LD_{80/30}$ (radiation dose that kills 80% of the animals in 30 days) of radiation and monitored for survival over 30 days. The body weight of the animals was also recorded every alternate day for analyzing the effect of IL-6 on the radiation-induced decline in body weight. 7.5 Gy was selected as $LD_{80/30}$ for C57BL/6 mice. As it kills 80% of the animals within 30 days by both bone marrow and gastrointestinal syndrome. The actuarial survival curves were drawn by the Kaplan- Meier method (Fayers, 1985).

The experimental details are as follows:

Animals were randomized into the following weight-matched (22-25gm) experimental groups:

i) Control (n= 10)

ii) IR (7.5 Gy) (n= 10)

iii) IL-6 single dose + IR (10ng/mice) (n= 10)

iv) IL-6 multi dose + IR (40ng/mice.) (n= 10)

3.2.33 Peripheral blood counts

IL-6 was administered intramuscularly, 2 hrs prior to a whole-body radiation dose of 7.5 Gy or 2 Gy. Blood was withdrawn from the retro-orbital sinus of mice from different groups using a glass capillary in 1.5ml centrifuge tubes containing 10 µL of 5mM K_2-EDTA at 01, 03, 07, 14, 21 and 28 days post-treatment. Blood was allowed to mix thoroughly on a rotary shaker, and complete blood cell counts were taken within 30 minutes of blood collection using automated haematology analyzer Eurocount Plus (Medsource biomedicals, India). The analyzed parameters included total white blood cells (WBCs), lymphocyte number, granulocyte number, RBC and platelet count and Haemoglobin (Hb).

3.2.34 Bone marrow cellularity by enumeration of cell number

Animals were sacrificed by cervical dislocation. Both femurs of the mice were dissected out by cutting just above the pelvic joint, ensuring that the epiphysis is intact. The bones were then cleared off the residual muscle using lint-free tissue paper and trimmed at both the ends to expose the central marrow shaft. The contents of the bone were flushed with 2 ml of PBS containing 2% FBS using 1 ml syringe with a 26½ G needle and collected into a 15 ml centrifuge tube (The bones should appear white, once all the marrow has been expelled out completely). After making single-cell suspension, cells passed through 70 µM nylon mesh strainer (BD, USA) to remove any debris followed by centrifugation and lysis of the red blood cells by incubating with 1X RBC lysis buffer for 2 minutes at 4°C. Cells were washed twice, and the pellet was re-suspended in 1ml of PBS by gentle pipetting a few times to prepare a single-cell

suspension. The number of nucleated cells were then counted using a haemocytometer (Neubauer's, Marienfeld, Germany) and expressed as $\times 10^6$/ml.

3.2.35 Bone marrow cellularity by morphological analysis

Femurs were dissected out from the experimental animals as described above for observing the alterations in the bone marrow cellularity. The bones were fixed in 10% buffered formalin for at least 24 hrs at room temperature. The bones were then washed thoroughly with tap water, decalcified in 15 volumes (~15ml/ femur) of 10% K_2-EDTA (pH 7.2- 7.4) for 10-12 days at room temperature. The decalcifying solution was changed every alternate day. The decalcification process was complete when the bone was easily penetrated through by a needle without any force. Then paraffin-embedded bones sectioned longitudinally at 5µm thickness using a microtome. Afterwards, the bone samples were washed in running tap water before proceeding with the staining procedure. After de-waxing and rehydration, the femur sections were stained with haematoxylin and eosin and observed by bright field microscopy at 10X and 40X magnifications under an Olympus (IX51) microscope (Japan).

3.2.36 Measurement of spleen size, spleen mass index and spleen histology

At day 03 post-treatment, every individual mouse from all groups was weighed prior to being sacrificed. The animals were dissected, spleen excised and washed with PBS, blotted dry on a tissue paper to dry the wet surface and weighed immediately. Spleen length was measured using a centimetre-scale, and the spleen was weighed in milligram scale. Spleen index was calculated by dividing spleen weight with body weight. For spleen sectioning, the excised spleen was fixed in 10% buffered formalin,

and the paraffin-embedded spleen was sectioned horizontally. After de-waxing and rehydration, the spleen sections were stained with haematoxylin and eosin and observed by bright field microscopy at 4X, 10X and 40X magnifications under an Olympus (IX51) microscope (Japan).

3.2.37 Stem Cell enumeration in bone marrow

Femurs were harvested from the experimental animals at 24 hrs post-irradiation. The bone marrow cells were collected as described earlier in section 3.3.34. Further, the RBCs were lysed by treating with ice-cold 1× RBC lysis solution for 2 minutes on ice. Then, washed 2 times with cold PBS+2%FBS solution, followed by counting prior to staining. Around $5x10^6$cell population was stained with biotin labelled lineage (Lin) cocktail (BD biosciences) along with anti-SCA1-PE-CY7 (BD), anti-cKIT-PE-CY5 (BD) and anti-CD34-FITC (eBiosciences) (antibody dilution 1ul/10^6cells) in PBS plus 2% FBS solution (100µl) and incubated on ice in the dark. After 20 minutes incubation, the extra stain was washed off by washing 2 times with cold PBS followed by incubation with PE labelled streptavidin to stain biotin labelled lineage cells for 10 minutes on ice in the dark. To identify the live and dead population, cells were also stained with Dapi. After proper washing, cells were analyzed by FACSAria III cell sorter (Becton Dickinson, USA) using a blue and violet laser. At least 20,000 cells of the gated population were acquired for each sample. The gating strategy followed to identify stem cells is illustrated below-

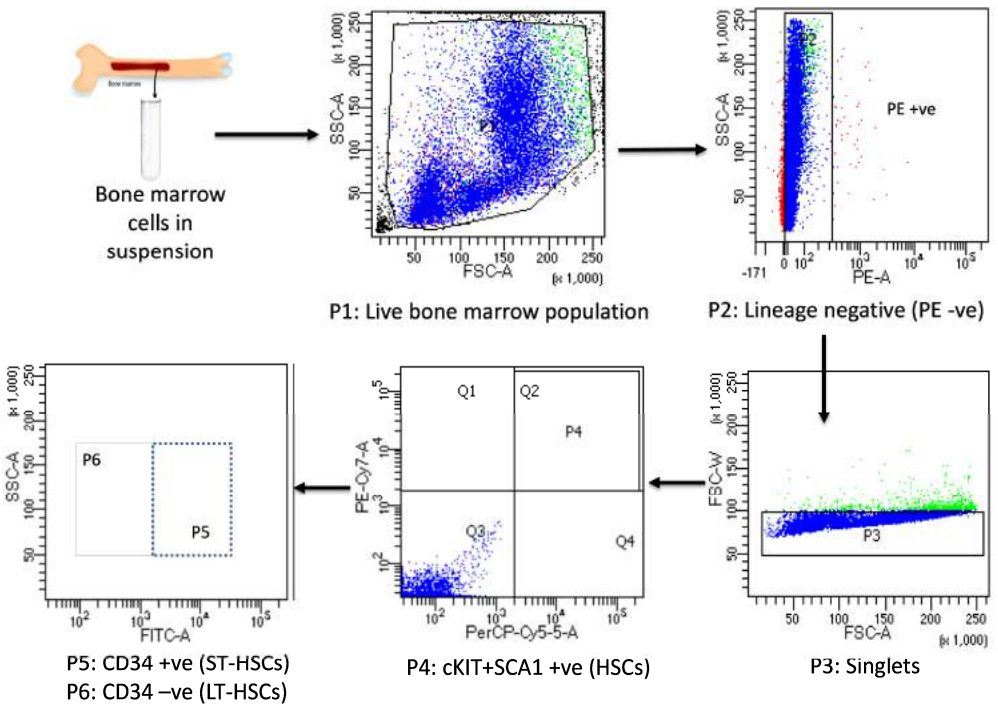

Figure 3.3: Gating strategy for hematopoietic stem cell (HSC) population selection (Lin-, SCA1+, cKit+, LSK cells) along with the short term (ST) or long term (LT) HSC. These dot-plot and quadrant graphs obtained from the unstained control sample.

3.2.38 γ- H2AX foci formation in PBMCs

Mice were subjected to a WBI of 2 Gy, 2 hrs after IL-6 administration. DNA damage and repair were assessed by visualizing and quantifying the γ-H2AX foci formed in peripheral blood mononuclear cells (PBMCs) after 1, 4, and 24 hrs of irradiation. Blood was collected into heparinized 1.5ml centrifuge tubes (HiMedia, India) by puncturing the retro-orbital plexus and PBMCs were isolated as per the following protocol:

1. 500 µL blood was mixed in 1:1 ratio with an equal volume of PBS.
2. The diluted blood was slowly layered on top of 2 ml (double of diluted blood) of Histopaque®-1083 (Sigma- Aldrich, USA) contained in a 15 ml centrifuge tube, minimizing any mixing of blood with Ficoll.

3. The tubes were centrifuged at 500g for 30 minutes at 20^{o}C, without brakes.
4. The top layer of plasma was carefully removed and discarded, and the buffy coat layer (containing the PBMCs) seen at the plasma-Ficoll interface was collected (avoiding the Histopaque underneath) into a new 15 ml tube.
5. The cells washed twice with three volumes of PBS by spinning at 200g for 10 minutes at 20^{o}C to remove the contaminating Ficoll/ platelets/ plasma proteins.
6. The final pellet was then re-suspended in 1ml PBS, and cells counted using a hemocytometer.

About 1x10^{5} cells were evenly spread on clean, poly-L-lysine pre-coated (with 0.01%, Sigma- Aldrich, USA) glass slides and left undisturbed for 20 minutes at 4^{o}C to adhere. Excess cells were discarded by shaking off the suspension, followed by fixation and permeabilization with chilled Acetone: Methanol (1:1) solution for 20 minutes at -20°C. The similar protocol was followed as discussed in section 3.2.25. Each slide was pre-scanned under 10X objective followed by γ- H2AX foci counting at 63X magnification in an automated Metafer microscope (MetaSystems, Germany) using the MetaCyte γ- H2AX foci scan software. About 500 nuclei were scanned to determine the frequency of γ- H2AX foci as well as the number of foci per cell.

3.2.39 Assessment of cytogenetic damage (Micronuclei Induction) in bone marrow

For the MN assay, mice (irradiated with 2 Gy with or without IL-6 administration) were euthanized to isolate the femurs, and the bone marrow cell suspension was made as described earlier under section 3.2.34. After centrifugation cell pellet was re-suspended in 500 µL of PBS. Out of that, 5 µL of cell suspension mixed with 5 µL of FBS and was smeared on clean, dry glass slides. The air-dried smears were then fixed with

methanol for 5 minutes, washed with water and left to dry after soaking extra water on tissue paper. Thereafter, slides were stained with Hoechst (10µg/ml) satin in phosphate buffer in the dark, at room temperature for 10 minutes. Then, slides were washed with PBS, mounted 1:1 v/v, PBS-Glycerol solution and observed under a fluorescence microscope (Olympus IX51, Japan) at 40X magnification using a UV excitation filter. One thousand cells were scored per group to calculate the M-fraction (MF).

3.2.40 Measurement of IL-6 levels

Anti-IL-6 ELISA was performed according to the manufacturers' protocol (murine IL-6 ELISA kit Affymetrix, eBiosciences, San Diego) in serum samples collected at 1 and 2 hrs post IL-6 treatment. The brief contract is as follows-

1. Corning 96-well plate was coated with 100µL/well of capture antibody in 1X coating buffer. The plate was sealed and kept at 4º C for overnight.
2. Next day, washed 3 times with 300 µL/well wash buffer. At least soaked for 1 minute during each wash and the residual buffer was removed by blotting the plate on absorbent paper.
3. Then, non-specific sites were blocked by 200µL/well 1X ELISA/ELISPOT diluent for 1hr at room temperature.
4. 100 µL of sample/standard has been added per well along with two wells of blank (1X Diluent only) and was incubated overnight at 4º C for maximal sensitivity. Next day again washed for a total of 3-5 washes.
5. Then, 100µL/well of detection antibody was added for 1hr at room temperature.
6. After 3-5 washing, avidin-HRP (100µL/well) was added for 30 minutes at room temperature followed by 5-7 washes with 2 minutes soaking time.

7. Next, 100 µL/well 1X TMB solution was added for 15 minutes at room temperature, followed by addition of 50 µL of stop solution.
8. The plate read at 450nm in a microplate reader, and data were analyzed.

Composition of wash Buffer- 1X PBS with 0.05% Tween 20

3.2.41 Protein expression analysis in animal tissues by Western blots

Bone marrow cells were recovered as described in section 3.2.34. PBMCs were isolated, as discussed in section 3.2.38. Spleen was cut into pieces and crushed between two frosted slides. The GI tissues were flushed with PBS to remove intestinal contents, and a small piece of tissue was chopped off and smashed. A single-cell suspension was prepared from all type of samples and passed through 70 µM nylon mesh strainer to remove any debris (except PBMCs) and lysed in 200-500µL RIPA buffer containing protease inhibitor cocktail. Samples were incubated on ice for 45 minutes and sonicated for 30 seconds followed by centrifugation at 14000 rpm for 15 minutes at 4ºC, and clear supernatant fractions were collected and stored at −80ºC. After estimating the protein concentration with the BCA method, the equal level of proteins for each sample (40-50µg) was separated on SDS-PAGE, which followed the similar protocol as discussed in section 3.2.18.

3.2.42 Histological assessment of intestinal injury

At day 01 and 07 after irradiation, jejunal tissues were excised from the small intestine (2 cm below the gastro-duodenal junction) of a minimum of 3 mice from each group. The tissues were flushed with PBS to remove intestinal contents, immersion fixed in 10% formalin buffer at room temperature (20:1 volume of fixative) and embedded vertically in paraffin (58- 60^{o}C) following the standard procedure of tissue preparation

(Humanson, 1961). 5 µm cross-sections were stained with haematoxylin and eosin (H&E) after de-waxing and rehydration and analyzed by bright field microscopy under Olympus (IX51) microscope (Japan) at 10X magnification.

3.2.43 Immunohistochemistry (IHC) for BrdU proliferation assay in GI

Mice injected with Bromodeoxyuridine (BrdU) (100µl from 10mg/ml) through intra-peritoneal route 2 hrs before dissection. GI sections were prepared as described above at day 07 after irradiation and then deparaffinized by sequential treatment with xylene (3 times, 5 min each), 100% ethanol (2 times, 10 min each) and 95% ethanol (2 times, 10 min each) followed by 5 minutes in water. Antigen retrieval was done in 10mM sodium citrate buffer for 5 minutes at 95^{o}C; this process was repeated twice and left for cooling at room temperature. After antigen retrieval, sections were rinsed with TBST, permeabilized with 0.1% Triton X 100 for 10 minutes in a humidity chamber and endogenous peroxidase activity was quenched by treating the parts with 3% H_2O_2 (peroxidase block). Non-specific sites were blocked by 5% BSA for 1 hr at room temperature before incubating the sections with anti- BrdU antibody (diluted 1:100 in 1% BSA in TBST) for overnight at 4^{o}C in a humid chamber. Thereafter, articles washed with TBST and incubated with FITC labelled secondary antibody in the dark for 1 hr at room temperature. Then, washed thrice with TBST and counterstained with Dapi to visualize nuclei. Finally, images were captured by fluorescence microscopy under Olympus (IX51) microscope (Japan) using blue and UV filters.

3.2.44 Biochemical analysis of GI tissue

Malondialdehyde (MDA) and GSH levels in the gut were determined at day 1 and 7 post-irradiation by measuring the absorbance of coloured product produced from

TBARS assay and DTNB or Ellman's reagent respectively. The intestinal tissue was flushed and rinsed thoroughly with PBS, blotted dry, and a small portion was weighed and chopped off to homogenize further. Tissue homogenate (10% (w/v)) was prepared in ice-cold Tris-KCl buffer followed by centrifugation at 10,000g for 15 minutes at 4ºC. This homogenate was further processed for TABRS and GSH assay as the detailed protocol discussed in section 3.2.14 and 3.2.16, respectively. Both MDA and GSH levels were calculated as nanomoles per milligram of protein.

3.2.45 TUNEL Assay for cell death in GI

Terminal Deoxynucleotidyl Transferase dUTP Nick End Labeling (TUNEL) assay was used to determine the fragmented DNA (a hallmark of apoptosis) in the GI tissue by the In Situ Cell Death Detection Kit as per the manufacturer's guidelines. GI tissue was harvested at 03 days post-irradiation and cleaned by flushing with PBS, minced off to fine pieces followed by enzymatic digestion with 0.1% Collagenase Type IV (MP Biomedicals Inc., USA) prepared in HBSS with 2.5 mM $CaCl_2$, for 1 hr at 37^{o}C. The digest solution was then passed through a 70µm Falcon cell strainer to eliminate any debris and further washed with HBSS. After preparing single-cell suspension, 100 µL of cell suspension (containing ~2 x 10^6 cells) was mixed with 100 µL of freshly prepared 4% PFA solution (final concentration 2% PFA) and incubated for 1 hr at room temperature. After washing with PBS, cells were permeabilized with 0.1% Triton X 100 in 0.1% sodium citrate) for 2 minutes on ice. Again, cells were washed and incubated in 50 µL of TUNEL reaction mixture (containing fluorescein-labelled nucleotides and terminal deoxynucleotidyl transferase enzyme) for 60 minutes at 37^{o}C in the dark followed by washing with PBS and finally cell pellets was re-suspended in

500 µL PBS. The acquisition was made in flow cytometer, FACSAria III cell sorter (BD, USA), and data were analyzed by the FACSDiva software (BD, USA).

3.2.46 Statistical Analysis

Data were plotted using Origin 5.0 or Graph pad prism software, and the experimental results were expressed as mean ± SEM of three independent experiments. Student's t-test and one-way or two-way ANOVA was used to test the significance of any differences between groups. Data of survival studies were analyzed using the Kaplan-Meier method followed by Mantel-Cox (log-rank) and Wilcoxon tests for assessment of significant differences. Results were considered significant at $p < 0.05$.

Chapter 4
Results

CHAPTER 4

RESULTS

4.1 IL-6 induced STAT-3 signalling protects cells from radiation-induced cell death and confers radio-resistance

Introduction

Protection of normal cells from radiation insult is a major challenge in the field of radiation biology and medicine. Nowadays, radio-protective agents are of great interest for application in radiotherapy and as civic health medicine in accidental radiation exposures. Although a plethora of compounds synthesized for this purpose has demonstrated radio-protective efficacy *in-vitro*, the majority of them failed *in-vivo* because of their acute toxicity and short time window of the application. Thus, the search for a safe and effective radio-protector that protects healthy tissues from radiation still exists. IL-6 is the multi-functional cytokine controlling the humoral immunity and inflammation. In cancer cells, it showed multi-functional behaviour by regulating multiple signalling pathways of cell death and survival. IL-6 induced therapeutic resistance is an obstacle for therapeutic gain in cancer patients. However, its mechanism causing radio-resistance is un-explored, particularly in healthy cells. Therefore, we tested the hypothesis if IL-6 can protect normal cells from radiation-induced cytotoxicity. Because of this, studies were undertaken to evaluate their radio-protective potential *in-vitro*. We treated RAW264.7 cells with IL-6 1-2 hours (hrs) before irradiation (IR) and examined the cell survival, proliferation, antioxidant defence mechanism and cell death.

4.1.1 Cytotoxicity analysis of Interleukin-6

Drug dose-response relationships are essential to analyze for a new drug or molecule either from a natural source or synthesized while assessing the safety and effective

concentrations of drugs. Therefore, cytotoxicity was studied in multiple cell lines of different nature and origin, i.e. hematopoietic (RAW264.7), gastrointestinal (INT407, IEC-6), and fibroblasts (NIH3T3). Here, we performed Sulphorhodamine B assay, a well-known cell proliferation assay, which is based on estimating the total cellular mass (Orellana & Kasinski, n.d.). IL-6 concentrations in the range from 0.1ng/ml to 10ng/ml were analyzed to identify the best concentration for further experiments (Fig;4.1.1). Cells were grown in respective IL-6 concentration, and SRB assay was performed at 48 hrs post-treatment. Results obtained from different cell lines showed no cytotoxicity at any concentration used in all four cell lines; however, there was marginally higher but statistically insignificant proliferation.

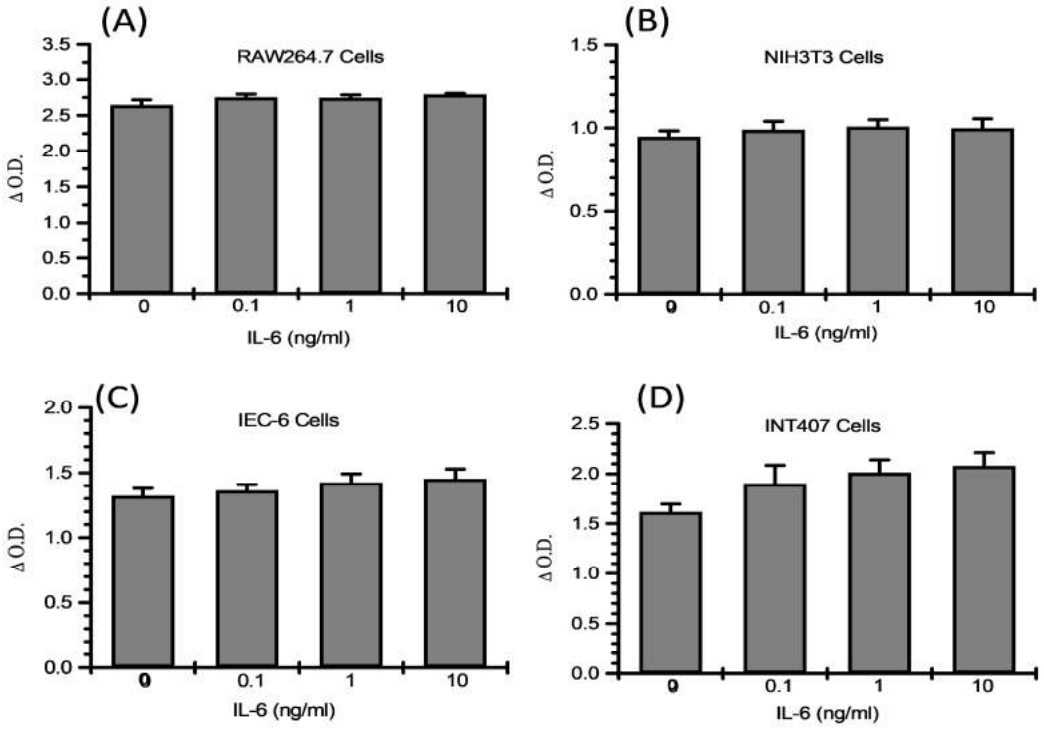

Figure 4.1.1: Sulphorhodamine B assay for drug-dose response in RAW264.7, NIH3T3, IEC-6 and INT407 cells. SRB assay carried out at 48 hr post-irradiation using different concentrations of IL-6 (0.1-10 ng/ml). Graph (OD 340 nm) plotted, and treatment groups were compared with their respective control. Data points represent mean ± S.E.M from 3 independent experiments at 48 hrs.

4.1.2 Examination of Radio-protective potential of IL-6 in various cellular models

4.1.2.1 SRB assay

Our next aim was to select the safe dose range of IL-6 at which it shows its maximum radioprotection. Since IL-6 was safe between the range of 0.1ng/ml to 10ng/ml, we further validated the efficacy of IL-6 at different concentrations ranging from 0.1 to 10ng/ml in multiple cell lines RAW264.7, NIH3T3, IEC-6 and INT407 at a respective LD50 radiation dose of each cell. The LD50 radiation dose for RAW264.7 is found nearly 2 Gy, for NIH3T3 and IEC-6 it is 4 Gy, and for INT407 it is almost 6 Gy. In this study, the human intestinal epithelial cell line INT407 was found to be relatively most radio-resistant among the investigated cellular models. The cells were incubated with a respective concentration of IL-6 for 2 hrs before radiation exposure; then the SRB assay was performed at 48 hrs to investigate the efficacious dose of IL-6. Results showed a significant increase in cell number after radiation exposure at both 1 and 10ng/ml IL-6 as compared to radiation alone (Fig;4.1.2A-D). Further to confirm, the gold standard cell counting method of growth kinetics assay was performed under a similar experimental condition at 48 hours to analyze and validate the efficacious concentration range of IL-6. The result showed maximum radioprotection at 1ng/ml of IL-6 concentration (Fig;4.1.2E). Thereafter, 1ng/ml IL-6 was used for all further experiments.

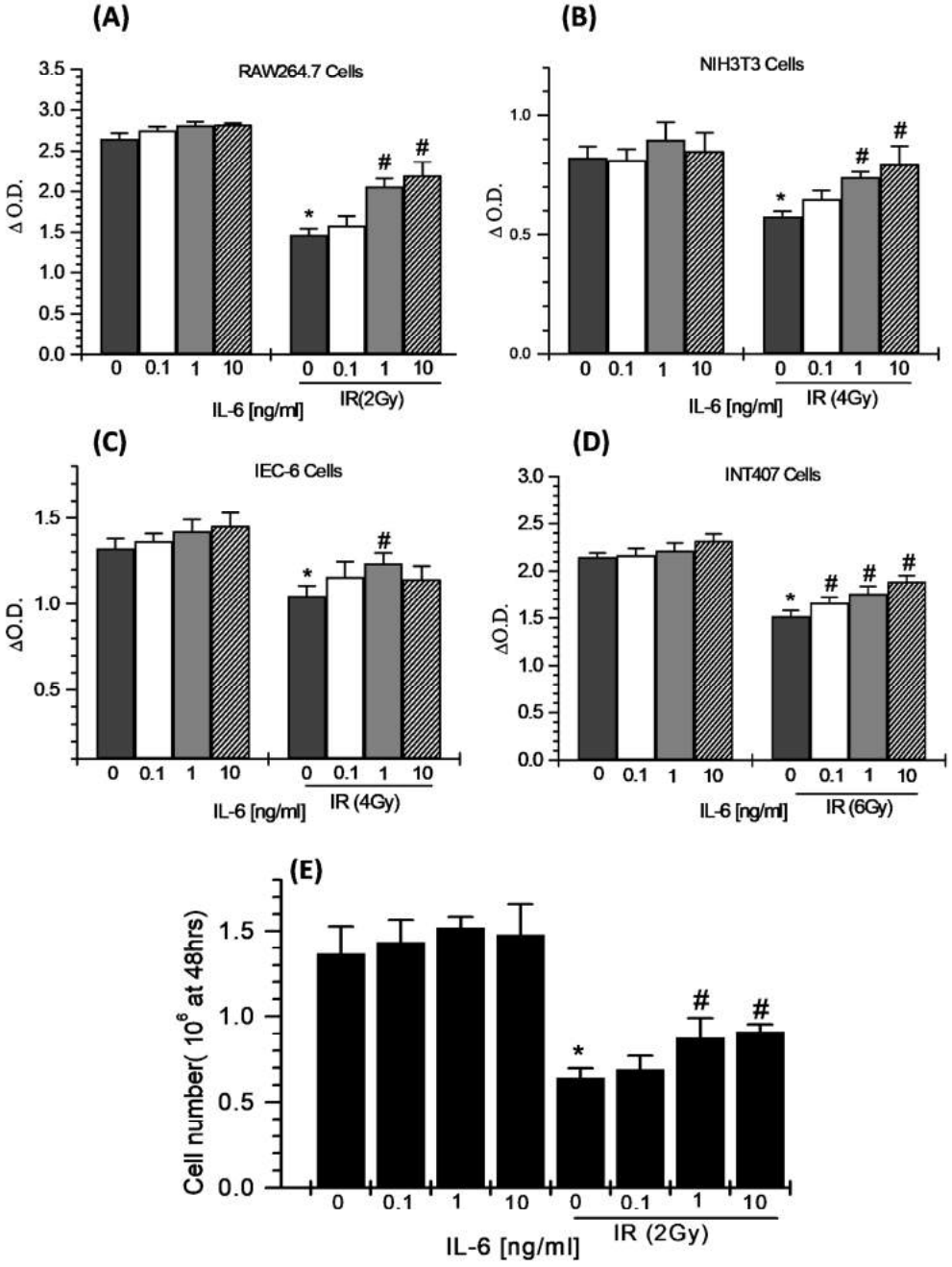

Figure 4.1.2: (A-D) Sulphorhodamine assay to identify the efficacious dose of IL-6 for radioprotection in RAW264.7, NIH3T3, IEC-6 and INT407 cells. SRB assay carried out at 48 hr post-irradiation using different concentrations of IL-6 (0.1-10 ng/ml) combined with radiation (E) Growth Kinetics assay was performed again at 48 hrs in RAW264.7 cells to pick the best concentration of IL-6. Star shows significance w.r.t. the control group and # show significance w.r.t. to the IR group. Data points represent mean ± S.E.M from 3 independent experiments.

4.1.2.2 Growth kinetics

Radiation-induced cell growth inhibition due to perturbed cell cycle progression and cell death, is the major limitation for cell survival (Kim et al., 2019). Cells were pre-treated with IL-6 (1ng/ml) followed by irradiation and then enumerated at various time points (24, 48 and 72 hours) post-treatment using an improved Neubauer's chamber. In all three cell lines (RAW264.7, NIH3T3and INT407 cells) IL-6 treatment prior to irradiation reduced the effect of radiation-induced cell growth inhibition observed by a substantial increase in cell number post-irradiation compared to their respective control groups. Assessment of growth kinetics from 24-72 hrs indicated that radiation inhibited the cell proliferation in all the cell lines studied. In NIH3T3 and INT407 cells, this inhibition was more pronounced at 72 hrs while in RAW264.7 cells, which are relatively more sensitive and fast proliferating, this inhibition was evident at 48 hours. In RAW264.7 cells, irradiation led to a 50% reduction in cell number at 24 hrs, which was restored up to 50% by 48 hrs with IL-6 treatment. The 48 hrs count (in a million) was 1.55±0.049, 1.78±0.054 in control and IL-6 groups while 0.635±0.025 in radiation alone and 0.9250±.01291 in IL-6 treated irradiated group (Fig;4.1.3A). Similarly, the 72 hrs count of NIH3T3 cells was 1.98±0.158 and 2.01±0.062 while 1.34±0.017 in radiation control and 1.65±0.079 in IL-6 treated irradiated groups (Fig;4.1.3B). INT407 cells also displayed the same pattern with cell number as 1.07±0.102, 1.007±0.097 in Control groups while 0.39±0.024 and 0.52±0.062 in IR and IL-6+IR groups (Fig;4.1.3C).

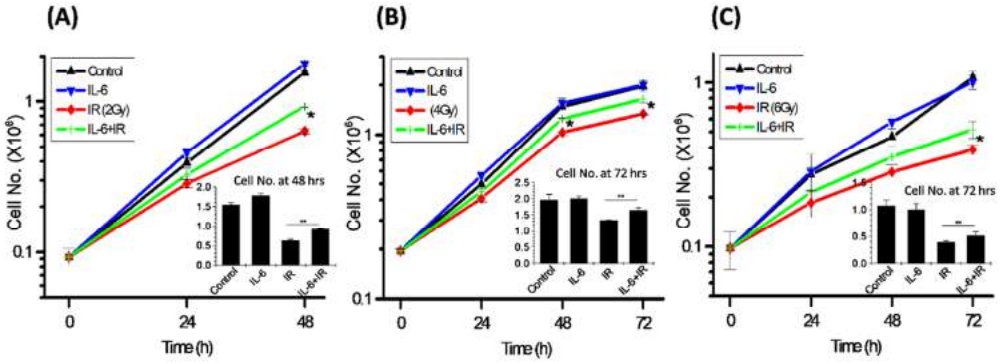

Figure 4.1.3: Growth kinetics assay, radiation-induced cell growth inhibition (A-C) Cell number quantified from 0-72hrs at a single dose of IL-6(1ng/ml), given 2 hrs prior to IR in RAW264.7 (A), NIH3T3 (B), and INT407 cells (C), and plotted as a line graph. Inset graph represents the cell no. at a single time point (48/72 hrs) for better understanding. Data points represent mean ± S.E.M from 3 independent experiments. *: $p<0.05$;

4.1.2.3 Clonogenic cell survival assay

Clonogenic assay is the technique to determine cells reproductive death after exposure to ionizing radiation. Only a fraction of seeded cells retain the ability to produce colonies (Franken, Rodermond, Stap, Haveman, & van Bree, 2006). This assay is the best method to check *in-vitro* cell survival which exploits the capability of a single cell to propagate into a colony. The effect of IL-6 on the radiation-induced loss of clonogenicity was assessed from the dose-response curve of the cells after exposure to different absorbed doses of gamma radiation (1Gy to 8Gy) in all three cell lines following pre-treatment with the IL-6 (1ng/ml) (Fig;4.1.4). The results of radio-modification studies with the IL-6 indicated that IL-6 significantly enhanced the surviving fraction (SF) of RAW264.7 cells at radiation dose from 1–6Gy. However, it did not protect the same cell line from radiation-induced loss of clonogenicity at higher doses (LD90). On the other hand, INT407 cells and NIH3T3 cells showed a significant increase in S.F. at doses 2-8 Gy. The S.F. values of different cell lines after exposure to radiation in the presence/ absence of the IL-6 are presented in table (4.1.1).

Table 4.1.1: Surviving fraction (SF) values of different cells on different radiation doses

Cell Lines	IR Dose (Gy)	0	1	2	4	6	8
RAW264.7	IR Control	1	0.756	0.544	0.138	0.02488	0.00303
	IL-6+IR	1.143	0.876	0.734*	0.219*	0.04532*	0.00417
NIH3T3	IR Control	1	0.854	0.596	0.371	0.174	0.048
	IL-6+IR	1.053	0.954*	0.709*	0.5*	0.22*	0.081*
INT407	IR Control	1	0.867	0.601	0.267	0.117	0.037
	IL-6+IR	0.985	1.01*	0.74*	0.371*	0.188*	0.052*

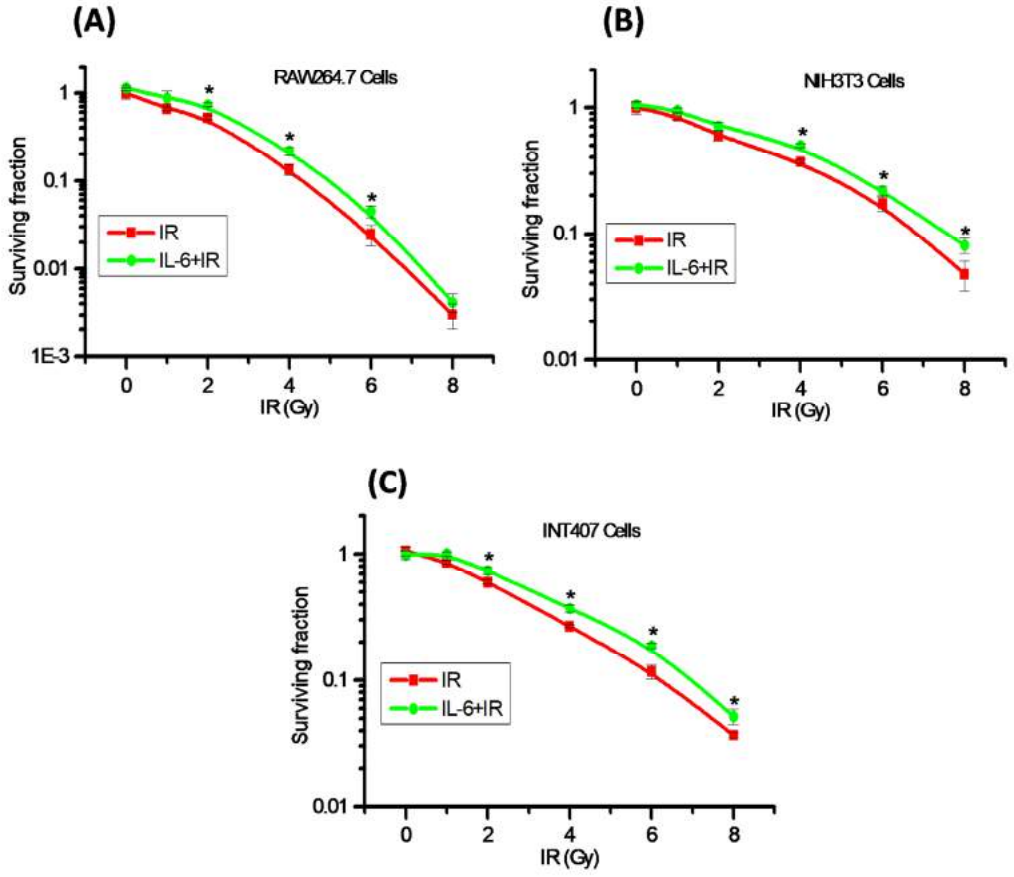

Figure 4.1.4: (A-C) Radiation dose-response in RAW264.7, NIH3T3, and INT407 cells. Surviving fraction was plotted against increasing dose of radiation dose (1-8 Gy). Star shows significance w.r.t. IR group. Data points represent mean ± S.E.M from 3 independent experiments.

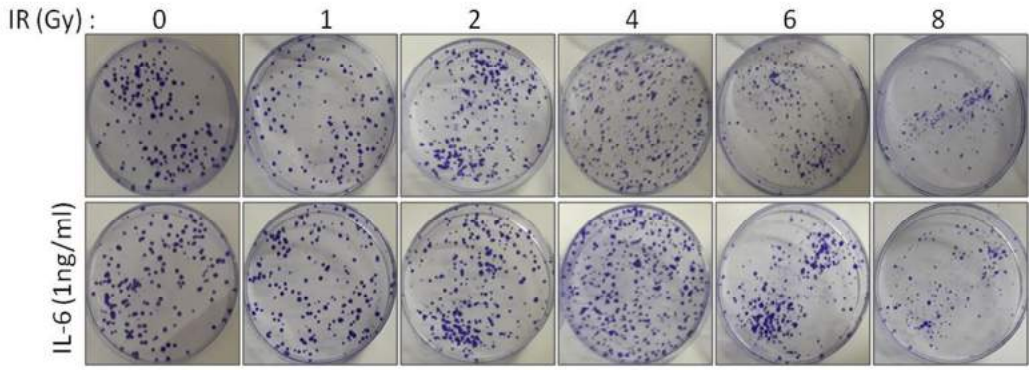

Figure 4.1.4 (D) Representative images of Macro colony formation in INT407 cells at increasing radiation doses. Cells were seeded in increasing number with increasing radiation dose. Controls and 1 Gy groups had 100 cells per Petri plate, 200 for 2 Gy, 400 for 4 Gy, 600 for 6 Gy and 800 cells for 8 Gy. Colony formations observed at 12-14 days.

4.1.3 Cell proliferation and cell cycle distribution:

The flowcytometric DNA content analysis was carried out from 2-48 hrs post-IR to analyze the radiation-induced cell cycle perturbation, and cell cycle checkpoint activation along with radiation-induced growth inhibition in IL-6 treated vs untreated RAW264.7 cells. The results revealed that exposure to 2 Gy IR causes a significant increase in S phase block at 2 hrs which progresses with time to appear as late S phase block at 4 hrs (Fig;4.1.5A). The S phase block initiated just at 2 hrs post-irradiation followed by prominent G2/M block at 4 hrs and gradually resolved till 16 hrs. The IL-6 pre-treated cells showed relatively less number of cells in radiation-induced S-phase block, whereas a massive difference in SubG1 population was observed, which indicates apoptotic cells. Bar graph representing the SubG1 population in all groups at different time points (Fig;4.1.5B).

(A)

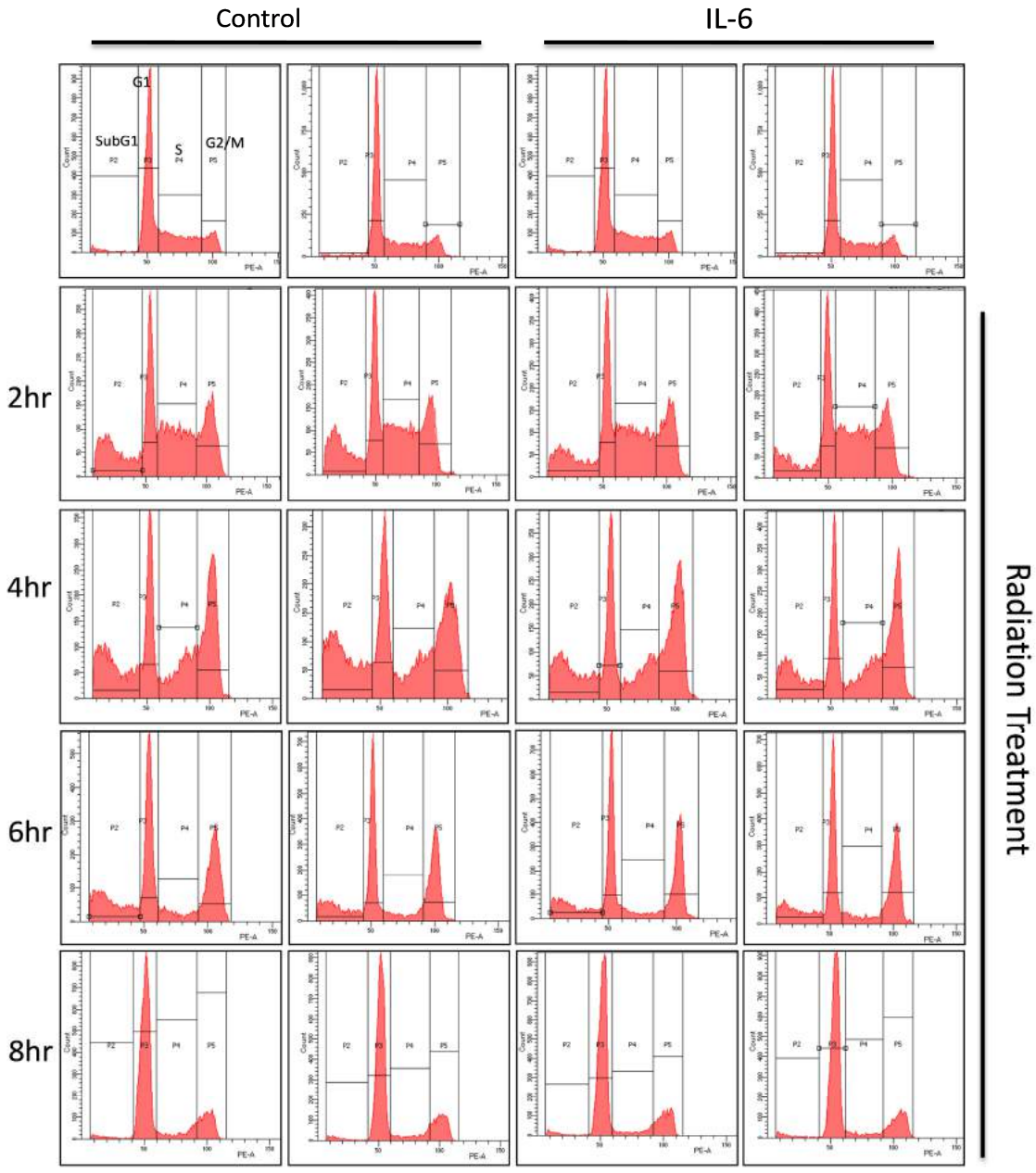
Control
IL-6
G1
SubG1
S
G2/M
2hr
4hr
6hr
8hr
Radiation Treatment

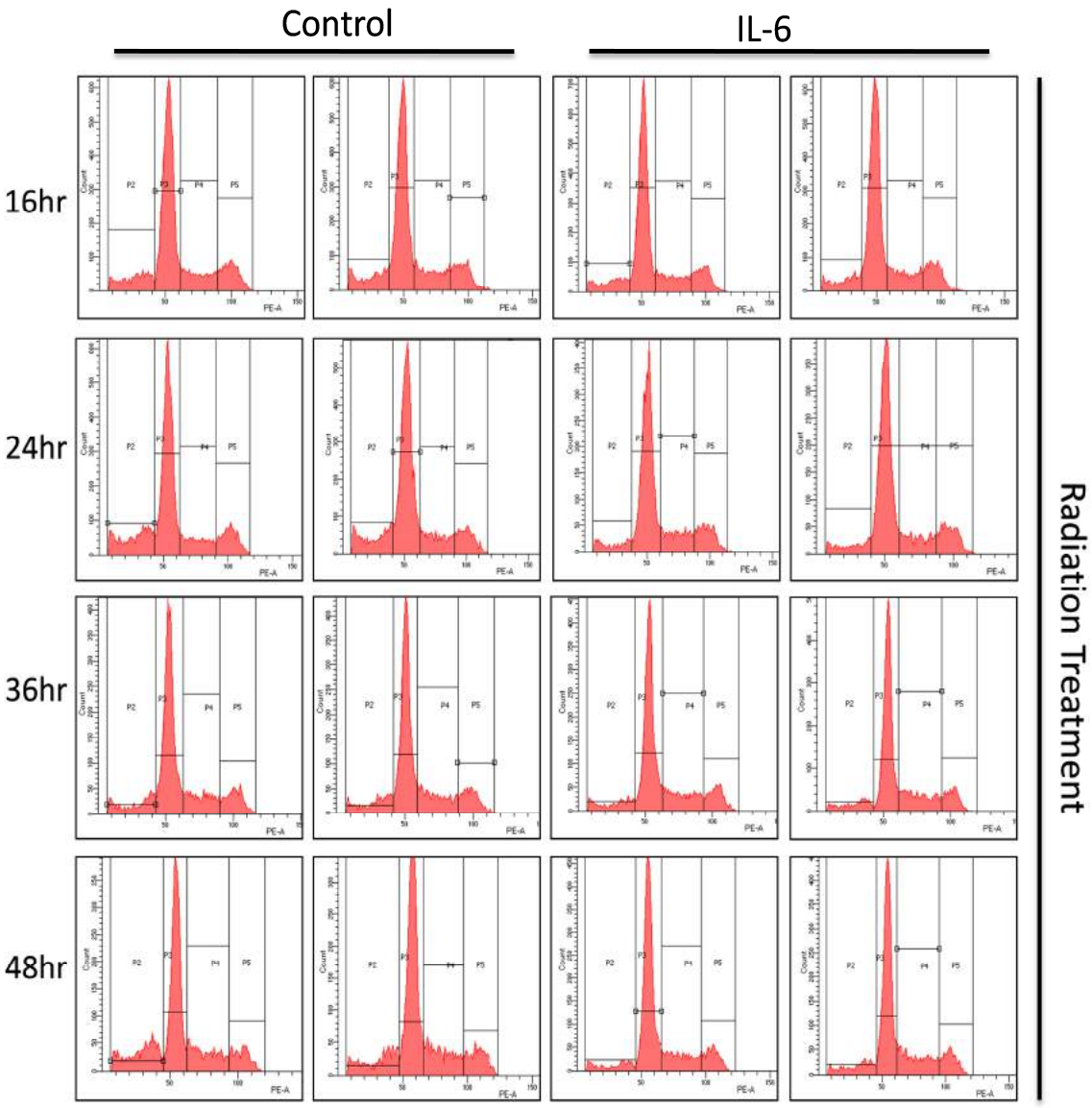
Control
IL-6
16hr
24hr
36hr
48hr
Radiation Treatment

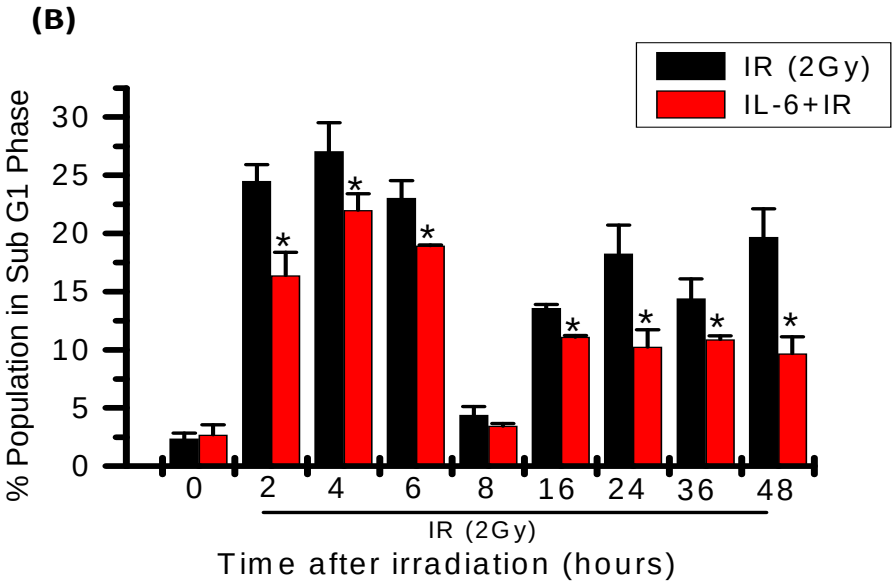

Figure 4.1.5: Effect of IL-6 on cell cycle perturbations caused by radiation**. (A)** DNA flow cytograms showing cell cycle distribution in RAW264.7 cells at indicated time points after irradiation. **(B)** Bar graph represents percent population in the sub G1 phase of the cell cycle from 0-48 hrs. Star shows significance w.r.t to the IR group.

IL-6 induced enhanced survival and proliferation in radiation treated samples have been further strengthened by assaying cell proliferation through Carboxyfluorescein succinimidyl ester (CFSE) labelling. The CFSE labelled cells were grown after IL-6 and radiation treatments and evaluated by flow cytometry (Fig;4.1.6). The fluorescence shift (shown by overlay graph) at 48 hrs is representing proliferation (Fig;4.1.6A). The cells displaying high fluorescence are signifying low proliferation. Thus, the visibly high fluorescence in IR and combined treatment (IL-6+IR) groups indicating low proliferation with respect to control group (Fig;4.1.6B). However, the fluorescence of IR was significantly high as compared with IL-6+IR, which represents a slow rate of proliferation due to irradiation which was conquered by IL-6 treatment. The primary regulator of cell survival and apoptotic inhibitor, Survivin was probed at 4 hrs post-irradiation (Fig;4.1.6C). Significant changes were observed in IL-6 treatment groups with respect to sham irradiated and irradiated group. Cdk/Cyclins

are the essential proteins required for cell cycle progression and division. Here, we checked the levels of cyclin D1 and found upregulated in IL-6 pre-treated, radiation-exposed cells (Fig;4.1.6C). This data suggest that IL-6 pre-treated cells showed faster proliferation after radiation exposure as compared to untreated cells, could be due to IL-6 induced enhanced proliferation, or reduced cell death.

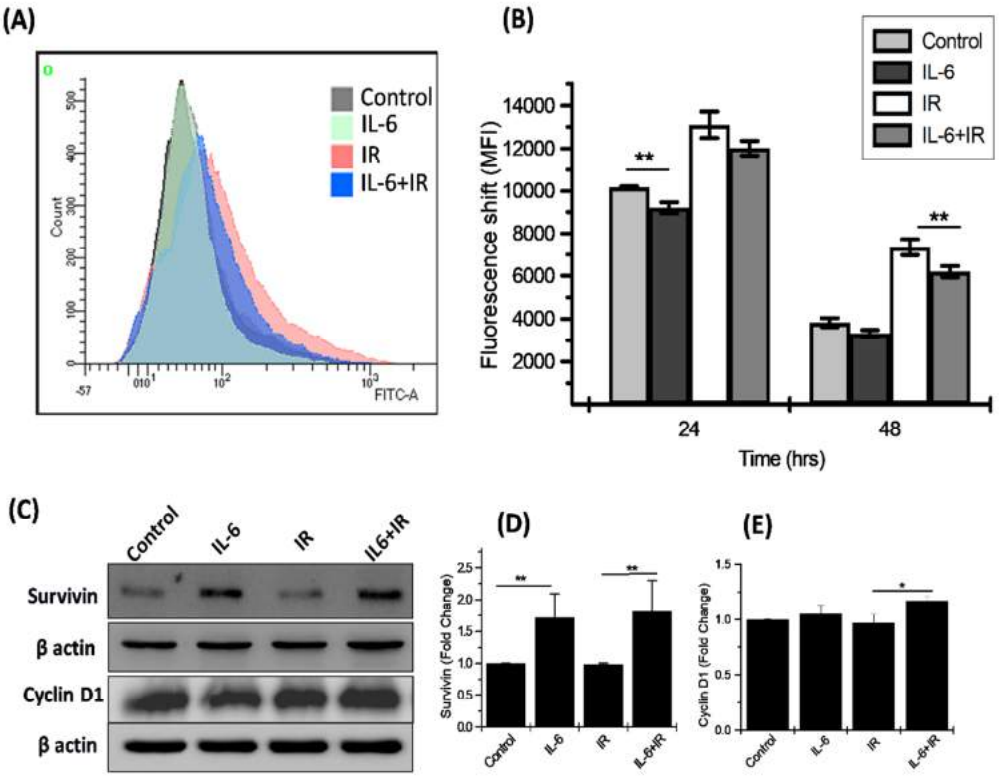

Figure 4.1.6: Cell proliferation assay (A) Overlay histogram represents the fluorescence shift with increased proliferation in samples. (B) Mean fluorescence intensity (MFI) as derived information from histogram plotted as bar diagram at 24 and 48h.(C) Immunoblots of Survivin and Cyclin D1 and their respective quantitative analysis is represented as bar diagram (D&E) Beta Actin was used as the loading control. Data points represent mean ± S.E.M from 2 independent experiments.

4.1.4 IL-6 recuperate redox balance altered by radiation

4.1.4.1 ROS (reactive oxygen species) kinetics: IR is known to induce the generation of intracellular ROS through radiolysis of water (Hall and Giaccia, 2006).

As described earlier, ROS may lead to cell death through damage to DNA and oxidation of other macromolecules and subsequent activation of signalling pathways related to cell death. We, therefore, investigated the effects of IL-6 on the modulation of radiation-induced ROS generation by using CM-H2DCFDA - a ROS indicator probe. The dye passively diffuses in cells, and the reduced non-fluorescent dye is oxidized to a fluorescence compound 2', 7'–dichlorofluorescein (DCF) by cellular ROS. The fluorescence produced is directly proportional to the amount of oxidized DCFDA to DCF or ROS. Fluorescence microscopic images are showing that green colour fluorescence was increased after irradiation of cells as compared to control cells. Spectrofluorometric study in RAW264.7 cells revealed the ROS kinetics from 0 to 48 hrs post-irradiation. Radiation (2 Gy) induced an oxidative burst immediately after exposure, evidenced by approximately 1.6 fold increase in total ROS at 0 hr. ROS levels again rise to 2 fold at 4 hrs followed by a dip at 12 hrs and then again a profound ROS burst of 3-5 folds higher than control was noted between 24 to 36 hrs. ROS level was returned to normal at 48 hrs post-irradiation (Fig;4.1.7A&B). This is clear from our and other studies that IR not only leads to the generation of ROS derived from water radiolysis, immediately after irradiation but it also uses other biological sources to derive secondary and delayed subsequent ROS burst after several hours of exposure. The secondary generated ROS have a variety of physiological functions, including apoptotic signalling, which ultimately affects cellular integrity and survival (Sharma, Jha, Dubey, & Pessarakli, 2012). IL-6 pre-treatment significantly reduced the delayed ROS burst and avoided the later consequences. However, it does not counter the radiation-induced first ROS burst. Typically, electron leak from mitochondrial electron transport chain (ETC) complexes to molecular oxygen results in the generation of superoxide radical ($O_2^{\bullet -}$) and other

derivatives in mitochondria. Radiation-induced disturbance in mitochondrial bioenergetics also contributed to enhanced mitochondrial ROS production and delayed oxidative stress (Ježek, Cooper, & Strich, 2018). Therefore, we analyzed the mitochondrial ROS 24 hrs post-irradiation (Fig;4.1.7D). IR exposed cells showed 1.4 fold increased mitochondrial ROS as compared to control while; IL-6 pre-treatment significantly brought it down to the normal level (1.1 fold with respect to control).

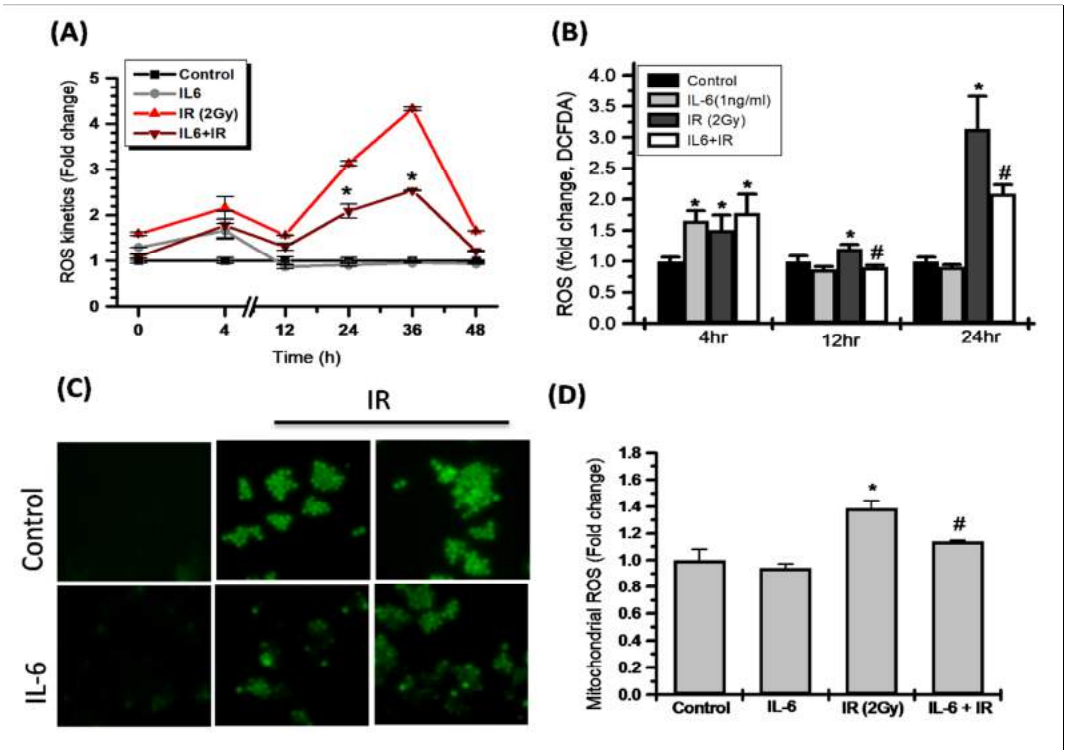

Figure 4.1.7: Modulation of radiation-induced ROS after IL-6 pre-treatment in RAW264.7 cells. (A & B) Total ROS kinetics estimated using CM-H2DCFDA (10µg/ml) from 0-48 hrs post-irradiation. (C) Photomicrograph is showing total ROS as DCF fluorescence at 24 hrs after radiation exposure. (D) Mitochondrial ROS at 24 hrs post-irradiation analyzed by Mitosox Red. Star shows significance w.r.t. the control group and # show significance w.r.t. to the IR group. Data points represent mean ± S.E.M from 3 independent experiments.

4.1.4.2 Assessment of radiation-induced macromolecular oxidation: An imbalance between the overproduction of ROS and the cell's antioxidant defence machinery is central to irradiation-induced cellular damage leading to apoptosis (Lee et al., 2007). We,

therefore, measured the levels of Malondialdehyde (MDA), protein carbonyl content and 8-hydroxy-2' -deoxyguanosine (8-OHdG) for lipid, protein and DNA oxidation, respectively as markers of oxidative stress-induced damages. RAW264.7 cells were irradiated with 2 Gy IR dose, and the lipid peroxidation marker MDA was measured at 4 and 24 hrs post-irradiation (Fig;4.1.8A). There was a slight increase at 4 hr post-irradiation however, a significant, 2 fold increase in MDA level was observed at 24 hrs post-irradiation. IL-6 pre-treatment reduced the radiation-induced MDA levels, nearly to the normal levels in combined treatment. The lipid peroxidation values were expressed as nanomoles of malondialdehyde (MDA) per mg of protein.

Further, we checked the carbonyl content of protein, a marker of protein oxidation (Fig;4.1.8B). Protein carbonylation is irreversible oxidative damage, often leads to loss of protein function (Dalle-Donne et al., 2006). Our study indicated that radiation causes a robust 3 fold increase (15.82±2.910 vs 5.04±0.473 nanomoles/mg protein) at 4 hrs time point, which further increased to approx. 7 fold increase (36.20±0.390 nanomoles/mg protein) with respect to control at 24 hrs post-irradiation. However, IL-6 pre-treatment to irradiated cells significantly reduced the protein carbonylation by approx. 35% at 4 hrs and 60% at 24 hrs post-irradiation, the corresponding values are 10.62± 0.89 and 14.56 ±2.468 nanomoles/mg respectively.

In the series of macromolecular damages caused by radiation, DNA oxidation is also a very important parameter to analyze radiation-induced macromolecular damage. The deoxyguanosine residue of DNA gets hydrolyzed at C-8 position to form 8-hydoxyguanosine (8-OHdG) by various oxygen radical producing agents like gamma radiation (Gao et al., 2019). The RAW264.7 cells were irradiated with 2Gy of radiation dose and DNA isolated at 1 and 4 hrs post-irradiation to analyze the levels of 8-OHdG

using competitive ELISA kit. The irradiated DNA samples showed 5 fold higher 8-OHdG level compared to un-irradiated control both at 1 and 4 hrs after irradiation which were estimated as 27±0.169 pg/ug and 15±0.149 pg/ug of DNA respectively (Fig;4.1.8C). IL-6 pre-treatment to irradiated cells significantly reduced the 8-OHdG content to 20.31±0.203 (approx. 30%) and 12.82±0.020 pg/ug of DNA at 1 and 4 hrs, respectively. It is essential to know here that IL-6 treatment alone also showed a marginally higher level of 8-OHdG (8.55±0.70 pg/ug of DNA), which could be due to relatively high ROS levels as compared to control in IL-6 treated sample (Fig;4.1.7A).

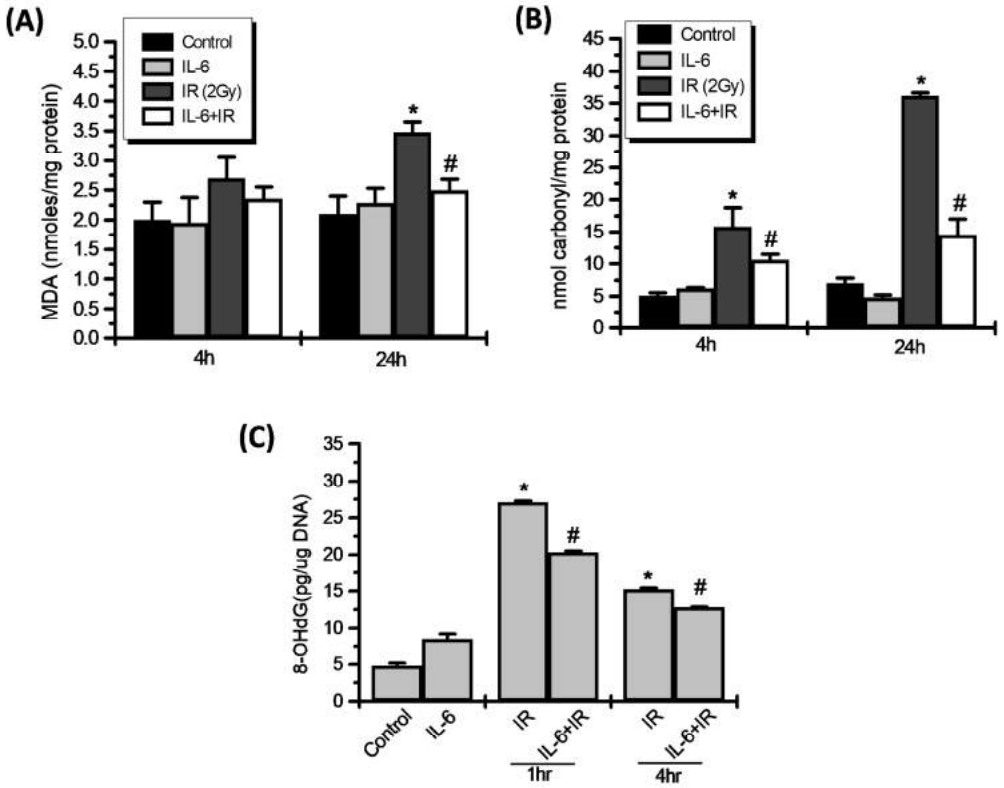

Figure 4.1.8: Assessment of macromolecular damage after irradiation (A) Lipid peroxidation measured as MDA content at 4 and 24 hrs post-IR (B) Protein Carbonyl content nmol/mg protein at 4 and 24 hrs post-IR (C) DNA oxidation measurement by 8-OHdG content at 1 and 4 hrs post-IR. Star shows significance w.r.t. the control group and # show significance w.r.t. to the IR group. Data points represent mean ± S.E.M from 3 independent experiments.

4.1.5 Evaluation of IL-6 induced Antioxidant defence mechanism:

IL-6 is not an anti-oxidant molecule, which can directly suppress the radiation-induced ROS. Therefore, we studied the mechanism of how IL-6 modulates the redox balance in radiation-induced oxidative stress; consequently, it is crucial to study the underlying defence mechanism. We estimated the total antioxidant capacity of cells under similar experimental conditions. A significant decrease in total antioxidant capacity in radiation sample was noted as 0.74±0.034 fold at 4 hrs and 0.76±0.019 at 24 hrs compared to un-irradiated control (Fig;4.1.9A). However, IL-6 pre-treatment was able to maintain the total antioxidant capacity at both the time points.

The major antioxidant defence molecule, Glutathione (GSH) efficiently scavenges free radicals like ROS and RNS moieties either directly or indirectly through enzymatic reactions. Notably, the thiol group of GSH (reduced glutathione) is very crucial for its antioxidant role, and in the direct scavenging of free radicals (Aquilano, Baldelli, & Ciriolo, 2014). Therefore we checked the levels of glutathione after irradiation and IL-6 treatment. Cells were treated with IL-6, followed by irradiation and harvested at different time points to estimate the levels of reduced glutathione at 4 and 24 hrs post-irradiation. IR significantly decreased the GSH levels at 24 hrs post-irradiation while there was noted only a slight dip at 4 hrs. However, IL-6 pre-treatment maintained and strengthened the GSH levels at both 4 and 24 hrs (Fig;4.1.9B). The corresponding values at 4 hrs are 2.4±0.04 of control, 2.6±0.25 of IL-6, 2.2±0.06 of IR alone and 2.6±0.14 of IL-6 plus IR. At 24 hrs, radiation alone has 2.3±0.1 and IL-6 plus IR have 3.2±0.04. Values were expressed as nanomoles/ug protein. This data suggested that IL-6 mediated elevation in GSH levels at 24 hrs post-treatment, played an essential role in recovering the cells from radiation-induced

oxidative stress. GSH is also known to involve in the detoxification of products derived from ROS mediated oxidation of lipids such as Malondialdehyde and 4-hydroxy-2-nonenal (4-HNE) (Aquilano et al., 2014). Therefore, increased GSH level is probably the reason for reduced macromolecular damage (Fig;4.1.8).

Being the crucial enzyme of antioxidant defence mechanism superoxide dismutase activity is requisite to make out the role of IL-6 in oxidative defence mechanism. The superoxide dismutase enzyme converts the highly toxic superoxide radicals to less toxic hydrogen peroxide, and its increased activity is shown to be radio-protective (Petkau, 1987). SOD activity declined to half (0.54±0.244) just after 4 hrs post-IR as compared to control (1±0.053), and IL-6 pre-treatment in irradiated samples maintained the SOD activity up to the control level (0.98±0.11). Further, at 24 hrs, nearly 1.7 fold and 2.6 fold significantly high SOD activity were estimated in IR and combined treatment with respect to control (Fig;4.1.9C). Apart from enzymatic studies, protein expression of SOD2 (manganese superoxide dismutase, MnSOD) was estimated at 24 hrs post-IR, under similar experimental conditions. Immunoblot results were in line with the enzymatic activity of total SOD, showed 2.5 fold reduction in SOD2 levels in IR alone group, which was comparable to control in IL-6 plus IR group (Fig;4.1.9D). The high levels of SOD2 in IL-6 treated irradiated in contrast to IR alone cells also suggested mitochondrial protection. The analysis of Nrf2 levels under similar experimental conditions showed that IL-6 induces Nrf2 signalling, which may be contributing to the maintenance of redox balance in radiation-exposed cells (Fig;4.1.9D). The Nrf2 expression was 1.4 fold in IL-6 alone, 1.6 fold in IR and 3.1 fold in IL-6 plus IR group with respect to the untreated control group at 24 hrs post-IR. Radiation is known to induce Nrf2 levels; however, IL-6

induced Nrf2 is not known. The up-regulated Nrf-2 suggested the activation of Nrf-2 mediated anti-oxidant defence.

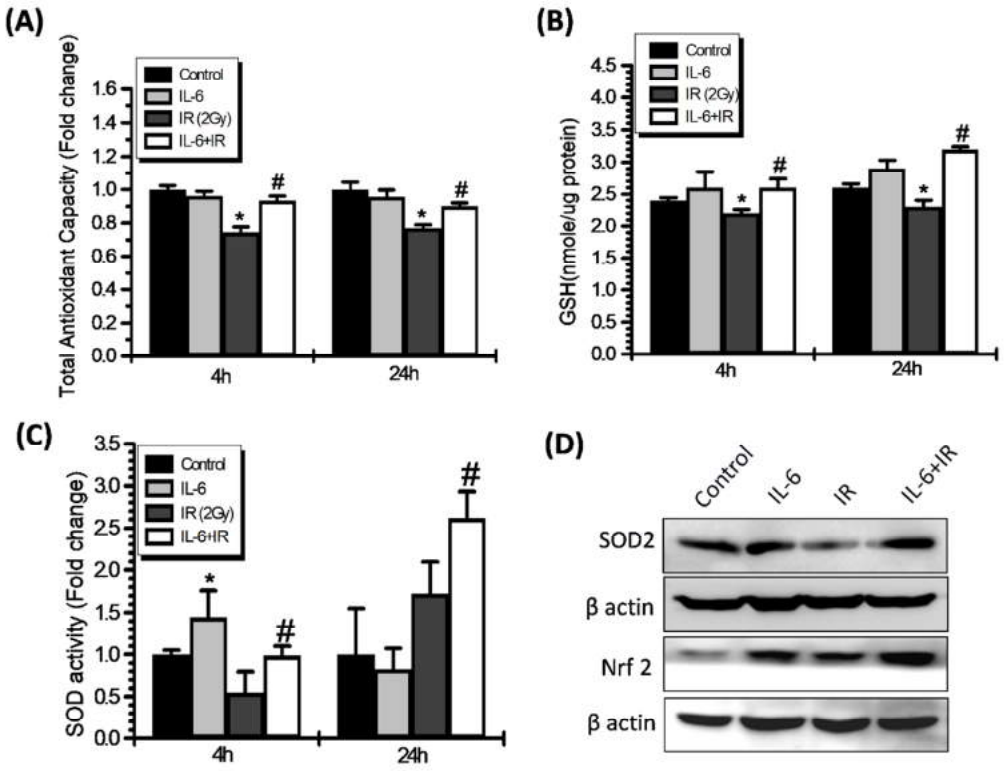

Figure 4.1.9: IL-6 induced modulation of antioxidant capacity post-irradiation (A) Relative fold change in total antioxidant capacity at 4 and 24 hrs post-IR (2Gy). (B) Graph showing reduced glutathione (GSH) levels calculated as nmoles/ug protein. (C) Relative fold change in superoxide dismutase activity at 4 and 24 hrs post IR (2Gy). (D) Immunoblots of SOD2 and Nrf2 at 24h post IR. Star shows significance w.r.t. the control group and # show significance w.r.t. to the IR group calculated by paired Student's t-test. Data are expressed as mean ± SD (n = 4) *#p <0.05

4.1.6 Modulation of ionizing radiation-induced Cell death by IL-6

It is established from decades that IR exposure triggers ROS production, and the resultant oxidative stress is due to an imbalance between the overproduction of ROS and the cellular antioxidant defence machinery which is pivotal in irradiation-induced cellular damage and thus, apoptosis (Lee et al., 2007). Therefore, our next aim was to

study the radiation-induced cell death parameters. Preliminary observations were made by dual staining of the cells with acridine orange and ethidium bromide (1:1) after 24 and 48 hrs of irradiation. The AO/EtBr staining results were correlated with growth kinetics at 24 hrs (Fig;4.1.3A). Radiation alone clearly showed more population of orange-red colour stained cells demarcated as apoptotic and necrotic cell population (Fig;4.1.10A). The number of dual positive cells (AO+EtBr) was significantly higher in the radiation alone group as compared to IL-6 pre-treated irradiated group in both the time points.

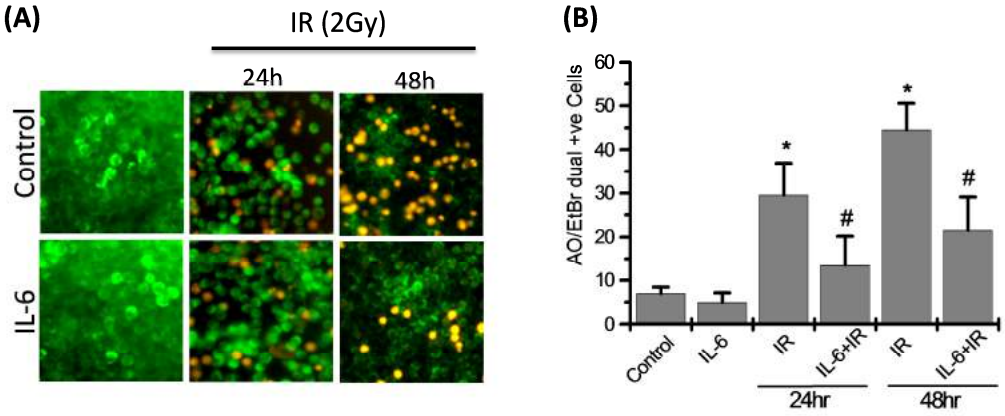

Figure 4.1.10: Analysis of radiation-induced apoptosis and its modulation by IL-6 using Acridine Orange/ Ethidium bromide staining for live and dead cells (A) in RAW264.7 cells at 24 and 48 hrs post-IR. Green fluorescent cells are live while the orange colour represents dead cells. (B) The graph plotted between groups showing the number of AO/EtBr +ve cells per view in RAW264.7 cells. The total of 10 views was analyzed to compute this data. Star shows significance w.r.t. the control group and # show significance w.r.t. to the IR group calculated by paired Student's t-test.

Next, we performed the quantitative validation of cell death induction by analyzing phosphatidylserine externalization using flow cytometry with annexin-V-Alexafluor 488 and propidium iodide staining, which differentiated the early and late apoptotic cell population. The cumulative apoptotic and necrotic population was approx. 62% in

radiation alone group with respect to IL-6 pre-treated irradiated group, having 46% (Fig 4.1.11). Here, the RAW264.7 cells showed a slightly higher percentage (12-13%) of annexin-V and PI (dual positivity) in control and IL-6 treated samples, though which is very low compare to irradiated cells. The percent apoptotic or dying population estimated by highly sensitive AnnexinV/PI assay was much higher than the EtBr/AO staining, however, the significant reduction in radiation-induced cell death offered by IL-6 was found similar, by the both cell death analysis assays.

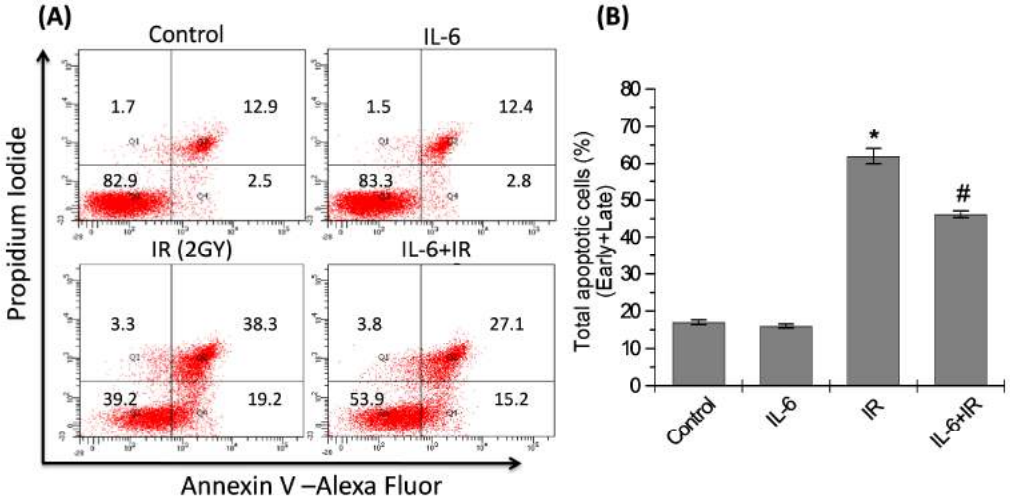

Figure 4.1.11: (A) Flow cytometric analysis of cell death by Annexin-V-Alexa Fluor and PI staining in RAW264.7 cells treated with IL-6 and IR (2Gy). The values given in quadrants represent the % cells in that particular quadrant (B) Total apoptotic cells (early+late) percentage shown by bar graph in the right panel. The experiment was performed 3 times in triplicates. Star shows significance w.r.t. the control group and # show significance w.r.t. to the IR group calculated by paired Student's t-test.

Further radiation-induced apoptosis was confirmed by the fluorescence microscopic evaluation of caspase 3/7 activity and by western blotting of cleaved caspase3 and PARP1 (poly [ADP-ribose] polymerase family, member 1) (Fig;4.1.12A&B). The Caspase 3 and 7 are serine proteases, which gets activated on cell death activation, and its activity is considered an important marker of cell apoptosis. In this

fluorescence assay, the activated caspase3/7 digest the peptide given, into a fluorescent peptide. Therefore, the cells with bright green nuclei represent activated caspase-3/7 in apoptotic cells, while the non-apoptotic cells (without activated caspase 3/7) carried no or very minimal fluorescent signal (J. Zhang et al., 2013). Further, the protein expression analysis of cleaved caspase and PARP confirmed the radiation-induced apoptosis. However, the extent of radiation-induced cleavage was considerably down in IL-6 pre-treated cells, suggesting a low number of apoptotic cells in IL-6 pre-treated sample (Fig;4.1.12A&B). This data further validates the results obtained by cell death assays that IL-6 minimizes radiation-induced cell death.

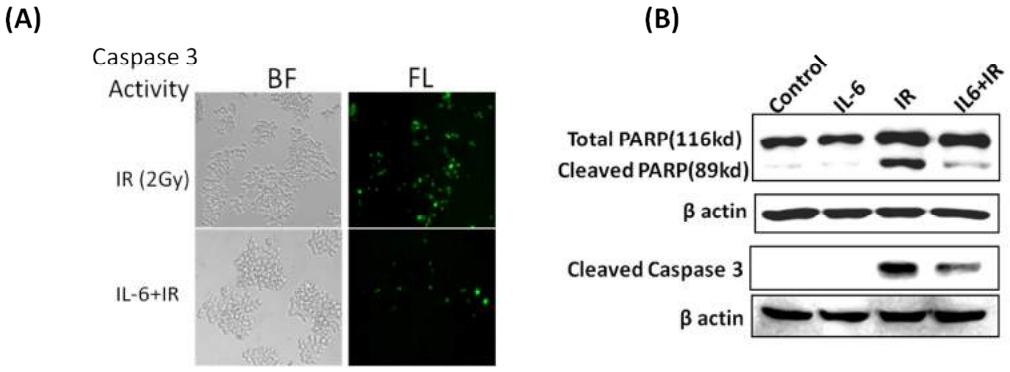

Figure 4.1.12: Analysis of apoptotic markers (A) Caspase 3/7 activity visualized by Cell Event™ Caspase-3/7 detection probe (5 μM) at 4hr post-irradiation. Images captured at 10x magnification in both white and fluorescence light (B) Immunoblots of PARP and Caspase 3 cleavage at 4 hrs post IR. Beta actin was the loading control.

Moreover, other markers of apoptosis, like p53, p21, Bax was also found to be increased in the radiation treatment group with respect to un-irradiated (Fig;4.1.13A), however IL-6 treatment appreciably resist the increase in these pro-apoptotic proteins. The balance between pro-apoptotic and anti-apoptotic proteins is essential for the apoptotic decision, the ratio of pro-apoptotic to anti-apoptotic factors is increased with oxidative stress, but the IL-6 pre-treatment may alter this ratio in favour of anti-

apoptotic signalling, leading to cell survival. IL-6 treatment not only decreases the expression of pro-apoptotic proteins but simultaneously increase the expression of anti-apoptotic proteins (Bcl2, Bcl-xl, Mcl-1) (Fig;4.1.13B). The Bcl2/Bax ratio was also significantly increased after IL-6 treatment evident as 1.37±0.08 fold in the IL-6 treatment group, 1.84±0.092 fold in IL-6 treatment plus irradiation group and 0.76±0.151 in radiation alone group concerning control 1.00±0.031 (Fig;4.1.13C).

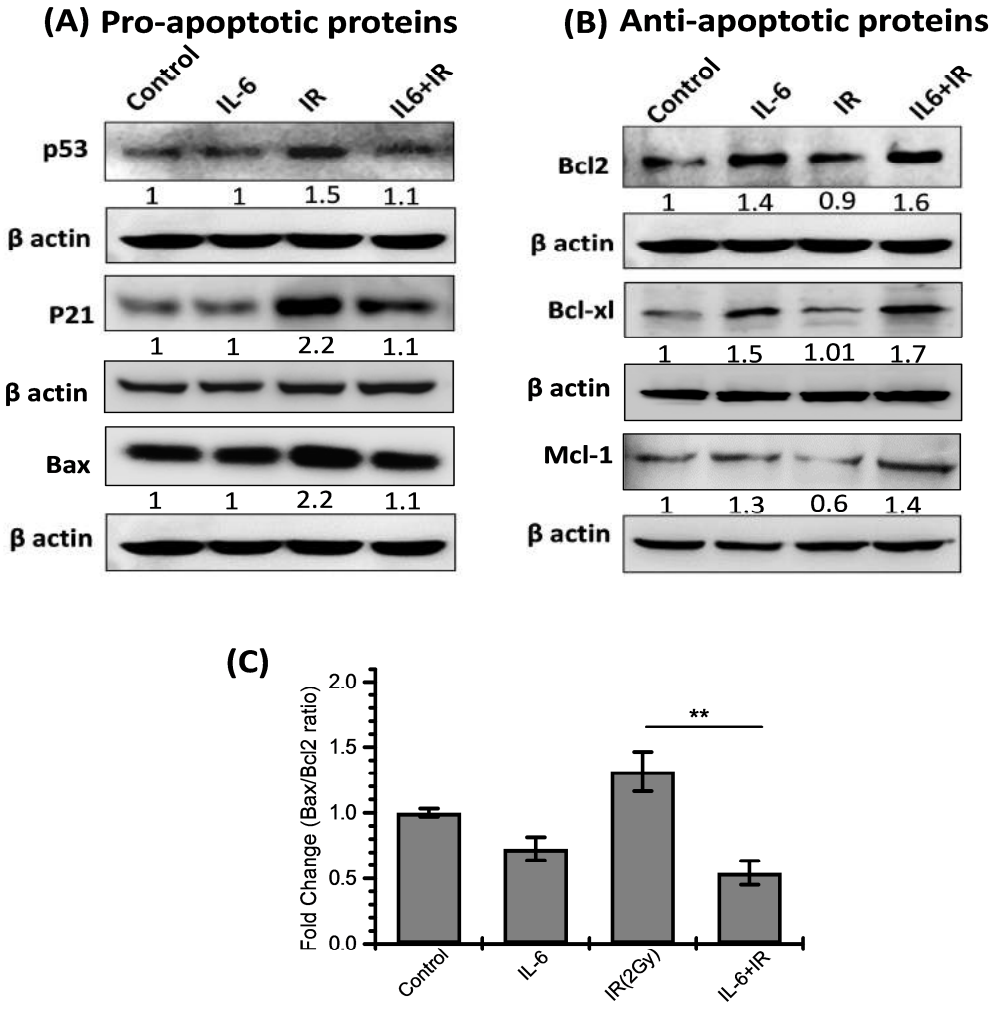

Figure 4.1.13: Analysis of apoptotic regulators (A & B) Immunoblots of P53, P21, Bax, Bcl2, Bcl-xl, Mcl-1 at 4 hrs post-irradiation. Values shown in between the blots are the average fold change value of densitometric analysis of 3 blots, normalized with respective β-Actin. (C) Relative fold change in Bax/Bcl2 ratio. Datapoint derived from 3 independent experiments.

4.1.7 Role of STAT-3 signalling in IL-6 mediated radioprotection:

IL-6 induced STAT-3 activation is the main leading pathway that further regulates the downstream proteins. In cancer cells, it is known to cause chemo and radio-resistance (Kumari et al., 2016). We performed a time-dependent and concentration-dependent induction of STAT-3 phosphorylation (Tyr705) in the presence of IL-6. We observed an increased level of phosphorylation with increasing concentration of IL-6 from 0.1 to 10ng/ml. Moreover, we found phosphorylation of STAT-3 as early as 30 min post-IL-6 treatment and remain phosphorylated up to 2 hrs (Fig;4.1.14A). Further, alone radiation treatment was not able to induce the STAT-3 phosphorylation at any time point (Fig;4.1.14B). The pSTAT-3 levels were normalized by STAT-3 and Beta actin. STAT-3 after phosphorylation undergoes dimerization and subsequent localization to nucleus, where it triggers the transcription of target genes and regulates multiple pathways. Therefore, we checked the translocation of pSTAT-3 to the nucleus. Western blot analysis exhibited differential expression of pSTAT-3 in cytoplasm and nucleus at 1 and 4 hrs post IL-6 treatment having more expression in cytoplasm and less in the nucleus at 1 hr or vice versa at 4 hrs (Fig;4.1.14C). Thus, it suggested the activation and translocation of STAT-3 to the nucleus, which might result in the activation of pro-survival signalling. Subsequently, STAT-3 mediated activation of pro-survival signalling was confirmed by using a pharmacological inhibitor of pSTAT-3 (JSI 124). Cells treated with JSI 124 (10µM) 15 min prior to IL-6 treatment prevented the IL-6 mediated phosphorylation of STAT-3 hence, reverted radioprotection (Fig;4.1.14D). Cells counted at 48 hrs post-irradiation showed reduced cell number in JSI-124 plus IL-6 plus IR treated group compared to IL-6 plus IR group as 0.405±0.031 and 0.60±0.05, respectively. While untreated, IL-6 treated,

and IR treated groups had 1.27±0.125, 1.30±0.085, and 0.43±0.053 cells correspondingly (Fig;4.1.15A). STAT-3 inhibition not only alters cell number, but it also modulated pro and anti-apoptotic proteins expression. The intensity of pro-apoptotic proteins like cleaved PARP, cleaved Caspase 3, Bax was reversed along with anti-apoptotic proteins (Mcl-1, Bcl2, Bcl-xL) after JSI-124 treatment to IL-6 plus IR treated group (Fig;4.1.15B&C). These results suggested the involvement of STAT-3 signalling in IL-6 induced radioprotection.

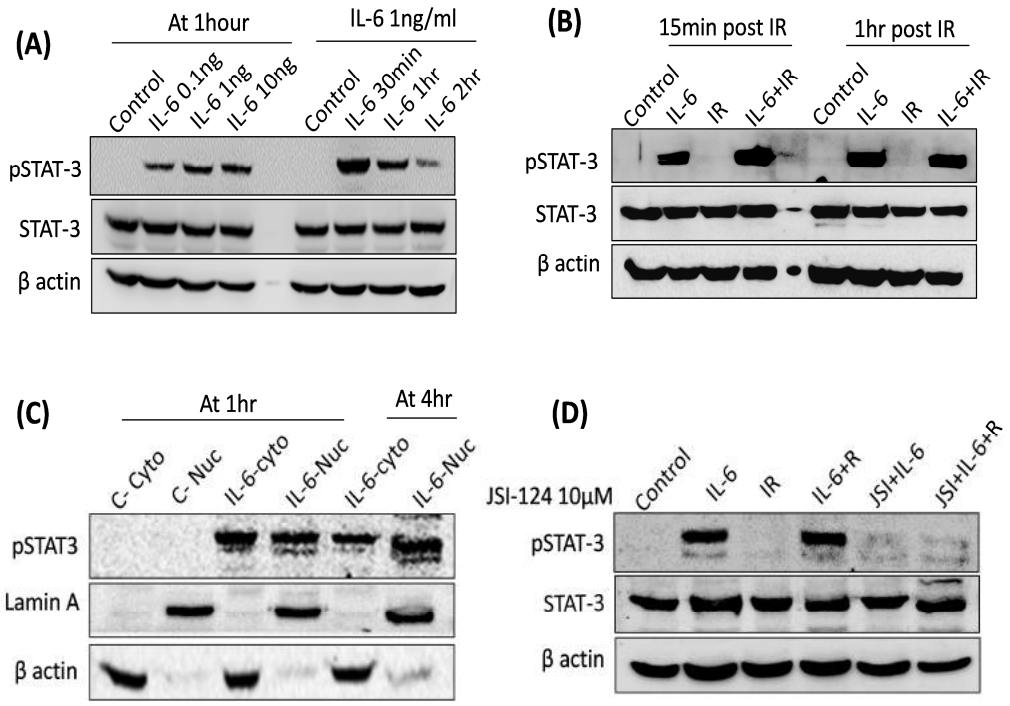

Figure 4.1.14: Activation of STAT-3 Signalling (A) Immunoblot of STAT-3 phosphorylation (Tyr705) at various concentrations of IL-6 (1-10ng/ml) and at multiple time points (0.5 to 2 hour). (B) Immunoblot of STAT-3 phosphorylation after IL-6 treatment (1ng/ml) and irradiation (2Gy) (C) Immunoblot showing nuclear translocation of phospho STAT-3 after IL-6 treatment. (D) Immunoblot showing Inhibition of STAT-3 phosphorylation by JSI 124 (10μM) given just 15 min prior to IL-6 treatment. pSTAT-3 levels were normalized with total STAT-3 levels. Lamin A and Beta actin were loading controls for nuclear and cytosolic proteins, respectively.

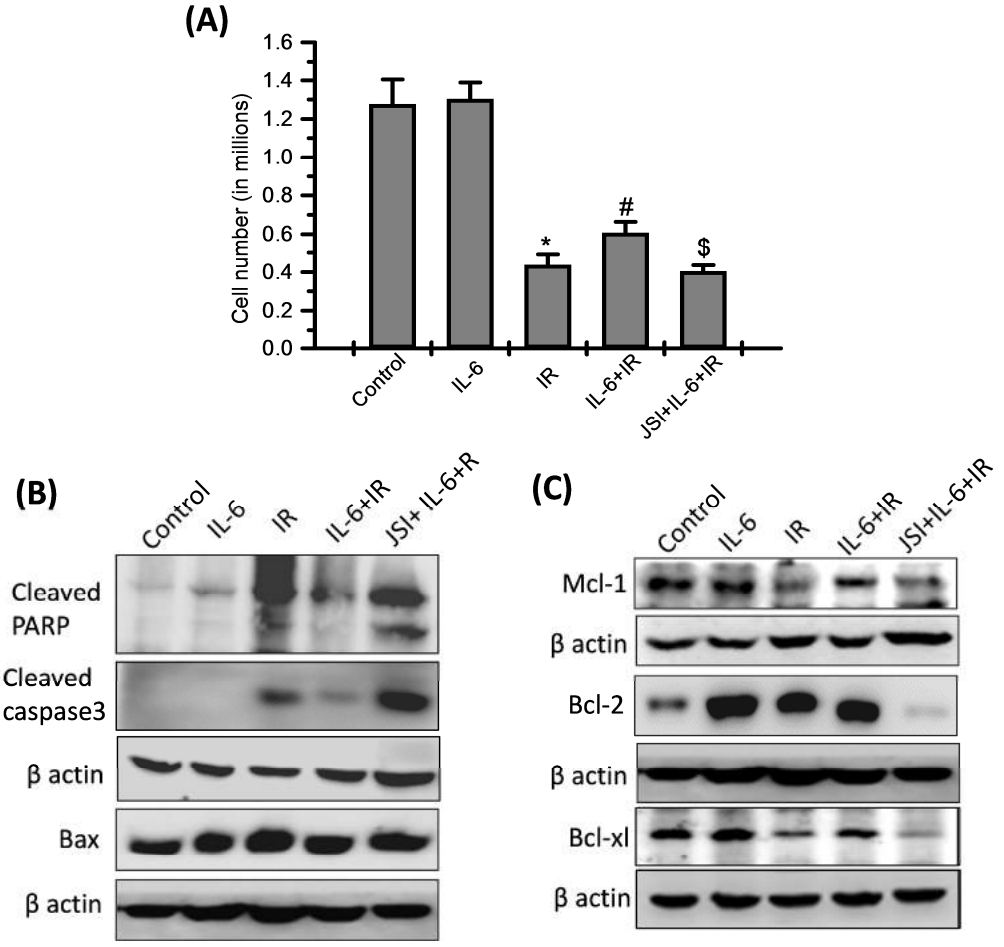

Figure 4.1.15: STAT-3 inhibition reverses the IL-6 mediated radioprotection (A) The cell number in control and treatment group was quantified at 48 hrs post-irradiation and graph presented on a linear scale as cell number in millions on the Y axis. (B & C) Immunoblots performed after STAT-3 inhibition. Star shows significance w.r.t. the control group, # shows significance w.r.t. to the IR group, and $ shows significance w.r.t. IL-6+IR group calculated by paired Student's t-test. Data are expressed as mean ± SD (n = 4) *p <0.05

4.1.8 Summary

This study summarizes as; IL-6 treatment phosphorylates STAT-3, a transcription factor that enters to the nucleus and facilitates cell survival and proliferation by reducing radiation-induced ROS generation, activation of antioxidant defence machinery and modulates pro- and anti-apoptotic proteins. The antioxidant defence mechanism is probably via Nrf2 activation. Further, the inhibition of STAT-3

phosphorylation by JSI-124 results in loss of STAT-3 activation and dimerization followed by nuclear translocation. Hence, IL-6 mediated protection abolished, and cells get sensitized to irradiation.

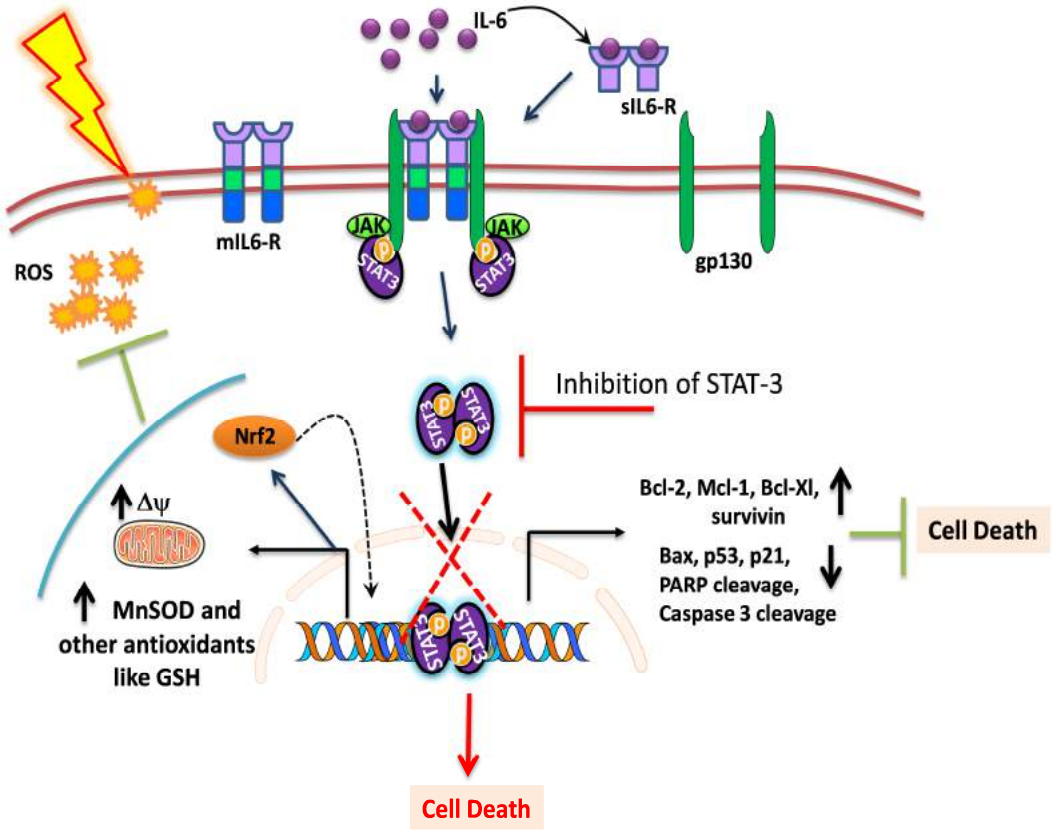

Figure 4.1.16: IL-6 in resisting oxidative stress and cell death; IL-6-induced JAK/STAT-3 facilitates the translocation of STAT-3 in the nucleus, which activates antioxidant defence pathways such as Nrf2 and leads to reduction in oxidative stress followed by macromolecular damage. IL-6 signalling results in the enhanced expression of anti-apoptotic genes (Bcl-2, Bcl-xL, Mcl-1, survivin,etc.) and reduction in pro-apoptotic proteins (Bax, p53, cleaved PARP and cleaved caspase).

4.2 Interleukin-6 confers radio-resistance by inducing Akt mediated glycolysis and reducing mitochondrial damage in cells

Introduction

Enhanced aerobic glycolysis is one of the prominent phenotypes of a majority of cancer cells which facilitate proliferation and confer protection against death, besides energy production (Bhatt et al., 2015). This induced glycolysis is one of the significant factors that contribute to IL-6-induced therapeutic resistance in cancer. The cancer cells and also the normal cells during various types of stress primarily depend on glycolysis for energy production even in the presence of oxygen, due to faster rate of ATP synthesis, this phenomenon is known as Warburg effect (Warburg, 1956). Moreover, glycolysis over the oxidative phosphorylation is the predominant pathway of energy metabolism in all the cells involved in the inflammatory response. Hence, it is clear that this phenomenon of aerobic glycolysis, which was initially discovered in cancer cells, is not restricted to cancer cells only. Therefore we investigated metabolic switch toward glycolysis in RAW264.7 cells, we treated RAW264.7 cells with IL-6 and examined the glycolytic flux. Increased expression of mRNA and protein levels of key glycolytic enzymes was observed after IL-6 treatment, which conferred glycolysis dependent resistance from radiation-induced cell death. We further investigated the role of IL-6-Akt signalling in IL-6 mediated glycolysis, and also studied the effect of IL-6 induced glycolysis on radiation-induced mitochondrial damage.

4.2.1 IL-6 induces Glycolysis

We first tested if IL-6 can induce glycolysis in Raw 264.7 cells. Thus we measured glucose uptake using non metabolizing, fluorescent glucose analogue 2-NBDG (2-(*N*-(7-Nitrobenz-2-oxa-1,3-diazol-4-yl)Amino)-2-Deoxyglucose) in RAW264.7 cells. IL-6 treatment

showed significant increase in glucose consumption at both 1 and 10 ng/ml IL-6 with highest 1.5 fold consumption at 1ng/ml (Fig;4.2.1A). Therefore, it was confirmed that 1ng/ml concentration of IL-6 is precise to use for other experiments. Consequently, lactate production, which is the end product of glycolysis was also increased by 1.65 fold after IL-6 treatment (Fig;4.2.1B). Further to understand if the high rate of glycolysis is achieved by IL-6 induced enhanced levels of glycolytic enzymes, we checked the levels of key glycolytic enzymes HK-1, HK-2, PFK-1 and PKM2 after IL-6 treatment.

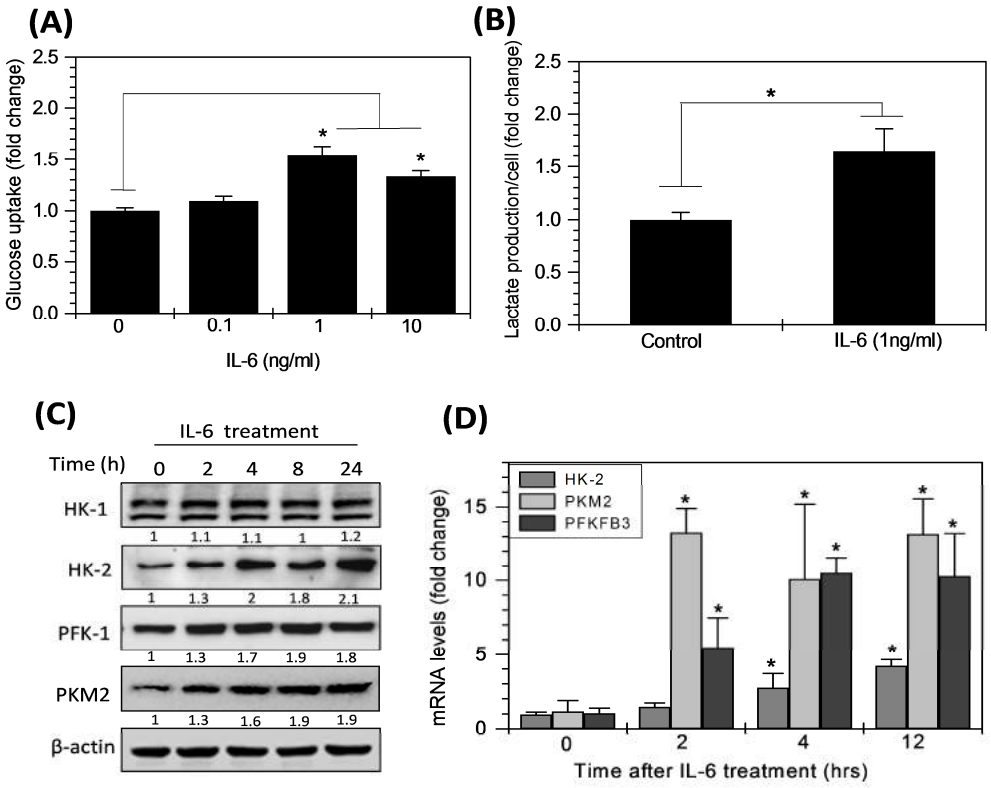

Figure 4.2.1: IL-6 induced rate of glycolysis was measured by observing glucose uptake and lactate production in cells after IL-6 treatment. Glucose uptake (A) and lactate production (B) was measured in culture media, 2 hours after IL-6 treatment. (C) Protein levels of various glycolytic regulatory enzymes (indicated in figure) were measured in untreated and IL-6 (1ng/ml) treated cells at given time points. β-Actin was used as loading control. Values shown in between the blots are the average fold change value of densitometric analysis of 3 blots, normalized with respective β-Actin. (D) The mRNA levels of HK-2, PKM2 and PFKFB3 genes at indicated time points after IL-6 (1ng/ml) treatment. Statistical significance calculated by one way ANOVA and Student's t test between the groups. Data are expressed as mean ± SD (n = 4) *p <0.05

We found nearly 1.3 to 2 fold time-dependent increase in the protein levels of HK-2, PFK-1, and PKM2, while the protein level of HK-1 was found unchanged (Fig;4.2.1C). Enhanced levels of HK-2 and PKM2 protein was further supported by the time-dependent increase in HK-2 and PKM2 mRNA levels (Fig;4.2.1D).We also checked the IL-6 induced gene expression of PFKFB3 gene, which produces Glucose 2,6 bis phosphate (G2,6BP) for allosteric activation of PFK-1 enzyme (Berg JM, Tymoczko JL, 2002) We found, IL-6 induced the mRNA levels of PFKFB3 gene also, suggesting it regulates the flow of glucose through glycolysis (Fig;4.2.1D). These findings suggest that IL-6 induces glycolysis by inducing the expression of glycolytic regulatory enzymes in RAW264.7 cells.

Since a significant and nearly equal increase in glucose consumption and radioprotection (Fig;4.1.2) were observed at both 1ng/ml and 10 ng/ml doses of IL-6; therefore we used 1 ng/ml concentration for all further experiments.

4.2.2 IL-6 induced radio-resistance is glycolysis dependent

Further, to validate the correlation between IL-6 induced glycolysis and radio-resistance; we analyzed the levels of glucose uptake and lactate production after radiation exposure in IL-6 pre-treated samples. Radiation alone group also showed increase in glucose uptake; however, it was significantly less (~1.5 fold) as compared to IL-6 alone and combined (IL-6 pre-treatment followed by irradiation) treatment groups (~2 fold) (Fig;4.2.2A). Similarly, the lactate production was also found significantly higher in IL-6 and radiation combined treatment as compared to radiation-exposed cells (Fig;4.2.2A). This result is substantiated by several fold increased protein levels of glycolytic enzymes (HK-2, PFK-1, PKM2), glucose transporter GLUT4 (Fig;4.2.2B) and mRNA expression of HK-2, PKM2 and PFKFB3 gene (Fig;4.2.2C) in cells co-treated with IL-6 and radiation as compared to radiation alone. We also found about 1.9 fold increased ATP level at 4 hours post-irradiation in IL-6 pre-treated cells with respect to control and radiation alone (Fig;4.2.2D).

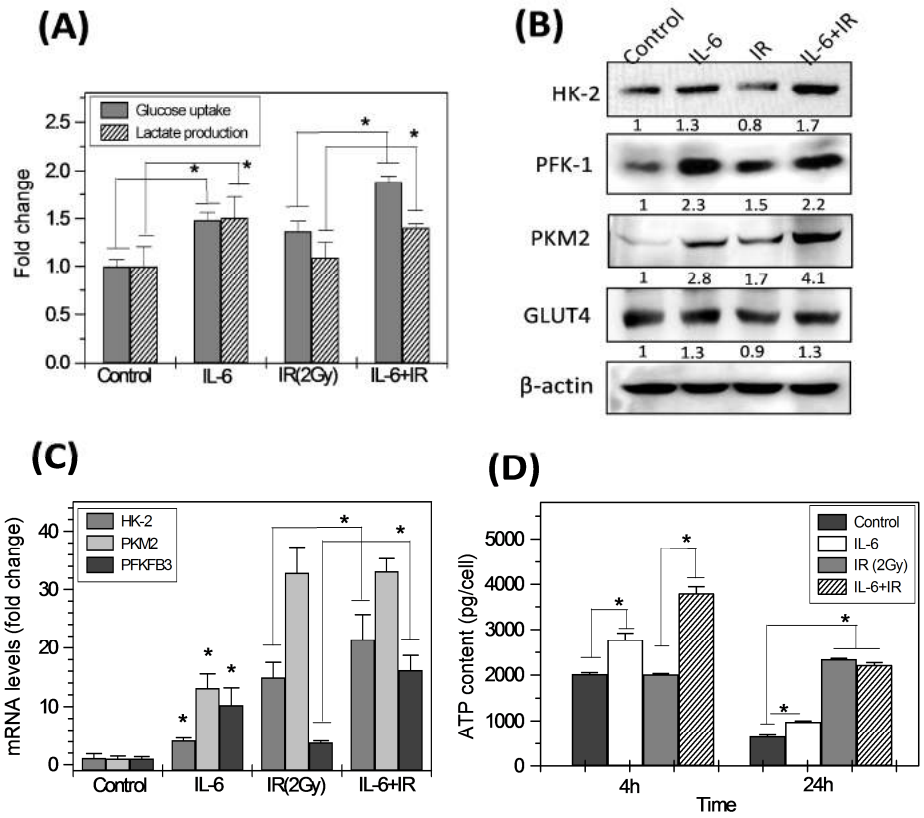

Figure 4.2.2: IL-6 induced radio-resistance is glycolysis dependent; (A) Glucose uptake, and lactate production measured 2 hours post-irradiation, as described (B) Immunoblotting of key regulatory glycolytic enzymes was performed at 24 hours post-irradiation. β-Actin was used as loading control. Values shown in between the blots are the average fold change value of densitometric analysis of 3 blots, normalized with respective β-Actin. (C) The mRNA levels of HK-2, PKM2 and PFKFB3 with respect to control were observed after 12 hours post-irradiation (D) ATP levels in cells was measured by bioluminescence ATP assay kit at indicated time points and represented as ATP concentration per cell calculated from standard.

We further inhibited the glycolysis using non-toxic concentrations of 2-dexoy-D-Glucose (2-DG) and 3-bromo pyruvate (3-B4.1P) in IL-6 pre-treated cells before exposing to radiation and performed growth kinetics. Both the glycolytic inhibitors 2-DG and 3-BP reversed the IL-6 induced protection from radiation-induced cell death (Fig;4.2.3A&B). This observation from growth kinetics assay was correlated with qualitative imaging of ethidium bromide and acridine orange (apoptosis assay) at 24 hours. Radiation alone and in combination with glycolytic inhibitors (2-DG and 3-BP) in IL-6 pre-treated group

showed nearly similar number of apoptotic and necrotic cell population, which was significantly higher as compared to IL-6 pre-treated and radiation-exposed treatment group (Fig;4.2.3C&D). Therefore, these findings evidently validate our earlier observation that induced glycolysis confers radio-resistance. It also suggests that IL-6 induced radio-resistance in RAW264.7 cells is glycolysis dependent.

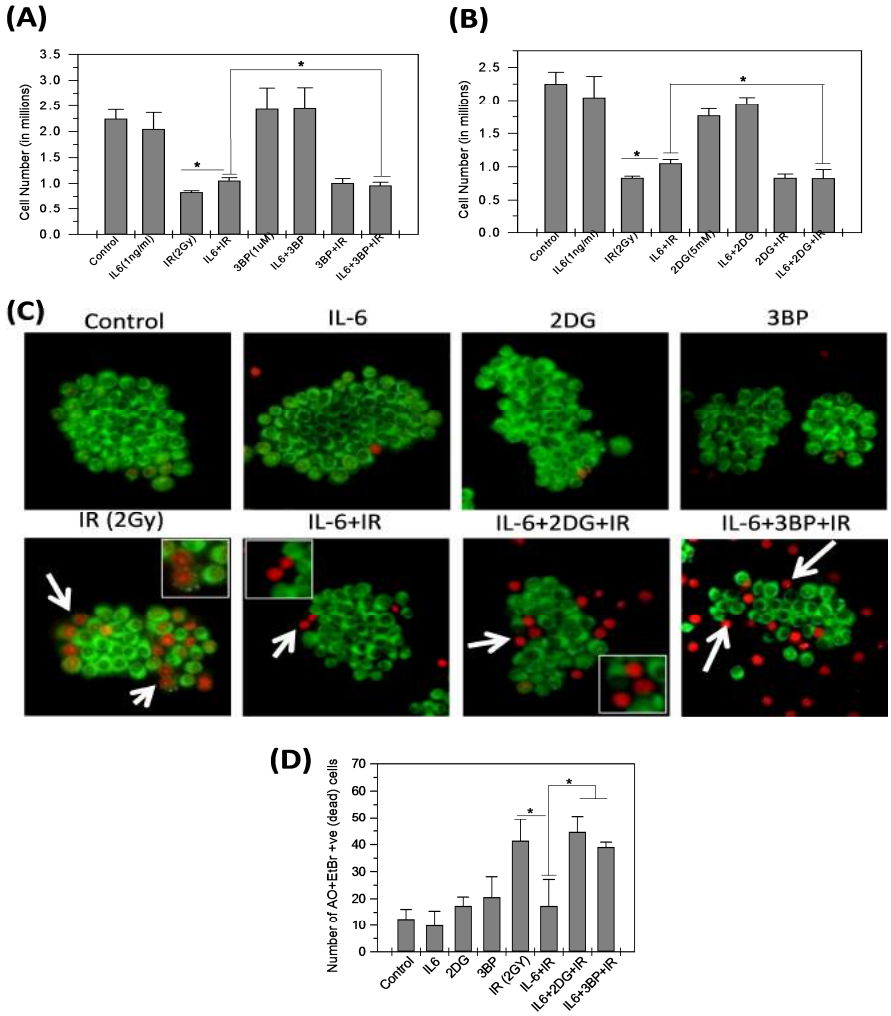

Figure 4.2.3: Inhibition of glycolysis reverted the IL-6 mediated radioprotection; (A & B) Cell number was quantified at 48 hrs. post-irradiation in various treatment groups and plotted as bar graph with cell number on Y axis. (C & D) Cells were stained with AO/EtBr 24 hr post-irradiation and examined under a fluorescent microscope at 10x magnification. Zoomed images of dying cells are shown in inset for an improved view. Dead cells (red) were counted from multiple images and the mean of dead cells per group was plotted as bar graph. Star shows the statistical significance of change between the groups calculated by Student's t-test. Data are expressed as mean ± SD (n = 4) *p <0.05

4.2.3 IL-6 protects from radiation-induced mitochondrial damage

Ionizing radiation is known to damage mitochondria and affect its energy metabolism (Rai et al., 2018; Verma et al., 2011). Therefore, we tested if IL-6 protects from radiation-induced mitochondrial damage also. To test the mitochondrial energy metabolism, we analyzed complex II activity of mitochondrial respiratory chain by monitoring formazan formation. We found, radiation induces nearly 2.5 fold increased formazan formation in IL-6 untreated and treated cells at early time point (4hr), which comes down to normal at later time point (24hr, Fig;4.2.4A). Mitochondrial enzymatic activity depends on the mitochondrial mass in cells and we have shown in our earlier study that radiation-induced mitochondrial damage can induce mitochondrial biogenesis and thereby increases the mitochondrial mass and formazan formation in cells (Rai et al., 2018). Interestingly, we noted nearly similar formazan formation in IL-6 untreated and treated cells after radiation exposure from 1.8 and 1.25 fold increased mitochondrial mass, respectively (Fig;4.2.4B). This observation shows that radiation-exposed cells have 80% more mitochondrial mass, but all may not be contributing to enhanced complex II activity. However, similar formazan formation from only 25% increased mitochondrial mass and nearly similar SDH level (Fig;4.2.4C&D) after radiation exposures in IL-6 pre-treated cells as compared to radiation alone exposed cells suggest reduced mitochondrial damage and higher efficiency of mitochondrial respiration in IL-6 pre-treated cells.

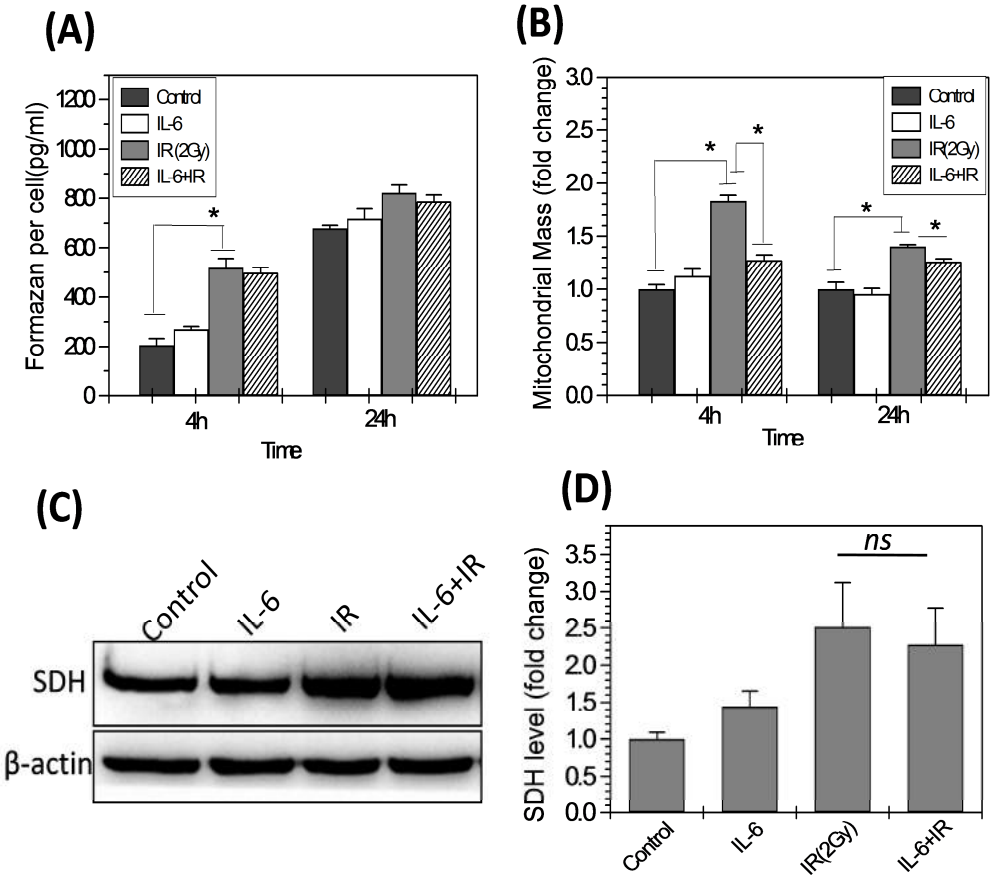

Figure 4.2.4: IL-6 prevents mitochondrial damage from radiation (A) The Formazan formed per cell was quantified spectro-photometrically and presented as bar graph at indicated time points. (B) The mitochondrial mass was analyzed by staining cells with MitoTracker Green FM (100 nM; 20 min) at indicated time points. Graph showing mean fluorescence intensity (MFI), presented as fold change with respect to control. (C&D) Immunoblot showing protein expression of mitochondrial complex-II subunit SDH-A presented in RAW264.7 cells. The bar graph represents the fold increase in SDH levels quantified by densitometry and normalized with β-Actin.

Further, we also analyzed the mitochondrial membrane potential (MMP) under similar experimental conditions to examine the mitochondrial status in radiation-exposed cells using fluorescent potentiometric dyes JC-1 and TMRM (Fig;4.2.5A&B). We observed radiation-induced increased MMP in IL-6 and radiation treated cells (Fig;4.2.5A); however, radiation-induced hyperpolarized mitochondria and increased mitochondrial mass (Fig;4.2.5B) can also show higher dyes uptake in cells giving false information of higher MMP (Rai et al., 2018). Therefore, we normalized the MMP values with mitochondrial mass of the respective sample to obtain the accurate MMP of the cells. When radiation-induced increased MMP was normalized with enhanced mitochondrial mass, it showed significant 30% decrease in MMP, which was restored in IL-6 pre-treated and radiation-exposed samples both at 4 and 24 hours (Fig;4.2.5B). This was further validated by microscopic observation of radiation-induced damaged mitochondria using A23187 dye (Verma et al., 2011). We found highly reduced numbers of A23187 puncta positive cells and much smaller intracellular bodies (showing damaged mitochondria) in IL-6 pre-treated cells as compared to radiation alone (Fig;4.2.5C&D). Interestingly, glycolysis inhibition using 2-DG in IL-6 pre-treated cells reverses the protective effects of IL-6 from radiation-induced mitochondrial damage. These observations suggest that IL-6 protects from radiation-induced mitochondrial damage and this protective effect is also linked with IL-6 induced glycolysis.

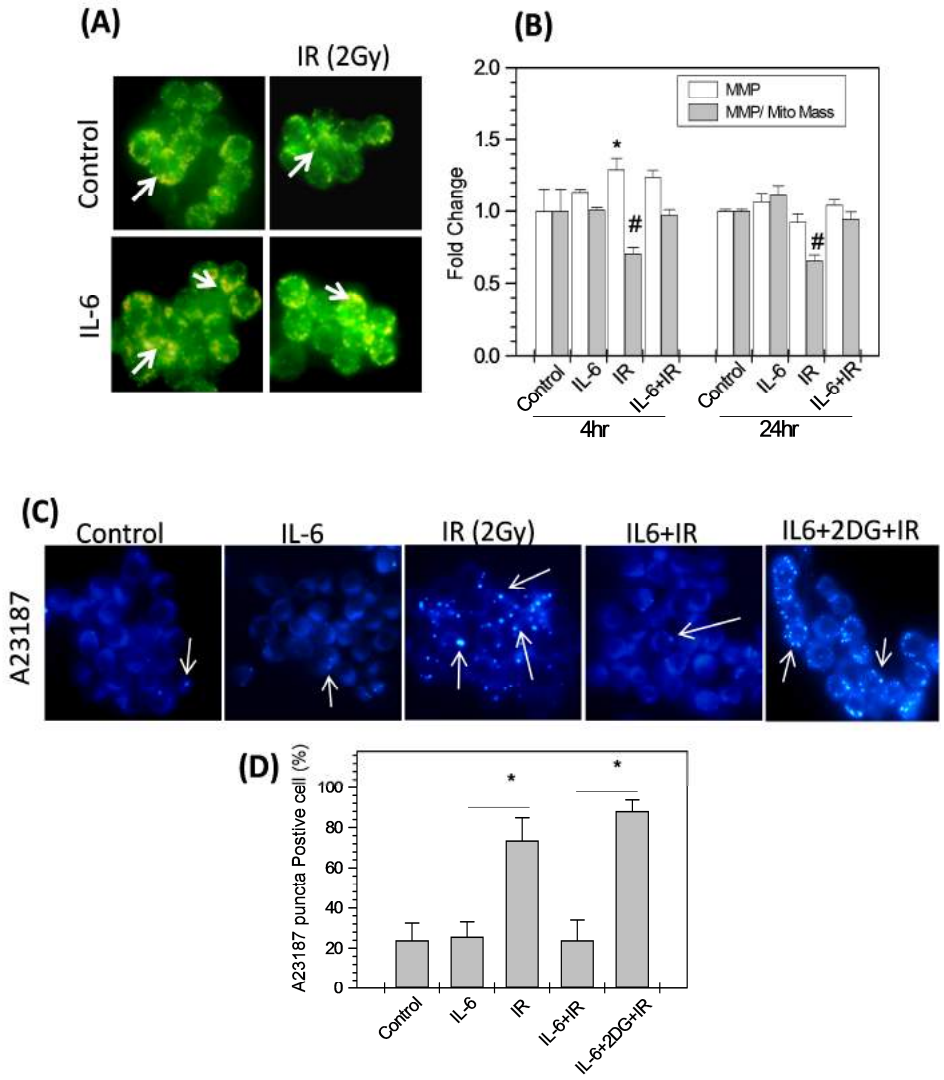

Figure 4.2.5: IL-6 prevents mitochondrial damage from radiation (A) Microscopic evaluation of mitochondrial membrane potential shown by distribution of JC-1-loaded mitochondria in response to radiation, the retention of green (monomer) and orange/yellow (aggregates) colour represents the shift in mitochondrial membrane potential. Images were captures at 40x (objective) and 10x (eyepiece) magnification. (B) Quantitative estimation of MMP by TMRM and normalized with respective mitochondrial content (data obtained from Mitotracker green, fig;4.2.4B) at 4 and 24h post-irradiation. (C) Photomicrograph shows the radiation change in mitochondrial calcium by staining the cells with A23187 (6 μM, 30 mins). Images were captured under a fluorescence microscope with 40X objective. (D) Graph representing quantification of I-bodies formation per cell in different treatment groups. Data obtained from n=10 fields per group. Star shows the statistical significance of change between the groups calculated by Student's t-test. Data are expressed as mean ± SD (n = 4) *p <0.05, # represents the significance with respect to the MMP/ mitochondrial mass of control group.

4.2.4 IL-6 induced Akt signalling promotes glycolysis and confers radio-resistance

Enhanced glycolytic metabolism is known to be regulated by two main signalling pathways in normal cells namely, HIF1α and Akt. IL-6 activates both HIF1α and Akt signalling pathway (Kumari et al., 2016; F. Zhang et al., 2016). Whereas, we found that IL-6 at 1ng/ml concentration does not induce detectable levels HIF1α in RAW264.7 cells. Therefore, we tested Akt pathway by estimating the time-dependent protein levels of pAkt (active form) in IL-6 treated cells. We found more than 2 fold increase in pAkt levels as early as 1 hr. of IL-6 treatment (Fig;4.2.6A). Further, to authenticate if IL-6 induced radio-resistance is dependent on Akt signalling and enhanced glycolysis mediated by it; we inhibited Akt signalling using pan Akt inhibitor MK2206 (Oki et al., 2015) and also knock down the Akt expression (53% depletion in Akt1/2 level) using Akt1/2 siRNA. Downregulation of Akt signalling not only reduced the IL-6 induced pAkt levels to un-induced basal level (Fig;4.2.6B) but also significantly brought down the level of IL-6 induced glucose uptake, and lactate production to the basal level (Fig;4.2.6C). Further, low pAkt level reduced the IL-6 induced total and mitochondrial bound fraction of HK-2 (Fig;4.2.6D&F) and reversed the IL-6 induced radio-resistance, indicated by significant reduction in cell number of IL-6 pre-treatment combined with Akt1/2 siRNA and MK2206 in irradiated cells nearly to the level of radiation control (Fig;4.2.6E). These results suggest that IL-6 induced Akt signalling upregulate the levels of glycolytic enzymes, which leads to enhanced glycolysis and radio-resistance in RAW264.7 cells.

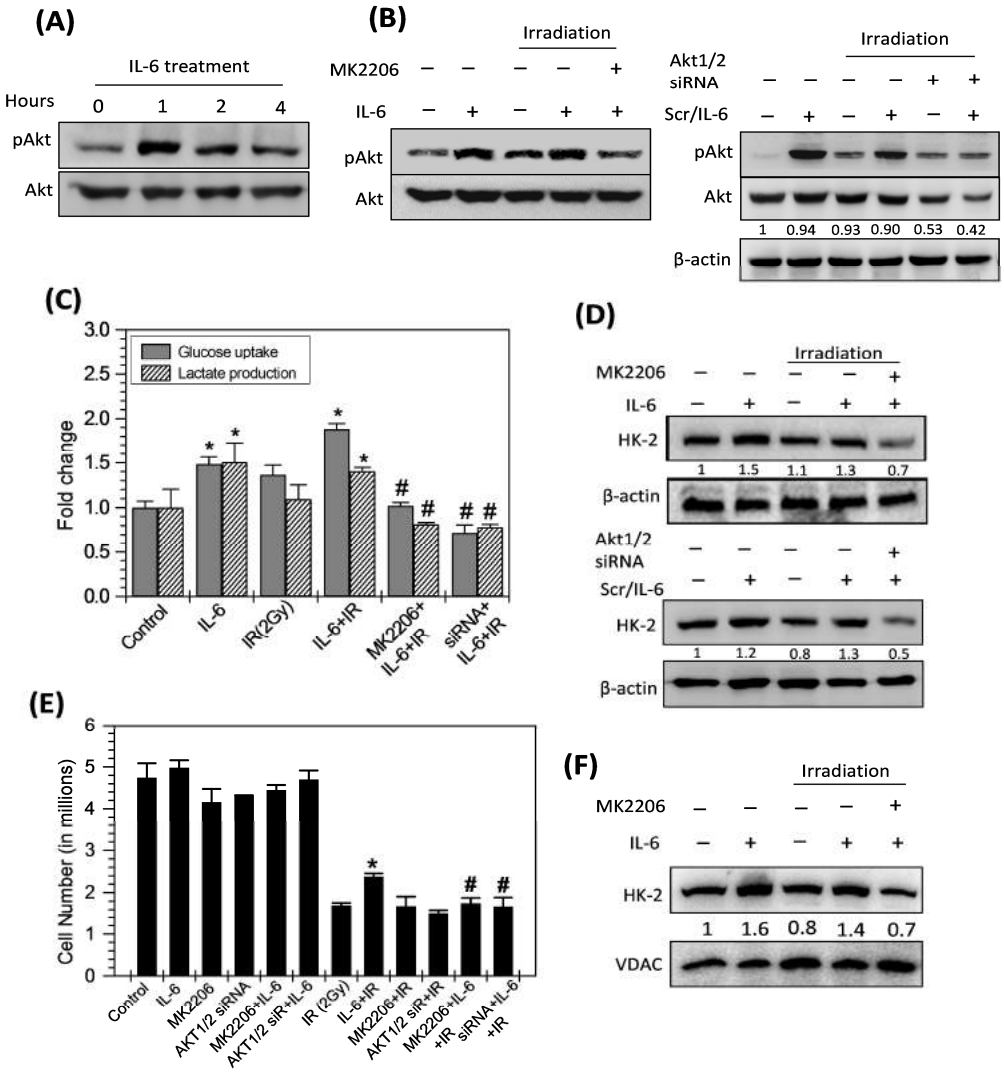

Figure 4.2.6: IL-6 induced glycolysis is Akt dependent (A) Phosphorylation of Akt at ser473 was detected at indicated time points after IL-6 treatment. (B) Cells treated with MK2206 (2.5uM) 15 min prior to IL-6 treatment followed by irradiation were harvested 1hr post-irradiation for Western blotting. Akt1/2 siRNA (100nM) and Control (scramble) siRNA transfected cells were also treated with IL-6 followed by irradiation and harvested for Western blotting of pAkt and Akt levels. Total Akt levels was normalized with the values of beta actin (loading control). (C) Graph represents fold change in glucose uptake and lactate production per cell respectively in various treatment groups at 2hr post-irradiation. (D) Immuno-blot of total HK-2 protein with MK2206 and Akt siRNA. β-Actin used as loading control and (E) Cell number quantified at 48 hr. post-irradiation in various treatment groups is presented as bar diagram. (F) Showing immunoblot of mitochondrial bound fraction of HK-2 where VDAC used as loading control. Values shown in between the blots are the average fold change value of densitometric analysis of 3 blots, normalized with respective β-Actin. Star shows the statistical significance of change between the groups calculated by one way ANOVA and Student's t test. # represents the statistical significance between siRNA or MK2206 group with respect to IL-6 pre-treated irradiated group. Data are expressed as mean ± SD (n = 4) *p <0.05

4.2.5 Summary

The results of this study suggest that IL-6 induced the glycolysis in RAW264.7 cells by activating Akt signalling, which further induced the expression of key regulatory glycolytic enzymes and glucose trans-porters. The IL-6-induced aerobic glycolysis and reduced mitochondrial damage at the time of radiation exposure ensures continuous and sufficient supply of energy for repair of radiation-induced macro-molecular and cellular damages, thereby causing radio-resistance.

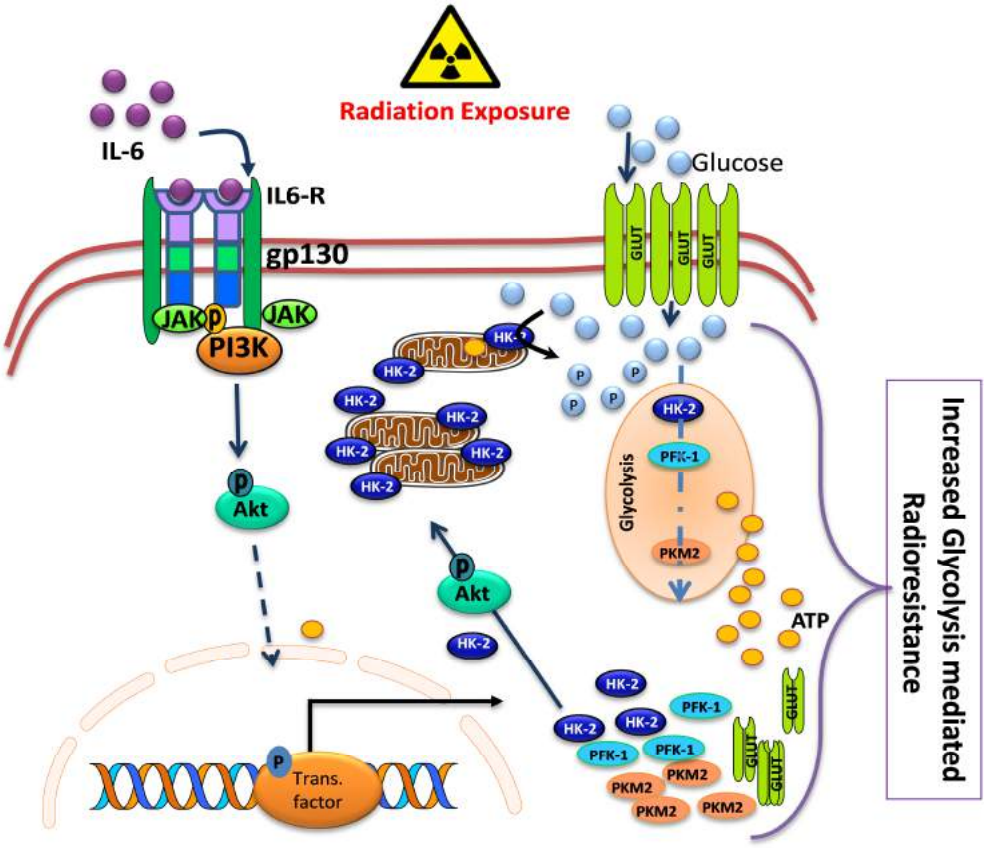

Figure 4.2.7: Role of IL-6 in Glycolysis; The picture illustrates that IL-6 treatment before irradiation activates PI3K-Akt pathway, which resulted in the up-regulation of important regulatory genes of glycolysis. Akt also phosphorylates HK-2, which allows its binding to outer membrane of mitochondria where it facilitates efficient glucose phosphorylation using mitochondrial ATP and ensures rapid rate of glycolysis. Efficient supply of energy (ATP) for the repair of radiation-induced macro-molecular and cellular damages and moonlighting functions of glycolytic enzymes like prevention of cytochrome C release from mitochondria by HK-2 resulted in IL-6-induced radio-resistance.

4.3 Role of IL-6 in cellular responses to radiation-induced DNA damage

The free radicals generated after irradiation accounts for 60-70% of DNA lesions else 30-40% is due to direct effects of radiation on the DNA molecule. Radiation affects cells in multiple ways; but most importantly, through DNA damage. In response to these damaged DNA lesions, especially double-strand breaks (DSBs), cells trigger the highly sophisticated and regulated repair response against DNA damage. Since the high fidelity during genome replication is decisive for appropriate cell proliferation, if cells succeed in the repair of DNA lesions will continue the cell cycle, else failed refurbishment can trigger cell death in damaged cells. Ionizing radiation induces apoptotic cell death in myeloid cells and DNA damage-induced mitotic catastrophe in epithelial cells (Wu et al., 2017). Since we observed IL-6 induced radioprotection in both myeloid cellular model (RAW264.7 cells) and epithelial cellular model (INT407 cells), we tested the hypothesis, if IL-6 treatment 2 hrs before IR defends the cells from IR mediated cell death by either minimizing the radiation-induced DNA damage or maximizing/ facilitating the DNA repair, and further to find out the possible contribution of DNA damage and repair in IL-6 induced radioprotection

4.3.1 DNA damage and repair: γ-H2AX foci formation

The observations on the assessment of intracellular ROS levels and clonogenic cell survival suggested that accelerated oxidative stress might be linked to DNA damage, and essentially playing an important role in the overall radio-modifying effects of IL-6 in RAW264.7 cells. Since, DNA damage following radiation exposure is the main contributing factor for the loss of clonogenicity (Celeste et al., 2002); therefore, the effects of IL-6 in the repair of DNA damage were studied. Histone-2A

phosphorylation at Ser-139 position (γ-H2AX), an appropriate biomarker of mainly DNA double-strand breaks (Rogakou et al., 1998), was used to assess DNA damage aroused in cells by exposure to radiation and correlated with effects on cell proliferation and survival. The intracellular levels of γ-H2AX were measured microscopically at 2 Gy IR dose in RAW264.7 cells from 30 minutes to 4 hrs.

Radiation led to a drastic elevation in the frequency of γ-H2AX foci formation at just 30 minutes post-exposure. The extent of damage induction was marginally but significantly low in the presence of IL-6. This was evident by the number of foci/cell (15.9±0.989 in IR vs 13.05±0.212 in IL-6+IR at 30 minutes) (Fig;4.3.1A&B). The number of foci per cell went significantly down just at 1hr post IR due to the presence of IL-6 and approached to control at 4 hrs post-treatment. The similar decreasing pattern was observed in the IR alone group; however, the recovery was not comparable to the IL-6 treatment and decline was observed with a slow rate. The average foci per cell at 4 hrs post IR was still 8.50±0.84 while IL-6 pre-treatment group had 4.85±0.353, Fig;4.3.1B. It was further validated by the western blot analysis of γ-H2AX protein at 1, 2 and 4 hrs. The decreased level of the phosphorylated form of this protein with increasing time indicated a faster rate of damage removal/repair of DNA strand breaks in IL-6 pre-treated cells. This observation indicated that IL-6 not only prevents the induction of DNA damage marginally but also facilitates faster repair. These findings corroborated with the observations from oxidative stress (ROS levels; Fig;4.1.7 as well as clonogenic cell survival (Fig;4.1.4) studies.

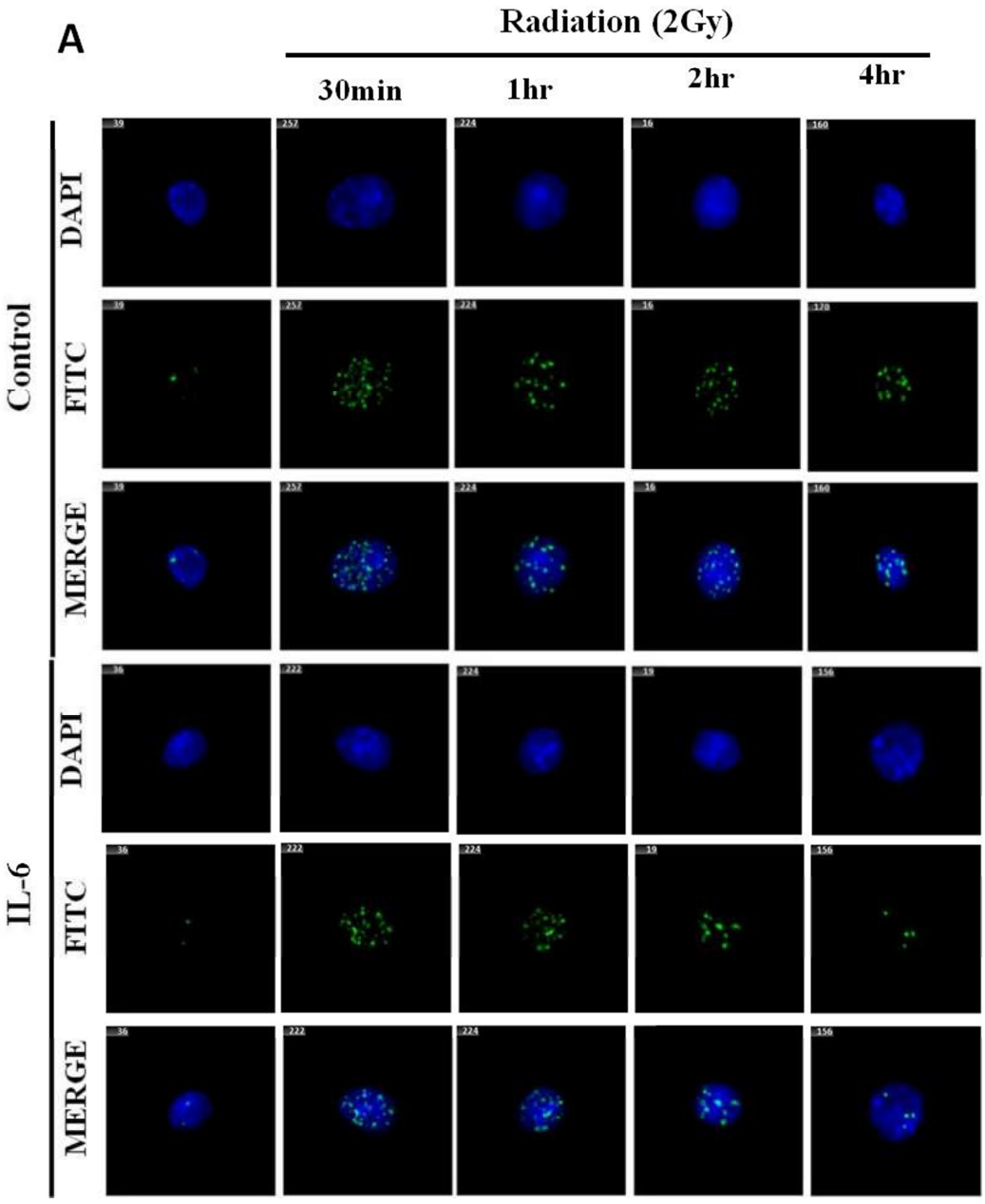

Figure 4.3.1: Effect of IL-6 on radiation-induced DNA damage- γ- H2AX assay (A) Photomicrographs showing distinct γ- H2AX foci at different time intervals from 0.5 to 4 hrs post-irradiation (after 2 hrs of IL-6 treatment). Images were captured under Metafer microscope at 100x.

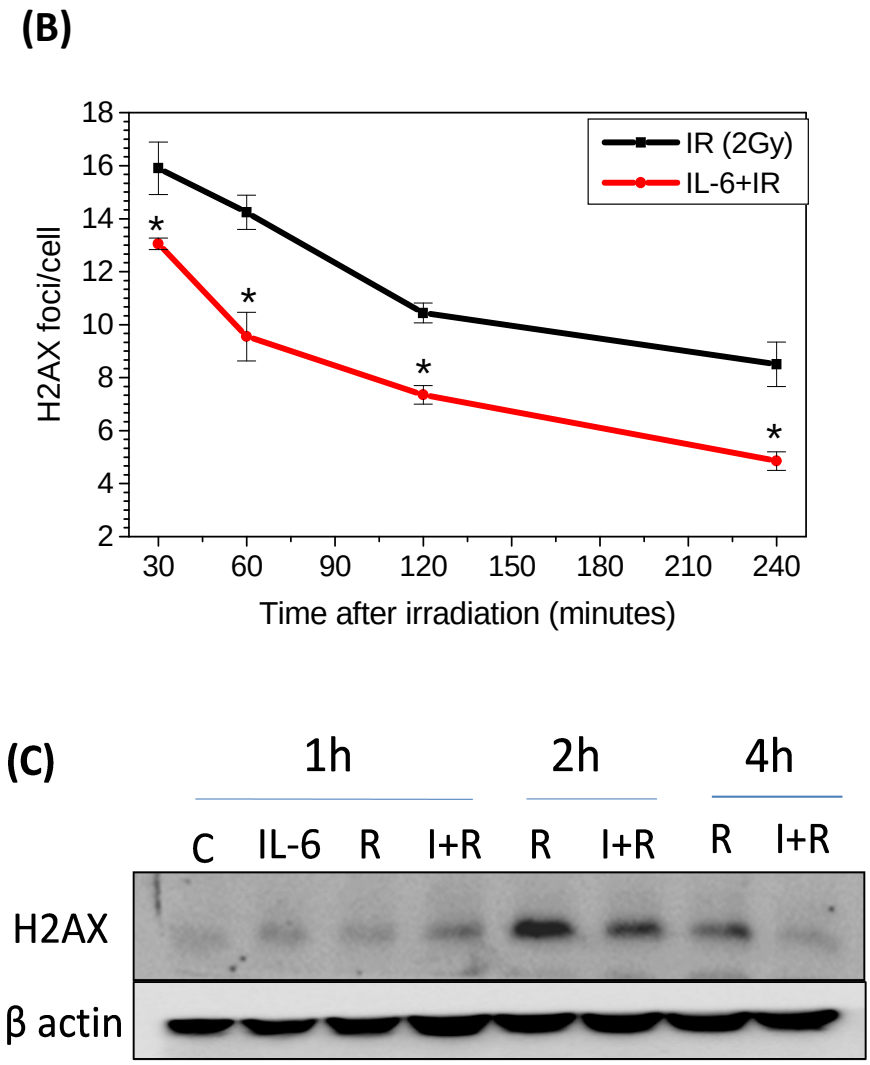

Figure 4.3.1: (B) Quantitative analysis of γ- H2AX foci formation at various time points using the MetaCyte γ- H2AX foci scan software in automated Metafer microscope. (C) Immunoblot of γ- H2AX at 1, 2 and 4 hrs post-irradiation. *: $p<0.05$.

4.3.2 DNA damage analysis by alkaline comet assay

Radiation exposure causes both types of DNA breaks (single and double-strand) leading to fragmentation of DNA in cells, which on the electrophoretic run in high PH buffer migrates towards positive electrode and acquires a shape resembling comets. Increase in radiation-induced DNA damage leads to an increased amount of

broken DNA in the comet tail. The results of the comet assay in different treatment groups at multiple time points from (0.5, 2 and 4 hrs) are represented by % DNA in tail, olive moment, tail moment and length of tail. IR alone group has increased % DNA in tail (23.8±0.79) compared with untreated control (3±0.2) (Fig;4.3.2). However, IL-6 pre-treatment significantly reduced the radiation mediated rise in % DNA to 14.53 ± 2.71 at 30 minutes of post-radiation exposure. The kinetics followed up to 4-hour post-exposure showed a similar pattern to γ- H2AX results, % DNA in the tail was less at 30 minutes (0.5 hrs) post-irradiation after IL-6 treatment and subsequently decreased % DNA was observed in IL-6+IR group till 4 hrs, which is almost equivalent to the untreated control group. Other parameters like the olive moment, tail moment, and tail length also showed the same pattern from 0.5 to 4 hrs after irradiation. Olive moment of tail post IR exposure was highest at 30 minutes (5.37±0.22 in IR vs 0.98±0.063 in Control) and subsequently goes down attaining the lowest at 4 hrs (2.24±0.077). IL-6 treatment effectively modulated the olive moment and achieved the lowest value at 4hr of IR exposure (1.12±0.15). Tail length also seems to be high at 30 minutes post IR exposure (20.23±0.61), which is quite low in the IL-6 treatment group (12.89±1.91). Therefore, all four parameters were significantly reduced by IL-6 treatment ($p<0.05$). Though IR alone showed self-recovery of the damaged DNA with time, as reflected by the kinetics of all parameters but still not attained the lowest value comparable to IL-6 treatment, hence displayed slow recovery. Thus, this data is indicating a faster rate of repair in the presence of IL-6 compared to IR alone group.

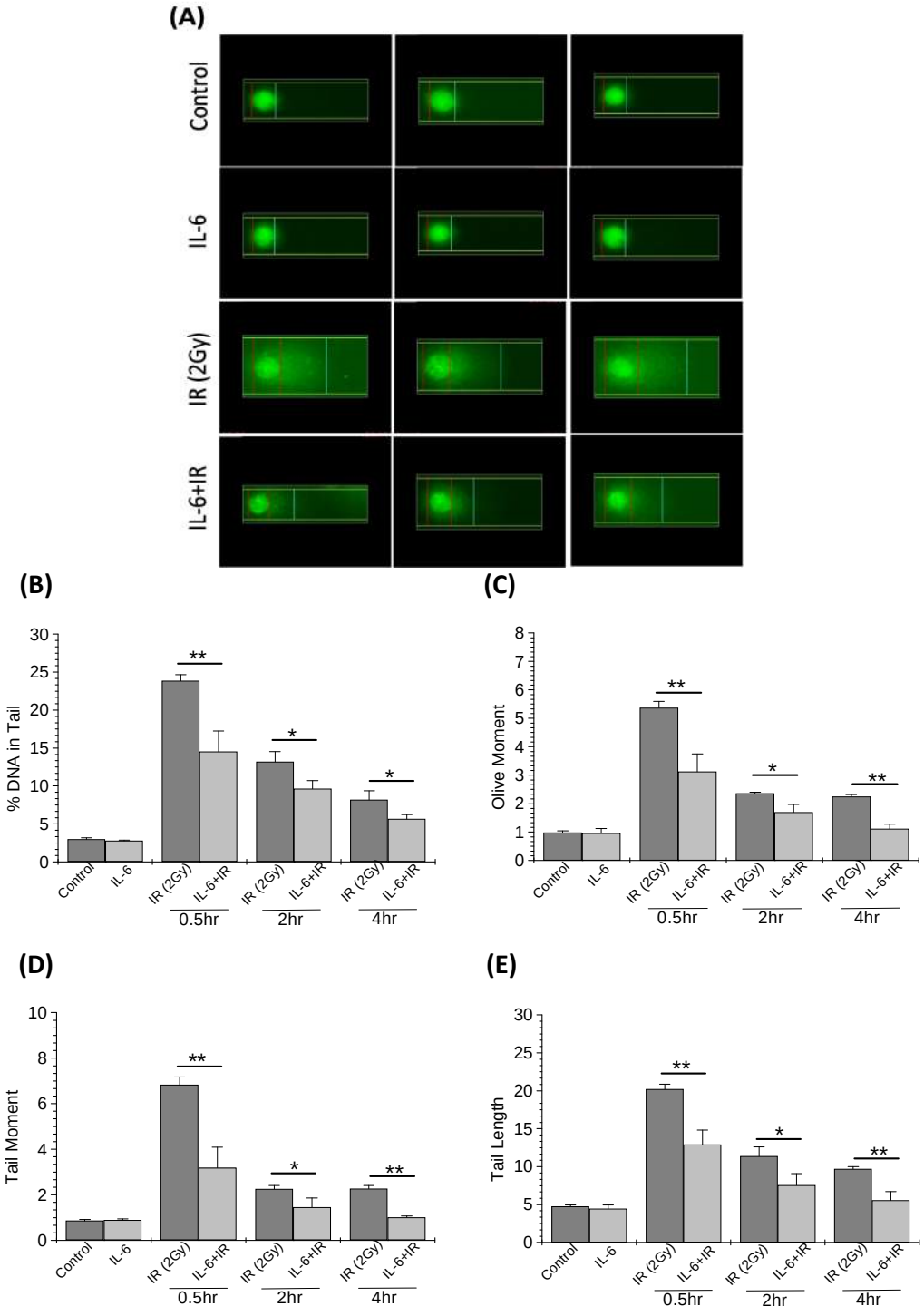

Figure 4.3.2: Effect of IL-6 on radiation-induced DNA damage- alkaline comet assay (A) Typical images of comet formation observed at 20X objective under a fluorescence microscope, Comet images were analyzed by MetaCyte comet scan software. (B) The graph represents % DNA in the comet tail. (B) Olive moment of the tail (C) Tail Moment and (E) Tail Length from 0.5 to 4 hrs post-irradiation; *: $p<0.05$, **: $p<0.01$.

4.3.3 Radiation-induced Micronuclei formation

Ionizing radiation primarily causes mitotic catastrophe linked death at moderate doses, where a cell is smashed during mitosis. However, if the cell survives with chromosomal aberrations during cell division like micronuclei, it dies in the next cycle (Kalsbeek & Golsteyn, 2017). Micronuclei are basically extra-nuclear bodies including chromosomal fragments or whole chromosomes, which failed to incorporate into the main nucleus following cell division. Instead, they enwrapped by the nuclear membrane and bear a resemblance to the central nucleus though tiny in size. Micronuclei can be formed by faulty repair machinery that may result in the accumulation of damaged DNA and non-reparable chromosomal aberrations (Luzhna, Kathiria, & Kovalchuk, 2013). Here, we investigated radiation-induced cytogenetic damage by enumerating the cells with micronuclei, which might be aroused due to unrepaired/mis-repaired DNA double-stranded breaks after irradiation. The time kinetics of micronuclei formation was followed up to 72 hrs post-IR exposure (Fig;4.3.3B). The micronuclei frequency was highest at 24 hrs (10±0.212 in IR vs 7.5±0.919 in IL-6+IR). The decrease was found to be significant but less at 12 hrs time point is probably because of radiation induced cell cycle delay in exposed cells; however the differences were visibly very prominent at later time points viz. 24, 36 and 48 hours because the divided daughter cells carry the micronuclei. The data clearly displayed a substantial reduction in the cell population with micronuclei in IL-6 pre-treated irradiated cells compared to irradiation alone at all-time points (Fig;4.3.3B) suggestive of decreased residual DNA damage due to efficient repair, correlated with the results of H2AX and comet (Fig;4.3.1 and 4.3.2)

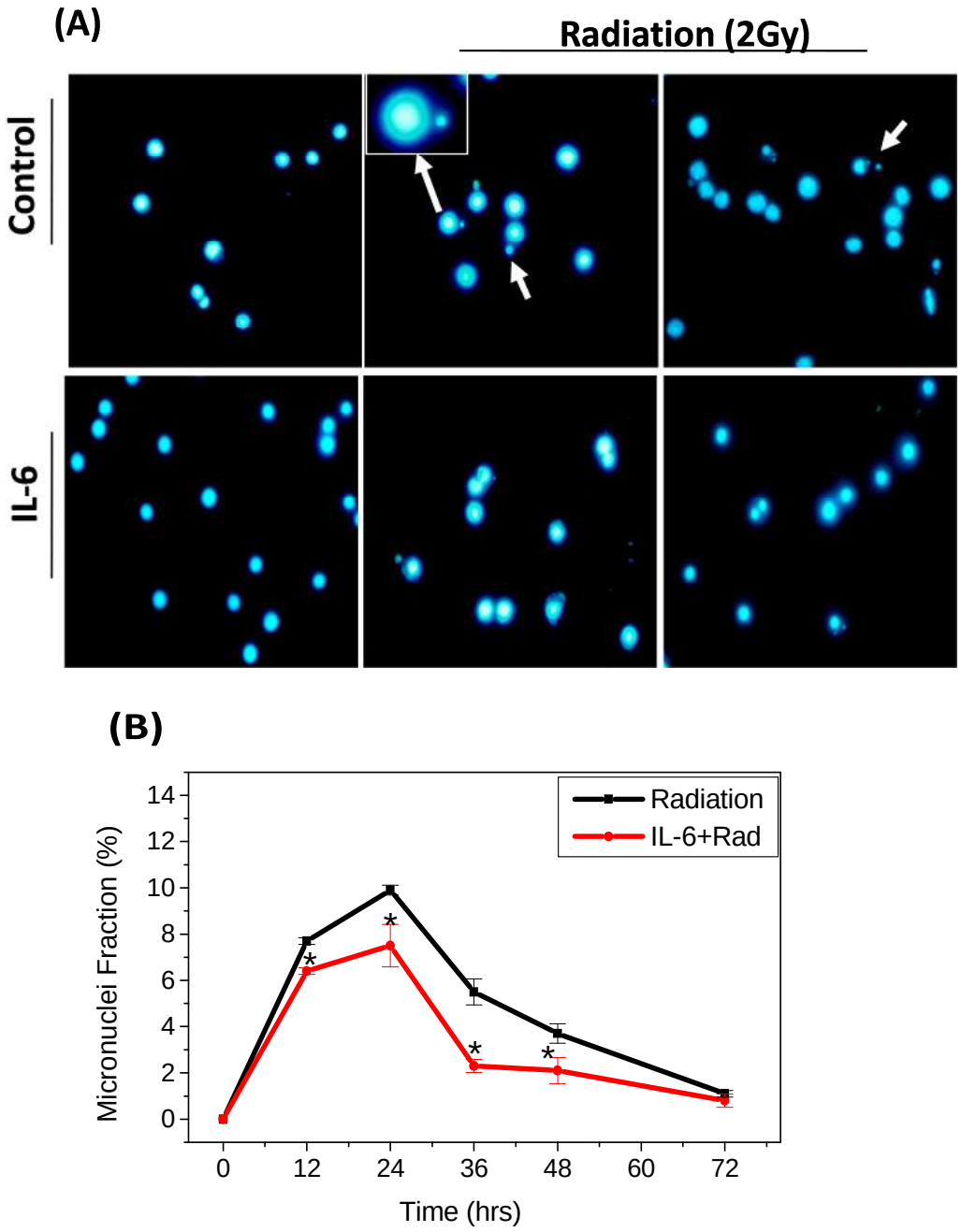

Figure 4.3.3: Effect of IL-6 on radiation impelled cytogenetic damages (A) Representative images of micronuclei along with main nucleus, captured at 20X, enlarged view of micronuclei is shown in Inset (B) Kinetics of Micronuclei fraction from 0-72 hrs at 2Gy radiation dose. *: $p<0.05$.

4.3.4 Assessment of 53BP1 foci formation

53BP1 is basically a p53 binding protein, which binds to p53 by interacting with its DNA binding domain. 53BP1 is known to be involved in DNA damage response, where it undergoes phosphorylation and rapidly relocated to the spots of DNA double-strand breaks in response to IR and is a putative substrate of ATM kinase (I. M. Ward, Minn, van Deursen, & Chen, 2003). The relocated 53BP1 could involve in chromosomal remodelling for assembly of DNA repair proteins at damaged sites or colocalized with repair proteins after several hours of exposure (Rappold, Iwabuchi, Date, & Chen, 2001). The DNA damage response (DDR) assist cells in sensing and countering damaged DNA by arresting cell cycle succession and repairing damage, if unrepaired, cells permanently entered into senescent phase. High dose of radiation upshots persistent DNA damage usually irreparable, compels the cells to senescence (Xurui Zhang et al., 2016). The occurrence of DNA double-strand breaks (DSBs) was also evaluated by visualizing 53BP1 foci formation similar to γ-H2AX foci. A GFP-tagged 53BP1 plasmid was stably transfected to HEK cells. The cells subjected to ionizing radiation manifested the recruitment of 53BP1 to the sites of DNA double-strand breaks, marked by its arrangement in the form of foci that are dispersed in the nucleus. These foci correspond to the spots of DNA DSB (Rappold et al., 2001). We observed distinct 53BP1–GFP 'punctum' like foci within 24 to 48 hrs of irradiation (Fig;4.3.4A) suggestive of radiation triggers DNA damage response (DDR) by creating DSBs, followed by recruitment of 53BP1 at the site of DNA lesions and stimulates ATM kinase (R. R. Nair, Bagheri, & Saini, 2015). The appearance of puncta formation with high frequency at a prolonged time period (48hrs) after

irradiation suggested that cells are still under the effect of radiation. Though the GFP-53BP1 cells started responding to irradiation (in terms of foci formation) within early hours, but the fluorescence intensity of puncta was very low which found to be increased with time along with an increase in number per cell. 5Gy of gamma radiation showed brightly illuminated small foci dispersed throughout the nucleus (Fig;4.3.4A). The number of cells containing foci has discrete distribution among different groups, as control groups (Untreated control and IL-6 alone treatment) have more than 70% cells with less than 0-5 foci per cell. However, IR alone group have approximately 40% cell with average 5-10 foci per cell, ~30% with 11-20 foci, 20% cell having 21-30 foci and the rest 10% contain more than 30 foci in each cell, none of the cell observed had less than 5 foci. Though IL-6+IR group had a high number of cells with more foci per cell with respect to controls, regardless of irradiation IL-6 treatment effectively modulated this distribution pattern and displayed reduced frequency of 53BP1 foci as compared to irradiation only group as around 15% cells with less than 5 puncta, 30% contain 5-10 foci, 25% have 11-20 foci and rest 15% cells have 21-30 foci, moreover none of the cell observed have more than 30 foci. Therefore, it can be projected that IL-6 pre-treatment profoundly reduced the foci frequency compared to IR group alone.

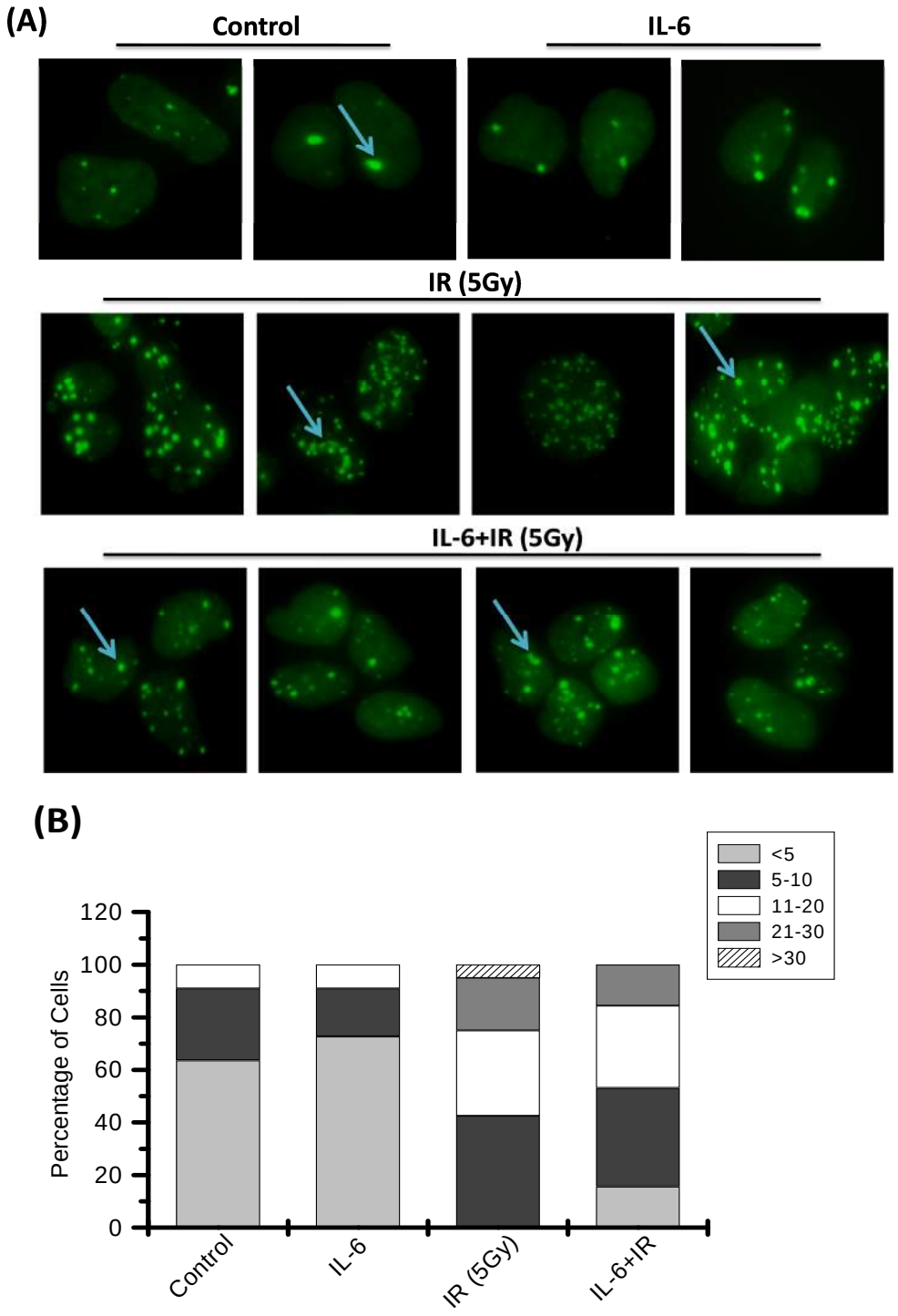

Figure 4.3.4: GFP-53BP1 foci formation in response to radiation (A) Photomicrograph showing 53BP1 'puncta' at 48 hrs post-irradiation captured under a fluorescence microscope at 40X magnification using a blue filter. (B) Graph representing the distribution of 53BP1 foci in percent cell population at 48 hrs post-irradiation. Number of foci counted in each view from all cells for at least 20 images per group.

4.3.5 Expression of DNA damage response (DDR) proteins

Eukaryotic cells gradually evolved machinery called DNA damage response (DDR) to prevent erroneous replication of DNA and to maintain genomic stability. DDR constituted of a network of biochemical pathways that detects the damage, signals to the DNA repair machinery, and repairs the DNA lesions, in coordination with transient cell cycle arrest (Delia & Mizutani, 2017). Key modules of this pathway are the sensors of DNA double-strand break, such as the Mre11-Rad50-NBS1 complex (MRN complex). Here, we observed that IL-6 treatment induces the expression of NBS1 at 1hr post-irradiation, which is known to be co-localized at γ-H2AX foci sites (Saito, Fujimoto, & Kobayashi, 2013). This early and enhanced activation of NBS1 after IL-6 treatment to irradiated cells as compared to the IR alone group, suggesting the timely detection of damage and start off repair machinery (Fig;4.3.5A). The MRN complex activation resulted in the activation of the ATM pathway that signals to the cell, leading to either cell cycle arrest or commences the repair kinetics. The ATM phosphorylation is evidenced by the visibly upshift of protein band (slow migration in the gel) in western blot that usually considered as of phosphorylated form, as the phospho form of proteins moves slower on SDS-PAGE in contrast to their non-phosphorylated form (Wegener & Jones, 1984). The ATM activation after IL-6+IR treatment with respect to IR alone suggested that IL-6 treatment is not only accountable for the early detection of damage but also executes fast DNA damage response as compared to IR treatment alone (Fig;4.3.5B). Moreover, we found enhanced expression of RAD51, a homologous recombination repair protein that is also known to respond in case of replication stress. After receiving the signal of DNA damage or replication halt, RAD51 recruited at the DSB sites along with other repair proteins like NBS1 (Bhattacharya et al., 2017). The

RAD51 expression was observed upto 4 hour after irradiation and found to be enhanced by IL-6 treatment to irradiated cells as compared to IR alone treatment which is also suggesting that IL-6 treatment not only enhances the expression of RAD51 but also causes the early recruitment at DSB sites to facilitate repair. These results are well correlated with our previous data of H2AX (Fig;4.3.1) and cell cycle (Fig;4.1.5) which indicated the generations of DSBs and cell cycle block. Cell cycle data showed that cell cycle block initiated just at 2 hrs post irradiation in both IR alone and IL-6+IR group and resolved completely at 8 hrs (Fig; 4.1.5). This observation propose that only IL-6 treatment facilitates DDR and resulted in successful completion of cell cycle, thereafter. Though cell cycle block resolved at same time in both the groups however, the levels of DDR are not equal in both groups which resulted the cells to enter in apoptosis in the IR group (Fig;4.1.12).

Apart from this, we also found enhanced mRNA expression of DNA repair enzymes Neil-1 (endonuclease VIII-like protein 1) and OGG-1 (8-oxoguanine-DNA-glycosylase 1). These two DNA glycosylases are known to repair 8-oxoAde:Cyt pairs consequence of DNA oxidation (Grin, Dianov, & Zharkov, 2010). We observed that IL-6 alone as well as with IR induces a several-fold increase in mRNA expression of both the enzymes as 42.24±8.725 fold of Neil-1 and 67.94±20.059 fold of OGG-1 at 12 hrs of IL-6 treatment compared with untreated control (Fig;4.3.5C). The basal level of these enzymes in the untreated group was approximately one. Irradiation also induced the mRNA expression as 21.24±5.380 of Neil-1 and 21.36±3.7 of OGG-1; however, combined treatment of IL-6 and radiation causes more expression as 48.49±3.58 in Neil-1 and 60.30±7.73 in OGG-1 as compared to radiation alone treatment. Our study implies that radiation causes damage to DNA either by direct

effect or via oxidative stress resulted in the commencement of DNA damage response which is found to boost up by IL-6 treatment.

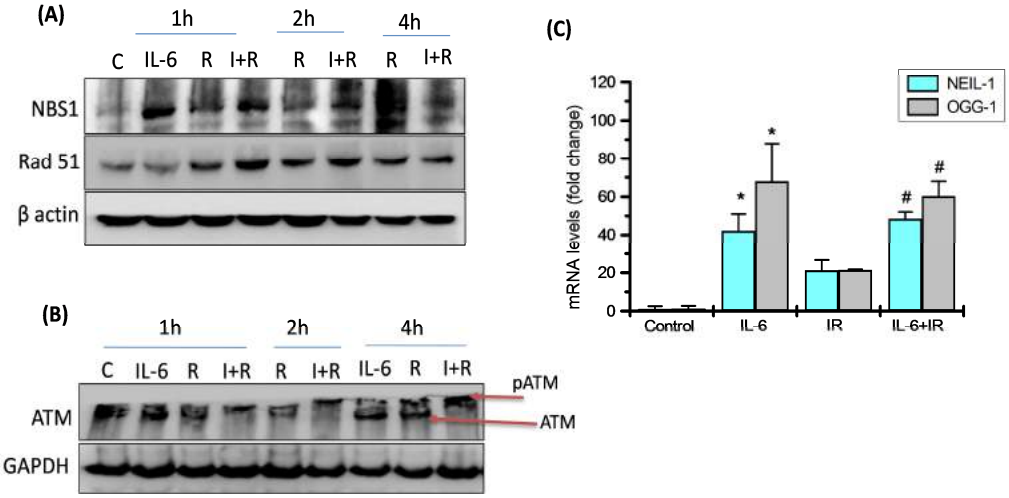

Figure 4.3.5: Activation of DDR and HR pathway after irradiation (A&B) Immunoblots of NBS1 (MRN complex protein), Rad51, and ATM at 1, 2 and 4 hrs post-irradiation in RAW264.7 cells treated with IL-6 for 2 hrs followed by irradiation with 2Gy. Beta actin and GAPDH were the loading controls, respectively. (C) Graph representing fold change in mRNA levels of Neil-1 and OGG-1. Data represents *#P>0.001; * represents significance with respect to the control group and, # represents significance with respect to the IR group.

4.3.6 Summary

The above study summarizes as; IL-6 facilitates DNA repair by inducing the expression of DNA repair enzymes. The induction of DNA damage phosphorylates the H2AX, a vital DSB marker which may lead to genomic instabilities. IL-6 treatment before radiation exposure activates the MRN complex proteins and ATM followed by recruitment to the DSB sites for the effective execution of DDR, and efficient repair of damaged DNA. Further, there we verified that the extent of DNA damage in both the IR alone group and the IL-6+IR groups differ considerably, followed by less cytogenetic damage after IL-6 treatment.

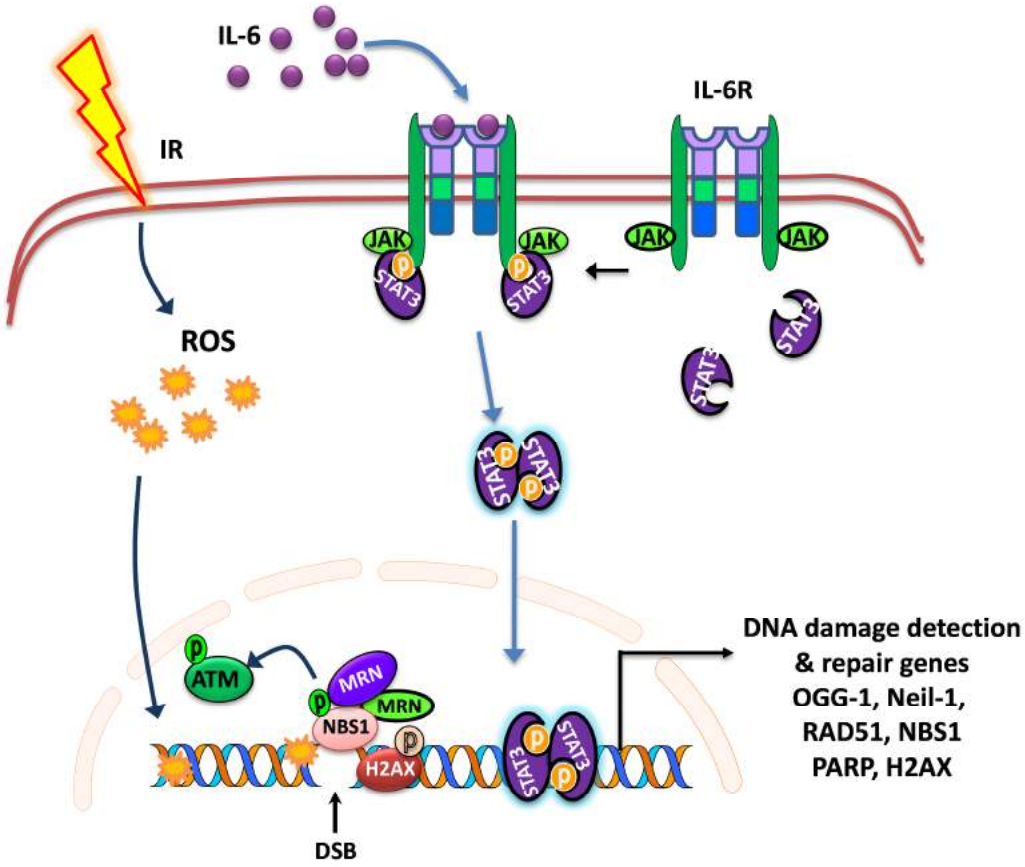

Figure 4.3.6: Role of IL-6 in DNA repair: IL-6 treatment to cells facilitates activation of DDR including, activation of MRN complex proteins along with ATM followed by recruitment to the DSBs sites. IL-6 treatment leads to the efficient repair of DNA lesions by activating several DNA repair enzymes.

4.4 Evaluation of radio-protective efficacy of IL-6 in *mice models*

Introduction

Exposure to lethal doses of IR may cause hematopoietic acute radiation syndrome (H-ARS) and gastrointestinal (GI) syndromes which are characterized by severe myelosuppression, diarrhoea, abdominal pain and weight loss followed by mortality. The acute effects are primarily manifested in tissues having a rapid rate of cell turnover, i.e., the hematopoietic (H- ARS) and the gastrointestinal systems (GI-ARS). This is because they house the critical and highly radio-sensitive cell population *viz.* the stem/ progenitor cells of the bone marrow (BM) and gastrointestinal crypts. In humans, a dose above 1 Gy may result in the compromised hematopoietic system, and death may occur at the dose range between 2.5-5 Gy due to BM failure. A radiation dose above 8 Gy, predominantly contributes to mortality due to GI injury (Dubois & Walker, 1988). The compromised immune system after irradiation and the damaged GI tract may result in bacterial translocation (gut microflora) to blood and other sterile organs which leads to sepsis and become the primary cause of mortality following radiation exposure (Berg, 1995). Therefore, the development of radiation countermeasures is based on their potential to overcome peripheral blood cell depletion, restore BM HSPC (haematopoietic stem/progenitor cell) population and regenerate intestinal stem cells. In this chapter, we studied whether IL-6 can give in vivo radioprotection also, similarly as it showed in in-vitro models. Further, studies were undertaken to investigate if the survival advantage conferred by the IL-6 to lethally irradiated mice is due to the amelioration of radiation induced hematopoietic and gastrointestinal damage.

4.4.1 IL-6 treatment activates STAT-3 and Akt phosphorylation in haematopoietic tissues of mice

We learned from our *in-vitro* studies that 1-2 hrs of IL-6 treatment is sufficient to activate STAT-3 signalling, the however same approach will not work until we know the effective concentration of IL-6 reaching in the blood at 1 and 2 hrs post IL-6 injection. Since IL-6 is also known as myokine and secreted by muscles after physical exercise; we chose to inject the cytokine through i.m. (intramuscular) route. C57BL/6 mice were given an intramuscular injection of IL-6 (10ng/mice of 25 gram average weight in 50 µl water), and blood was withdrawn at 1 and 2 hrs post-injection for serum collection. An IL-6 level in serum was detected by the ELISA method. We found a non-detectable (n.d.) concentration in untreated control mice serum samples. We detected around 800pg/ml IL-6 in Serum samples after 1 hr of intramuscular IL-6 injection whereas, this level was increased to1500pg/ml at 2 hrs (which is little higher than our 1ng/ml concentration used *in-vitro*) (Fig;4.4.1A).

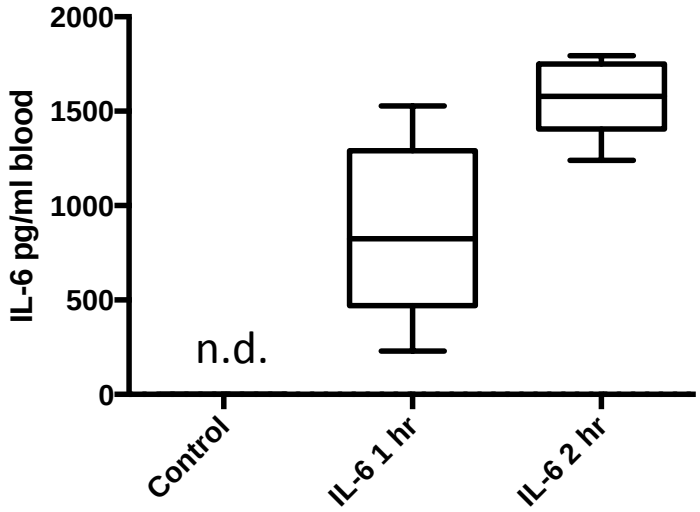

Figure 4.4.1A: IL-6 level in blood. IL-6 level was detected in serum at 1, and 2 hrs post IL-6 injection (10ng/mice) by ELISA method. n.d.- non-detectable. Data represents mean ± S.E.M from 2 independent experiments; n= 6 mice per group

The function of IL-6 is regulated by signal transducer and activator of transcription 3 (STAT-3). It has been known to facilitate various cellular services of a cell such as proliferation and survival (Stepkowski, Chen, Ross, Nagy, & Kirken, 2008). Similar to the *in-vitro* studies we determined whether STAT-3 signalling is activated *in-vivo* following IL-6 intramuscular injection (10ng/mice of 25 gram average weight in 50µl water) in C57BL/6 mice and first analyzed the phosphorylation of STAT-3. We found increased phosphorylated STAT-3 (active form) levels at 2 hrs of IL-6 treatment in all the target radio-sensitive haematopoietic organs such as blood, bone marrow and spleen (Fig;4.4.1B).

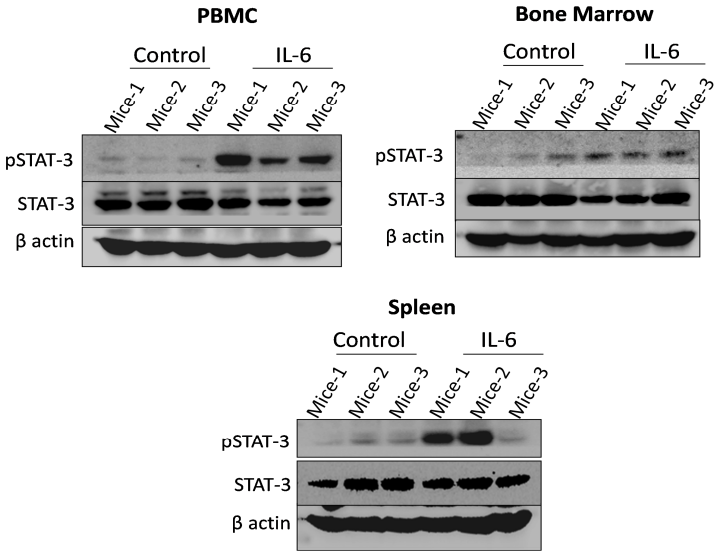

Figure 4.4.1B: Immunoblots of pSTAT-3 and STAT-3 in blood, bone marrow and spleen of three different mice (1, 2 &3) at 2 hrs post-treatment. Protein levels were normalized by beta actin.

Along with STAT-3, Akt pathway was also found activated as demonstrated by the elevated levels of pAkt in all the similar haematopoietic organs at 2 hrs post IL-6 treatment (Fig;4.4.1C).

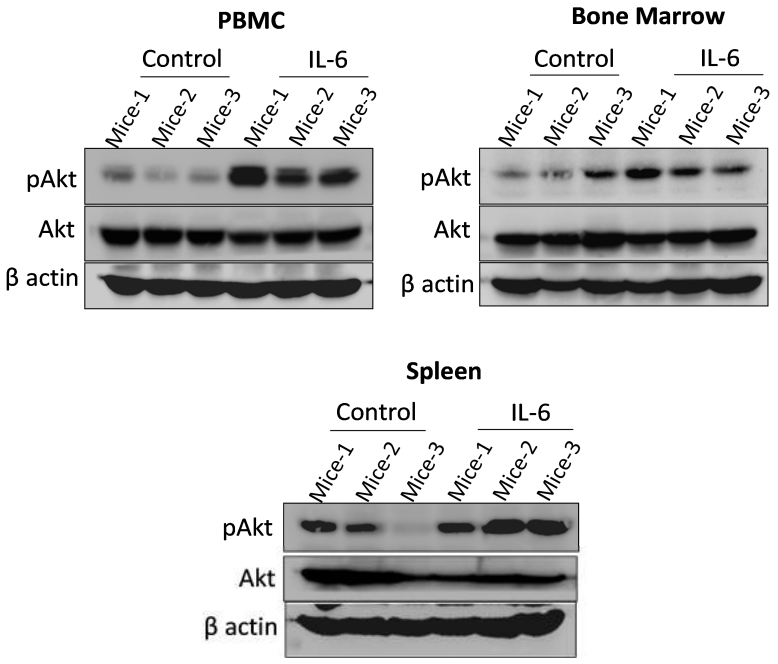

Figure 4.4.1C: Immunoblots of pAkt and Akt at 2 hrs post-IL-6 treatment in blood, bone marrow and spleen in three different mice of control and IL-6 treated group. Beta actin was used as an internal protein loading control.

Together these results suggest that IL-6 induced phosphorylation stimulates STAT-3 and Akt signalling that may provide a survival advantage to the animals, as we observed in cellular models. The intramuscular route of IL-6 dose was adopted due to the myokine nature of IL-6 and two hrs after injection was sufficient time to reach IL-6 which activated STAT-3 and Akt signalling even in deep sitting organs of the mice, as observed in bone marrow and spleen.

4.4.2 IL-6 protects C57BL/6 mice from lethal irradiation:

Next, we checked the radio-protective potential of IL-6 in C57BL/6 mice. The animals were administered with 10ng IL-6 per mice (average weight, 25 gm), intramuscular (i.m.), 2 hrs before being exposed to a single lethal dose of 7.5 Gy

using Co^{60} based irradiator LDI2000. The two different treatment groups of mice were treated with a single (pre-irradiation dose) and multiple (one pre and three post-irradiation at 24, 48 and 72 hrs.) doses of IL-6. The animals were observed for signs of radiation illness and mortality for 30 days post-radiation treatment. Animal survival was then analyzed using Kaplan Meier survival curve (Fig; 4.4.2). At this lethal radiation dose, the percent survival of vehicle-treated irradiated animals was 20%, accompanied by indications of radiation sickness such as loss of appetite, loss of thirst, weight loss, ruffled hair, diarrhoea, facial edema and lethargy (Macià i Garau et al., 2011). Irradiation of the mice resulted in the appearance of these symptoms within 2–4 days after exposure. Some animals also showed difficulty in movement during second-week post-exposure. Mice treated with single and multiple doses of IL-6 along with irradiation showed delayed onset of symptoms of illness and significantly improved survival after irradiation. The beginning of mortality was also delayed by 4-5 days in multi-dose IL-6 treatment; however, it is same in radiation alone and single-dose treatment groups. The number of survivors increased significantly in both the groups of drug treatment ($p< 0.001$ for multiple doses and $p< 0.01$ for a single dose of IL-6), compared to the radiation group. IL-6 conferred 50% survival with a single dose of IL-6 and 80% survival with multi doses of IL-6.

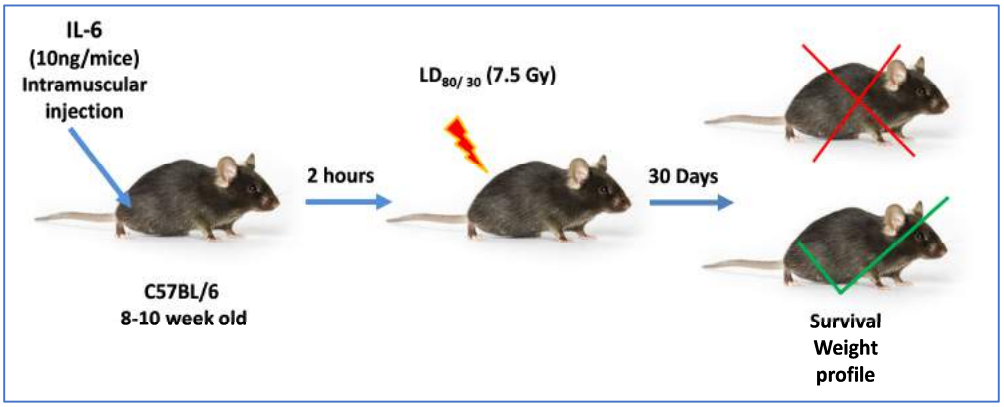

Survival study procedure followed for 30 days

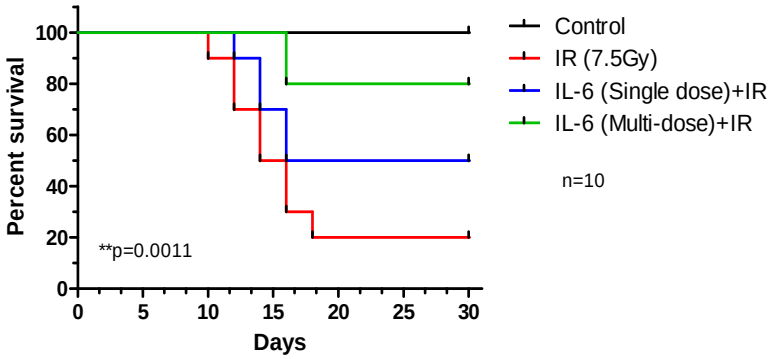

Figure 4.4.2: Radioprotection by IL-6 treatment- survival analysis: Kaplan-Meier curve illustrates the 30 days survival of C57BL/6 mice given intramuscular injection of IL-6 (10ng/mice), 2 hrs before being exposed to a lethal dose of IR (n= 10 mice per group). In a multi-dose group, 3 more doses of IL-6 (10ng/mice) at 24, 48 and 72 hrs had been given post-radiation exposure.

The average weight of the untreated control animals gradually increased over the 30 days period. However, the mice belonging to the radiation alone group displayed a sharp decline in their average body weight (from 22.2±1.32 at day 01 to 17.8±2.21 at day 15) in contrast to IL-6 multi-dose treated animals who showed no change till day 23 (22.7±1.06 at day 01 to 22.6±1.33 at day 23). The IL-6 (single dose) treated animals also showed a slightly decreasing trend until day 13, after which the animals began to recover and displayed an increase in their body weight (Fig;4.4.3). The survivors left in radiation also began regaining their body weight. Table 4.4.1 shows the 30 days mean weights of mice exposed to a lethal dose of γ-radiation with or without administration of IL-6. The average food

intake per mice per day during 30 days survival period was significantly low in irradiated animals (1.73 ± 0.703 vs 2.64±0.481 in control p=0.0025) though IL-6 treatment to irradiated animals prevented the loss of appetite and had food intake similar to sham irradiated animals (2.69 ± 0.91, p=0.023). Irradiated animals initially showed loss of appetite till day 15, and later they had gained their natural diet; still, the average intake was low. In contrast, IL-6 treated irradiated animals showed a constant diet till day 30 (Fig; 4.4.4A). Irradiated animals not only showed loss of appetite, but their water intake capacity was also compromised. The average water intake in IR alone and IL-6+IR animals were significantly low with respect to control and observed non-significant change between IR and IL-6+IR (4.19 ±1.040 in control vs. 2.51±0.722, 2.77±0.541 in IR and IL-6+IR, respectively, (Fig;4.4.4B).

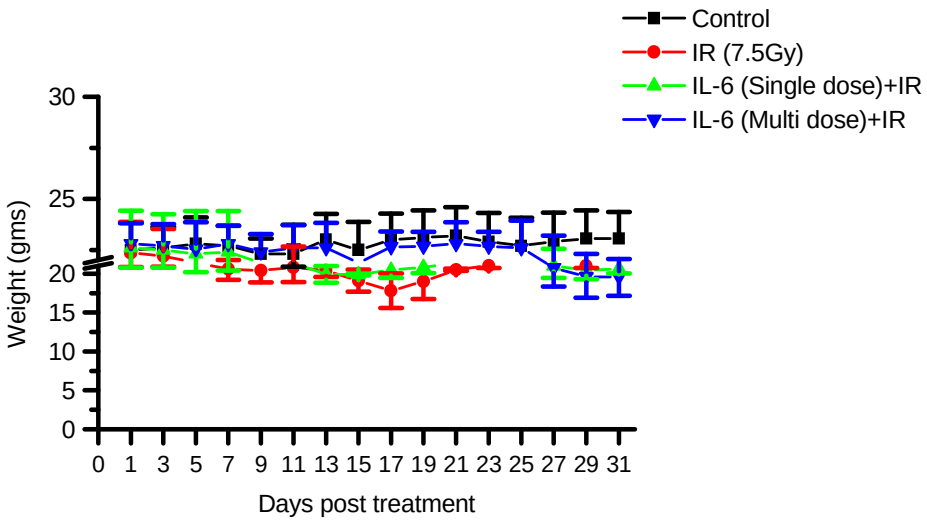

Figure 4.4.3: Effect of IL-6 on the bodyweight profile of irradiated mice. C57BL/6 mice were irradiated with 7.5 Gy WBI (Whole-Body Irradiation) after 2 hrs of intramuscular injection of IL-6. Their body weight was recorded every alternate day for a period of 30 days. Data represent mean ± S.E.M. of n= 10 mice per group.

Table 4.4.1: Bodyweight profile of mice of different treatment groups over an observation period of 30 days

Days post-treatment	Control	Radiation	IL-6 (Single dose) + IR	IL-6 (Multiple doses + IR
0	22.49 ± 1.33	22.35 ± 1.52	22.6 ± 1.82	22.8 ± 1.01
1	22.6 ± 1.02	22.2 ± 1.32	22.5 ± 1.75	22.7 ± 1.06
3	22.8 ± 1.29	21.5 ± 1.23	22.3 ± 2.1	22.53 ± 1.33
5	22.7 ± 0.99	20.6 ± 1.41	22.4 ± 2.0	22.8 ± 0.89
7	22.3 ± 0.76	20.4 ± 1.53	21.9 ± 1.86	22.4 ± 0.87
9	22.3 ± 1.43	20.8 ± 1.87	19.7 ± 5.03	22.6 ± 1.11
11	23 ± 1.27	20.4 ± 0.83	19.9 ± 1.08	22.6 ± 1.22
13	22.5 ± 1.37	19.1 ± 1.42	19.88 ± 0.11	21.5 ± 2.24
15	23 ± 1.28	17.8 ± 2.21	20.46 ± 1.02	22.65 ± 0.75
17	23.1 ± 1.34	19 ± 2.26	20.8 ± 0.75	22.68 ± 0.71
19	23.2 ± 1.39	20.5 ± .141	21.3 ± 0.90	22.8 ± 1.06
21	22.9 ± 1.41	21 ± 0.28	21.6 ± 0.91	22.68 ± 0.715
23	22.7 ± 1.37	21.1 ± 0.701	21.26 ± 0.98	22.6 ± 1.33
25	22. 9 ± 1.42	21.3 ± 0.707	21 ± 1.56	20.76 ± 2.43
27	23.06 ± 1.37	21 ± 0.28	20.46 ± 1.17	19.6 ± 2.70
29	23.06 ± 1.30	21.4 ± 0.84	20.5 ± 0.866	19.4 ± 2.59
31	23.2 ± 1.02	21.2 ± 0.741	20.62 ± 0.586	19.6 ± 2.46

* Values represent mean ± S.E.M.

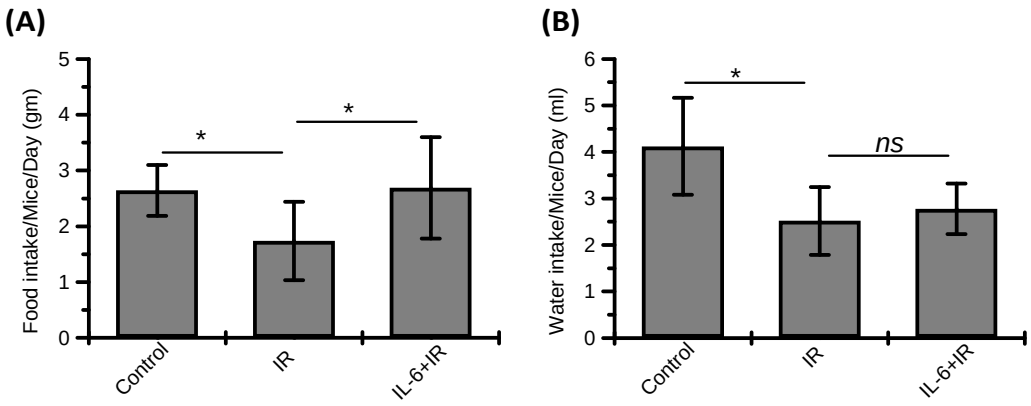

Figure 4.4.4: Effect of IL-6 on food and water intake of irradiated mice. The C57BL/6 mice were exposed to 7.5 Gy WBI 2 hrs following intramuscular administration of IL-6. Their food and water intake recorded every alternate day for 30 days. (A) Average food intake/mice/day in grams. (B) Average water intake/mice/day in ml.

4.4.3 Modification of radiation-induced hematopoietic damage by IL-6

The hematopoietic system is the most susceptible to the deleterious effects of radiation. H-ARS is characterized by sterilization of the mitotically active BM progenitor cells, leading to neutropenia, thrombocytopenia and anaemia (Mauch et al., 1995). Subsequent defects in the adaptive immune system, due to the depletion of lymphocytes, leads to immunosuppression and enhanced susceptibility of subjects to secondary infections (Dainiak, Waselenko, Armitage, MacVittie, & Farese, 2003). Haemorrhage, occurring as a result of thrombocytopenia, can further complicate the situation and lead to mortality (Kiang et al., 2015). Therefore, survival after myeloablative doses of IR is critically reliant on the self-renewal capacity and proliferation of the surviving stem cells for achieving hematopoietic reconstitution.

The animals sacrificed after 30 days survival showed complete recovery in terms of bone marrow cell count and spleen size in IL-6 treated group. There was a significant change in bone marrow cell density of IR treated animals with respect to control; however IL-6 treatment regains the complete cell density (30.34±2.51, 21.032±2.77 and 31.34±3.34 million cells in control, IR and IL-6+IR respectively, $p< 0.05$, Fig; 4.4.5A). Loss of splenocytes because of IR induced apoptosis results in the overall decline in the size and weight of the spleen (splenic atrophy) (Singh et al., 2015). There was a significant difference in spleen weight of IR alone animals with respect to IL-6+IR and un-irradiated animals (119.3±1.3 vs90.25±2.25 in IR vs 124±6 in IL-6+IR, $p< 0.001$, Fig; 4.4.5B). Albeit irradiated animals showed the signs of revitalization but not entirely recovered from radiation sickness day 30 post-

irradiation. Because the multiple doses of IL-6 treatment gave maximum survival advantage, we used multi-dose protocol for future experiments.

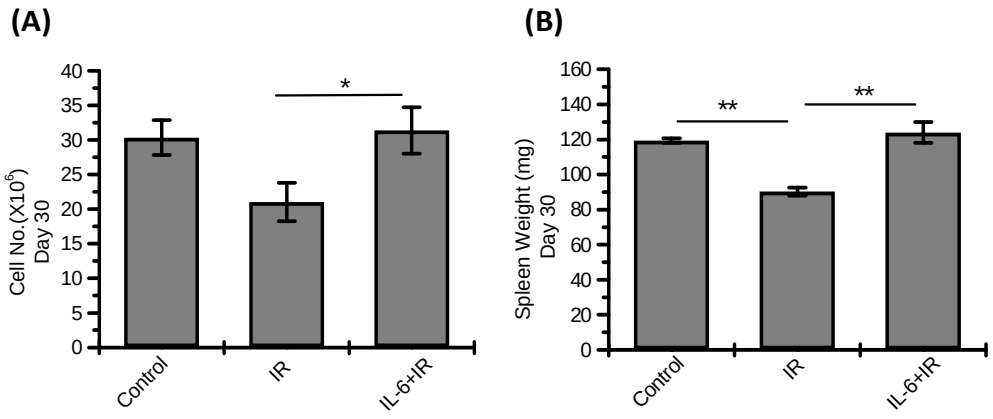

Figure 4.4.5: Effect of IL-6 on bone marrow and spleen at day 30 post-irradiation. C57BL/6 mice were dissected following 30-day survival analysis. (A) A total number of live nucleated cells in bone marrow at 30 days of treatment. (B) Spleen weight index at day 30 post-treatment.

4.4.3.1 Effects of IL-6 on radiation-induced cytopenia

Analysis of the peripheral blood cell indices is a simple and reliable assay for assessment of hematopoietic injury and its amelioration by a countermeasure agent. The hematopoietic recovery was studied in mice irradiated with a lethal dose of 7.5 Gy and compared with the effects of IL-6 on hematopoietic recovery following radiation exposure in C57BL/6 mice. Blood was collected at day 01, 03, 07, 14, 21 and 28 post-treatment and assessed for its constituent parameters. Radiation-induced severe depletion of blood cell counts were obtained in mice 24 hrs following 7.5 Gy WBI in both IL-6 treated as well as vehicle-treated mice ($p < 0.001$). However, for platelets, red blood cells (RBCs) and haemoglobin (Hb), the nadir (maximum decrease in the value) was observed at day 14 post-WBI in the IL-6 pre-treated as well as vehicle-treated mice ($p < 0.001$) (Fig;4.4.6A-F). The total leukocyte count in irradiated mice

began to increase from day 21, but still remained significantly low and did not unveil complete recovery ($p < 0.05$) till day 28, as compared with untreated control mice. However, IL-6 treatment induced a profound accelerated recovery in the WBC index, leading to the achievement of baseline values by day 21, which was almost 4 folds higher ($p < 0.001$) than the levels seen in the WBI alone cohort (Fig;4.4.6A). The lymphocyte and granulocyte number also reached their nadir values just after 24 hrs post-WBI. Lymphocytes showed a slight recovery at day 21 but still did not enter the same benefits as the untreated control (6.34±2.41 in control vs 0.855±0.572 in IR, $p < 0.001$). However, IL-6 treatment most effectively mediated the recovery from radiation-induced lymphocytopenia, leading to the achievement of the baseline point (7.39±2.56, $p < 0.001$) (Fig;4.4.6B). Further, radiation alone failed to attain the normal level up to day 28 (1.98±0.091 in IR vs 6.3±0.113 in IL-6+IR).

For granulocytes, the decline was similar to that of lymphocytes until day 14 after WBI. The counts were very low till day 14, which was indicative of severe neutropenia in both IL-6 treated and untreated cohort. IL-6 showed the recovery at day 21 and 28 after irradiation leading to a significantly higher number of granulocytes in IL-6+WBI (1.82±0.056 vs 3.25±0.646 in WBI at day 21) ($p < 0.05$) at day 28 post-treatment, with the numbers reaching the baseline values in IL-6 + WBI mice (Fig; 4.4.6C).

The platelet count began to decline by day 03 after radiation, reaching its nadir on day 14 in both drug- and vehicle-treated groups, though the levels were not reduced to the same extent in drug-treated mice as that in radiation alone group. Platelet count was still significantly higher in IL-6+ WBI ($p < 0.05$) than WBI cohort at day 14. Although the platelet levels

increased by day 21 in IL-6 treated as well as radiation alone mice, only IL-6 treated cohort recovered completely at day 28 and reached the same values as those of untreated control mice (653±12.727 in control, 487±53.740 in IR and 647±43.840 in IL-6+IR) (Fig;4.4.6D). The RBC counts in radiation alone group exhibited a similar pattern, reaching its minimum value at day 14 ($p < 0.001$), and failed to attain complete recovery even at day 21 ($p < 0.001$). In contrast, IL-6 treatment significantly prevented the decline in RBC counts from day 7 to 14 and showed complete recovery at day 21 (7.09±0.806 in IR vs 9.40±0.271 in IL-6 +IR). However, RBC counts in the IR alone group get recovered at day 28 (8.38±0.07 in IR vs 9.39±0.325in IL-6 +IR) (Fig;4.4.6E). The Hb levels also presented a decreasing trend from day 07 till day 14 following irradiation. IL-6 treatment cohort had significantly higher Hb level at day 14 with respect to IR alone (4.9±0.217 in IR vs 7.6±0.707in IL-6+IR). Both the groups attained the baseline values at day 21 (Fig; 4.4.6F). Thus, these results revealed the potential of IL-6 in mediating recovery from radiation-induced cytopenia and, hence protecting C57BL/6 mice from WBI-induced lethality.

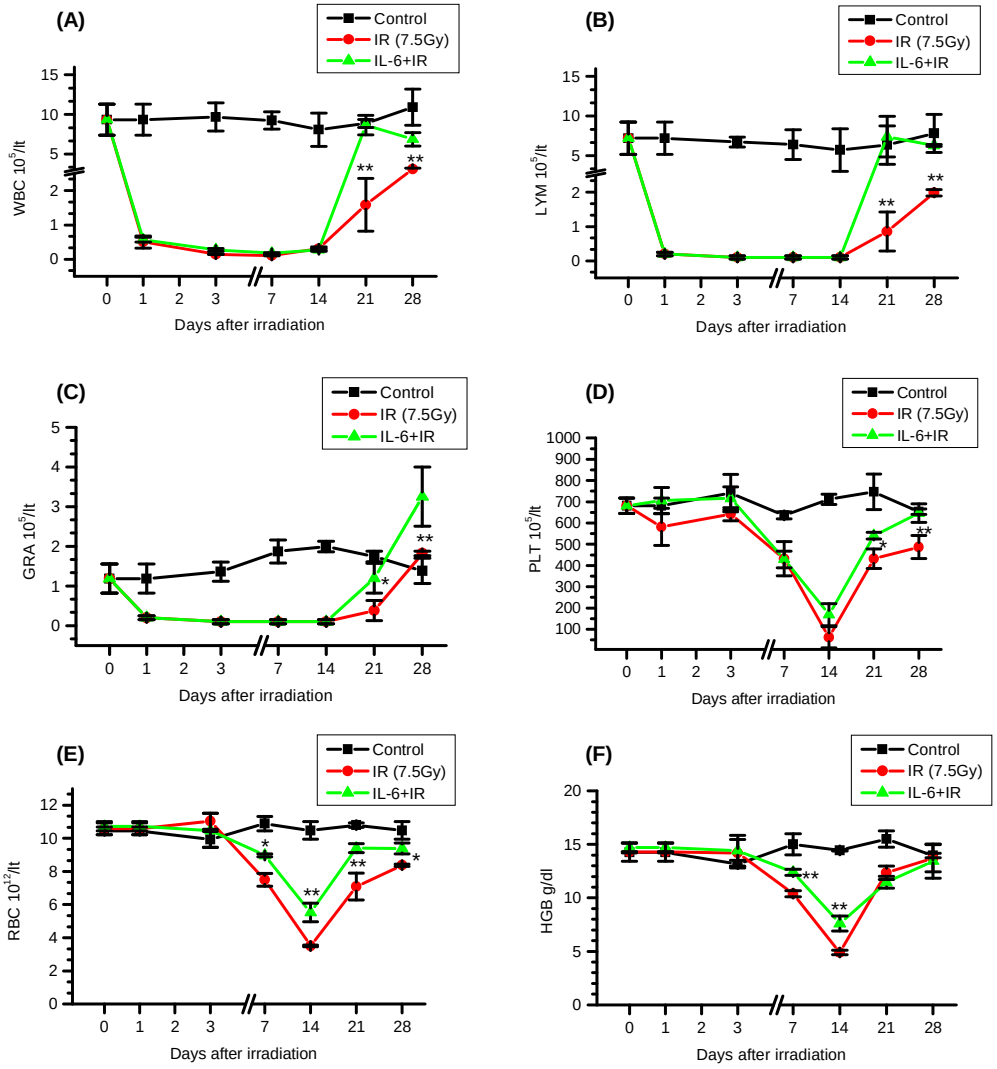

Figure 4.4.6: Effect of IL-6 on radiation-induced alterations in peripheral blood cell populations. C57BL/6 mice were administered IL-6, 2 hr prior to 7.5 Gy WBI and 3 doses post Irradiation at 24, 48, and 72 hrs (A) Total WBC count (B) Lymphocyte number (C) Granulocyte number (D) Platelet count (E) RBC (F) Haemoglobin at 01, 03, 07, 14, 21 and 28 days post-treatment. *: $p<0.05$; **: $p<0.001$.

Although, IL-6 showed significant recovery of the haematopoietic system on 7.5 Gy, which was a relatively high dose for H-ARS. Therefore, we also evaluated the effect of low dose ionizing radiation on peripheral blood count. Radiation-induced severe depletion of white blood cell counts has obtained in mice 24 hrs following 2 Gy WBI

in both IL-6 pre-treated as well as vehicle-treated mice ($p < 0.01$). In contrast to the animals receiving high IR dose, 2 Gy irradiated animals exhibited fast recovery. The total leukocyte count began to increase after day 3 in IR treated animals but remained significantly low as compared to control and IL-6+IR group till day 28 and did not show complete recovery ($p < 0.05$). The lymphocyte and granulocyte number also reached their nadir values just after 24 hrs post-WBI and started recovering from day 3 onwards. However, IL-6 treatment significantly reduced the initial dip at 24 hrs, and the difference was more than 2 fold at day 3 in lymphocyte count (0.69±0.12 in IR vs 1.52±0.253 in IL-6+IR cohort, p=0.001) (Fig; 4.4.7B).

Lymphocytes showed a significant recovery in radiation alone but still did not reach the same values as the untreated control at day 28 (7.81±2.40 in untreated vs 4.1±0.55 in IR, $p < 0.01$). However, IL-6 treatment most effectively mediated the recovery from radiation-induced lymphocytopenia (7.82±2.241). Granulocyte count was also modulated by 2 Gy after WBI but recovered completely till day 28 (Fig;4.4.7C). However, IL-6 treatment resisted the initial dip in granulocyte count at 01, 03 and 07 day post-IR and maintained significantly high as compared to IR alone cohort. After day 7, irradiated animals also showed accelerated recovery and achieved normal count by day 21(1.745±0.134 in control vs 1.47±0.43 in IR vs 1.63±0.37 in IL-6 +IR cohorts). There was a non-significant alteration in platelets, RBC and haemoglobin following 2 Gy irradiation (Fig;4.4.7D, E, F).

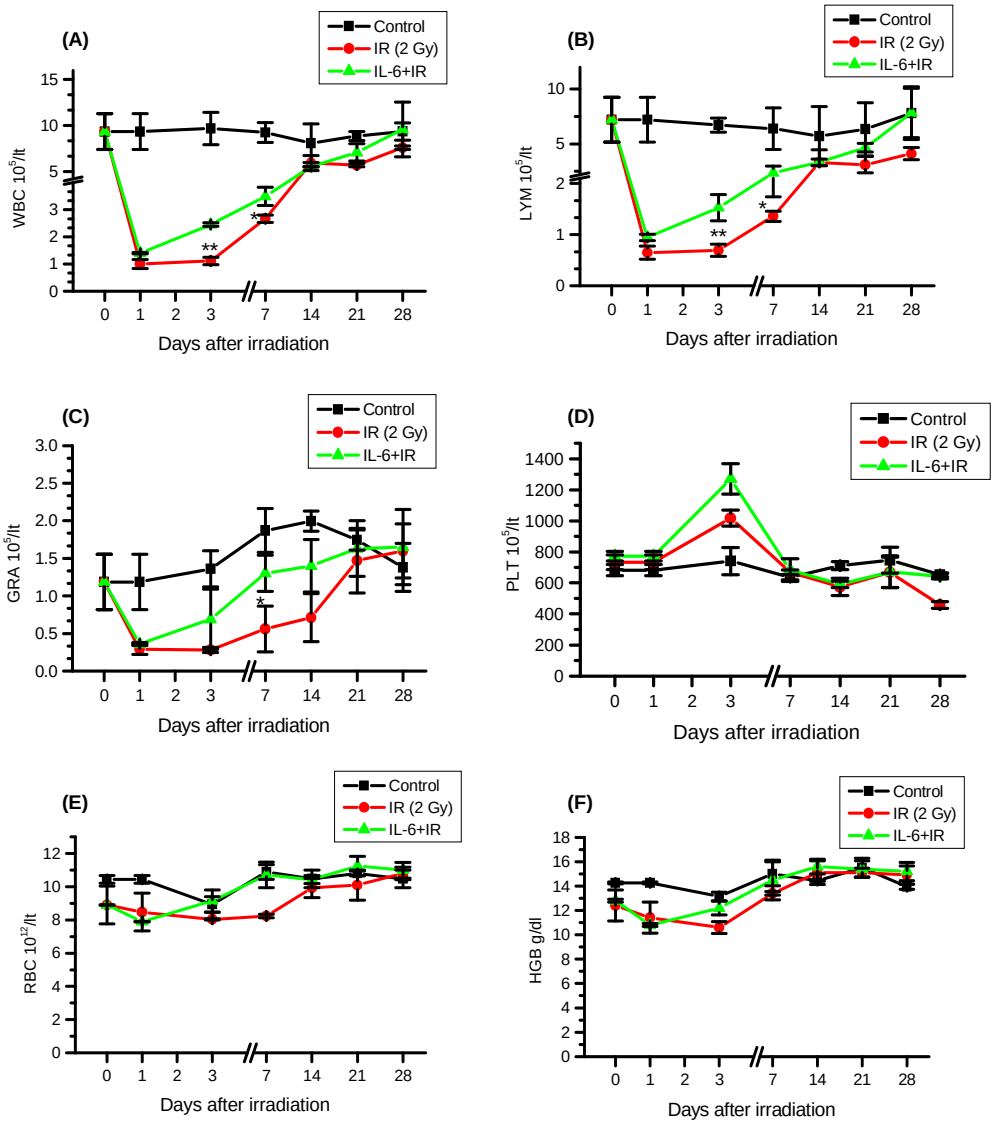

Figure 4.4.7: Effect of IL-6 on radiation-induced alterations in peripheral blood cell populations at low IR dose (2 Gy). C57BL/6 mice were administered IL-6, 2 hr prior to 2 Gy WBI followed by 3 doses post WBI at 24, 48, and 72 hrs (A) Total WBC count (B) Lymphocyte number (C) Granulocyte number (D) Platelet count (E) RBC count (E) Haemoglobin at 01, 03, 07, 14, 21 and 28 days after treatment. *: $p<0.05$; **: $p<0.001$.

4.4.3.2 Effects on bone marrow cellularity

Bone marrow is a critical target of ionizing radiation and myelotoxicity resulting from acute exposure of low to moderate doses of radiation and is the major contributing

factor for radiation-induced haematological toxicity. Myelotoxicity/myelosuppression or bone marrow depression is indicated by loss of bone marrow cellularity, resulting in compromised haematopoiesis and increased susceptibility to infections (Shao, Luo, & Zhou, 2014; V. K. Singh, Newman, Berg, & MacVittie, 2015). To evaluate the effect of IL-6 on radiation-induced damage to the bone marrow compartment, we did a histological analysis of the femur and assessed the number of nucleated cells in bone marrow on day 14 post-irradiation in C57BL/6 mice. It was observed that the number of bone marrow cells was nearly 60% low in WBI group, as compared to the un-irradiated control group ($8.8\pm2.21 \times 10^6$ vs $29\pm3.82 \times 10^6$ in control; $p< 0.001$) at day 14 post-irradiation. IL-6 pre-treatment to irradiated mice showed a significantly higher bone marrow cell number, with the count being 2.4 folds elevated (20.5 ± 2.828; $p< 0.01$) (Fig;4.4.8A).These results corroborated well with the histopathological changes observed in the femur of mice belonging to different treatment groups at both the IR doses. Disruption of bone architecture and severe marrow hypoplasia, evidenced by reduced cellular density was evident in WBI mice. Radiation-induced depletion of bone marrow stem cells was overcome by IL-6 treatment. The cellularity of the femur in animals treated with IL-6 was comparable to the naïve animals (Fig; 4.4.8B&C). Taken together, this data indicated that IL-6 has the potential to ameliorate WBI-induced BM hypo-cellularity by facilitating the proliferation of stem cells, thus accelerating hematopoietic recovery and BM regeneration.

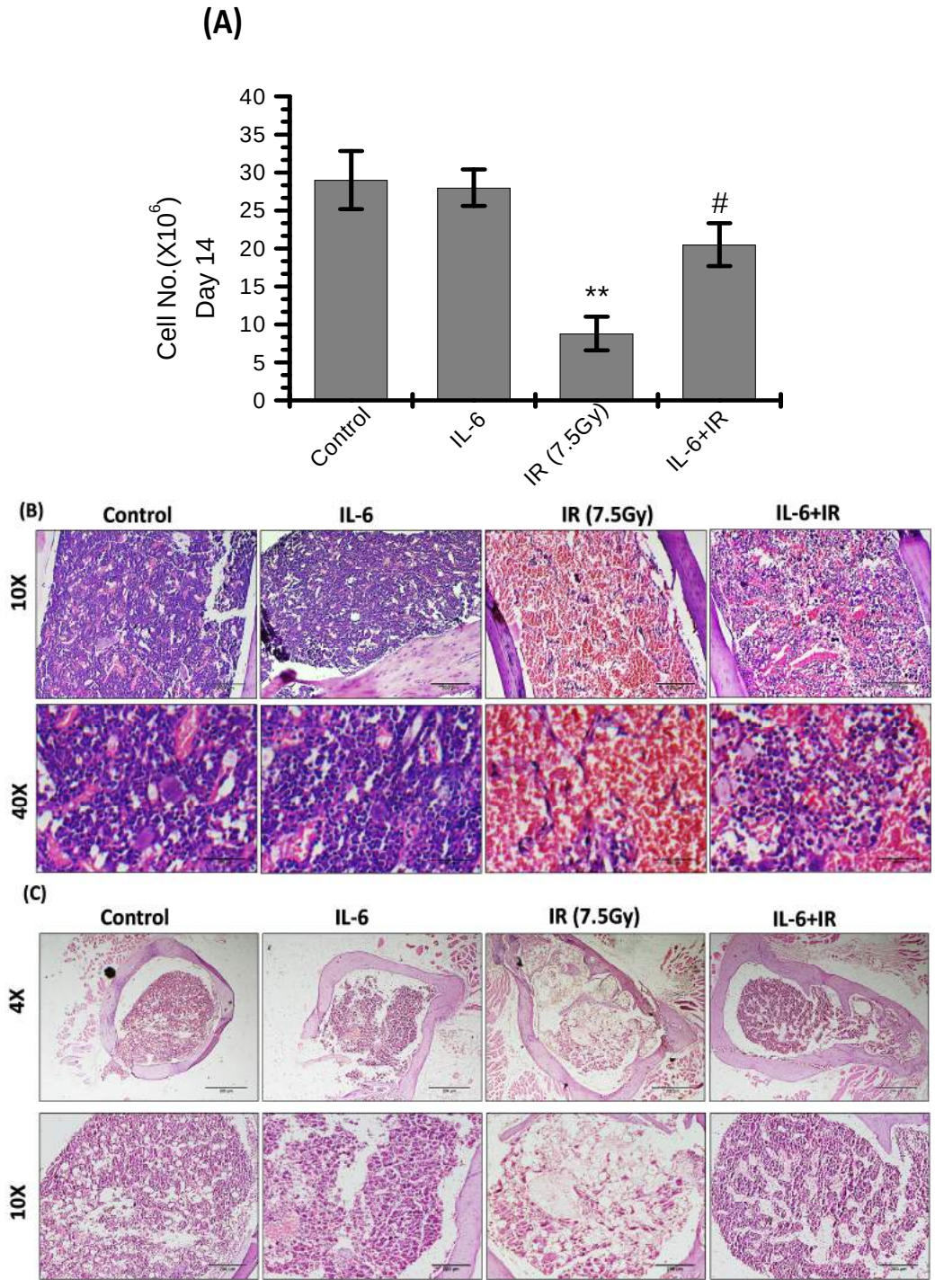

Figure 4.4.8: Effect of IL-6 on the bone marrow cellularity of irradiated C57BL/6 mice (A& B) Bone marrow nucleated cell count at day 14 of treatment at 7.5Gy. **: $p<0.01$ (C) Images are showing vertical sections (D) and horizontal sections of Haematoxylin and Eosin stained femur at 14 days post 7.5 Gy irradiation. IL-6 treatment was followed according to the multi-dose protocol.

4.4.3.3 Effects on radiation-induced spleen atrophy and splenocyte death

The spleen is the secondary lymphoid organ composed of numerous round, long or irregular aggregations called white pulp (W.P.) located in the red pulp (R.P.) with the clear and prominent marginal area in between them. These compartments (W.P. and R.P.) are enclosed by the compact connective tissue capsule from which trabeculae extend deep into the interior of the spleen. Lymphoid organs are highly radio-sensitive because of their high turnover rate; therefore, IR induced cell death can be easily observed in these organs (Kulkarni et al., 2010; Mauch et al., 1995). Loss of splenocytes because of IR induced apoptosis results in the overall loss in the size and weight of the spleen (splenic atrophy) (Ha, Li, Fu, Xiao, & Landauer, 2013). To determine the effect of IL-6 on WBI (7.5 Gy) mediated splenic atrophy, spleen size and weight were taken at day 3 post-WBI. A significant contraction in the spleen size was observed in WBI mice, which was around 25% lower in comparison to the size of normal spleen in un-irradiated mice ($p < 0.01$). A similar observation was made with the spleen weight, which displayed a 3- fold reduction in the WBI group in contrast to the un-irradiated control mice ($p< 0.001$). This radiation induced splenic atrophy was countered by IL-6 treatment and the spleen size was found to be marginally reduced but comparable to the size of the naive mice ($p< 0.05$; Fig; 4.4.9A&B). The spleen weight was also found to be markedly increased in the IL-6+WBI mice ($p < 0.05$), but it still remained significantly lower than that of the naive animals (Fig; 4.4.9C). Further spleen to body weight ratio confirmed the radiation induced spleen shrinkage independent of body weight ($p < 0.01$) (Fig; 4.4.9D). Furthermore, flow cytometric analysis of apoptosis in spleen revealed that IL-6 significantly reduced the percent increase in total apoptotic cells as compared to WBI alone (12.75±0.353 in WBI vs 7.5 ±0.707 in IL-6+WBI, Fig; 4.4.9E). Haematoxylin and eosin (H&E) staining of

transverse sections of spleen revealed that the width and density of white pulp in spleen at day 3 post irradiation was disorganized and compromised in comparison to control mice. It was followed by spleen contraction and the decreased cellularity of the white and red pulp. The white pulp is the site of B and T cells differentiation and interaction to blood borne antigens. IL-6 pre-treatment to irradiated animals prevented the loss of cellularity in the white and red pulp and the deformation of spleen morphology (Fig; 4.4.9F). These findings proposed that the alleviation of WBI-mediated injury by IL-6, also contributed to the hematopoietic recovery in secondary lymphoid organs.

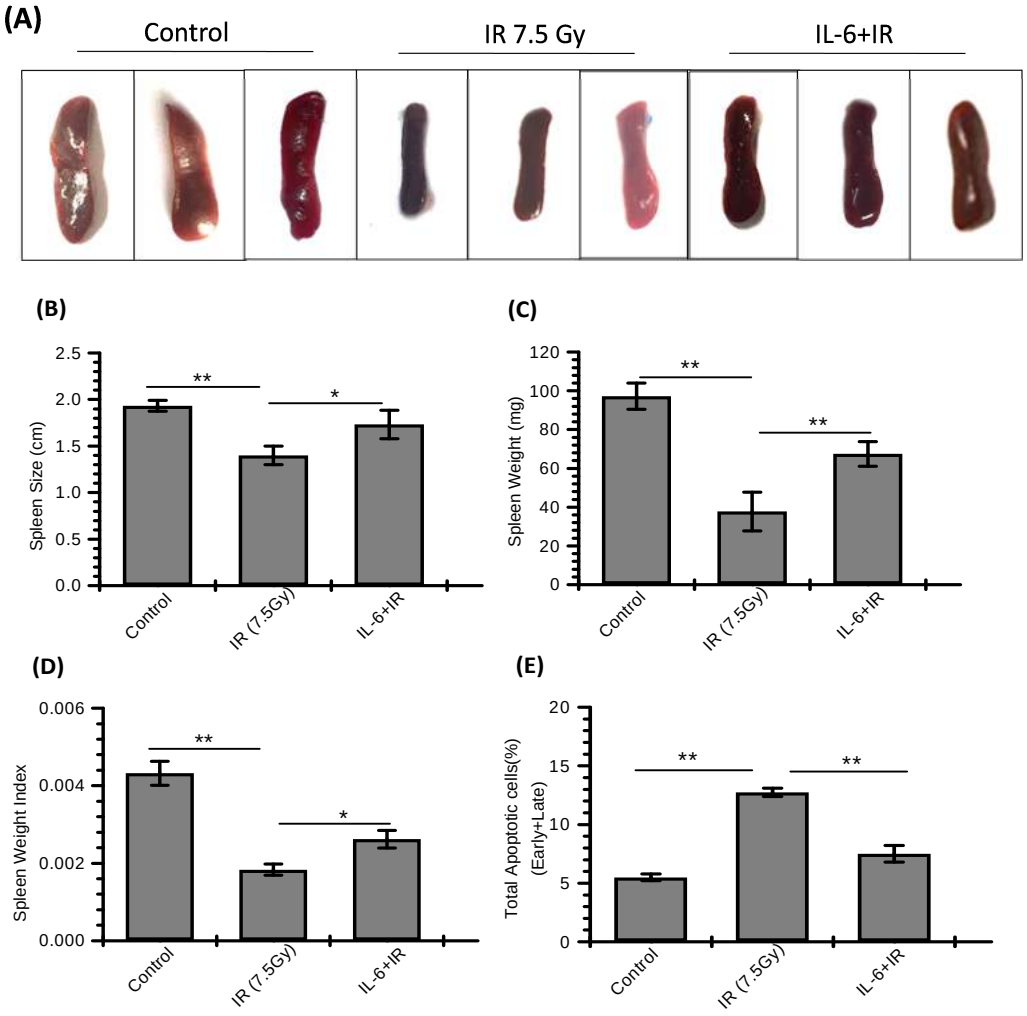

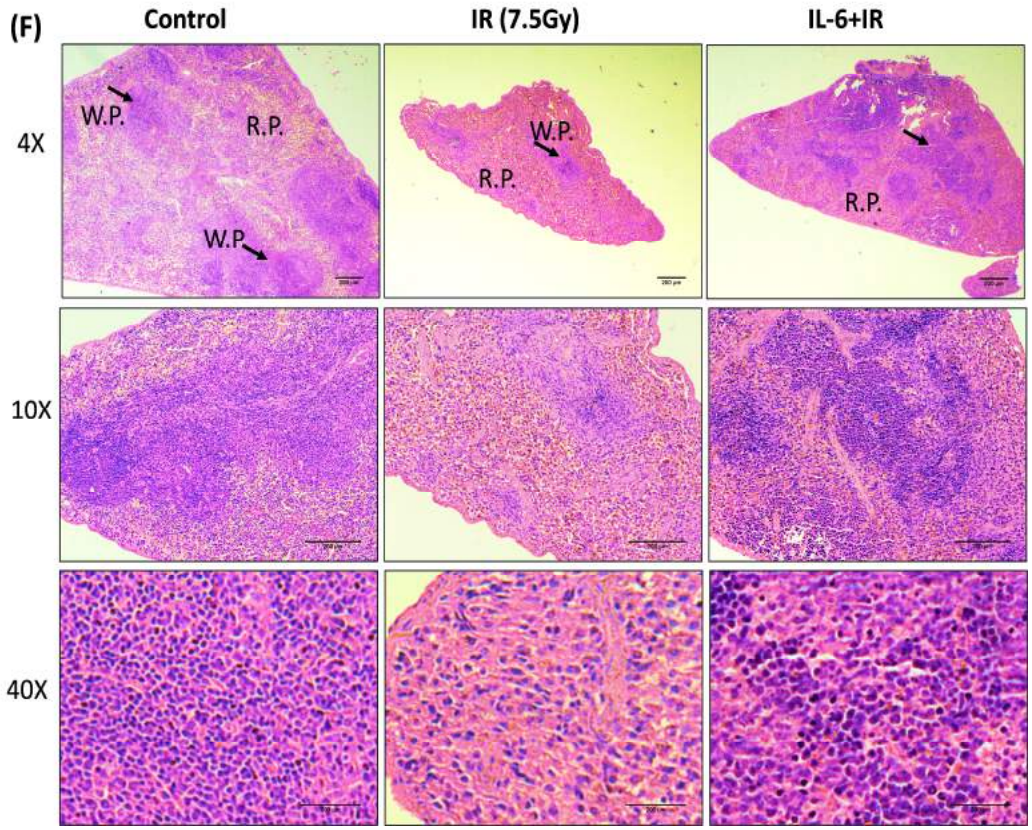

Figure 4.4.9: Effect of IL-6 on spleen atrophy (A) Representative images of spleen (B) spleen size and (C) spleen weight (in mg) (D) Spleen weight index of irradiated C57BL/6 mice analyzed at day 3 post-treatment (E)Total apoptotic cells at 24 hrs post-irradiation. (F) H&E staining of spleen sections was performed 3 days after WB (7.5Gy), (Arrowheads show white pulp). IL-6 treatment was followed according to the multi-dose protocol. *: $p<0.05$; **: $p<0.01$.

4.4.3.4 Effect of IL-6 on radiation-induced DNA damage and repair in PBMCs

Radiation-induced oxidative stress causes damage to the cellular macromolecules, the most sensitive target being the DNA. DNA DSBs represent the most critical lesions induced by ionizing radiation, which can be assessed by detecting the γ-H2AX foci formation at DSB sites by immunostaining, as it had been established that the ratio of visible γ-H2AX foci to DSBs is nearly 1 (1:1) (Moroni, Maeda, Whitnall, Bonner, & Redon, 2013). Since IL-6 had shown the potential to reduce the radiation-induced oxidative stress; it prompted us to study its action on DNA damage induction and repair

in the peripheral blood lymphocytes (PBMCs). The whole body irradiation with 2 Gy dose of C57BL/6 mice induced a significant amount of DNA damage in the PBMCs, as nearly a 10 fold rise in the average number of foci was observed in the irradiated cells, 1hr post-exposure (7±2.5 vs 2±0.5in control; $p< 0.01$). The pattern of foci suggested discrete sites of damage induction. These observations are depicted in the photomicrographs presented in Fig; 4.4.10, which showed the appearance and clearance of γ-H2AX foci after irradiation at 1, 4 and 24 hrs. The level of damage induction was markedly reduced in IL-6 and IR co-treated cells, as the average foci per cell were about 30% lesser in these cells (5±0.5 vs 7.3±1.5 in radiation alone; $p< 0.05$). At 24 hrs post-treatment, unrepaired lesions accounted for a statistically significant higher residual damage in the irradiated cells, while in IL-6 administered mice, the residual damage was only 50% of the WBI alone cohort (3±0.5 vs 6±1in radiation alone $p< 0.05$) (Fig;4.4.10A) suggestive of an efficient repair of the DSBs. A temporal reduction in the number of foci was indicative of ongoing repair, which was compromised in the radiation alone cells as compared to the IL-6 pre-treated ones.

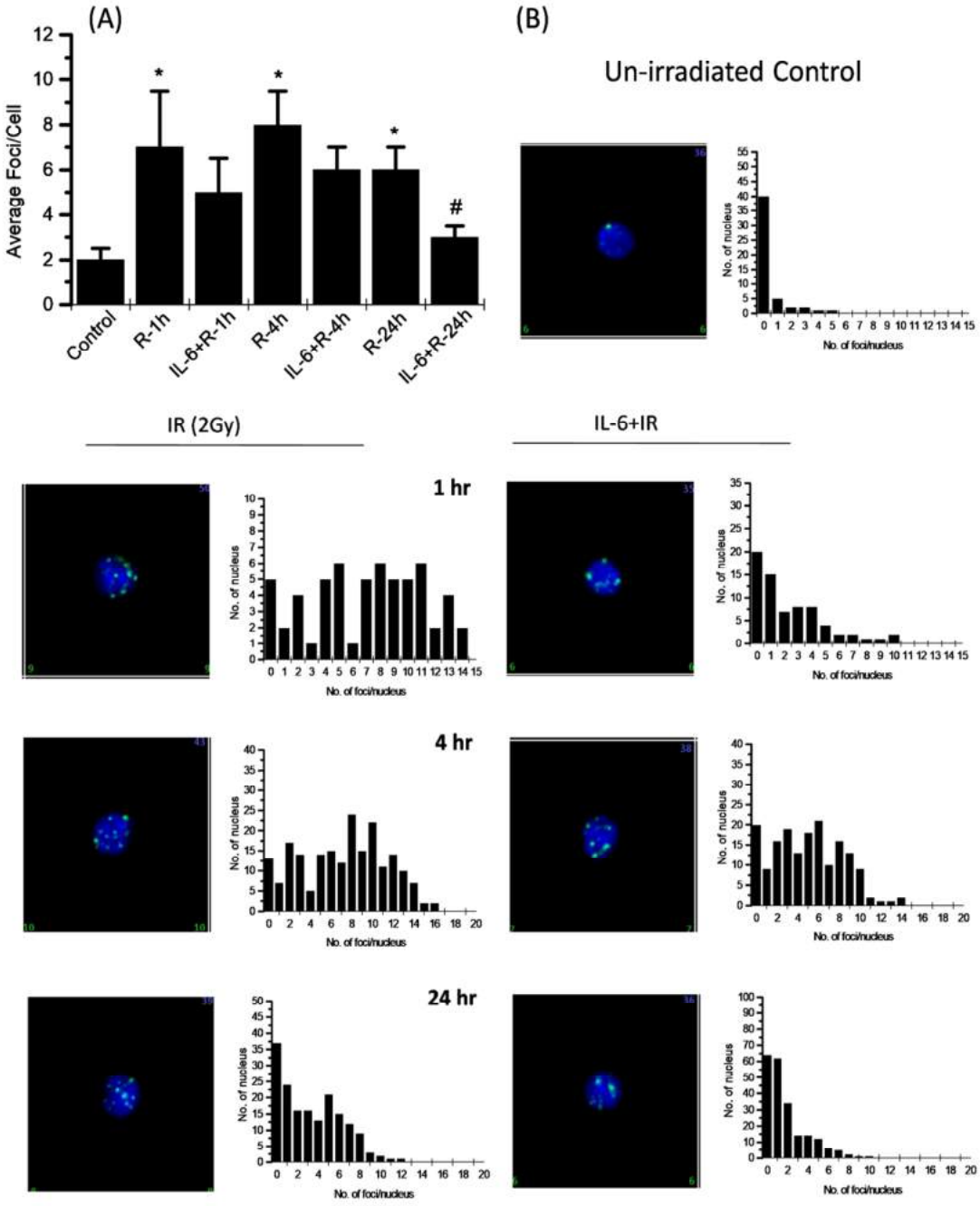

Figure 4.4.10: Effect of IL-6 on radiation (2 Gy) mediated DNA damage and repair in peripheral blood mononuclear cells of C57BL/6 mice (A) Quantitative analysis of γ- H2AX foci at varied time points (B) The representative photomicrographs showing distinct γ-H2AX foci at varying time intervals, with a frequency histogram of the number of foci/ nucleus. $*^{\#}$: $p<0.05$; Star shows significance w.r.t. to control and # showed with respect to IR.

4.4.3.5 Effects of IL-6 on radiation-induced cell cycle perturbations in Bone marrow cells

Since the imbalance in cell proliferation and death determines the size of the hematopoietic stem cell pool, we analyzed the cell cycle progression of BM cells to deduce the effect of IL-6 on radiation-induced apoptosis and proliferation in these cells. Cell cycle checkpoint activation forms an inherent component of the DNA repair machinery and ensures damage-free proliferation of cells. Radiation treatment accumulated cells in S and G2/M phase of cell cycle at 72 hrs post-exposure, followed by a significantly higher proportion of cells with hypodiploid DNA content (sub-G1 population, an indication of apoptotic/degenerating cells) at 48 and 72 hrs (11.8 ±0.424% at 48 hrs and 13.9 ±3.39% at 72 hrs vs 5.58±1.21 % in control $p< 0.01$). This could be due to a high level of unrepaired/ mis-repaired DNA damage that ensued the initiation of cell death in these cells. This data was consistent with the γ-H2AX foci observed at 24 hrs of IR exposure (Fig; 4.4.10). The fraction of cells that accumulated in the S and G2/M phase was released following IL-6 treatment, and there was a reduced population in sub-G1 phase at 24, 48 and 72 hrs (2.46±0.45% at 24 hrs, 1.7 ±0.98% at 48 hrs and 2.66 ±1.401 at 72 hrs; $p< 0.01$; Fig; 4.4.11B) which suggested proliferation, repair and reduced apoptosis by IL-6.

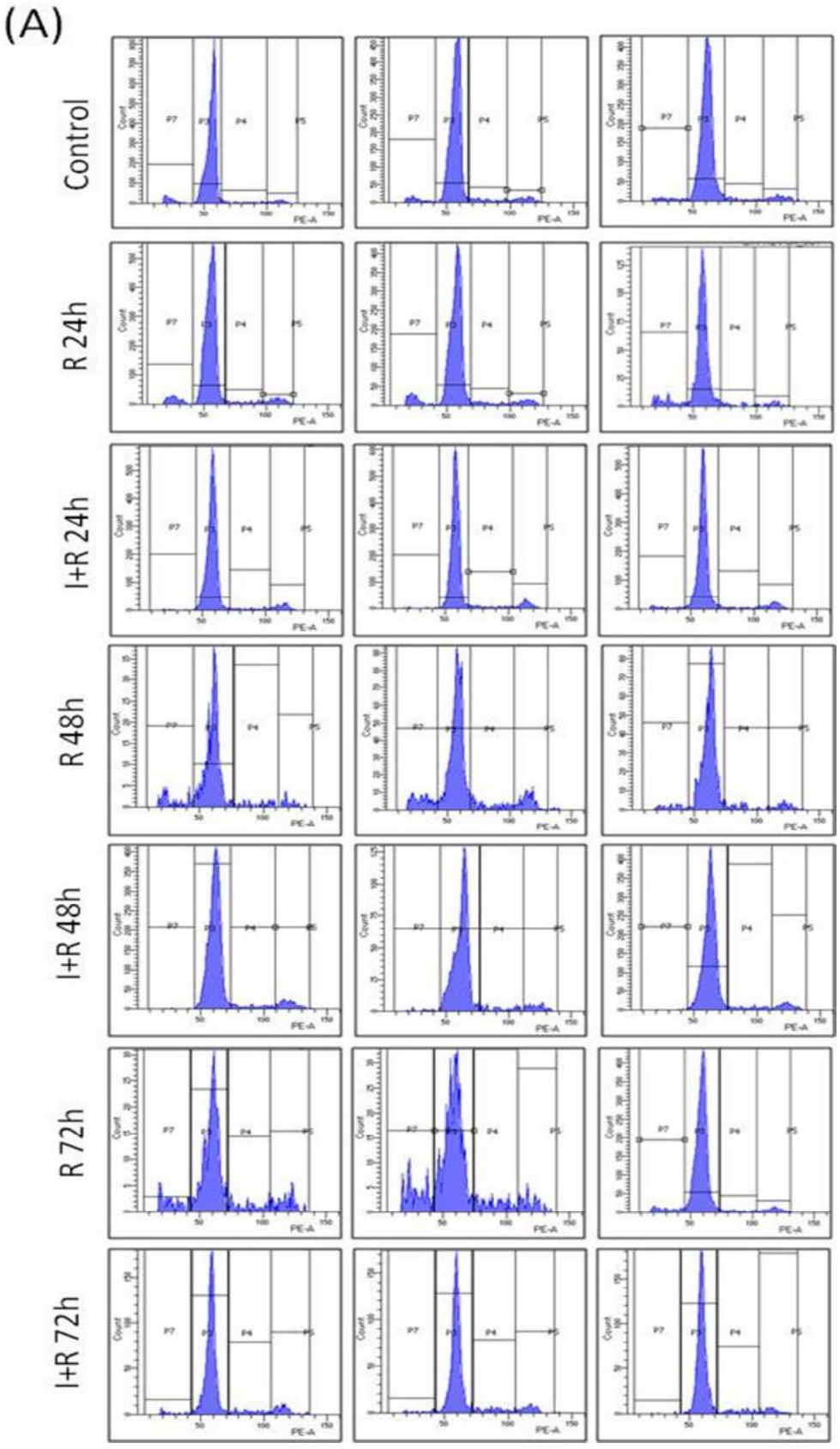
(A)
Control
R 24h
I+R 24h
R 48h
I+R 48h
R 72h
I+R 72h

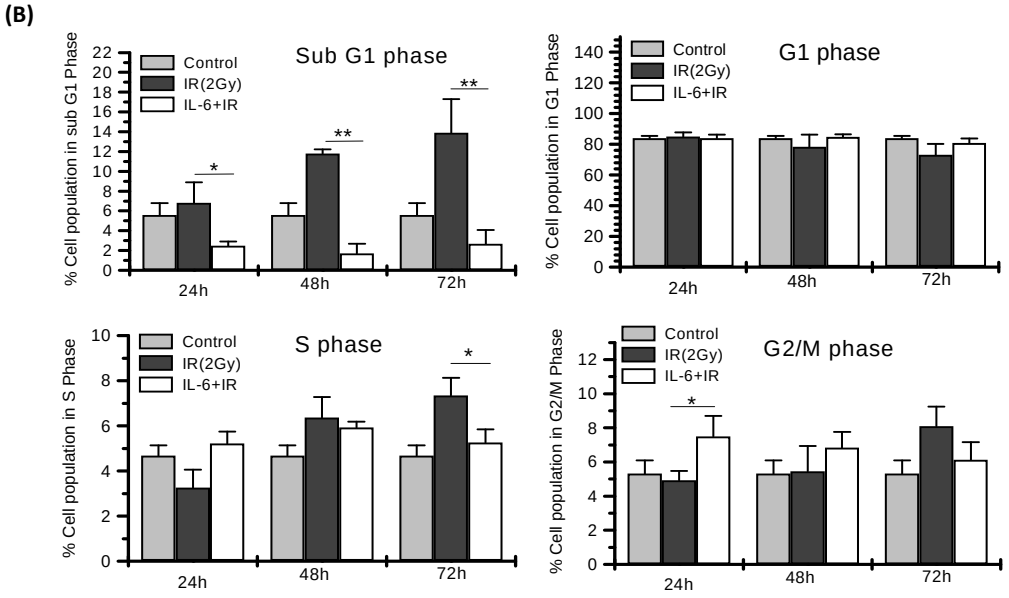

Figure 4.4.11: Effect of IL-6 on radiation-induced cell cycle perturbations in the bone marrow cells of C57BL/6 mice. (A) Representative flow cytometric DNA histograms presenting the cell cycle distribution pattern in naïve, WBI and IL-6+ WBI mice at 24, 48 and 72 hrs of treatment. (B) Graphs represent the percentage of cells in the distinct phases of the cell cycle at 24 -72 hrs. *: $p<0.05$; **: $p<0.01$.

4.4.3.6 Effects of IL-6 on radiation mediated cytogenetic damage in the cells of Bone marrow

Radiation induces free radical-mediated DNA damage which further results in interphase and/or mitotic cell death in different hematopoietic compartments and contributes significantly in WBI induced lethality (Maier, Hartmann, Wenz, & Herskind, 2016). Radiation causes residual DNA (cytogenetic) damage which can be visualized as micronuclei in the nucleated cells in the bone marrow compartment. There was a substantially higher (~4 fold) M-fraction in the BM nucleated cells of WBI cohort than its un-irradiated counterparts at 48 hrs ($p<0.01$; Fig;4.4.12A). IL-6 offered protection against radiation-induced micronuclei formation as it reduced the M-fraction by 50%, i.e., from (12.25±2.42) to (6.5±2.38)($p< 0. 01$) at 48 hrs and (5.83±0.752) to (1.993±0.75) at 72 hrs after treatments. The bone marrow cell

enumeration at the same time was correlated and suggestive of the fact that cells having micronucleus were removed from the system and maintained a low cell number in IR group as compared to IL-6 +IR cohort till 72 hrs (0.912 x 10^6±0.152 in IR vs 1.77 x 10^6±0.191 in IL-6+IR groups) (Fig;4.4.12B). These observations, together with the results of the γ-H2AX assay (Fig;4.4.10), strongly suggested the geno-protective potential of IL-6.

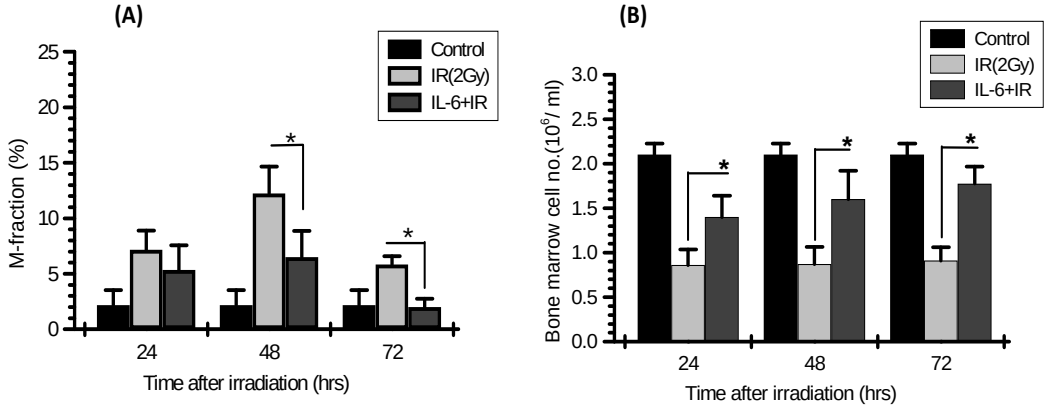

Figure 4.4.12: Effect of IL-6 on radiation mediated cytogenetic damage in the BM cells of C57BL/6 mice (A) Number of micronucleated bone marrow cells (M-fraction) at 24, 48, 72 hrs of treatment. (B) Bone marrow nucleated cells per ml at 24, 48 and 72 hrs. *: $p<0.05$.

4.4.3.7 Effects of IL-6 on BM hematopoietic stem cells

Bone marrow is a kind of reservoir for many types of cells, including both blood-forming (hematopoietic) and non-blood forming (stromal and endothelial) progenitor cells. Hematopoietic stem cells (HSCs) are most sensitive to radiation injury and results in the manifestations of acute radiation injuries like haemorrhage, illness, and bone marrow failure (Dainiak, 2002; Shao et al., 2014). All the immune and blood cells including B and T lymphocytes, natural killer cells, platelets, erythrocytes, myeloid cells, mast cells and dendritic cells (DCs) are continuously replenished by HSCs throughout the life span of an organism. Radiation injury to the BM can affect the niches for stem cell development and

therefore, the recovery from hematopoietic injury. Thus, preservation of the stem cell pool is essential for stem cell rejuvenation and differentiation (Kulkarni et al., 2010; Yin & Li, 2006). HSCs constitute long-term HSCs (LT-HSCs), short-term HSCs (ST-HSCs), and multipotent progenitors (MPPs), which can be characterized with specific cell-surface markers through immunostaining and detection using flow cytometric technique. The murine HSCs are typically lineage negative (Lin-), stem cell antigen-1 positive (Sca-1+), and cKit+ (together called LSK cells).

Flow cytometric analysis at 24 hrs post-irradiation revealed that 2 Gy radiation dose is sufficient to cause stem cell transition from quiescent to proliferation phase. Therefore, the percentage of LSK cells was increased by irradiation (6.3%) as compared to non-irradiated control (3.7%) (Fig;4.4.13). However, IL-6 pre-treatment before irradiation significantly increased the LSK population to 10.4%, which is suggestive of increased proliferation. Further, the LSK population was differentiated to short term HSCs to recover the ablation of blood cells. Under no stress condition, e.g. un-irradiated control, out of 3.7% LSK, 91% were LT-HSCs, and only 9% were ST-HSCs (which were required to maintain the hematopoietic pool). Irradiation (or any genotoxic stress) brought the conversion of LSK cells more towards ST-HSCs to hasten the recovery, therefore out of 6.3% LSK cells 70% were LT-HSCs, and 30% were ST-HSCs in IR while the IL-6 pre-treatment increased the ST-HSCs to 40% signifying intense recovery compared to IR alone. The data were correlated with our haematological counts at 24 hrs post 2 Gy irradiation which had more blood cell count in IL-6 pre-treated irradiated group in comparison with IR alone (Fig; 4.4.7). These results indicated that IL-6 facilitated hematopoietic recovery following irradiation by augmenting the proliferation and differentiation of HSCs.

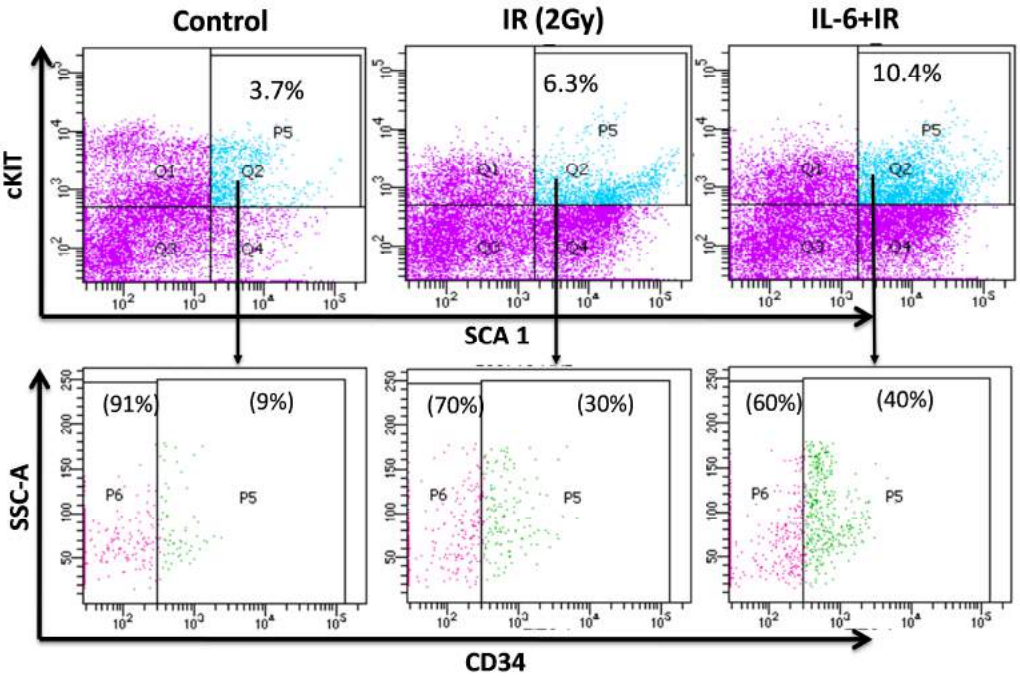

Figure 4.4.13: Effect of IL-6 on hematopoietic stem cell pool in the bone marrow of C57BL/6 mice; percentage of LSK (Lin−, SCA1+, cKit+) cells (P5 population) out of the total population with representative FACs plots (upper panel). LSK cells were dragged to differentiate between LT-HSC (CD34−) and ST-HSC (CD34+) (lower panel).

4.4.4 Modification of radiation-induced gastrointestinal (GI) damage by IL-6

The intestinal epithelium is a rapidly renewing tissue, damage to which can be a cause of mortality following moderate to high doses of IR. It is an early responding tissue because of the high sensitivity of intestinal stem cells (P. K. Singh et al., 2012). An acute injury is caused by the rapid stem cell apoptosis at the crypt base, leading to an inadequate supply of cells required for maintaining the mucosal lining, followed by the mitotic cell death 24-48 hrs post-radiation (Bonnaud et al., 2010). Radiation exposure elicits injury not only in the mucosal elements but also in the vascular compartment. This results in intestinal barrier disruption and vascular permeability, which then initiates or perpetuates inflammatory mediator release, causing damage to

distant organs as well (Buell & Harding, 1989). Thus, injury to the gut may be regarded as the key player in the initiation of multiple organ dysfunction syndromes or failure (Monti, Wysocki, van der Meeren, & Griffiths, 2005). GI injury in the lack of recovery can be devastating and can result in the death of animals within 10-15 days, thus underscoring the importance of intestinal regeneration as an essential criterion in the development of radiation countermeasure agents.

4.4.4.1 Modification of radiation-induced gastrointestinal injury

The severity of injuries to the bone marrow and GI tract is the primary determinant of survival after receiving moderate doses of ionizing radiation (Williams & McBride, 2011a). The induced apoptosis is primarily responsible for the decreased survival (cell loss), which leads to structural and functional alterations in these two compartments (Duckworth & Pritchard, 2009). To assess the potential of IL-6 in ameliorating radiation-induced gastrointestinal injury, we carried out the histopathological analysis of the small intestine at day 01 and 07 following treatment in C57BL/6 mice. The jejunum was selected as the primary tissue for histopathological analysis. Fig;4.4.14A shows the representative photomicrographs of H&E-stained jejunum sections obtained from mice of the different treatment groups. The jejunum from irradiated mice showed marked structural distortions characterized by denuded mucosa, shortening of villi, cellular desquamation at villus tips and epithelial detachment.

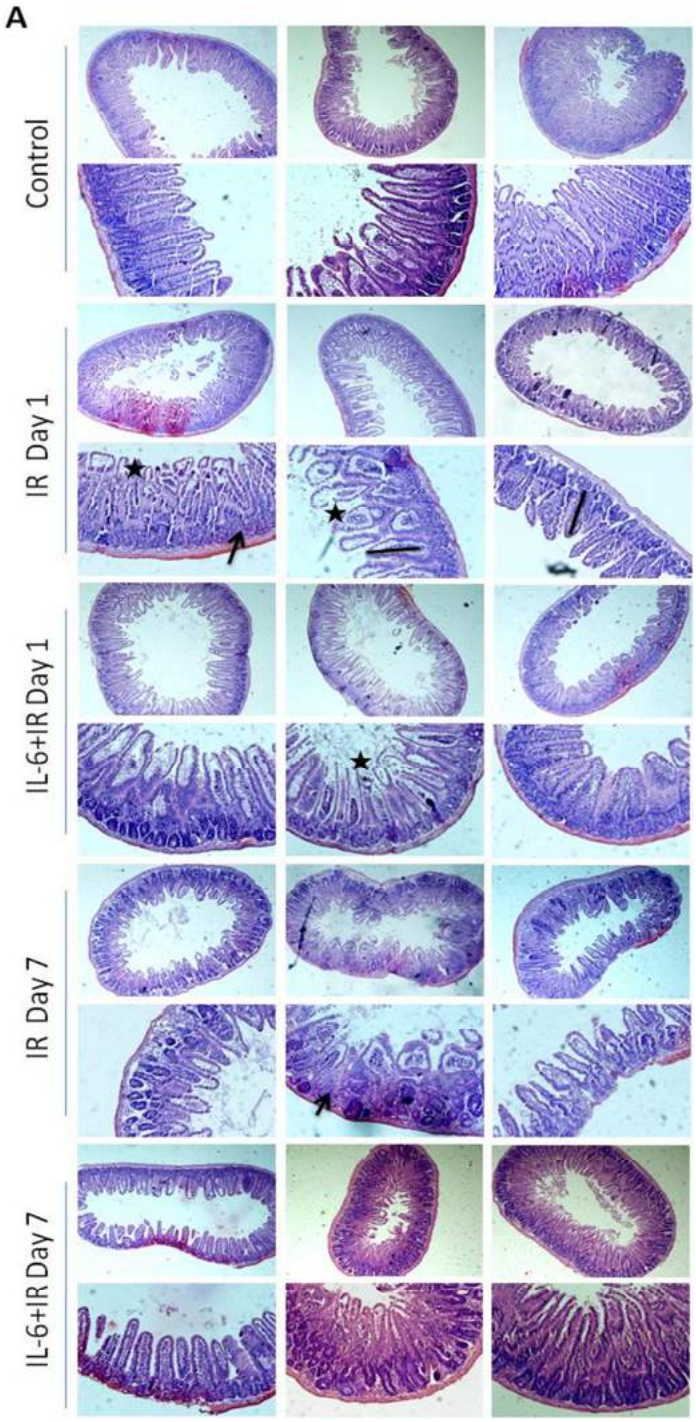

Figure 4.4.14: Effect of IL-6 on jejunal histology of irradiated mice. Representative photomicrographs of H & E stained jejunal sections harvested from C57BL/6 mice, treated with IL-6 prior and post-irradiation with 7.5 Gy. Irradiated mice showed shortening of villi (vertical line), sloughed off mucosa (*) and loss of crypts (arrows) at day 01 with marginal recovery at day 07. Scale bar= 200µm

The damage induction was more pronounced in irradiated mice; however, IL-6 treatment reduced the structural abnormalities caused by WBI at day 01. This was evident by the preserved villi length at day 07, and the overall structural integrity. The mucosal morphology was retained to the level of control in IL-6+WBI mice as compared to WBI at day 07 post IR, and discernible differences in the histology of WBI and IL-6+ WBI mice could be clearly observed. However, the differences were significant between control and IL-6+WBI as shown by substantial changes in mucosal architecture and a few interspersed shorter villi, indicating partial injured mucosa. These results demonstrated the remarkable potential of IL-6, in restoring the structural integrity of the small intestine following radiation injury.

4.4.4.2 Effects of radiation-induced oxidative stress and apoptosis on GI tissue and its modulation by IL-6

It is well established that IR exposure leads to the ROS generation, and the oxidative stress resulting from an imbalance in the overproduction of ROS and the cell's antioxidant defence machinery has a key role in irradiation-induced cellular damage and thus, apoptosis (Jin, Sung, In, & Park, 2007). We, therefore, measured the levels of MDA, a consistent indicator of oxidative stress-mediated tissue damage (Del Rio, Stewart, & Pellegrini, 2005), and protein carbonylation to evaluate the effect of IL-6 on radiation-induced oxidative stress and measured the expression pattern of anti-apoptotic proteins. MDA levels in the jejunum of the irradiated mice were increased by approx. 2.5 fold at 24 hrs of IR treatment ($p < 0.001$) (Fig;4.4.15A).Pre-treatment with IL-6 reduced the IR-induced elevation in MDA levels up to the normal extent. The MDA content was found around 3 fold less in IL-6+ WBI mice ($p < 0.001$ vs radiation) at 24 hrs post IR. Further, at day 07 post-IR, the MDA level came near to

control 2.45±0.467 nmol/mg protein in control vs. 3.44±0.534 in IR alone. However, in IL-6 and radiation treated animals, the MDA levels were found below control (1.32±0.26) at day 07 (Fig; 4.4.15A). ROS not only damages the membrane lipid but also another important macromolecule that is protein, therefore protein carbonylation was also checked as a result of radiation injury. We observed a robust increase in protein oxidation due to irradiation but, IL-6 treatment prevented protein oxidation significantly and the level did not exceed to 50% of the irradiation (27.23±4.20 in IR vs 13.20±0.377 in IL-6+IR; $p < 0.001$, Fig; 4.4.15B) at day 01 post irradiation. However, at day 07 the values observed were comparable to control in all groups. The differences in the lipid peroxidation and protein carbonylation in different treatment groups suggested lower oxidative stress followed by lower apoptosis.

In response to gamma radiation, the intestinal crypt cells rapidly undergo apoptosis and cause gastrointestinal toxicity (Rotten & Grant, 1998; P. K. Singh et al., 2012). Apoptosis was investigated in GI tissue following radiation exposure using TUNEL assay by flow cytometric analysis at day 03 post-irradiation. The mean fluorescence intensity (MFI), representing TUNEL positive cells, was compared between the different treatment groups. Irradiation led to the initiation of apoptosis in the jejunum cells, indicated by around 3 fold enhancement ($p< 0.05$) in the MFI as compared to the un-irradiated control, which was decreased by ~ 1.5 fold upon IL-6 pre-treatment ($p< 0.05$; Fig;4.4.15C). Reduced apoptosis was further validated by the increased expression of anti-apoptotic proteins like Bcl-2 and Mcl-1 in GI tissues (Fig; 4.4.15D). These results suggested that IL-6 has a strong potential of protecting mice from radiation-induced GI injury owing to its potent antioxidant and anti-apoptotic properties.

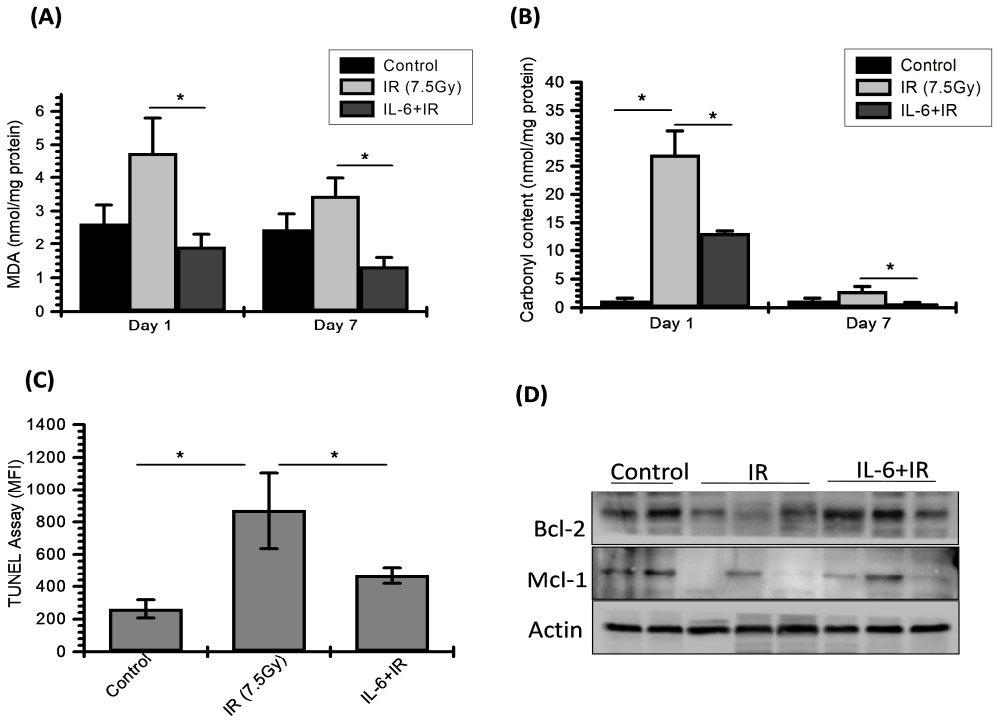

Figure 4.4.15: Effects of IL-6 on radiation-induced oxidative stress and apoptosis. (A) MDA content and (B) Protein carbonyl content at day 01 and 07 post-irradiation with 7.5 Gy (C) Graph represent the Mean fluorescence intensity of TUNEL positive cells with respect to control at day 3 post-irradiation (D) Protein expression pattern of cleaved Bcl-2, Mcl-1 in naïve, IR and IL-6+ IR mice at day 3 post-irradiation. ns: non- significant; *: $p<0.01$.

4.4.4.3 Effect of IL-6 on radiation-induced alterations in cellular antioxidants in GI tissues

Since IL-6 was found to reduce the level of oxidation of biomolecules (lipid and proteins) following radiation exposure (Fig; 4.4.15), we sought to investigate if this was because of the modulation of the antioxidant defence system. In accordance with the lipid peroxidation and protein carbonylation results, irradiation compromised the cellular antioxidant defence mechanism. There was a considerable reduction in total antioxidant capacity at day 01 post IR compared to control (1.00±0.094 vs 0.56±0.037 in IR, $p < 0.001$). However, IL-6 pre-treatment resisted this IR mediated change (0.86±0.095) and maintained the antioxidant levels comparable to control

(Fig;4.4.16A). Further, IR caused depletion of GSH in the GI tissue of both IR alone and IL-6+IR, and non-significant changes were observed between the two groups on day 1. Conversely, IL-6 significantly recovered from GSH depletion concerning irradiation cohort at day 07 post IR (8.55±0.59 in IL-6+IR vs 5.16±1.01 in IR), though still significantly low from un-irradiated control (14.71±2.92) (Fig; 4.4.16B). Values of GSH expressed as nanomoles/mg protein. Non-significant changes in GSH between IR and IL-6+IR groups at 24 hrs post-irradiation suggested the contribution of other antioxidant enzymes in maintaining total antioxidant capacity and recovering from oxidative stress damages. Overall results showed that IL-6 prevents the harmful consequences of oxidative stress produced from radiation exposure in GI by strengthening the antioxidant defence machinery.

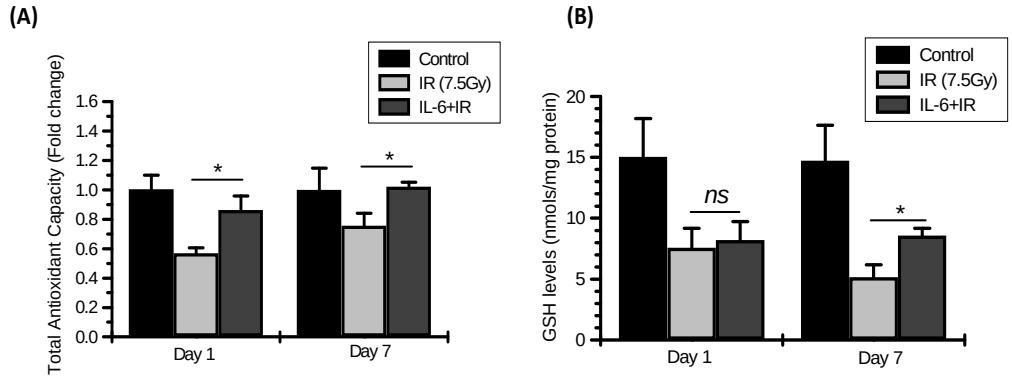

Figure 4.4.16: Effect of IL-6 on radiation-induced alterations in the level of cellular antioxidants (A) Total antioxidant capacity (B) GSH level in the GI tissues at day 01 and 07 post IR treatment. *: $p<0.01$; *ns*=non-significant.

4.4.4.4 Effect of IL-6 on Intestinal Epithelial cell proliferation

The mammalian intestinal epithelium has the capability to self-renew, and the entire epithelium can be replaced in approx. 3–5 days depending upon the severity of the damage. Therefore, the period between 3-7 days post IR is crucial to observe cell

proliferation. 5-bromo-2′-deoxyruidine (BrdU) immunohistochemistry have been used to level dividing cells (Jin et al., 2007; P. K. Singh et al., 2012). Two hrs after BrdU injection, mice were euthanized, and GI was removed and fixed in formalin, then sectioned and stained for BrdU. Slides were counterstained with Dapi. There was a visual difference between all groups in BrdU+ cells. The green colour dots showing anti-BrdU FITC labelled cells. The IR exposed samples showed very low proliferation in GI crypts; however, IL-6 treatment enhanced the regeneration, which could be observed by more BrdU FITC positive cells in IL-6+IR section. This data is in line with the H&E staining data (Fig;4.4.17) where IR alone group showed marginal recovery till day 07 that might be the outcome of radiation-induced loss of stem cells and slow or very minimal proliferation ability, evidenced by BrdU staining in different groups.

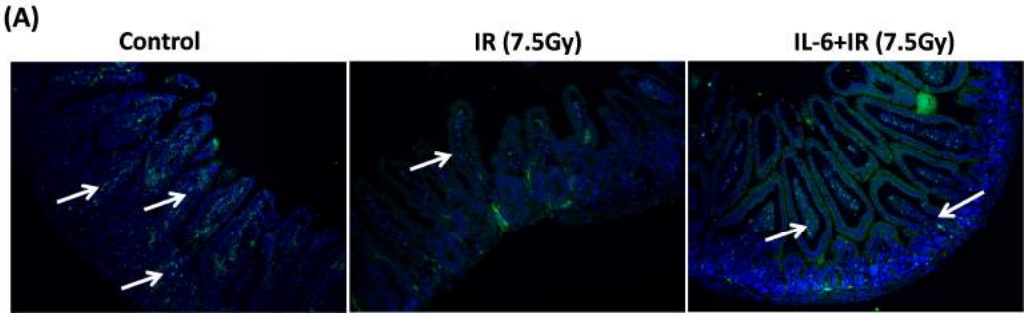

Figure 4.4.17: Effect of IL-6 on intestinal epithelial cell proliferation (A) Photomicrographs showing GI jejunum sections stained with FITC tagged anti-BrdU antibody (Green dot) at daPy 07 post-irradiation. Cells, undergoing proliferation accumulated BrdU (represented by arrow). Slides were counterstained with Dapi for nuclear staining. Image captured at 10X.

4.4.5 Inhibition of STAT-3 signalling reverted the IL-6 mediated radioprotection

In-vitro studies confirmed the role of STAT-3 in IL-6 mediated radioprotection (Fig;4.1.16). Similarly, intraperitoneal injection of STAT-3 inhibitor JSI-124 (1mg/kg body weight) to mice 30 minutes prior to IL-6 and radiation treatment resulted in

radio-sensitization of animal, observed by decreased survival. There was an early onset of radiation sickness in the presence of JSI-124

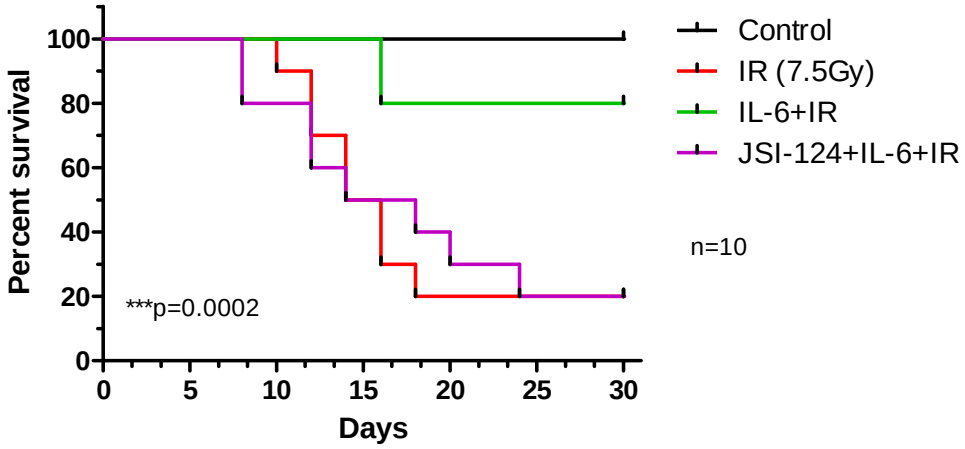

Figure 4.4.18: JSI-124 treatment reverses IL-6 mediated radioprotection. Kaplan-Meier survival curve showing the 30-day survival of C57BL/6 mice given an intraperitoneal injection of JSI124 (1mg/kg body weight) 30 minutes before followed by intramuscular injection of IL-6 (10ng/mice) for 2 hrs before being exposed to a lethal dose of radiation (7.5Gy) (n= 10 mice per group). Three post-exposure doses of IL-6 were given as per multi-dose protocol at 24, 48 and 72 hrs in IL-6+IR and JSI-124+IL-6+IR groups.

4.4.6 Summary

The study reveals that intramuscular injection of IL-6 to animals 2 hours before radiation followed by 3 doses post-irradiation protects them from lethal effects of radiation by activating STAT-3 signalling. The radiation-induced reduction in peripheral blood indices, bone marrow cellularity, and spleen atrophy was recovered after IL-6 treatment suggesting the protection from radiation-induced hematopoietic acute radiation syndrome (H-ARS). Further the proliferation of GI crypts cells, regeneration of villi, reduced macromolecular damages, reduced apoptosis and enhanced antioxidants in GI suggested that IL-6 treatment also protects from

gastrointestinal acute radiation syndrome (GI-ARS). Further, the inhibition of STAT-3 reverted the IL-6 mediated radioprotection to animals.

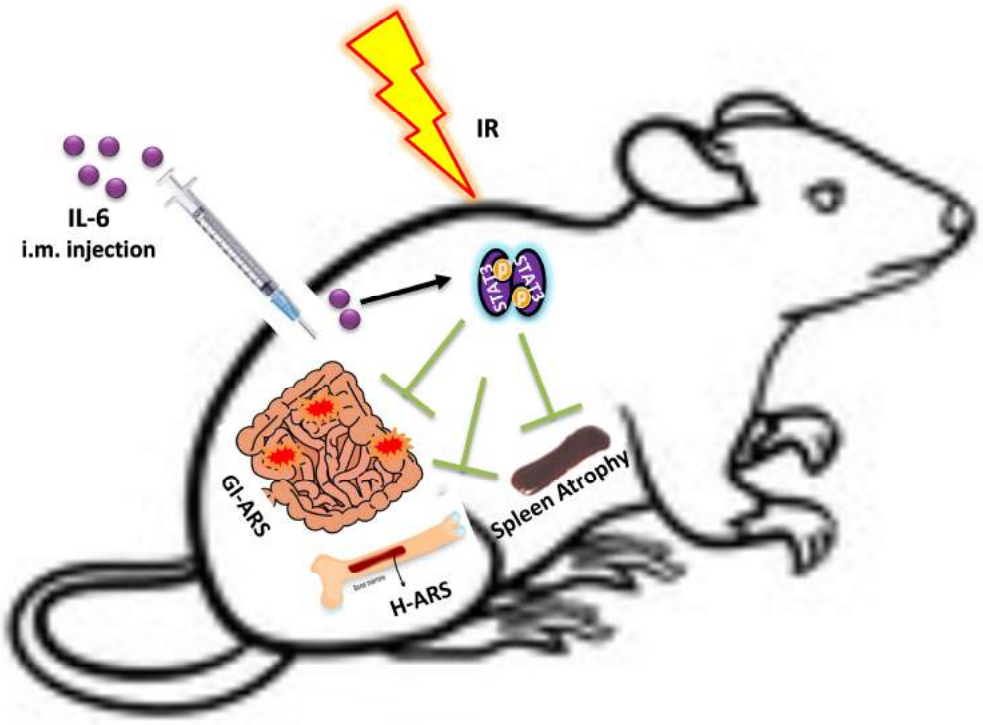

Figure 4.4.19: IL-6 protects from H-ARS and GI-ARS; IL-6 treatment prevent radiation-induced haematopoietic and gastrointestinal acute radiation syndromes by activating IL-6-STAT-3 signalling and resulted in survival at a lethal dose of irradiation.

Chapter 5
Discussion & Conclusion

CHAPTER 5
DISCUSSION & CONCLUSION

Literature survey shows a lot of reports about IL-6 being secreted from tumours and its associated stromal cells causing IL-6 mediated chemo- and radio-resistance in cancer, thus posing a major limitation in therapies (Kumari et al., 2016). It protects the cells from therapeutic stress-induced cell death by activating various pro-survival signalling cascades, proliferation, anti-oxidant defence system and inhibition of apoptosis. The IL-6 mediated radio-resistance in cells upon activation of cellular protective response has been attributed to be activated by IL-6 induced STAT-3 signalling (Brown et al., 2012)(X. Chen et al., 2018). Therefore, we tested whether IL-6 can also protect the normal and healthy cells from radiation.

The process of drug discovery involves comprehensive studies at the pre-clinical (non-human) level, involving cell cultures, tissue, and experimental animals as well as computational simulations for gathering information about the toxicity, efficacy and pharmacokinetics (PK) of a potential drug, before considering evaluation at the clinical level. For this, we started with finding the *in-vitro* cytotoxicity of IL-6 in multiple cell lines of different origins like hematopoietic (RAW264.7), gastrointestinal (INT-407) and fibroblasts (NIH3T3) cells. In literature, researchers have used varying concentration of 1pg/ml to 500ng/ml, which is suggestive of non-toxic range. We tested the concentrations from 0.1 to 10ng/ml and observed no toxicity at any of the concentrations screened in all three cell lines (Fig;4.1.1). Radio-protectors are basically the compounds given before irradiation that prevents radiation injury. In our study, we used IL-6 as a prophylactic approach that will protect the cells/animal against radiation insult. Further, we checked the radio-protective potential of these concentrations (0.1 to 10ng/ml) and foun 0.1ng/ml to be

ineffective in all the cell lines, but 1 and 10ng turned out to be effective doses at which radioprotection was observed. We wanted to use the minimal and best effective concentration therefore we pursued 1ng/ml dose for future experiments. Growth kinetics and Clonogenic assays are commonly used to investigate radiation-induced cell growth inhibition and survival of irradiated cells. Interestingly, IL-6 pre-treatment showed recovery of all the cell lines from radiation-induced growth delay; this was apparent from growth kinetics results and validated by clonogenic cell survival assay (Fig;4.1.3&4). Since the objective of the study was to protect the radio-sensitive cells from ionizing radiation; we selected cellular radio-sensitivity as a major factor for choosing cellular models for radio-protective studies. In preliminary studies, we worked on a range of radio-sensitive cells of hematopoietic and GI origin to moderately sensitive fibroblast cells. Since the haematopoietic system is one of the most vulnerable systems to ionizing radiation; we performed most of our study on murine monocytic RAW264.7 cells.

Cellular exposure to ionizing radiation initiates certain oxidizing events through direct or indirect (via the products of water hydrolysis) interactions with radiation that may lead to alterations in the atomic structure of biomolecules, hence results in damaged DNA, proteins, and lipids (Hall, Eric J. Giaccia, 2006). Biochemical modifications that arise in cells due to radiation exposure are the primary cause for most of the deleterious effects in mammalian cells. The primary ROS burst occurs just after irradiation, which eventually goes down but not before initiating a cascade of events inside the cell through which the second wave of ROS appears later ("secondary" ROS) either directly or typically through enzyme or metal catalysed processes. Consequently, oxidative modifications may endure till days or months from the first exposure due to continuous secondary ROS generation (Azzam, Jay-Gerin, & Pain, 2012). Therefore it is crucial to observe the kinetics of IR induced oxidative stress.

We followed the ROS kinetics from 0-48 hrs post-irradiation (Fig;4.1.7A). There was significant ROS burst just after irradiation, but more prominent ROS levels were seen after 24 hrs suggesting the secondary ROS burst. The organism survives such kind of oxidative stress by eliciting a response at the molecular, cellular and tissue level that neutralize the toxic effects of ionizing radiation (Azzam et al., 2012).

Consequently, IL-6 treatment aided the cells to survive such IR induced oxidative stress by reducing both early and delayed ROS. Since mitochondria occupy a considerable fraction of cell volume, almost 4-25% depending upon the cell type and size (Leach, Tuyle, Lin, Schmidt-ullrich, & Mikkelsen, 2001) and consumes around 90% of the body's oxygen, which makes it a prime target of radiation and are the chief source of ROS (Cadenas & Davies, 2000), this is also indicated by our results that IR induced delayed ROS is mainly produced by mitochondria (Fig;4.1.7D), which was reversed by IL-6 pre-treatment. A decrease in mitochondrial membrane potential after irradiation indicates the poor mitochondrial health while IL-6 treatment resists this depolarization and improve mitochondrial health and function (Fig;4.2.5). This increased ROS and low energy to overcome stress due to poor mitochondrial health lead to macromolecular damages observed by oxidation of DNA, peroxidation of lipids and carbonylation of proteins after irradiation (Fig;4.1.8). IL-6 treatment prior to irradiation reduces ROS and subsequently less macromolecular (DNA, protein and lipid) damage was observed in IL-6 pre-treated group (Fig;4.1.8).

The ROS generation in cells encountered by a variety of antioxidant defence mechanisms, including enzymatic and non-enzymatic scavengers. The most effective antioxidants having enzymatic activity are catalases, superoxide dismutases (SOD), glutathione peroxidase and peroxiredoxins which converts the dangerous superoxides

and other oxidative products to H_2O_2 and then water, on the other hand, non-enzymatic scavengers like vitamin C, vitamin E, glutathiones (GSH), carotenoids, lipoic acid, and flavonoids interrupts the free radical generating chain reactions (Redza-Dutordoir & Averill-Bates, 2016). Ionizing radiation-exposed cells stand with the oxidative insult by activation of ROS generating-oxidases, leading to altered redox and metabolic activity. Subsequently, in our study we observed that total antioxidant capacity was reduced after irradiation; however, IL-6 pre-treated cells were protected from the effect of IR by upregulating IL-6 induced total antioxidant capacity (Fig;4.1.9A). Further, the high levels of reduced glutathione (GSH)in IL-6 pre-treated irradiated cells is the indication of increased activity of glutathione reductase, an enzyme that converts the oxidized glutathione to reduced glutathione(Schmidt, Krieg, & Vedder, 2005). The IL-6 mediated increase in GSH, and the SOD activity neutralizes the IR induced oxidative stress (Fig;4.1.9B&C). Since the IL-6 predominantly alleviates the delayed ROS (24h post-IR), thus by virtue of this, alterations in oxidative damage, antioxidants capacity and reduced cell death were observed at 24 hr post-IR, mainly. Since the mitochondrial health is very crucial in the initiation of apoptosis in myeloid cells, the IL-6 mediated increase in MnSOD expression level also suggested the protection of mitochondria and later apoptosis. Furthermore, the above observations advocate the earlier published results in cancer cells, of reduction in ROS and macromolecular damages that may be the result of IL-6 induced increased antioxidant capacity in a cell that quenches ROS burst and the subsequent ROS mediated damage (Brown et al., 2012).

Apoptosis plays a very crucial role in maintaining genomic integrity by selectively removing the population of heavily damaged cells. Apoptosis can be triggered by any kind of stress, including oxidative stress, DNA damage, hypoxia, starvation, temperature

shock and infection (Redza-Dutordoir & Averill-Bates, 2016). Under these circumstances, the relative expression of pro-apoptotic and anti-apoptotic proteins is altered that leads to apoptosis. Our results showed the radiation-induced cell death by AO/EtBr staining and apoptosis by tracking phosphatidylserine externalization through annexin V binding along with propidium iodide permeation (Fig;4.1.10&11). The suicidal process of a cell under stress conditions is carried out by activation of certain caspases (initiator or executioner), e.g. Caspase 3. Caspase-3 is regularly expressed in its inactive form and can be activated through proteolysis during the apoptotic signal. Active caspase-3 (cleaved form) will cleave its cellular substrate poly (ADP-ribose) or PARP. Cleavage of these factors contributes to the apoptotic changes inside cells(Yu & Little2, 1998) as clearly seen in our study (Fig;4.1.12). The higher Bax/Bcl2 ratio observed after irradiation favouring apoptosis was reversed by IL-6 treatment resulting in a lower Bax/Bcl2 ratio. In ischemic conditions, high Bcl2/Bax ratio inhibits ROS production and found to be involved in increasing antioxidants like GSH(Waxman & Kolliputi, 2009). This is how IL-6 prevents oxidative stress-induced cell death. In stress-free condition, cells maintained the basal level of p53 without affecting their normal functioning. The activation and stabilization of p53 occur in response to irradiation followed by upregulation of p21, leading to cell growth arrest or p53 dependent apoptosis usually initiated by radiation-induced DNA damage. The p53 regulates the transcriptional activation of certain pro- or anti-apoptotic genes, thereby increasing the ratio of pro- to anti-apoptotic proteins (Bax/Bcl2) and thus favoured apoptosis (Fig;4.1.13). Other anti-apoptotic proteins of Bcl2 family, like Bcl-xl, Mcl-1 along with survivin, the member of the inhibitor of apoptosis (AIP) family that negatively regulates apoptosis were also upregulated by IL-6 treatment suggested that IL-6 attributes to a reduction in apoptosis (Fig;4.1.5&13). IL-6 triggers the STAT-3 pathway in many cancers where it mainly

regulates cell proliferation and survival. Majority of the genes that regulate cell survival and proliferation, such as Bcl-2, Bcl-xL, Mcl-1, cyclin D, p21, and survivin are direct targets of STAT-3 (Kumari et al., 2016). In our study, we checked the time and concentration-dependent phosphorylation in the presence of IL-6 and found that STAT-3 get phosphorylated as early as 30 min post-IL-6 treatment with 1ng/ml dose and remain phosphorylated up to 2 hours (Fig;4.1.14A). Moreover, there was increased phosphorylation noted with increasing IL-6 concentration from 0.1 to 10ng/ml; however, the difference between 1 and 10ng/ml was not significant. Furthermore, there was no phosphorylation of STAT-3 without treatment of IL-6 in any of the groups, either irradiated or non-irradiated control was observed (Fig;4.1.14 B). This data further strengthened our usage of IL-6 dose, i.e. 1ng/ml and 2 hour pre-treatment time before irradiation which is also supported by induction of glycolysis at 2 hour post IL-6 treatment (Fig;4.2.1A&B). Since, STAT-3 is a transcription factor, it translocate to nucleus upon phosphorylation which is clearly demonstrated by fractionation of nuclear and cytosolic proteins. We observed more STAT-3 phosphorylation in cytosolic fraction compared to nucleus at 1 hour post IL-6 treatment, however pSTAT-3 level was found more in nucleus at 4 hours, suggesting the nuclear translocation and activation of pro-survival signalling (Fig;4.1.14C). Further, the nuclear translocation of pSTAT-3 at 4 hours also reinforced the 4 hour time period at which the expression of pro-survival proteins has been inspected. IL-6 regulates the process of apoptosis by activating STAT-3 and NF-kB signalling, which trans-activates the expression of many anti-apoptotic proteins such as Bcl-2, Bcl-xL, Mcl-1 in many cancers (Grivennikov & Karin, 2010). However, in our study, we did not detect any significant increase in NF-kB at this concentration of IL-6. It may also be possible that IL-6 alone at this concentration is not sufficient for NF-kB activation and other cytokines like TNF-α etc. are also required to

activate the pro-inflammatory NF-kB. Therefore, it may be considered that IL-6-STAT-3 pathway is solely operated in favour of radioprotection, and maybe a mild inflammation that is beneficial to cells (Fleit, 2014). IL-6 is known to protect cardiac myocytes (normal cell) from oxidative stress-induced apoptosis through STAT-3 signalling and gastric cancer cells by upregulating Mcl-1 expression (Lin MT, Juan CY, Chang KJ, Chen WJ, 2001). Besides Bcl-2, Bcl-xL and Mcl-1, IL-6 also supports tumour cell survival by inducing the expression of survivin through direct binding of STAT-3 to the survivin promoter (Gritsko et al., 2006). Thus, the incorporation of STAT-3 inhibitor (JSI-124) inhibits phosphorylation (Fig;4.1.14D) and reverted the IL-6 mediated radio-resistance and modulated the expression of downstream survival proteins (Fig;4.1.15). Hence, it appears that cells rely over IL-6-STAT-3 axis which is very crucial for survival after irradiation. IL-6 induced STAT-3 phosphorylation induces anti-oxidant defence system and facilitates pro-survival signalling to protect the cells from ionizing radiation. However, one cannot deny the involvement of some other possible pathways in IL-6 mediated cellular radio-resistance. Therefore, we explored the role of IL-6 induced metabolic alterations in radio-resistance.

Previous reports from our laboratory demonstrated that the transient elevation of glycolysis could protect from radiation-induced cell death (Bhatt et al., 2015). IL-6 also induced glycolysis in hematopoietic RAW264.7cells. It induced the glycolysis by increasing the levels of many regulatory glycolytic enzymes viz. HK-2, PFK-1 and PKM2 (Fig;4.2.1)(Kumari, Das, & Narayan Bhatt, n.d.).Enhanced expression of HK-2 and its association with mitochondria ensures rapid phosphorylation of glucose using mitochondrial ATP (Z. Chen, Zhang, Lu, & Huang, 2009). The PFK-1 is the first critical and irreversible step of glycolysis which diverts the glucose through glycolysis (catabolic pathway). It ensures that glucose does not enter the pentose

phosphate pathway or gluconeogenesis (anabolic pathways). At the time of stress or cellular injury, ATP generated from catabolic pathways is required for macromolecular repair and cell survival, therefore, diverting glucose towards glycolysis for more ATP production is vital and decisive for cell survival (Berg JM, Tymoczko JL, 2002). We found higher ATP levels in IL-6 treated cells (Fig;4.2.2D), which acts as an inhibitor of PFK-1, however, increased expression of PFKFB3 (Fig;4.2.2C) produces fructose 2,6bisphosphate (F2,6BP), which acts as an allosteric activator of PFK-1 and ensures the continuous activation of PFK-1 even in the presence of high ATP (Ando et al., 2010; Berg JM, Tymoczko JL, 2002). Further, IL-6 induced higher protein levels of PKM2 (Fig;4.2.2B) maintains the smooth running of glucose through glycolysis by reducing the level of its substrate Phosphoenolpyruvate (PEP), which can inhibit the PFK-1 and stop the flow of glucose towards glycolysis. These results suggest that IL-6 induces the glycolysis by elevating the levels of all the crucial regulatory enzymes of this pathway.

Interestingly, IL-6 pre-treatment to induce glycolysis could protect the radio-sensitive RAW264.7 cells from radiation-induced cell death (Fig;4.2.3). The protein levels of glucose transporter and glycolytic enzymes, which got decreased after radiation exposure was found elevated in IL-6 alone and combined treatment group, suggesting that IL-6 induced the glycolysis in radiation-exposed cells also. Radiation is also known to induce the glycolysis (Zhong et al., 2013), which can be observed by enhanced glucose uptake, lactate production and higher levels of glycolytic enzymes, HK-2, PFK-1 and PKM2 in a radiation-exposed sample as compared to control (Fig;4.2.2B). However, these levels were found further increased in IL-6 pre-treated and radiation-exposed (combined treatment) sample. These findings suggest that radiation-induced glycolysis, which is marginally higher than the control cannot meet

the requirement of energy to rescue the cells from radiation-induced cell death; however, IL-6 can induce the glycolysis at a sufficiently higher level to accomplish the requirement of energy for repair and survival of cells battling with radiation-induced damage. This proposition is further confirmed by significantly higher levels of ATP in radiation-exposed cells pre-treated with IL-6 as compared to control and radiation alone (Fig;4.2.2D). The IL-6 induced high levels of ATP in IL-6 alone and combined treatment was noted at an early time point (4 hrs.), when it was obligatory to rescue the cells, as ATP is essentially required for energy-consuming processes like macromolecular repair, mainly DNA (Bhatt et al., 2015). The reversal of IL-6 induced radio-resistance by glycolytic inhibitors 3-BP and 2-DG (Fig;4.2.3) authenticated the role of glycolysis in IL-6 induced radio-resistance. Radiation-induced mitochondrial damage also contributes to radiation-induced cell death; we observed that IL-6 reduced the mitochondrial damage in IL-6 pre-treated cells. Interestingly, inhibition of IL-6 induced glycolysis also reverses the protective effect of IL-6 from radiation-induced mitochondrial damage (Fig;4.2.4).

IL-6, after binding to its receptor on the cell surface, induces the phosphorylation of STAT-3 and PI3K (Phosphoinositol-3-kinase), which further phosphorylates the Akt (Kumari et al., 2016). Increased Akt phosphorylation is found to be associated with increased rates of glucose metabolism in cells (Elstrom et al., 2004). Akt signalling influence the glycolysis directly by regulating the localization of GLUT to the plasma membrane (Barthel et al., 1999), HK-2 expression and mitochondrial interaction (Miyamoto, Murphy, & Brown, 2008), and expression of PFK-1 and PFKFB3 (Deprez, Vertommen, Alessi, Hue, & Rider, 1997). Similarly, IL-6 induced Akt phosphorylation suggested the involvement of Akt signalling in IL-6 induced enhanced glycolysis, which was further verified by knocking down the Akt expression and inhibition of Akt

signalling under similar experimental settings (Fig;4.2.5A). Downregulation of Akt signalling in IL-6 pre-treated samples not only reduced the glycolysis (glucose uptake and lactate production) but also the expression level of key glycolytic enzyme HK-2 and its association with mitochondria, which resulted in the reversal of IL-6 induced radio-resistance (Fig;4.2.5E). HK-2 association with mitochondrial outer membrane not only facilitates the quick phosphorylation of glucose using mitochondrial ATP but also prevents cytochrome C release from mitochondria, thereby inhibiting apoptosis (Pastorino, Shulga, & Hoek, 2002). Therefore, IL-6 induced and Akt mediated translocation of HK-2 to mitochondrial membrane may also cause radio-resistance besides glycolysis. Moreover, besides the direct role of PKM2 in glucose catabolism, it was demonstrated to facilitate the homologous recombination of DNA repair in the nucleus (Sizemore et al., 2018). Hence, we can assume that IL-6 induced high levels of PKM2, and HK-2 may be causing radio-resistance through glycolysis along with STAT-3 pathway. Therefore, these results suggest that IL-6 induced glycolysis is a favourable metabolic change, partly responsible for radio-resistance. This study adds induced glycolysis as one of the major pathways along with IL-6/STAT3, responsible for IL-6 induced radio-resistance.

Since the radiation-induced cell cycle arrest observed in S/G2 phase was similar as initiated at 2hr post-IR and subsequently disappears at 8 hr in both IR alone group and combination with IL-6 treatment (Fig;4.1.5). The activation of p53 and p21 facilitates the cell cycle arrest. Interestingly, p53, as well as p21 levels, were high in IR alone group compared with the combination group suggesting two conditions; first, there is more DNA damage in IR exposed cells that could not be repaired during this arrest, and therefore cells decided to undergo p53 dependent apoptosis which is later confirmed by noting more population in subG1 phase at 16 and 24hr post IR

exposure. Second, there is low DNA damage in IL-6-pretreated irradiated cells which could be easily repaired during this block; as a result, low p53 and p21 were observed. Moreover, radiation-induced ROS generation causes extensive damage to DNA that may also lead to apoptosis(Simon, Haj-Yehia, & Levi-Schaffer, 2000). Therefore it is imperative to see the extent of DNA damage and repair in the presence of IL-6. DNA damage and repair is a continuous on-off switching process, depending on the endogenous as well as exogenous stress posed to cells. Radiation-induced DNA damage is considered as potentially lethal damage (PLD) than any other endogenous stress. Ionizing radiation often creates clustered damage sites, known as double-strand breaks (DSB) which leads to breakage of the phosphodiester backbone of both the strands. In response to these DSBs cells activates the DNA damage response (DDR), a very efficient and sophisticated process to detect DNA damage and then initiate repair. The manifestation of DSBs triggers phosphorylation of H2AX histone protein, a more reliable marker of DNA damage. The phosphorylation of H2AX protein is crucial to initiate DDR and is requisite to attract other repair proteins surrounding the lesion (Lomax, Folkes, & O'neill, 2013). Our study showed the time kinetics of H2AX phosphorylation from 30min to 4hr at 2 Gy dose of γ-radiation. The phosphorylation was at a peak as early as 30 min post IR and then gradually decreases up to 4hrs. In IL-6 pre-treated cells, not only the initial damage induction was low but also the damage removal kinetics was much faster. IL-6 pre-treatment controlled these kinetics and resulted in almost complete disappearance of H2AX foci till 4hr (Fig;4.3.1). The phosphorylation of histone H2AX in yeast and mammalian cells is known to cause adaptation in a genomic structure that assist DNA repair by making the genome accessible to DNA repair proteins (Bassing et al., 2002). Therefore, H2AX foci formation leads to the recruitment of MRN complex proteins

(MRE11/RAD50/NBS1) to co-localize at the site of DNA damage (Bassing et al., 2002). In our study, we found the up-regulation of NBS1 protein in IL-6+IR groups, detected as early as 1hr post IR that may have resulted in faster removal of damaged lesions and could be the possible reason for the reduction in the frequency of H2AX foci and the percent DNA damage (Fig;4.3.5). Since ATM activates itself via auto-phosphorylation at Ser residue in response to IR irrespective of any treatment, and later initiate phosphorylation of its target proteins (Podhorecka, Skladanowski, & Bozko, 2010). IL-6 treatment further enhances its activation which appears to be delayed in IR alone group. The phosphorylation of H2AX proteins initiated the recruitment of MRN complex proteins that identify DNA damage and subsequently directs ATM protein to the site of a lesion which further amplifies the signals to activates other DDR proteins like RAD51 for chromatin remodelling and repair (Saito & Komatsu, 2015). The NBS activation and localization at DSB sites followed by IL-6 mediated ATM activation/phosphorylation (Fig;4.3.5B) promote the activation of RAD51 mediated homologous recombination (HR) and repair (Bhattacharya et al., 2017). Similarly, in our study, we found upregulated RAD51 post-IL-6 treatment which proposed the initiation of HR pathway for repair. The upregulation of RAD51 also implicated in the smooth progression of replication fork after DNA repair. IR causes not only DSBs but also the Single-strand break (SSB), DNA cross-links and base damages. The alkaline comet assay was used to detect all these types of DNA damages comprising SSBs, DSBs, and alkali-labile sites ((M. Zhang et al., 2018)). The comet assay states the extent of physical damage to DNA, instead of getting involved in activating damage response as done by phosphorylation of 53BP1/H2AX. Comet assay showed that IL-6 suppresses IR induced DNA damage. The length of the comet tail and percent DNA in tail suggested the incidence of DNA damage. IL-6

treatment significantly recovered cells from IR induced DNA damage, revealed by tail length, tail moment, olive moment and percent DNA in tail. These were all comparable to that of un-irradiated cells at 4hr post-IL-6 and irradiation treatment (Fig;4.3.2). All this data indicates the early recognition of damage and the follow-up response to IR by IL-6 treatment. If the damaged DNA could not be repaired, the cells undergo apoptosis which can be observed by annexin-V/PI staining at 24hr post IR (Fig;4.1.11). Further, the radiation-induced genomic instabilities cannot be overlooked. If the DSBs are not repaired efficiently, it may result in micronucleus formation which is a small fragment of DNA aligned with the whole genome during anaphase of cell division and get enclosed by cell membrane along with the nucleus; generally, it appears after cell division. Thus the radiation-induced late effects were assessed by cytogenetic damages in cells. Therefore we followed the kinetics of micronucleus (MN) formation from 24 to72 hour post-irradiation (Fig;4.3.3). The occurrence of MN indicates that the cells suffered from loss of reproductive ability due to the damaged genome by irradiation. In such cases, cells are doomed to die; thus micronuclei frequency relates to cell survival. In our study, we observed a decrease in cell number and increase in MN formation in irradiation alone group, and vice versa in IL-6+IR group at 24 to 48 hour. Reduction in DNA damage observed by H2AX foci in IL-6+IR group might be the reason in lowering the MN count in the same group. Thus, the low frequency of MN in IL-6 treated irradiated group compared to IR alone advocates the role of IL-6 in reduction of cytogenetic damage. Since, the frequency of MN was more in IR at both 24 and 48 hrs directs that DSBs are not repaired or removed properly and can also be witnessed by appearance of 53BP1 foci at 48hour post irradiation. However, diminished 53BP1 foci in IL-6 pretreatment group suggested efficient repair and removal of DSBs and the following

reduction in genomic instabilities (Fig;4.3.4). Moreover, 53BP1 might be involved in the damage repair or in control of checkpoints associated with the damage persisting for several hours. Since radiation cause damage to DNA either through base excision or via oxidation of bases in both the nuclear and mitochondrial genome. We observed the enhanced mRNA levels of important DNA repair enzymes Neil-1 and OGG-1 (DNA glycosylases) in the presence of IL-6 which further facilitate base excision repair and repair oxidized bases (such as 8-OHdG), and suggested the role of IL-6 in DNA repair. Previously, high expression of Neil-1 specifically reported in S phase of cell cycle suggesting the involvement in DNA repair during replication (Dou et al., 2008). However, both the enzymes were known to repair the oxidized and excised bases in both mitochondria and nucleus (Dou et al., 2008; Prakash & Doublié, 2015). Moreover, these enzymes were also reported to protect the mitochondrial DNA from excessive consumption of ethanol and showed improved recovery in case of partial hepatectomy (Tachibana et al., 2014; Xiuying Zhang et al., 2010). Thus, IL-6 mediated DDR, and other repair proteins resulted in the faster repair of DNA damage.

After observing significant cellular protection from IL-6 in the *in-vitro* model, we tested its radio-protective efficacy in the *in-vivo* model (C57/BL6 black mice). The results have clearly demonstrated that IL-6 could protect mice from radiation-induced mortality when given intramuscular injection 2hr before irradiation and IL-6 doses continued till 72hr, given a total of four doses at 24 hours interval (Fig;4.4.2). This 2hrs of IL-6 intramuscular injection is sufficient to reach the blood and to other vital organs, where it activates STAT-3 and Akt pathways. The blood was withdrawn at 1, and 2hrs post-IL-6 treatment and IL-6 level in serum were measured, the data showed more IL-6 in blood at 2hr as compared to 1hr suggesting that 2hr pre-treatment before irradiation is required to have sufficient and effective concentration (nearly 1ng/ml) of IL-6 in blood. Further, we checked the IL-6

induced STAT-3 and Akt phosphorylation/activation in haematopoietic organs such as blood, bone marrow and spleen at 2hr post-IL-6 treatment. It can be clearly observed from this data, that significantly high phosphorylation of STAT-3 in blood cells indicates 2hr to be sufficient enough time for IL-6 to reach in circulation; however, relatively low phosphorylation in bone marrow cells was observed at a similar time point, suggesting either low reach of exogenous IL-6 to these tissues or more time is required. But once it gets in the blood, it is going to activate signalling in all the organs sooner or later. (Fig;4.4.1A&B). The 30-day survival analysis with IL-6 treatment before and after irradiation had given 80% survival against 7.5 Gy IR dose (Fig;4.4.2) which comprised of delayed onset of symptoms like weakness, reduced appetite, dehydration/loss of thirst and loss of body weight. At the systemic level, damage to the hematopoietic and gastrointestinal systems is the major determinant of the survival of the organism following whole-body irradiation (WBI) because of their susceptibility to radiation damage linked to the high proliferation status (Williams & McBride, 2011b). Therefore, we inspected the role of IL-6 on radiation impairment to these two organ systems. Exposure to radiation doses above 2 Gy can lead to myelosuppression, leading to the development of neutropenia, thrombocytopenia and anaemia due to higher radio-sensitivity of the progenitors of these lineages. As a result, there is a severe diminution in the peripheral blood count, particularly lymphocytes, leading to immunosuppression and susceptibility of subjects to secondary infections and death (Dainiak et al., 2003). Thrombocytopenia, haemorrhage and defects in the adaptive immune system due to the depletion of lymphocytes can further complicate the situation (Hendry and Feng-Tong, 1995). Whole blood analysis at multiple time points from 24hr to 28 days post-irradiation (7.5 Gy) showed radiation-induced cytopenia; however, IL-6 treatment initiated the recovery from day 14 onwards and the value reached to their normal level at day 21 (Fig;4.4.6).

Furthermore, peripheral blood counts at 2Gy radiation doses from 24hr to 28 days revealed a different pattern than lethal radiation exposure (7.5Gy), where the nadir values in blood cell count observed at just 24hr post IR and started recovering from day 14 onwards. Whereas in 2Gy of radiation the nadir values achieved at 24hr post-irradiation but start recovering very early, from day 03 onwards and by the day 14 all groups recovered and have a comparable count to that of un-irradiated control mice (Fig;4.4.7). Thus, the result indicates that animals can survive at a low dose of radiation with the slow recovery rate at no cost of life however at the high dose of radiation animals cannot survive without the treatments like IL-6. Further, the peripheral blood count is not the true representative of the hematopoietic damage and could not exactly reflect the stem cell reservoir. Bone marrow is the main hematopoietic tissue, produces all type of blood cells. Therefore, the hematopoietic recovery after IL-6 treatment was further confirmed by the enumeration of bone marrow stem cell pool (Fig;4.4.13). Low doses of radiation may also be deleterious as observed earlier in case of peripheral blood count and may efficiently degrade the stem cell pool, which is required to recover from radiation-induced cytopenia. Under any kind of stress, the protected stem cells forced to move from quiescent to the proliferation phase. This transition is required to convert long term stem cell (those having self-renewal ability) to short term stem cells (can differentiate into any type of blood cells) to facilitate recovery (Pazhanisamy, 2009). In our study, we observed a similar phenomenon which can be clearly indicated by a differential change in percent population of short term and long term HSCs in a hematopoietic pool of IL-6 treated *vs* un-treated animals (Fig;4.4.13) and found that the remaining pool of stem cells in IL-6 treatment after irradiation is enough to help in quick recovery from radiation-induced cytopenia (Fig;4.4.7). Moreover, histopathological analysis of bone marrow at day 14 post-IR revealed that IL-6 administration significantly ameliorates the IR induced bone marrow aplasia (Fig;4.4.8), which may be due to recovery

in blood cell count. It has been demonstrated that IR induced myelosuppression or failure of HSC renewal is a direct consequence of DNA damage in the BM compartment. Cell death occurring in HSCs as a result of un- or mis-repaired DNA damage then manifests as BM hypoplasia or aplasia, leading to a haematological crisis in the marrow(Wang, Liu, Pazhanisamy, Meng, & Zhou, 2009). Therefore, the radiation-induced DNA damage or cytogenetic damage was assessed in the PBMCs and BM cells. The γ- H2AX foci frequency in PBMCs isolated from irradiated animals represents the number of DNA DSBs formed after irradiation and is directly proportional to the number of foci formed (Firsanov, Solovjeva, & Svetlova, 2011). The kinetics of formation and removal of γ-H2AX foci in the presence of IL-6 was greatly modulated as compared to the PBMCs from IR alone mice (Fig;4.4.10). Similarly, the cytogenetic damage in BM cells observed as M-fraction was also greatly reduced by IL-6 treatment. Hence, we could say that the accelerated removal of damage indicated that IL-6 promoted the survival of hematopoietic cells by reducing damage induction as well as enhancing repair. Further, the secondary lymphoid organ, like the spleen, has an important role in the immune system and renewal of RBCs. A variety of splenocytes population residing in spleen comprises of B and T lymphocytes, monocytes, macrophages, and dendritic cells playing diverse immune functions, T cells are specifically known to involve in cell-mediated immunity while B cells produce antibodies or humoral immunity. WBI resulted in a reduction in spleen volume, reduction in germinal centres, decreasing cell number and vascular damage. Any pathological condition or inefficient haematopoiesis may also result in reduced cellularity to other distant organs such as the spleen (Hall, 2000). However, IL-6 administration significantly protects from radiation induced shrinkage in spleen morphology and the histopathological alterations including vasculature of spleen (Fig;4.4.8& 9).

Mortality in mice after full body exposure to a high dose of radiation from 8–20 Gy occur due to GI syndrome. Irradiation causes loss of clonogenic crypts, that may result in shortening of villi length due to the inability of replacement of new cells (Macià i Garau et al., 2011). At higher doses (≥10 Gy), animals succumb to death purely by GI syndrome in 7-10 days; however, we performed our study at 7.5 Gy (which is $LD_{80/30}$) only to delineate the mode of injuries. The clinical death within ten days presumed to be the indirect indicator of GI syndrome (Mason, Withers, & Davis, 1989; Terry & Travis, 1989). Results of the current study performed on GI tissues at 7.5 Gy radiation dose revealed that IL-6 could rescue mice from GI lethality or gastrointestinal-ARS (GI-ARS). Since, the prime cause of mortality following irradiation due to GI damage is the loss of the stem cells that reside in the crypts of the intestine, which maintains the epithelial lining of the GI tract. BrdU incorporation 2 hr before animal dissection, showed less proliferating crypt cells in irradiated animals, however IL-6 treatment not only protect crypt cells from radiation-induced mitosis but also maintain their proliferating ability which is crucial to migrating these newly formed villi to sustain or regenerate the villi and epithelial lining (Fig; 4.4.17). Further, the histopathological examination of GI tissue showed the denudation of epithelial lining following irradiation and their initiation of recovery by 3 to 5 days upon IL-6 treatment (Fig; 4.4.14). Moreover, radiation-induced damage is widely embraced of oxidative damage due to overproduction of ROS (Martinel Lamas et al., 2013). Our data showed that IL-6 administration before irradiation significantly alleviates oxidative damage to biomolecules such as lipids and proteins in GI tissues. Hence, IL-6 reduces radiation-induced apoptosis and augments expression of anti-apoptotic proteins such as Bcl-2 and Mcl-1 in these intestinal cells (Fig;4.4.15). Furthermore, the mechanism underlying in minimizing the oxidative damage and

apoptosis may be the IL-6 mediated elevation in total antioxidant capacity and availability of free thiols (GSH) that quenches oxidative stress in GI tissue (Fig;4.4.16). This study overall suggests that IR mediated death is via both haematopoietic-ARS and GI-ARS.

Similar to our *in-vitro* study (Fig;4.1.15), inhibition of STAT-3 pathway using JSI-124 along with IL-6 administration *in-vivo*, reversed the effect of IL-6 induced radioprotection in C57/BL6 mice (Fig;4.4.18), validating the proposition that IL-6 induced radioprotection is primarily STAT-3 dependent.

Conclusion

The findings of our study clearly confirmed that IL-6 exhibits radio-protective effects on multiple cell lines of different tissue origins. Further, it protects the hematopoietic system and GI system against whole-body exposure to gamma-radiation in *in-vivo* C57/BL6 mice model. IL-6 primarily employed IL-6-STAT-3 pathway but also utilized IL-6-Akt pathway for metabolic modifications to add on radioprotection. For this reason, IL-6 is a promising radio-protective agent and has the potential to be developed as a drug against nuclear emergencies. Though this study intensely discussed the role of IL-6 in radioprotection; however, it will be interesting to study the link between IL-6 mediated metabolic modification and DNA repair. We observed only 80% radioprotection in C57/BL6 mice model; further, it will be pertinent to test if variation in IL-6 dose or pre-treatment time or supportive care like the use of antibiotics against bacterial infection in GI to improve the radioprotection in-vivo to 100%. Later, for the development of a drug, it warrants the testing and trial in non-human primates (NHP) for further validation.

Bibliography

BIBLIOGRAPHY

Abraham, R. T. (2001, September 1). Cell cycle checkpoint signaling through the ATM and ATR kinases. *Genes and Development*, Vol. 15, pp. 2177–2196. https://doi.org/10.1101/gad.914401

Ahmed, S. T., Mayer, A., Ji, J.-D., & Ivashkiv, L. B. (2002). Inhibition of IL-6 signaling by a p38-dependent pathway occurs in the absence of new protein synthesis. *Journal of Leukocyte Biology*, *72*(1), 154–162. Retrieved from http://www.ncbi.nlm.nih.gov/pubmed/12101275

Akira, S., & Kishimoto+, T. (1992). IL-6 and NF-IL6 in Acute-Phase Response and Viral Infection. *Immunological Reviews*, *127*(1), 25–50. https://doi.org/10.1111/j.1600-065X.1992.tb01407.x

Akleyev, A. V. (2016). Normal tissue reactions to chronic radiation exposure in man. *Radiation Protection Dosimetry*, *171*(1), 107–116. https://doi.org/10.1093/rpd/ncw207

Ando, M., Uehara, I., Kogure, K., Asano, Y., Nakajima, W., Abe, Y., … Tanaka, N. (2010). Interleukin 6 enhances glycolysis through expression of the glycolytic enzymes hexokinase 2 and 6-phosphofructo-2-kinase/fructose-2,6-bisphosphatase-3. *Journal of Nippon Medical School = Nippon Ika Daigaku Zasshi*, *77*(2), 97–105. Retrieved from http://www.ncbi.nlm.nih.gov/pubmed/20453422

Aquilano, K., Baldelli, S., & Ciriolo, M. R. (2014). Glutathione: New roles in redox signalling for an old antioxidant. *Frontiers in Pharmacology*. https://doi.org/10.3389/fphar.2014.00196

Arora, R., Gupta, D., Chawla, R., Sagar, R., Sharma, A., Kumar, R., … Sharma, R. K. (2005, January). Radioprotection by plant products: Present status and future prospects. *Phytotherapy Research*, Vol. 19, pp. 1–22. https://doi.org/10.1002/ptr.1605

Awasthi, Y. C., Yang, Y., Tiwari, N. K., Patrick, B., Sharma, A., Li, J., & Awasthi, S. (2004). Regulation of 4-hydroxynonenal-mediated signaling by glutathione S-transferases. *Free Radical Biology & Medicine*, *37*(5), 607–619.

https://doi.org/10.1016/j.freeradbiomed.2004.05.033

Azzam, E. I., Jay-Gerin, J. P., & Pain, D. (2012). Ionizing radiation-induced metabolic oxidative stress and prolonged cell injury. *Cancer Letters*, *327*(1–2), 48–60. https://doi.org/10.1016/j.canlet.2011.12.012

Barthel, A., Okino, S. T., Liao, J., Nakatani, K., Li, J., Whitlock, J. P., & Roth, R. A. (1999). Regulation of GLUT1 gene transcription by the serine/threonine kinase Akt1. *The Journal of Biological Chemistry*, *274*(29), 20281–20286. https://doi.org/10.1074/jbc.274.29.20281

Bassing, C. H., Chua, K. F., Sekiguchi, J. A., Suh, H., Whitlow, S. R., Fleming, J. C., … Alt, F. W. (2002). Increased ionizing radiation sensitivity and genomic instability in the absence of histone H2AX. *Proceedings of the National Academy of Sciences of the United States of America*, *99*(12), 8173–8178. https://doi.org/10.1073/pnas.122228699

Bastard, J. P., Maachi, M., Van Nhieu, J. T., Jardel, C., Bruckert, E., Grimaldi, A., … Hainque, B. (2002). Adipose tissue IL-6 content correlates with resistance to insulin activation of glucose uptake both in vivo and in vitro. *Journal of Clinical Endocrinology and Metabolism*, *87*(5), 2084–2089. https://doi.org/10.1210/jcem.87.5.8450

Berg JM, Tymoczko JL, S. L. (2002). The Glycolytic Pathway Is Tightly Controlled. In *Biochemistry* (5th ed.). Retrieved from https://www.ncbi.nlm.nih.gov/books/NBK22395/

Berg, R. D. (1995). Bacterial translocation from the gastrointestinal tract. *Trends in Microbiology*, *3*(4), 149–154. https://doi.org/10.1016/s0966-842x(00)88906-4

Bhatt, A. N., Chauhan, A., Khanna, S., Rai, Y., Singh, S., Soni, R., … Dwarakanath, B. S. (2015). Transient elevation of glycolysis confers radio-resistance by facilitating DNA repair in cells. *BMC Cancer*, *15*, 335. https://doi.org/10.1186/s12885-015-1368-9

Bhattacharya, S., Srinivasan, K., Abdisalaam, S., Su, F., Raj, P., Dozmorov, I., … Asaithamby, A. (2017). RAD51 interconnects between DNA replication, DNA repair and immunity. *Nucleic Acids Research*, *45*(8), 4590–4605. https://doi.org/10.1093/nar/gkx126

Bian, L., Meng, Y., Zhang, M., & Li, D. (2019, November 26). MRE11-RAD50-NBS1 complex alterations and DNA damage response: Implications for cancer treatment. *Molecular Cancer*, Vol. 18, pp. 1–14. https://doi.org/10.1186/s12943-019-1100-5

Bode, J. G., Nimmesgern, A., Schmitz, J., Schaper, F., Schmitt, M., Frisch, W., … Graeve, L. (1999). LPS and TNFalpha induce SOCS3 mRNA and inhibit IL-6-induced activation of STAT3 in macrophages. *FEBS Letters*, *463*(3), 365–370. https://doi.org/10.1016/s0014-5793(99)01662-2

Bolus, N. E. (2017). Basic review of radiation biology and terminology. *Journal of Nuclear Medicine Technology*, *45*(4), 259–264. https://doi.org/10.2967/jnmt.117.195230

Bonnaud, S., Niaudet, C., Legoux, F., Corre, I., Delpon, G., Saulquin, X., … Paris, F. (2010). Sphingosine-1-phosphate activates the AKT pathway to protect small intestines from radiation-induced endothelial apoptosis. *Cancer Research*, *70*(23), 9905–9915. https://doi.org/10.1158/0008-5472.CAN-10-2043

Booth, C., Tudor, G., Tudor, J., Katz, B. P., & MacVittie, T. J. (2012). Acute gastrointestinal syndrome in high-dose irradiated mice. *Health Physics*, *103*(4), 383–399. https://doi.org/10.1097/HP.0b013e318266ee13

Borhani, N., Manoochehri, M., Saleh Gargari, S., Ghaffari Novin, M., Mansouri, A., & Omrani, M. D. (2014). Decreased expression of proapoptotic genes caspase-8- and BCL2-associated agonist of cell death (BAD) in ovarian cancer. *Clinical Ovarian and Other Gynecologic Cancer*, *7*(1–2), 18–23. https://doi.org/10.1016/j.cogc.2014.12.004

Brenner, D. J., & Ward, J. F. (1992). Constraints on energy deposition and target size of multiply damaged sites associated with DNA double-strand breaks. *International Journal of Radiation Biology*, *61*(6), 737–748. https://doi.org/10.1080/09553009214551591

Brown, C. O., Salem, K., Wagner, B. A., Bera, S., Singh, N., Tiwari, A., … Goel, A. (2012). Interleukin-6 counteracts therapy-induced cellular oxidative stress in multiple myeloma by up-regulating manganese superoxide dismutase. *The Biochemical Journal*, *444*(3), 515–527. https://doi.org/10.1042/BJ20112019

Buege, J. A., & Aust, S. D. (1978). Microsomal Lipid Peroxidation. *Methods in Enzymology*, *52*(C), 302–310. https://doi.org/10.1016/S0076-6879(78)52032-6

Buell, M. G., & Harding, R. K. (1989). Proinflammatory effects of local abdominal irradiation on rat gastrointestinal tract. *Digestive Diseases and Sciences*, *34*(3), 390–399. https://doi.org/10.1007/BF01536261

Cadenas, E., & Davies, K. J. A. (2000). Mitochondrial free radical generation, oxidative stress, and aging. *Free Radical Biology and Medicine*. https://doi.org/10.1016/S0891-5849(00)00317-8

Capizzi, R. L., & Oster, W. (1995). Protection of normal tissue from the cytotoxic effects of chemotherapy and radiation by amifostine: clinical experiences. *European Journal of Cancer (Oxford, England : 1990)*, *31A Suppl 1*, S8-13. https://doi.org/10.1016/0959-8049(95)00144-8

Chalaris, A., Garbers, C., Rabe, B., Rose-John, S., & Scheller, J. (2011, June). The soluble Interleukin 6 receptor: Generation and role in inflammation and cancer. *European Journal of Cell Biology*, Vol. 90, pp. 484–494. https://doi.org/10.1016/j.ejcb.2010.10.007

Chao, N. J. (2007). Accidental or intentional exposure to ionizing radiation: Biodosimetry and treatment options. *Experimental Hematology*, *35*(4 SUPPL.), 24–27. https://doi.org/10.1016/j.exphem.2007.01.008

Chen, X., Wei, J., Li, C., Pierson, C. R., Finlay, J. L., & Lin, J. (2018). Blocking interleukin-6 signaling inhibits cell viability/proliferation, glycolysis, and colony forming activity of human medulloblastoma cells. *International Journal of Oncology*, *52*(2), 571–578. https://doi.org/10.3892/ijo.2017.4211

Chen, Z., Zhang, H., Lu, W., & Huang, P. (2009). Role of mitochondria-associated hexokinase II in cancer cell death induced by 3-bromopyruvate. *Biochimica et Biophysica Acta*, *1787*(5), 553–560. https://doi.org/10.1016/j.bbabio.2009.03.003

Citrin, D., Cotrim, A. P., Hyodo, F., Baum, B. J., Krishna, M. C., & Mitchell, J. B. (2010). Radioprotectors and Mitigators of Radiation-Induced Normal Tissue Injury. *The Oncologist*, *15*(4), 360–371. https://doi.org/10.1634/theoncologist.2009-s104

Coleman, C. N., Blakely, W. F., Fike, J. R., MacVittie, T. J., Metting, N. F., Mitchell, J. B., … Wong, R. S. L. (2003). Molecular and cellular biology of moderate-dose (1-10 Gy) radiation and potential mechanisms of radiation protection: report of a workshop at Bethesda, Maryland, December 17-18, 2001. *Radiation Research*, *159*(6), 812–834. https://doi.org/10.1667/rr3021

Cox, A. A., Sagot, Y., Hedou, G., Grek, C., Wilkes, T., Vinik, A. I., & Ghatnekar, G. (2017, May 2). Low-dose pulsatile interleukin-6 as a treatment option for diabetic peripheral neuropathy. *Frontiers in Endocrinology*, Vol. 8. https://doi.org/10.3389/fendo.2017.00089

Croker, B. A., Krebs, D. L., Zhang, J. G., Wormald, S., Willson, T. A., Stanley, E. G., … Alexander, W. S. (2003). SOCS3 negatively regulates IL-6 signaling in vivo. *Nature Immunology*, *4*(6), 540–545. https://doi.org/10.1038/ni931

Curnow, S. J., Scheel-Toellner, D., Jenkinson, W., Raza, K., Durrani, O. M., Faint, J. M., … Salmon, M. (2004). Inhibition of T Cell Apoptosis in the Aqueous Humor of Patients with Uveitis by IL-6/Soluble IL-6 Receptor trans -Signaling . *The Journal of Immunology*, *173*(8), 5290–5297. https://doi.org/10.4049/jimmunol.173.8.5290

Dainiak, N. (2002). Hematologic consequences of exposure to ionizing radiation. *Experimental Hematology*, *30*(6), 513–528. https://doi.org/10.1016/S0301-472X(02)00802-0

Dainiak, N., Waselenko, J. K., Armitage, J. O., MacVittie, T. J., & Farese, A. M. (2003). The hematologist and radiation casualties. *Hematology / the Education Program of the American Society of Hematology. American Society of Hematology. Education Program*, pp. 473–496. https://doi.org/10.1182/asheducation-2003.1.473

Dalle-Donne, I., Aldini, G., Carini, M., Colombo, R., Rossi, R., & Milzani, A. (2006). Protein carbonylation, cellular dysfunction, and disease progression. *Journal of Cellular and Molecular Medicine*, Vol. 10, pp. 389–406. https://doi.org/10.1111/j.1582-4934.2006.tb00407.x

Deborah Ribble, Nathaniel B Goldstein, D. A. N. and, & Shellman, Y. G. (2005). A simple technique for quantifying apoptosis in 96-well plates. *BMC*

Biotechnology, *5*(12). https://doi.org/10.1186/1472-6750-5-12

Del Rio, D., Stewart, A. J., & Pellegrini, N. (2005). A review of recent studies on malondialdehyde as toxic molecule and biological marker of oxidative stress. *Nutrition, Metabolism and Cardiovascular Diseases*, Vol. 15, pp. 316–328. https://doi.org/10.1016/j.numecd.2005.05.003

Delia, D., & Mizutani, S. (2017, September 1). The DNA damage response pathway in normal hematopoiesis and malignancies. *International Journal of Hematology*, Vol. 106, pp. 328–334. https://doi.org/10.1007/s12185-017-2300-7

Deprez, J., Vertommen, D., Alessi, D. R., Hue, L., & Rider, M. H. (1997). Phosphorylation and activation of heart 6-phosphofructo-2-kinase by protein kinase B and other protein kinases of the insulin signaling cascades. *The Journal of Biological Chemistry*, *272*(28), 17269–17275. https://doi.org/10.1074/jbc.272.28.17269

Dörr, H., Baier, T., & Meineke, V. (2013). [Cutaneous damage after acute exposure to ionizing radiation: decisive for the prognosis of radiation accident victims]. *Der Hautarzt; Zeitschrift Fur Dermatologie, Venerologie, Und Verwandte Gebiete*, *64*(12), 904–909. https://doi.org/10.1007/s00105-013-2626-x

Dörthe Schaue, Evelyn L. Kachikwu, and W. H. M. (2012). *Dörthe Schaue1, Evelyn L. Kachikwu, and William H. McBride*. *100*(2), 130–134. https://doi.org/10.1016/j.pestbp.2011.02.012.Investigations

Dou, H., Theriot, C. A., Das, A., Hegde, M. L., Matsumoto, Y., Boldogh, I., … Mitra, S. (2008). Interaction of the human DNA glycosylase NEIL1 with proliferating cell nuclear antigen: The potential for replication-associated repair of oxidized bases in mammalian genomes. *Journal of Biological Chemistry*, *283*(6), 3130–3140. https://doi.org/10.1074/jbc.M709186200

Dubois, A., & Walker, R. I. (1988). Prospects for management of gastrointestinal injury associated with the acute radiation syndrome. *Gastroenterology*, Vol. 95, pp. 500–507. https://doi.org/10.1016/0016-5085(88)90512-4

Dubois, A., & Walker, R. I. (1989). Prospects for Management of Gastrointestinal Injury Associated With the Acute Radiation Syndrome. In

GASTROENTEROLOGY (Vol. 95).

Duckworth, C. A., & Pritchard, D. M. (2009). Suppression of Apoptosis, Crypt Hyperplasia, and Altered Differentiation in the Colonic Epithelia of Bak-Null Mice. *Gastroenterology*, *136*(3), 943–952. https://doi.org/10.1053/j.gastro.2008.11.036

Elstrom, R. L., Bauer, D. E., Buzzai, M., Karnauskas, R., Harris, M. H., Plas, D. R., … Thompson, C. B. (2004). Akt stimulates aerobic glycolysis in cancer cells. *Cancer Research*, *64*(11), 3892–3899. https://doi.org/10.1158/0008-5472.CAN-03-2904

Fayers, P. M. (1985). Using and understanding medical statistics. *International Journal of Cardiology*, *9*(2), 252–253. https://doi.org/10.1016/0167-5273(85)90210-4

Fenech, M., Chang, W. P., Kirsch-Volders, M., Holland, N., Bonassi, S., & Zeiger, E. (2003). HUMN project: Detailed description of the scoring criteria for the cytokinesis-block micronucleus assay using isolated human lymphocyte cultures. *Mutation Research - Genetic Toxicology and Environmental Mutagenesis*, *534*(1–2), 65–75. https://doi.org/10.1016/S1383-5718(02)00249-8

Firsanov, D. V., Solovjeva, L. V., & Svetlova, M. P. (2011, August). H2AX phosphorylation at the sites of DNA double-strand breaks in cultivated mammalian cells and tissues. *Clinical Epigenetics*, Vol. 2, pp. 283–297. https://doi.org/10.1007/s13148-011-0044-4

Fisman, E. Z., & Tenenbaum, A. (2010). The ubiquitous interleukin-6: a time for reappraisal. *Cardiovascular Diabetology*, *9*(1), 62. https://doi.org/10.1186/1475-2840-9-62

Fleit, H. B. (2014). Chronic Inflammation. In *Pathobiology of Human Disease: A Dynamic Encyclopedia of Disease Mechanisms* (pp. 300–314). https://doi.org/10.1016/B978-0-12-386456-7.01808-6

Franken, N. A. P., Rodermond, H. M., Stap, J., Haveman, J., & van Bree, C. (2006). Clonogenic assay of cells in vitro. *Nature Protocols*, *1*(5), 2315–2319. https://doi.org/10.1038/nprot.2006.339

Freeman, S. L., & MacNaughton, W. K. (2000). Ionizing radiation induces iNOS-mediated epithelial dysfunction in the absence of an inflammatory response. *American Journal of Physiology. Gastrointestinal and Liver Physiology*, *278*(2), G243-50. https://doi.org/10.1152/ajpgi.2000.278.2.G243

Fridovich, I. (1997). Superoxide anion radical (O2/-·), superoxide dismutases, and related matters. *Journal of Biological Chemistry*, Vol. 272, pp. 18515–18517. https://doi.org/10.1074/jbc.272.30.18515

Friedberg, E. C. (2003, January 23). DNA damage and repair. *Nature*, Vol. 421, pp. 436–440. https://doi.org/10.1038/nature01408

Gabay, C. (2006). Interleukin-6 and chronic inflammation. *Arthritis Research and Therapy*, *8*(SUPPL. 2). https://doi.org/10.1186/ar1917

Gao, Y., Wang, P., Wang, Z., Han, L., Li, J., Tian, C., … Lyu, Y. (2019). Serum 8-Hydroxy-2′-Deoxyguanosine Level as a Potential Biomarker of Oxidative DNA Damage Induced by Ionizing Radiation in Human Peripheral Blood. *Dose-Response*, *17*(1). https://doi.org/10.1177/1559325818820649

Goans, R. E., Holloway, E. C., Berger, M. E., & Ricks, R. C. (2001). Early dose assessment in criticality accidents. *Health Physics*, *81*(4), 446–449. https://doi.org/10.1097/00004032-200110000-00009

GRAY, L. H., CONGER, A. D., EBERT, M., HORNSEY, S., & SCOTT, O. C. (1953). The concentration of oxygen dissolved in tissues at the time of irradiation as a factor in radiotherapy. *The British Journal of Radiology*, *26*(312), 638–648. https://doi.org/10.1259/0007-1285-26-312-638

Grin, I. R., Dianov, G. L., & Zharkov, D. O. (2010). The role of mammalian NEIL1 protein in the repair of 8-oxo-7,8-dihydroadenine in DNA. *FEBS Letters*, *584*(8), 1553–1557. https://doi.org/10.1016/j.febslet.2010.03.009

Gritsko, T., Williams, A., Turkson, J., Kaneko, S., Bowman, T., Huang, M., … Jove, R. (2006). Persistent activation of Stat3 signaling induces survivin gene expression and confers resistance to apoptosis in human breast cancer cells. *Clinical Cancer Research*, *12*(1), 11–19. https://doi.org/10.1158/1078-0432.CCR-04-1752

Grivennikov, S. I., & Karin, M. (2010). Dangerous liaisons: STAT3 and NF-κB collaboration and crosstalk in cancer. *Cytokine and Growth Factor Reviews*, *21*(1), 11–19. https://doi.org/10.1016/j.cytogfr.2009.11.005

Guo, Y., Xu, F., Lu, T., Duan, Z., & Zhang, Z. (2012, November). Interleukin-6 signaling pathway in targeted therapy for cancer. *Cancer Treatment Reviews*, Vol. 38, pp. 904–910. https://doi.org/10.1016/j.ctrv.2012.04.007

Ha, C. T., Li, X.-H., Fu, D., Xiao, M., & Landauer, M. R. (2013). Genistein nanoparticles protect mouse hematopoietic system and prevent proinflammatory factors after gamma irradiation. *Radiation Research*, *180*(3), 316–325. https://doi.org/10.1667/RR3326.1

Hagen, U. (1994). Mechanisms of induction and repair of DNA double-strand breaks by ionizing radiation: Some contradictions. *Radiation and Environmental Biophysics*, *33*(1), 45–61. https://doi.org/10.1007/BF01255273

Hall, Eric J. Giaccia, A. j. (2006). *Radiobiology for the Radiologist* (6th Editio, Vol. 66). https://doi.org/10.1016/j.ijrobp.2006.06.027

Hall, E. J. (2000). The Physics and Chemistry of Radiation Absorption. *Radiobiology for the Radiologist*, 5–16. https://doi.org/10.1148/radiol.2242022530

Hammacher,', A., Ward,',', L. D., Weinstock, J., Treutlein, H., Yasukawa, K., & Simpson', R. J. (1994). Structure-function analysis of human IL-6: Identification of two distinct regions that are important for receptor binding. In *Protein Science* (Vol. 3). Cambridge University Press.

Hensley, M. L., Hagerty, K. L., Kewalramani, T., Green, D. M., Meropol, N. J., Wasserman, T. H., … Schuchter, L. M. (2009). American society of clinical oncology 2008 clinical practice guideline update: Use of chemotherapy and radiation therapy protectants. *Journal of Clinical Oncology*, *27*(1), 127–145. https://doi.org/10.1200/JCO.2008.17.2627

Hérodin, F., & Drouet, M. (2005, October). Cytokine-based treatment of accidentally irradiated victims and new approaches. *Experimental Hematology*, Vol. 33, pp. 1071–1080. https://doi.org/10.1016/j.exphem.2005.04.007

Hirano, T., Taga, T., Nakano, N., Yasukawa, K., Kashiwamura, S., Shimizu, K., … Kishimoto, T. (1985). Purification to homogeneity and characterization of human B-cell differentiation factor (BCDF or BSFp-2). *Proceedings of the National Academy of Sciences of the United States of America*, *82*(16), 5490–5494. https://doi.org/10.1073/pnas.82.16.5490

Huang, L., Snyder, A. R., & Morgan, W. F. (2003, September 1). Radiation-induced genomic instability and its implications for radiation carcinogenesis. *Oncogene*, Vol. 22, pp. 5848–5854. https://doi.org/10.1038/sj.onc.1206697

Humanson, G. L. (1961). *In: Basic Procedures- Animal Tissue Technique.*

I, C. on the A. of C. R. in P. near N. F.-P., Board, N. and R. S., Studies, D. on E. and L., & Council, N. R. (2012). *Radiation as a Carcinogen*.

Iliakis, G. E., Metzger, L., Denko, N., & Stamato, T. D. (1991). Detection of DNA double-Strand breaks in synchronous cultures of CHO cells by means of asymmetric field inversion gel electrophoresis. *International Journal of Radiation Biology*, *59*(2), 321–341. https://doi.org/10.1080/09553009114550311

Iliopoulos, D., Hirsch, H. A., & Struhl, K. (2009). An Epigenetic Switch Involving NF-κB, Lin28, Let-7 MicroRNA, and IL6 Links Inflammation to Cell Transformation. *Cell*, *139*(4), 693–706. https://doi.org/10.1016/j.cell.2009.10.014

Ježek, J., Cooper, K. F., & Strich, R. (2018, March 1). Reactive oxygen species and mitochondrial dynamics: The yin and yang of mitochondrial dysfunction and cancer progression. *Antioxidants*, Vol. 7. https://doi.org/10.3390/antiox7010013

Jia, Y., Zhou, F., Deng, P., Fan, Q., Li, C., Liu, Y., … Sun, X. (2012). Interleukin 6 protects H2O2-induced cardiomyocytes injury through upregulation of prohibitin via STAT3 phosphorylation. *Cell Biochemistry and Function*, *30*(5), 426–431. https://doi.org/10.1002/cbf.2820

Jin, H. L., Sung, Y. K., In, S. K., & Park, J. W. (2007). Regulation of ionizing radiation-induced apoptosis by mitochondrial NADP+-dependent isocitrate dehydrogenase. *Journal of Biological Chemistry*, *282*(18), 13385–13394. https://doi.org/10.1074/jbc.M700303200

Jones, S. A., Scheller, J., & Rose-John, S. (2011, September 1). Therapeutic strategies for the clinical blockade of IL-6/gp130 signaling. *Journal of Clinical Investigation*, Vol. 121, pp. 3375–3383. https://doi.org/10.1172/JCI57158

Kalechman, Y., Zuloff, A., Albeck, M., Strassmann, G., & Sredni, B. (1995). Role of endogenous cytokines secretion in radioprotection conferred by the immunomodulator ammonium trichloro(dioxyethylene-0-0')tellurate. *Blood*, *85*(6), 1555–1561. https://doi.org/10.1182/blood.V85.6.1555.bloodjournal8561555

Kalsbeek, D., & Golsteyn, R. M. (2017, November 6). G2/M-phase checkpoint adaptation and micronuclei formation as mechanisms that contribute to genomic instability in human cells. *International Journal of Molecular Sciences*, Vol. 18. https://doi.org/10.3390/ijms18112344

Kaplanski, G., Marin, V., Montero-Julian, F., Mantovani, A., & Farnarier, C. (2003). IL-6: A regulator of the transition from neutrophil to monocyte recruitment during inflammation. *Trends in Immunology*, *24*(1), 25–29. https://doi.org/10.1016/S1471-4906(02)00013-3

Keski-Nisula, L., Hirvonen, M. R., Roponen, M., Heinonen, S., & Pekkanen, J. (2004). Spontaneous and stimulated interleukin-6 and tumor necrosis factor-alpha production at delivery and three months after birth. *European Cytokine Network*, *15*(1), 67–72.

Kiang, J. G., Smith, J. T., Anderson, M. N., Swift, J. M., Christensen, C. L., Gupta, P., … Maheshwari, R. K. (2015). Hemorrhage Exacerbates Radiation Effects on Survival, Leukocytopenia, Thrombopenia, Erythropenia, Bone Marrow Cell Depletion and Hematopoiesis, and Inflammation-Associated microRNAs Expression in Kidney. *PLOS ONE*, *10*(9), e0139271. https://doi.org/10.1371/journal.pone.0139271

Kim, Lee, Seo, Kim, Kim, Kim, … Youn. (2019). Cellular Stress Responses in Radiotherapy. *Cells*, *8*(9), 1105. https://doi.org/10.3390/cells8091105

Kishimoto, T., Akira, S., Narazaki, M., & Taga, T. (1995). Interleukin-6 family of cytokines and gp130. *Blood*, Vol. 86, pp. 1243–1254. https://doi.org/10.1182/blood.v86.4.1243.bloodjournal8641243

Kouvaris, J. R., Kouloulias, V. E., & Vlahos, L. J. (2007). Amifostine: The First Selective-Target and Broad-Spectrum Radioprotector. *The Oncologist*, *12*(6), 738–747. https://doi.org/10.1634/theoncologist.12-6-738

Krishnamoorthy, N., oriss, T., Paglia, M., Ray, A., & Ray, P. (2007). A critical role for IL-6 secretion by dendritic cells promoting Th2 and limiting Th1 response (95.24). *The Journal of Immunology*, *178*(1 Supplement).

Kulkarni, S., Ghosh, S. P., Satyamitra, M., Mog, S., Hieber, K., Romanyukha, L., … Kumar, K. S. (2010). Gamma-tocotrienol protects hematopoietic stem and progenitor cells in mice after total-body irradiation. *Radiation Research*, *173*(6), 738–747. https://doi.org/10.1667/RR1824.1

Kumari, N., Das, A., & Narayan Bhatt, A. (n.d.). *Interleukin-6 confers radio-resistance by inducing Akt-mediated glycolysis and reducing mitochondrial damage in cells*. https://doi.org/10.1093/jb/mvz091

Kumari, N., Dwarakanath, B. S., Das, A., & Bhatt, A. N. (2016). Role of interleukin-6 in cancer progression and therapeutic resistance. *Tumor Biology*, *37*(9), 11553–11572. https://doi.org/10.1007/s13277-016-5098-7

Landskron, G., De La Fuente, M., Thuwajit, P., Thuwajit, C., & Hermoso, M. A. (2014). Chronic inflammation and cytokines in the tumor microenvironment. *Journal of Immunology Research*, Vol. 2014. https://doi.org/10.1155/2014/149185

Lauber, K., Ernst, A., Orth, M., Herrmann, M., & Belka, C. (2012). Dying cell clearance and its impact on the outcome of tumor radiotherapy. *Frontiers in Oncology*. https://doi.org/10.3389/fonc.2012.00116

Le Caër, S. (2011). Water Radiolysis: Influence of Oxide Surfaces on H2 Production under Ionizing Radiation. *Water*, *3*(1), 235–253. https://doi.org/10.3390/w3010235

Leach, J. K., Tuyle, G. Van, Lin, P., Schmidt-ullrich, R., & Mikkelsen, R. B. (2001). *Ionizing Radiation-induced , Mitochondria-dependent Generation of Reactive Oxygen / Nitrogen 1*. 3894–3901.

Leibowitz, B. J., Wei, L., Zhang, L., Ping, X., Epperly, M., Greenberger, J., … Yu, J. (2014). Ionizing irradiation induces acute haematopoietic syndrome and gastrointestinal syndrome independently in mice. *Nature Communications*, *5*(1), 1–10. https://doi.org/10.1038/ncomms4494

Lin MT, Juan CY, Chang KJ, Chen WJ, K. M. (2001). IL-6 inhibits apoptosis and retains oxidative DNA lesions in human gastric cancer AGS cells through up-regulation of anti-apoptotic gene mcl-1tle. *Carcinogenesis*, *22*(12), 1947–1953. Retrieved from doi:10.1093/carcin/22.12.1947

Liu, Z., Simpson, R. J., & Cheers, C. (1992). Recombinant interleukin-6 protects mice against experimental bacterial infection. *Infection and Immunity*, *60*(10), 4402–4406. Retrieved from http://www.ncbi.nlm.nih.gov/pubmed/1398949

Lomax, M. E., Folkes, L. K., & O'neill, P. (2013). Biological Consequences of Radiation-induced DNA Damage: Relevance to Radiotherapy Statement of Search Strategies Used and Sources of Information. *Clinical Oncology*, *25*, 578–585. https://doi.org/10.1016/j.clon.2013.06.007

López, M., & Martín, M. (2011). Medical management of the acute radiation syndrome. *Reports of Practical Oncology and Radiotherapy*, Vol. 16, pp. 138–146. https://doi.org/10.1016/j.rpor.2011.05.001

Luzhna, L., Kathiria, P., & Kovalchuk, O. (2013). Micronuclei in genotoxicity assessment: From genetics to epigenetics and beyond. *Frontiers in Genetics*, Vol. 4. https://doi.org/10.3389/fgene.2013.00131

Macià i Garau, M., Lucas Calduch, A., & López, E. C. (2011). Radiobiology of the acute radiation syndrome. *Reports of Practical Oncology and Radiotherapy*, Vol. 16, pp. 123–130. https://doi.org/10.1016/j.rpor.2011.06.001

Maier, P., Hartmann, L., Wenz, F., & Herskind, C. (2016, January 14). Cellular pathways in response to ionizing radiation and their targetability for tumor radiosensitization. *International Journal of Molecular Sciences*, Vol. 17. https://doi.org/10.3390/ijms17010102

Manda, K., Anzai, K., Kumari, S., & Bhatia, A. L. (2007). Melatonin attenuates radiation-induced learning deficit and brain oxidative stress in mice. *Acta Neurobiologiae Experimentalis*, *67*(1), 63–70.

Martinel Lamas, D. J., Carabajal, E., Prestifilippo, J. P., Rossi, L., Elverdin, J. C., Merani, S., … Medina, V. A. (2013). Protection of Radiation-Induced Damage to the Hematopoietic System, Small Intestine and Salivary Glands in Rats by JNJ7777120 Compound, a Histamine H4 Ligand. *PLoS ONE*, *8*(7). https://doi.org/10.1371/journal.pone.0069106

Mason, K. A., Withers, H. R., & Davis, C. A. (1989). Dose dependent latency of fatal gastrointestinal and bone marrow syndromes. *International Journal of Radiation Biology*, *55*(1), 1–5. https://doi.org/10.1080/09553008914550011

Mauch, P., Constine, L., Greenberger, J., Knospe, W., Sullivan, J., Liesveld, J. L., & Deeg, H. J. (1995). Hematopoietic stem cell compartment: Acute and late effects of radiation therapy and chemotherapy. *International Journal of Radiation Oncology, Biology, Physics*, *31*(5), 1319–1339. https://doi.org/10.1016/0360-3016(94)00430-S

McGinnis, G. R., Ballmann, C., Peters, B., Nanayakkara, G., Roberts, M., Amin, R., & Quindry, J. C. (2015). Interleukin-6 mediates exercise preconditioning against myocardial ischemia reperfusion injury. *American Journal of Physiology-Heart and Circulatory Physiology*, *308*(11), H1423–H1433. https://doi.org/10.1152/ajpheart.00850.2014

McLoughlin, R. M., Jenkins, B. J., Grail, D., Williams, A. S., Fielding, C. A., Parker, C. R., … Jones, S. A. (2005). IL-6 trans-signaling via STAT3 directs T cell infiltration in acute inflammation. *Proceedings of the National Academy of Sciences of the United States of America*, *102*(27), 9589–9594. https://doi.org/10.1073/pnas.0501794102

Méry, B., Guy, J. B., Vallard, A., Espenel, S., Ardail, D., Rodriguez-Lafrasse, C., … Magné, N. (2017, February 22). In Vitro Cell Death Determination for Drug Discovery: A Landscape Review of Real Issues. *Journal of Cell Death*, Vol. 10. https://doi.org/10.1177/1179670717691251

Midander, J., & Révész, L. (1980). The frequency of micronuclei as a measure of cell survival in irradiated cell populations. *International Journal of Radiation Biology*, Vol. 38, pp. 237–242. https://doi.org/10.1080/09553008014551161

Mihara, M., Hashizume, M., Yoshida, H., Suzuki, M., & Shiina, M. (2012). IL-6/IL-6 receptor system and its role in physiological and pathological conditions. *Clinical Science*, *122*, 143–159. https://doi.org/10.1042/CS20110340

Miyamoto, S., Murphy, A. N., & Brown, J. H. (2008). Akt mediates mitochondrial protection in cardiomyocytes through phosphorylation of mitochondrial hexokinase-II. *Cell Death and Differentiation*, *15*(3), 521–529. https://doi.org/10.1038/sj.cdd.4402285

Monti, P., Wysocki, J., van der Meeren, A., & Griffiths, N. M. (2005). The contribution of radiation-induced injury to the gastrointestinal tract in the development of multi-organ dysfunction syndrome or failure. *The British Journal of Radiology*, *Supplement_27*(1), 89–94. https://doi.org/10.1259/bjr/53186341

Moron, M. S., Depierre, J. W., & Mannervik, B. (1979). Levels of glutathione, glutathione reductase and glutathione S-transferase activities in rat lung and liver. *BBA - General Subjects*, *582*(1), 67–78. https://doi.org/10.1016/0304-4165(79)90289-7

Moroni, M., Maeda, D., Whitnall, M. H., Bonner, W. M., & Redon, C. E. (2013). Evaluation of the gamma-H2AX assay for radiation biodosimetry in a swine model. *International Journal of Molecular Sciences*, *14*(7), 14119–14135. https://doi.org/10.3390/ijms140714119

Müller, W. U., Nüsse, M., Miller, B. M., Slavotinek, A., Viaggi, S., & Streffer, C. (1996). Micronuclei: A biological indicator of radiation damage. *Mutation Research - Reviews in Genetic Toxicology*, *366*(2), 163–169. https://doi.org/10.1016/S0165-1110(96)90037-8

Muñoz-Cánoves, P., Scheele, C., Pedersen, B. K., & Serrano, A. L. (2013). Interleukin-6 myokine signaling in skeletal muscle: a double-edged sword? *The FEBS Journal*, *280*(17), 4131–4148. https://doi.org/10.1111/febs.12338

Nair, C. K., Parida, D. K., & Nomura, T. (2001). Radioprotectors in radiotherapy. *Journal of Radiation Research*, *42*(1), 21–37. https://doi.org/10.1269/jrr.42.21

Nair, R. R., Bagheri, M., & Saini, D. K. (2015). Temporally distinct roles of ATM and ROS in genotoxic-stressdependent induction and maintenance of cellular

senescence. *Journal of Cell Science*, *128*(2), 342–353. https://doi.org/10.1242/jcs.159517

Narbutt, J., Lukamowicz, J., Bogaczewicz, J., Sysa-Jedrzejowska, A., Torzecka, J. D., & Lesiak, A. (2008). Serum concentration of interleukin-6 is increased both in active and remission stages of pemphigus vulgaris. *Mediators of Inflammation*, *2008*. https://doi.org/10.1155/2008/875394

Neta, R, Perlstein, R., Vogel, S. N., Ledney, G. D., & Abrams, J. (1992). Role of interleukin 6 (IL-6) in protection from lethal irradiation and in endocrine responses to IL-1 and tumor necrosis factor. *The Journal of Experimental Medicine*, *175*(3), 689–694. https://doi.org/10.1084/jem.175.3.689

Neta, Ruth. (1988a). *Cytokines in radioprotection and therapy of radiation injury*. *45*, 41–45.

Neta, Ruth. (1988b). Role of cytokines in radioprotection. *Pharmacology and Therapeutics*, *39*(1–3), 261–266. https://doi.org/10.1016/0163-7258(88)90070-8

Nolen, B. M., Marks, J. R., Ta'san, S., Rand, A., Luong, T. M., Wang, Y., … Lokshin, A. E. (2008). Serum biomarker profiles and response to neoadjuvant chemotherapy for locally advanced breast cancer. *Breast Cancer Research*, *10*(3). https://doi.org/10.1186/bcr2096

Oki, Y., Fanale, M., Romaguera, J., Fayad, L., Fowler, N., Copeland, A., … Younes, A. (2015). Phase II study of an AKT inhibitor MK2206 in patients with relapsed or refractory lymphoma. *British Journal of Haematology*, *171*(4), 463–470. https://doi.org/10.1111/bjh.13603

Orellana, E. A., & Kasinski, A. L. (n.d.). *Sulforhodamine B (SRB) Assay in Cell Culture to Investigate Cell Proliferation*. https://doi.org/10.21769/BioProtoc.1984

Packard, C. (1930). The relation between division rate and the radiosensitivity of cells. *The Journal of Cancer Research*, *14*(3), 359–369. https://doi.org/10.1158/jcr.1930.359

Pastorino, J. G., Shulga, N., & Hoek, J. B. (2002). Mitochondrial binding of hexokinase II inhibits Bax-induced cytochrome c release and apoptosis. *The*

Journal of Biological Chemistry, *277*(9), 7610–7618. https://doi.org/10.1074/jbc.M109950200

Patchen, M. L., MacVittie, T. J., Williams, J. L., Schwartz, G. N., & Souza, L. M. (1991). Administration of interleukin-6 stimulates multilineage hematopoiesis and accelerates recovery from radiation-induced hematopoietic depression. *Blood*, *77*(3), 472–480. Retrieved from http://www.ncbi.nlm.nih.gov/pubmed/1991164

Patt, H. M., Tyree, E. B., Straube, R. L., & Smith, D. E. (1949). Cysteine Protection against X Irradiation. *Science (New York, N.Y.)*, *110*(2852), 213–214. https://doi.org/10.1126/science.110.2852.213

Pazhanisamy, S. K. (2009, July 1). Stem cells, DNA damage, ageing and cancer. *Hematology/ Oncology and Stem Cell Therapy*, Vol. 2, pp. 375–384. https://doi.org/10.1016/S1658-3876(09)50005-2

Peter, R. U., Steinert, M., & Gottlöber, P. (2001). The cutaneous radiation syndrome: Diagnosis and treatment. *Radioprotection*, *36*(4), 451–457. https://doi.org/10.1051/radiopro:2001103

Petkau, A. (1987). Role of superoxide dismutase in modification of radiation injury. *The British Journal of Cancer. Supplement*, *8*, 87–95. Retrieved from http://www.ncbi.nlm.nih.gov/pubmed/3307878

Podhorecka, M., Skladanowski, A., & Bozko, P. (2010). Access to. *Research Journal of Nucleic Acids*, *2010*. https://doi.org/10.4061/2010/920161

Prakash, A., & Doublié, S. (2015). Base Excision Repair in the Mitochondria. *Journal of Cellular Biochemistry*, *116*(8), 1490–1499. https://doi.org/10.1002/jcb.25103

Radtke, S., Wüller, S., Yang, X. P., Lippok, B. E., Mütze, B., Mais, C., … Hermanns, H. M. (2010). Cross-regulation of cytokine signalling: Pro-inflammatory cytokines restrict IL-6 signalling through receptor internalisation and degradation. *Journal of Cell Science*, *123*(6), 947–959. https://doi.org/10.1242/jcs.065326

Rai, Y., Pathak, R., Kumari, N., Sah, D. K., Pandey, S., Kalra, N., … Bhatt, A. N. (2018). Mitochondrial biogenesis and metabolic hyperactivation limits the application of MTT assay in the estimation of radiation induced growth inhibition. *Scientific Reports*, *8*(1). https://doi.org/10.1038/s41598-018-19930-w

Rappold, I., Iwabuchi, K., Date, T., & Chen, J. (2001). Tumor Suppressor p53 Binding Protein 1 (53BP1) Is Involved in DNA Damage-signaling Pathways. In *The Journal of Cell Biology* (Vol. 153). Retrieved from http://www.jcb.org/cgi/content/full/153/3/613

Redza-Dutordoir, M., & Averill-Bates, D. A. (2016). Activation of apoptosis signalling pathways by reactive oxygen species. *Biochimica et Biophysica Acta - Molecular Cell Research*. https://doi.org/10.1016/j.bbamcr.2016.09.012

Reihmane, D., & Dela, F. (2014). Interleukin-6: Possible biological roles during exercise. *European Journal of Sport Science*, Vol. 14, pp. 242–250. https://doi.org/10.1080/17461391.2013.776640

Riley, P. A. (1994). Free radicals in biology: oxidative stress and the effects of ionizing radiation. *International Journal of Radiation Biology*, *65*(1), 27–33. https://doi.org/10.1080/09553009414550041

Romano, M., Sironi, M., Toniatti, C., Polentarutti, N., Fruscella, P., Ghezzi, P., … Mantovani, A. (1997). Role of IL-6 and its soluble receptor in induction of chemokines and leukocyte recruitment. *Immunity*, *6*(3), 315–325. https://doi.org/10.1016/S1074-7613(00)80334-9

Rotten, C. S., & Grant, H. K. (1998). The relationship between ionizing radiation-induced apoptosis and stem cells in the small and large intestine. *British Journal of Cancer*, *78*(8), 993–1003. https://doi.org/10.1038/bjc.1998.618

Saito, Y., Fujimoto, H., & Kobayashi, J. (2013). Role of NBS1 in DNA damage response and its relationship with cancer development. *Translational Cancer Research*, *2*(3), 178–189. https://doi.org/10.3978/j.issn.2218-676X.2013.04.05

Saito, Y., & Komatsu, K. (2015, August 20). Functional role of NBS1 in radiation damage response and translesion DNA synthesis. *Biomolecules*, Vol. 5, pp. 1990–2002. https://doi.org/10.3390/biom5031990

Samstein, R. M., & Riaz, N. (2018, October 1). The DNA damage response in immunotherapy and radiation. *Advances in Radiation Oncology*, Vol. 3, pp. 527–533. https://doi.org/10.1016/j.adro.2018.08.017

Santivasi, W. L., & Xia, F. (2014). Ionizing radiation-induced DNA damage, response, and repair. *Antioxidants and Redox Signaling*, *21*(2), 251–259. https://doi.org/10.1089/ars.2013.5668

Saraste, A., & Pulkki, K. (2000, February). Morphologic and biochemical hallmarks of apoptosis. *Cardiovascular Research*, Vol. 45, pp. 528–537. https://doi.org/10.1016/S0008-6363(99)00384-3

Schaue, D., Kachikwu, E. L., & McBride, W. H. (2012). Cytokines in Radiobiological Responses: A Review. *Radiation Research*, *178*(6), 505–523. https://doi.org/10.1667/rr3031.1

Scheller, J., Chalaris, A., Schmidt-Arras, D., & Rose-John, S. (2011, May). The pro- and anti-inflammatory properties of the cytokine interleukin-6. *Biochimica et Biophysica Acta - Molecular Cell Research*, Vol. 1813, pp. 878–888. https://doi.org/10.1016/j.bbamcr.2011.01.034

Schmidt, A. J., Krieg, J. C., & Vedder, H. (2005). Interleukin-6 induces glutathione in hippocampal cells. *Progress in Neuro-Psychopharmacology and Biological Psychiatry*, *29*(2), 321–326. https://doi.org/10.1016/j.pnpbp.2004.11.018

Schulte, W., Bernhagen, J., & Bucala, R. (2013). Cytokines in sepsis: Potent immunoregulators and potential therapeutic targets - An updated view. *Mediators of Inflammation*, *2013*. https://doi.org/10.1155/2013/165974

Sebina, I., Fogg, L. G., James, K. R., Soon, M. S. F., Akter, J., Thomas, B. S., … Haque, A. (2017). IL-6 promotes CD4+ T-cell and B-cell activation during Plasmodium infection. *Parasite Immunology*, *39*(10). https://doi.org/10.1111/pim.12455

Shao, L., Luo, Y., & Zhou, D. (2014, March 20). Hematopoietic stem cell injury induced by ionizing radiation. *Antioxidants and Redox Signaling*, Vol. 20, pp. 1447–1462. https://doi.org/10.1089/ars.2013.5635

Sharma, P., Jha, A. B., Dubey, R. S., & Pessarakli, M. (2012). Reactive Oxygen Species, Oxidative Damage, and Antioxidative Defense Mechanism in Plants under Stressful Conditions. *Journal of Botany*, *2012*, 1–26. https://doi.org/10.1155/2012/217037

Shinohara, K., & Nakano, H. (1993). Interphase Death and Reproductive Death in X-Irradiated MOLT-4 Cells. *Radiation Research*, *135*(2), 197. https://doi.org/10.2307/3578295

Shinomiya, N. (2001). New concepts in radiation-induced apoptosis: 'premitotic apoptosis1 and "postmitotic apoptosis." *Journal of Cellular and Molecular Medicine*, *5*(3), 240–253. https://doi.org/10.1111/j.1582-4934.2001.tb00158.x

Simon, H. U., Haj-Yehia, A., & Levi-Schaffer, F. (2000). Role of reactive oxygen species (ROS) in apoptosis induction. *Apoptosis*, *5*(5), 415–418. https://doi.org/10.1023/A:1009616228304

Simpson, R. J., Hammacher, A., Smith, D. K., Hews, J. M. M., & Ward, L. D. (1997). *Interleukin-6 : Structure-function relationships*.

Singh, N. P., McCoy, M. T., Tice, R. R., & Schneider, E. L. (1988). A simple technique for quantitation of low levels of DNA damage in individual cells. *Experimental Cell Research*, *175*(1), 184–191. https://doi.org/10.1016/0014-4827(88)90265-0

Singh, P. K., Wise, S. Y., Ducey, E. J., Fatanmi, O. O., Elliott, T. B., & Singh, V. K. (2012). α-Tocopherol Succinate Protects Mice against Radiation-Induced Gastrointestinal Injury. *Radiation Research*, *177*(2), 133–145. https://doi.org/10.1667/rr2627.1

Singh, V. K., Newman, V. L., Berg, A. N., & MacVittie, T. J. (2015). Animal models for acute radiation syndrome drug discovery. *Expert Opinion on Drug Discovery*, *10*(5), 497–517. https://doi.org/10.1517/17460441.2015.1023290

Singh, V. K., & Seed, T. M. (2017, September 2). A review of radiation countermeasures focusing on injury-specific medicinals and regulatory approval status: part I. Radiation sub-syndromes, animal models and FDA-approved countermeasures. *International Journal of Radiation Biology*, Vol. 93, pp. 851–869. https://doi.org/10.1080/09553002.2017.1332438

Sizemore, S. T., Zhang, M., Cho, J. H., Sizemore, G. M., Hurwitz, B., Kaur, B., … Xia, F. (2018). Pyruvate kinase M2 regulates homologous recombination-mediated DNA double-strand break repair. *Cell Research*, *28*(11), 1090–1102. https://doi.org/10.1038/s41422-018-0086-7

Smart, N., Mojet, M. H., Latchman, D. S., Marber, M. S., Duchen, M. R., & Heads, R. J. (2006). IL-6 induces PI 3-kinase and nitric oxide-dependent protection and preserves mitochondrial function in cardiomyocytes. *Cardiovascular Research*, *69*(1), 164–177. https://doi.org/10.1016/j.cardiores.2005.08.017

Steensberg, A., Febbraio, M. A., Osada, T., Schjerling, P., Van Hall, G., Saltin, B., & Pedersen, B. K. (2001). Interleukin-6 production in contracting human skeletal muscle is influenced by pre-exercise muscle glycogen content. *Journal of Physiology*, *537*(2), 633–639. https://doi.org/10.1111/j.1469-7793.2001.00633.x

Stepkowski, S. M., Chen, W., Ross, J. A., Nagy, Z. S., & Kirken, R. A. (2008). STAT3: an important regulator of multiple cytokine functions. *Transplantation*, *85*(10), 1372–1377. https://doi.org/10.1097/TP.0b013e3181739d25

Streffer, C., Müller, W.-U., & Wuttke, K. (1994). The Formation of Micronuclei after Exposure to Ionizing Radiation. In *Chromosomal Alterations* (pp. 214–222). https://doi.org/10.1007/978-3-642-78887-1_22

Surova, O., & Zhivotovsky, B. (2013, August 15). Various modes of cell death induced by DNA damage. *Oncogene*, Vol. 32, pp. 3789–3797. https://doi.org/10.1038/onc.2012.556

Suzuki, K., Ojima, M., Kodama, S., & Watanabe, M. (2003). Radiation-induced DNA damage and delayed induced genomic instability. *Oncogene*, *22*(45), 6988–6993. https://doi.org/10.1038/sj.onc.1206881

Tachibana, S., Zhang, X., Ito, K., Ota, Y., Cameron, A. M., Williams, G. M., & Sun, Z. (2014). Interleukin-6 is required for cell cycle arrest and activation of DNA repair enzymes after partial hepatectomy in mice. *Cell & Bioscience*, *4*(1), 6. https://doi.org/10.1186/2045-3701-4-6

Tanaka, T., Narazaki, M., & Kishimoto, T. (2014). Il-6 in inflammation, Immunity, And disease. *Cold Spring Harbor Perspectives in Biology*, *6*(10). https://doi.org/10.1101/cshperspect.a016295

Tanaka, T., Narazaki, M., & Kishimoto, T. (2016, July 1). Immunotherapeutic implications of IL-6 blockade for cytokine storm. *Immunotherapy*, Vol. 8, pp. 959–970. https://doi.org/10.2217/imt-2016-0020

Terry, N. H. A., & Travis, E. L. (1989). The influence of bone marrow depletion on intestinal radiation damage. *International Journal of Radiation Oncology, Biology, Physics*, *17*(3), 569–573. https://doi.org/10.1016/0360-3016(89)90108-9

Tomida, J., Kitao, H., Kinoshita, E., & Takata, M. (2008). Detection of phosphorylation on large proteins by western blotting using Phos-tag containing gel. *Protocol Exchange*. https://doi.org/10.1038/nprot.2008.232

Varanda, E. A., & Tavares, D. C. (1998). Radioprotection: Mechanisms and radioprotective agents including honeybee venom. *Journal of Venomous Animals and Toxins*, *4*(1), 5–21. https://doi.org/10.1590/S0104-79301998000100002

Verma, A., Bhatt, A. N., Farooque, A., Khanna, S., Singh, S., & Dwarakanath, B. S. (2011). Calcium ionophore A23187 reveals calcium related cellular stress as "I-Bodies": An old actor in a new role. *Cell Calcium*, *50*(6), 510–522. https://doi.org/10.1016/j.ceca.2011.08.007

Vermes, I., Haanen, C., Steffens-Nakken, H., & Reutelingsperger, C. (1995). A novel assay for apoptosis Flow cytometric detection of phosphatidylserine. *Journal of Immunological Methods*, *184*(1), 39–51. https://doi.org/10.1016/j.physb.2005.01.398

Vichai, V., & Kirtikara, K. (2006). Sulforhodamine B colorimetric assay for cytotoxicity screening. *Nature Protocols*, *1*(3), 1112–1116. https://doi.org/10.1038/nprot.2006.179

Vral, A., Fenech, M., & Thierens, H. (2011). The micronucleus assay as a biological dosimeter of in vivo ionising radiation exposure. *Mutagenesis*, *26*(1), 11–17. https://doi.org/10.1093/mutage/geq078

Wang, Y., Liu, L., Pazhanisamy, S. K., Meng, A., & Zhou, D. (2009). Total Body Irradiation Causes Residual Bone Marrow Injury by Induction of Persistent Oxidative Stress in Murine Hematopoietic Stem Cells. *Blood*, *114*(22), 3209–3209. https://doi.org/10.1182/blood.v114.22.3209.3209

Warburg, O. (1956). On the origin of cancer cells. *Science*, *123*(3191), 309–314. https://doi.org/10.1126/science.123.3191.309

Ward, I., & Chen, J. (2004). Early Events in the DNA Damage Response. *Current Topics in Developmental Biology*, *63*, 1–35. https://doi.org/10.1016/S0070-2153(04)63001-8

Ward, I. M., Minn, K., van Deursen, J., & Chen, J. (2003). p53 Binding Protein 53BP1 Is Required for DNA Damage Responses and Tumor Suppression in Mice. *Molecular and Cellular Biology*, *23*(7), 2556–2563. https://doi.org/10.1128/mcb.23.7.2556-2563.2003

Ward, J. F. (1994). The complexity of DNA damage: Relevance to biological consequences. *International Journal of Radiation Biology*, *66*(5), 427–432. https://doi.org/10.1080/09553009414551401

Waselenko, J. K., MacVittie, T. J., Blakely, W. F., Pesik, N., Wiley, A. L., Dickerson, W. E., … Dainiak, N. (2004, June 15). Medical management of the acute radiation syndrome: Recommendations of the Strategic National Stockpile Radiation Working Group. *Annals of Internal Medicine*, Vol. 140. https://doi.org/10.7326/0003-4819-140-12-200406150-00015

Waxman, A. B., & Kolliputi, N. (2009). IL-6 protects against hyperoxia-induced mitochondrial damage via Bcl-2-induced Bak interactions with mitofusions. *American Journal of Respiratory Cell and Molecular Biology*, *41*(4), 385–396. https://doi.org/10.1165/rcmb.2008-0302OC

Wegener, A. D., & Jones, L. R. (1984). Phosphorylation-induced mobility shift in phospholamban in sodium dodecyl sulfate-polyacrylamide gels. Evidence for a protein structure consisting of multiple identical phosphorylatable subunits. *Journal of Biological Chemistry*, *259*(3), 1834–1841.

Wei, L. H., Kuo, M. L., Chen, C. A., Chou, C. H., Cheng, W. F., Chang, M. C., … Hsieh, C. Y. (2001). The anti-apoptotic role of interleukin-6 in human cervical

cancer is mediated by up-regulation of Mcl-1 through a PI 3-K/Akt pathway. *Oncogene*, *20*(41), 5799–5809. https://doi.org/10.1038/sj.onc.1204733

Weiss, J. F., & Landauer, M. R. (2009). History and development of radiation-protective agents. *International Journal of Radiation Biology*, *85*(7), 539–573. https://doi.org/10.1080/09553000902985144

Willers, H., Dahm-Daphi, J., & Powell, S. N. (2004, April 5). Repair of radiation damage to DNA. *British Journal of Cancer*, Vol. 90, pp. 1297–1301. https://doi.org/10.1038/sj.bjc.6601729

Williams, J. P., & McBride, W. H. (2011a, August). After the bomb drops: A new look at radiation-induced multiple organ dysfunction syndrome (MODS). *International Journal of Radiation Biology*, Vol. 87, pp. 851–868. https://doi.org/10.3109/09553002.2011.560996

Williams, J. P., & McBride, W. H. (2011b, August). After the bomb drops: A new look at radiation-induced multiple organ dysfunction syndrome (MODS). *International Journal of Radiation Biology*, Vol. 87, pp. 851–868. https://doi.org/10.3109/09553002.2011.560996

Wink, D. A., & Mitchell, J. B. (1998). Chemical biology of nitric oxide: Insights into regulatory, cytotoxic, and cytoprotective mechanisms of nitric oxide. *Free Radical Biology & Medicine*, *25*(4–5), 434–456. https://doi.org/10.1016/s0891-5849(98)00092-6

Wu, Q., Allouch, A., Martins, I., Brenner, C., Modjtahedi, N., Deutsch, E., & Perfettini, J. L. (2017, May 26). Modulating both tumor cell death and innate immunity is essential for improving radiation therapy effectiveness. *Frontiers in Immunology*, Vol. 8. https://doi.org/10.3389/fimmu.2017.00613

Xing, Z., Gauldie, J., Cox, G., Baumann, H., Jordana, M., Lei, X. F., & Achong, M. K. (1998). IL-6 is an antiinflammatory cytokine required for controlling local or systemic acute inflammatory responses. *Journal of Clinical Investigation*, *101*(2), 311–320. https://doi.org/10.1172/JCI1368

Yin, T., & Li, L. (2006, May 1). The stem cell niches in bone. *Journal of Clinical Investigation*, Vol. 116, pp. 1195–1201. https://doi.org/10.1172/JCI28568

Yoshida, K., Taga, T., Saito, M., Suematsu, S., Kumanogoh, A., Tanaka, T., … Kishimoto, T. (1996). Targeted disruption of gp130, a common signal transducer for the interleukin 6 family of cytokines, leads to myocardial and hematological disorders. *Proceedings of the National Academy of Sciences of the United States of America*, *93*(1), 407–411. https://doi.org/10.1073/pnas.93.1.407

Yu, Y., & Little2, J. B. (1998). p53 Is Involved in But Not Required for Ionizing Radiation-induced Caspase-3 Activation and Apoptosis in Human Lymphoblast Cell Lines1. In *CANCER RESEARCH* (Vol. 58).

Zhang, F., Duan, S., Tsai, Y., Keng, P. C., Chen, Y., Lee, S. O., & Chen, Y. (2016). Cisplatin treatment increases stemness through upregulation of hypoxia-inducible factors by interleukin-6 in non-small cell lung cancer. *Cancer Science*, *107*(6), 746–754. https://doi.org/10.1111/cas.12937

Zhang, J., Wang, X., Cui, W., Wang, W., Zhang, H., Liu, L., … Li, B. (2013). Visualization of caspase-3-like activity in cells using a genetically encoded fluorescent biosensor activated by protein cleavage. *Nature Communications*, *4*(1), 1–13. https://doi.org/10.1038/ncomms3157

Zhang, M., Cao, G., Guo, X., Gao, Y., Li, W., & Lu, D. (2018). A comet assay for DNA damage and repair after exposure to carbon-ion beams or X-rays in saccharomyces cerevisiae. *Dose-Response*, *16*(3). https://doi.org/10.1177/1559325818792467

Zhang, Xiuying, Tachibana, S., Wang, H., Hisada, M., Williams, G. M., Gao, B., & Sun, Z. (2010). Interleukin-6 is an important mediator for mitochondrial DNA repair after alcoholic liver injury in mice. *Hepatology*, *52*(6), 2137–2147. https://doi.org/10.1002/hep.23909

Zhang, Xurui, Ye, C., Sun, F., Wei, W., Hu, B., & Wang, J. (2016). Both complexity and location of DNA damage contribute to cellular senescence induced by ionizing radiation. *PLoS ONE*, *11*(5). https://doi.org/10.1371/journal.pone.0155725

Zhong, J., Rajaram, N., Brizel, D. M., Frees, A. E., Ramanujam, N., Batinic-Haberle, I., & Dewhirst, M. W. (2013). Radiation induces aerobic glycolysis through

reactive oxygen species. *Radiotherapy and Oncology : Journal of the European Society for Therapeutic Radiology and Oncology*, *106*(3), 390–396. https://doi.org/10.1016/j.radonc.2013.02.013

Zhuang, L., Lee, C. S., Scolyer, R. A., McCarthy, S. W., Zhang, X. D., Thompson, J. F., & Hersey, P. (2007). Mcl-1, Bcl-XL and Stat3 expression are associated with progression of melanoma whereas Bcl-2, AP-2 and MITF levels decrease during progression of melanoma. *Modern Pathology*, *20*(4), 416–426. https://doi.org/10.1038/modpathol.3800750

Zölzer, F., Speer, A., Pelzer, T., & Streffer, C. (1995). Evidence for quiescent S- and G_2 -phase cells in human colorectal carcinomas: a flow cytometric study with the Ki-67 antibody. *Cell Proliferation*, *28*(6), 313–327. https://doi.org/10.1111/j.1365-2184.1995.tb00073.x

Publication

Role of interleukin-6 in cancer progression and therapeutic resistance

Neeraj Kumari, B. S. Dwarakanath, Asmita Das & Anant Narayan Bhatt

Tumor Biology
Tumor Markers, Tumor Targeting and Translational Cancer Research

ISSN 1010-4283

Tumor Biol.
DOI 10.1007/s13277-016-5098-7

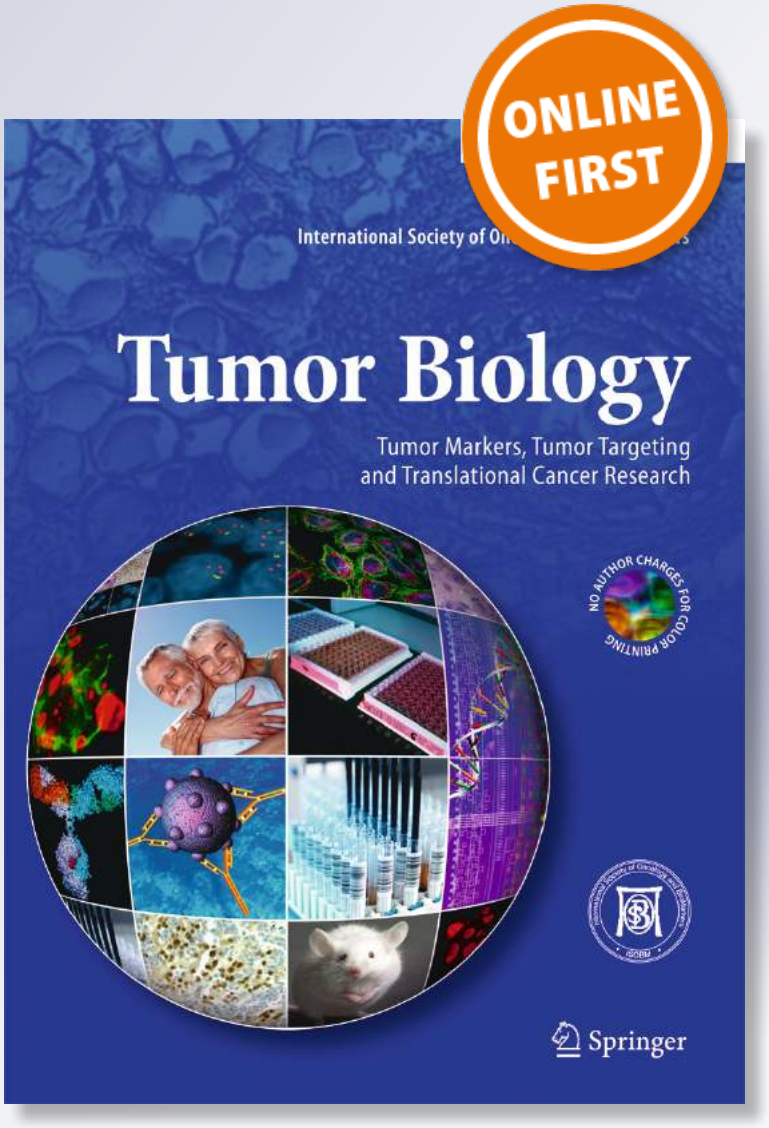

Springer

Your article is protected by copyright and all rights are held exclusively by International Society of Oncology and BioMarkers (ISOBM). This e-offprint is for personal use only and shall not be self-archived in electronic repositories. If you wish to self-archive your article, please use the accepted manuscript version for posting on your own website. You may further deposit the accepted manuscript version in any repository, provided it is only made publicly available 12 months after official publication or later and provided acknowledgement is given to the original source of publication and a link is inserted to the published article on Springer's website. The link must be accompanied by the following text: "The final publication is available at link.springer.com".

Author's personal copy

Tumor Biol.
DOI 10.1007/s13277-016-5098-7

REVIEW

Role of interleukin-6 in cancer progression and therapeutic resistance

Neeraj Kumari[1,2] · B. S. Dwarakanath[3] · Asmita Das[2] · Anant Narayan Bhatt[1]

Received: 3 February 2016 / Accepted: 22 May 2016
© International Society of Oncology and BioMarkers (ISOBM) 2016

Abstract In the last several decades, the number of people dying from cancer-related deaths has not reduced significantly despite phenomenal advances in the technologies related to diagnosis and therapeutic modalities. The principal cause behind limitations in the curability of this disease is the reducing sensitivity of the cancer cells towards conventional anticancer therapeutic modalities, particularly in advance stages of the disease. Amongst several reasons, certain secretory factors released by the tumour cells into the microenvironment have been found to confer resistance towards chemo- and radiotherapy, besides promoting growth. Interleukin-6 (IL-6), one of the major cytokines in the tumour microenvironment, is an important factor which is found at high concentrations and known to be deregulated in cancer. Its overexpression has been reported in almost all types of tumours. The strong association between inflammation and cancer is reflected by the high IL-6 levels in the tumour microenvironment, where it promotes tumorigenesis by regulating all hallmarks of cancer and multiple signalling pathways, including apoptosis, survival, proliferation, angiogenesis, invasiveness and metastasis, and, most importantly, the metabolism. Moreover, IL-6 protects the cancer cells from therapy-induced DNA damage, oxidative stress and apoptosis by facilitating the repair and induction of countersignalling (antioxidant and anti-apoptotic/pro-survival) pathways. Therefore, blocking IL-6 or inhibiting its associated signalling independently or in combination with conventional anticancer therapies could be a potential therapeutic strategy for the treatment of cancers with IL-6-dominated signalling.

Keywords IL-6 · Cancer · Therapeutic resistance · STAT-3 · Chemotherapy · Radio-resistance

Introduction

Inflammation has a very strong link with various types of cancer. Malignant cells are highly proliferative in nature, which is facilitated by the inflammatory molecules that are continuously being secreted by other cells and/or tumour cells themselves in a microenvironment [1, 2]. Interleukin-6 (IL-6) is one such inflammatory molecule, which is produced and secreted by various types of cells including the tumour cells. It is involved in the proliferation and differentiation of malignant cells and found to be high in serum and tumour tissues of a majority of cancers, viz. colorectal cancer [3], breast cancer [4], prostate cancer [5], ovarian carcinoma [6], pancreatic cancer [7], lung cancer [8], renal cell carcinoma [9], cervical cancer [10] and multiple myeloma [11]. Elevated levels of IL-6 are associated with aggressive tumour growth and response to therapies in many types of cancer [12, 13]. Patients with high levels of circulating IL-6 are generally associated with poor prognosis and shorter survival, whilst a lower level of IL-6 is associated with better response to therapy [14, 15].

Anticancer drugs and ionizing radiation used during cancer therapy induce inflammatory signalling, mainly in the form of the nuclear factor-kappa B (NF-kB) pathway [16, 17]. NF-kB regulates the expression of different pro-inflammatory

✉ Anant Narayan Bhatt
anant@inmas.drdo.in; anbhatt@yahoo.com

[1] Division of Metabolic Cell Signalling Research, Institute of Nuclear Medicine and Allied Sciences, Brig SK Mazumdar Road, Delhi 110 054, India

[2] Department of Biotechnology, Delhi Technological University, Delhi 110042, India

[3] Central Research Facility, Sri Ramachandra University, Chennai 600116, India

Published online: 03 June 2016

Author's personal copy

cytokines, chemokines and anti-apoptotic genes and acts as a key molecular link between inflammation and initiation as well as progression of oncogenesis [18]. Chemotherapeutic drugs and radiation also induce IL-6 expression in tumour and stromal cells [12, 13] through the activation of NF-kB signalling, leading to therapeutic resistance [19, 20]. These evidences suggest that blocking IL-6 or inhibiting the IL-6 downstream signalling pathways may provide therapeutic gain in those cancers which are associated with a higher level of IL-6. This review provides an insight into the current understanding of the role of IL-6 in the regulation of various hallmarks and associated signalling in cancer as well as its contribution to therapeutic resistance. It also provides an insight into how the anti-IL-6 antibody or the inhibitors of pathways downstream to IL-6 signalling can improve the effectiveness of cancer radio- and/or chemotherapy.

Interleukin-6

IL-6 is a glycosylated polypeptide chain having a molecular weight of nearly 25 kDa, depending on the glycosylation and the species. It has a characteristic structure made up of four long α-helices arranged in an up–up–down–down topology [21]. It was first discovered as a B cell differentiation factor (BSF-2) which induces the maturation of B cells into antibody-producing cells [22]. Besides its role in immune regulation, it plays an important role in the maintenance of hepatocytes, haematopoietic progenitor cells, the skeleton, the placenta, the cardiovascular system and the endocrine as well as nervous systems. In the murine haematopoietic system, IL-6 induces the expansion of progenitor cells by stimulating cells from the resting stage to enter the G1 phase [23]. IL-6 also supports various physiological functions by acting as a hepatocyte stimulatory factor and by inducing the acute-phase protein synthesis. It is also known to stimulate osteoclast formation, induce bone resorption and is responsible for neural differentiation [24]. IL-6 supports the survival of cholinergic neurons, induces adrenocorticotropic hormone synthesis, and, in placenta, causes the secretion of chorionic gonadotropin from trophoblasts [23]. IL-6 also plays a very important role in metabolism. For example, in the absence of IL-6, mice develop glucose intolerance and insulin resistance, whilst IL-$6^{-/-}$ mice exhibit signs of liver inflammation [25]. The secretion and availability of IL-6 is ubiquitous, and it can bind to various types of cells in different tissues. However, its binding on different cell types may differ, resulting in two different types of IL-6-dependent cell signalling (Fig. 1).

IL-6 binds to the IL-6 receptor (IL-6R) on the plasma membrane, and the resultant IL-6/IL-6R complex associates with gp130 and causes gp130 homodimerization to form an activated IL-6 receptor complex, which is a hexameric structure consisting of two molecules each of IL-6, IL-6R and gp130 [26, 27]. The binding of IL-6 to IL-6R occurs at three distinct receptor-binding sites of IL-6R and gp130. However, the Ig-like domain of the human IL-6R is not involved in the direct binding of IL-6 [28]. Upon binding to the receptor and gp130, IL-6 induces various functions by activating cell signalling events [24]. IL-6 triggers signal transduction via two forms of IL-6R: one a transmembrane 80-kDa receptor with a short cytoplasmic domain (mbIL-6R, also known as IL-6Rα, gp80 or CD126) and the other a small, extracellular, secretory soluble receptor (sIL-6R) [29]. Classical IL-6 signalling, which is the predominant form of IL-6 signalling, requires membrane-bound IL-6R (mbIL-6R) and is restricted to hepatocytes, some epithelial cells and certain leukocytes (Fig. 1) [26]. IL-6R contains a very short cytosolic domain that lacks the major potential motifs for transduction of intracellular cell signalling. However, gp130 (also known as IL-6Rβ or CD130) in the same hexameric complex is rich in all these potential motifs required for intracellular signalling, such as SHP-2 domain and YXXQ motif for JAK/STAT signalling. Upon binding with IL-6/IL-6R, the dimerization of gp130 leads to the activation of associated cytoplasmic tyrosine kinases, resulting in the phosphorylation of various transcription factors [24]. gp130 is expressed in almost all organs, including the brain, heart, lung, liver, kidney, spleen and placenta, where it plays an indispensable role in their development, cell survival, growth and tissue homeostasis [30]. gp130 is a common signal transducing receptor and is also used by other members of the IL-6 family cytokines, such as IL-11, IL-12, IL-27, leukaemia inhibitory factor, oncostatin M, etc. [31]. Although the expression of transmembrane IL-6R is limited to the hepatocytes and subsets of leukocytes, gp130 is expressed ubiquitously. Therefore, the IL-6/sIL-6R complex can transduce the IL-6 signal in various cells, which do not express transmembrane IL-6R but express gp130, through a trans-signalling mechanism. sIL-6R is generated by alternative splicing of IL-6R mRNA or by limited proteolysis of mbIL-6R by Zn-dependent metalloproteinase (ADAM10 and ADAM17, a disintegrin and metalloproteinases 10 and 17; Fig. 1) [29–32]. sIL-6R is devoid of the cytoplasmic and transmembrane domains and binds to IL-6 with comparable affinity as the membrane-bound form, thereby mediating gp130 activation in an autocrine or paracrine manner [21]. Consequently, by binding to sIL-6R, IL-6 increases its reach to a wide variety of cells. There is enough evidence to suggest that neural cell, neural stem cells, haematopoietic stem cells, liver progenitor cells and embryonic stem cells depend on sIL-6R in their response to IL-6 [33–36]. The level of sIL-6R present in the human sera increases during inflammation [32, 37]. Knockdown of the IL-6R gene in hepatocytes reduces the levels of sIL-6R by 32 % in the serum, whilst ablation of the IL-6R gene in haematopoietic cells reduces the sIL-6R serum levels by 60 % [38]. These observations suggest that hepatocytes and haematopoietic cells are the main sources of sIL-6R

Author's personal copy

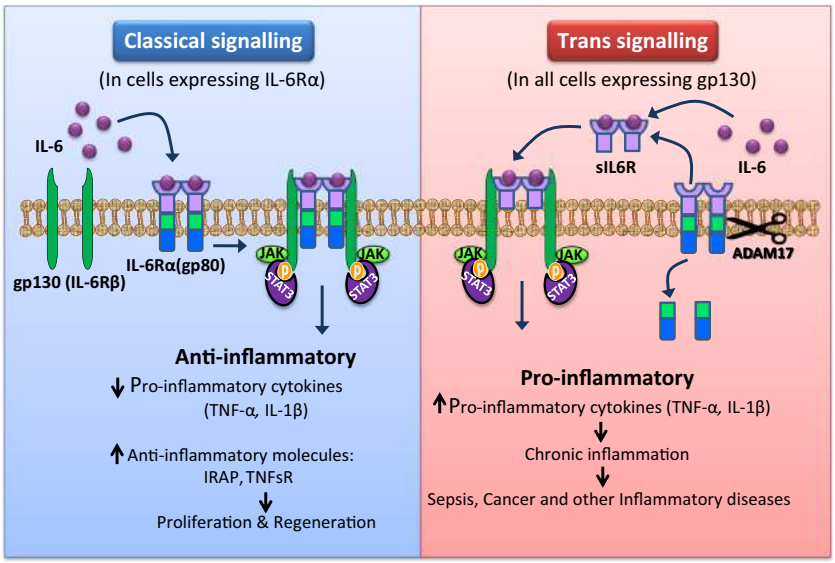

Fig. 1 Classical and trans-signalling of IL-6: In classical signalling, which occurs mainly in leukocytes and liver cells, IL-6 binds to the membrane-bound receptor mbIL-6Rα, which then forms a complex with the ubiquitously present cell receptor gp130 (*IL-6Rβ*). Trans-signalling can occur in any cell expressing gp130. In trans-signalling, IL-6 forms a complex with sIL-6R, which is a small part of mbIL-6Rα produced by either metalloproteinase or by alternative splicing. Furthermore, the IL-6–sIL-6R complex binds with gp130 on cells which do not express mbIL-6R. The inflammatory reactions induce the production of sIL-6R, which elicits response to IL-6 in cells that do not express IL-6 receptor (mbIL-6Rα) and/or remain inert to IL-6 signalling in normal physiological conditions. Classical signalling activates the anti-inflammatory pathways and promotes the regeneration of tissues, whereas trans-signalling activates pro-inflammatory pathways and is known to play a significant role in many diseases such as sepsis and cancer

found in the circulation [38]. Like sIL-6R, a soluble form of the signal transducer protein gp130 (sgp130) is also present in the circulation at relatively high concentrations during inflammation and cancer [37, 39]. sgp130 is mainly produced by alternative splicing rather than limited proteolysis, as in the case of sIL-6R generation. Since sgp130 binds to the IL-6/sIL-6R complex in the circulation, it acts as a specific inhibitor of IL-6-mediated trans-signalling [40]. Classic signalling via the mbIL-6R is not affected by sgp130. Its inhibitory action depends on the IL-6/sIL-6R ratio, with trans-signalling inhibition at low concentrations [37].

IL6 expression and secretion

The common characteristic of many of the stimuli that activate IL-6 is that they are associated with tissue damage or stress (e.g. ionizing radiation, UV, reactive oxygen species, viruses, microbial products and other pro-inflammatory cytokines) [12, 41, 42]. IL-6 production is predominantly regulated by changes in the gene expression of various transcription factors such as NF-kB, CCAAT/enhancer-binding protein a and activator protein 1, the major transcriptional regulator, although posttranscriptional modifications have also been identified [41, 43]. Though the activation of these transcription factors leads to the overexpression of this cytokine during inflammation, its expression is also known to be regulated epigenetically in breast cancer, hepatocellular carcinoma, colon cancer, prostate cancer and lung cancer through miRNAs (Lin28 and Let-7) [44].

The normal blood circulating level of IL-6 is nearly 1 pg/ml [45, 46], but an increase in its level is found under several conditions such as acute hyperglycemia [47], high-fat meal [48], normal menstrual cycle [49], physical activity [50] and during/after surgery [51]. Inconsistent levels of IL-6 have also been observed during pregnancy, with median values around 128 pg/ml registered at delivery, which drop by more than two fold (~58 pg/ml) immediately afterward [52]. Furthermore, serum IL-6 levels have been found to increase drastically during sepsis [53].

Many physiological factors such as diet, exercise and stress are known to regulate the secretion of IL-6 [47–53]. Exercise is an important stimulus for increased gene expression and production of IL-6 in skeletal muscle, and the majority of circulating IL-6 during exercise originates from contracting muscle, resulting in a 100-fold increase over the normal physiological level [50, 54]. IL-6 produced in the working muscle during physical activity acts as an energy sensor that activates AMP-activated kinase and enhances glucose uptake, metabolism, lipolysis and fat oxidation [50]. IL-6 is also known to sensitize myotubes to insulin and enhances glucose uptake in muscles for high glycogen synthesis. Moreover, the reduced level of muscle glycogen also augments IL-6 production and secretion from muscle cells [55]. In addition to exercise, the expression of IL-6 increases in skeletal muscles under other

Author's personal copy

conditions as well, such as denervation of muscles and muscular dystrophy, also resulting in the upregulated expression of muscle IL-6 [54]. The adipose tissue produces nearly 30 % of circulating systemic IL-6, where it is closely associated with obesity, impaired glucose tolerance and insulin resistance [56]. Plasma IL-6 concentrations are a predictor of the development of type 2 diabetes, and peripheral administration of IL-6 results in insulin resistance in rodents and humans by causing hyperlipidaemia and hyperglycaemia [56]. Besides muscle cells, e.g. macrophages, mast cells, dendritic cells, B cells and CD4 effector T helper cells in the immune system are amongst the major sources of IL-6 production [22, 57–59]. In addition, IL-6 is also secreted by a variety of non-haematopoietic cells such as fibroblasts, endothelial cells, epithelial cells, astrocytes and malignant cells [2, 33, 42, 60]. Enhanced levels of IL-6 have been found in many cancers, with an inverse relationship between IL-6 levels and response to chemotherapy and hormone therapy [61]. Furthermore, IL-6 expression has also been found higher in recurrent tumours as compared to primary tumours, as well as in recurrent metastatic lesion as compared to primary metastasis [15].

The primary sources of IL-6 in the tumour microenvironment are tumour cells as well as tumour-associated macrophages (TAMs), $CD4^+$ T cells, myeloid-derived suppressor cells (MDSCs) and fibroblasts [59–62]. In the tumour microenvironment, IL-6 supports tumorigenesis by directly affecting cancer cells through the modulation of both the intrinsic and extrinsic activities of tumour cells as well as by influencing stromal cells that indirectly support tumorigenesis [63]. For example, in skin and prostate cancer, the autocrine and paracrine secretion of IL-6 induces a complex of cytokine, growth factors and protease network consisting of granulocyte macrophage colony-stimulating factor (GM-CSF), IL-8, MCP-1, vascular endothelial growth factor (VEGF) and MMP-1 and stimulates malignant progression [64]. Basically, tumour cells produce IL-6 for promoting their survival and progression and do not depend on paracrine release of IL-6 by stromal cells [63]. However, both autocrine and paracrine mechanisms of IL-6 are known to influence tumour progression and metastasis through IL-6 trans-signalling [2, 64].

Pleiotropic role of IL-6

Cancer is an inflammatory disease, and the key feature of cancer-related inflammation is the expression of cytokines. Different cytokines play different roles in the onset and resolution of inflammation. However, a ubiquitous and functionally diverse cytokine, IL-6 is a pleiotropic cytokine with pro- and anti-inflammatory properties (Fig. 1). It is an important cytokine regulating the acute-phase response of inflammation [21]. During inflammatory response, tumour necrosis factor alpha (TNFα) induces the expression of IL-6 together with other inflammatory alarm cytokines, such as IL-1β, which are involved in the elicitation of acute-phase inflammatory reactions/responses (Fig. 1) [65]. Furthermore, IL-6 controls the level of acute inflammatory responses by downregulating the expression of pro-inflammatory cytokines and upregulating anti-inflammatory molecules, including IL-1 receptor antagonist protein, TNF-soluble receptor and extrahepatic protease inhibitors (Fig. 1) [66]. IL-6 has also been found to counter inflammation by inhibiting TNFα release in experimental endotoxemia [67]. This pleiotropic nature of IL-6 maintains the host–tumour homeostasis.

During switch between pro- and anti-inflammatory roles, TNFα and IL-1β negatively regulate IL-6 signalling at different levels by enhancing the IL-6-induced expression of the suppressor of cytokine signalling (SOCS3, feedback inhibitor) and/or targeting IL-6-induced gene expression via its action on target gene promoters [59, 68–70]. IL-1β also counteracts IL-6-mediated STAT-3 activation independent of SOCS3 expression [71]. IL-1β is the major regulator of the pro- and anti-inflammatory nature of IL-6; on the one hand, it reduces the pro-inflammatory activity of IL-6 that results in the inhibition of overshooting immunological reactivity, such as in inflammatory bowel disease or autoimmune arthritis, whilst on the other hand, it delays the anti-inflammatory effects of IL-6 to reinforce the pro-inflammatory processes in the initial phase of inflammation [70]. Similarly, the high concentration of IL-1β in the tumour microenvironment must maintain the chronic inflammatory environment by suppressing the anti-inflammatory processes of IL-6.

Emerging evidences suggest that IL-6 plays key roles in the acute as well as the transition (resolution) phase of inflammation [68]. Furthermore, IL-6 trans-signalling recruits T cells at the site of inflammation by triggering the expression of T cell-attracting chemokines (CCL4, CCL5, CCL17 and CXCL10) [72]. Moreover, IL-6 also rescues T cells from entering apoptosis by STAT-3-dependent upregulation of anti-apoptotic regulators (Bcl-2 and Bcl-xL) and modulation of Fas surface expression [73, 74]. IL-6 also regulates the differentiation of recruited T cells towards TH2 by inducing the expression of IL-4. Thus, IL-6 regulates some of the key steps in controlling inflammation and sets the anti-inflammatory environment by promoting TH2 response [57]. Collectively, these evidences suggest that endogenous IL-6 plays a vital anti-inflammatory role in both local and systemic acute inflammatory responses by controlling the level of pro-inflammatory cytokines, mainly. The trans-signalling of IL-6 regulates mainly the pro-inflammatory response; however, IL-6 classical signalling imparts its anti-inflammatory or regenerative activity (Fig. 1) such as regeneration [75], inhibition of epithelial apoptosis and the activation of the acute-phase response [76]. Understanding of the pleiotropic role of IL-6 in cancer

Author's personal copy

is not very clear; however, the information available from other inflammatory diseases suggest that IL-6 might play both pro- and anti-inflammatory roles in the tumour microenvironment, which is crucial for host–tumour interaction.

Role of IL-6 and associated signalling in cancer

The notion that inflammation drives cancer is now well established. One of the major drivers of this link is NF-kB, which plays a central role in the secretion and activation of numerous pro-inflammatory cytokines from multiple cell types in the tumour microenvironment, including macrophages, T cells and epithelial cells [43, 57, 58]. Several pro-inflammatory cytokines released by innate and adaptive immune cells regulate cancer cell growth and thereby contribute to tumour promotion and progression. Amongst these, IL-6 is important in the development of human cancer and activates oncogenic pathways, and it is known to be deregulated in cancer [77]. Overexpression of IL-6 in many types of tumours, such as colorectal cancer [3], prostate cancer [5], breast cancer [4], ovarian carcinoma [6], pancreatic cancer [7], lung cancer [8], renal cell carcinoma [9], cervical cancer [10], multiple myeloma [11] and lymphomas [78], suggests a strong link between this cytokine and cancer. The high susceptibility and incidence of liver cancer in males is also found to be associated with high levels of IL-6 [79]. However, in females, oestrogen steroid hormones inhibit IL-6 production and so protect female mice from cancer [79, 80]. Activation of the IL-6/STAT-3 signalling axis is an important event in cancer which promotes tumorigenesis by regulating multiple survival signalling pathways in cancer cells [24]. IL-6 regulates nearly all hallmarks of cancer, such as inhibition of apoptosis [81, 82], promotion of survival [8, 75], proliferation [35, 83], angiogenesis [10], invasiveness and metastasis [62, 84], and is also known to regulate cancer cell metabolism (Fig. 2) [85, 86]. Therefore, there exists a strong link between IL-6 and cancer, similar to the link between cancer and inflammation. Majority of the phenotypes or hallmarks of cancer which are influenced by IL-6 comprise many biological capabilities that are acquired during tumour development. The role of IL-6 in the regulation of hallmarks of cancer will be discussed in detail later.

Evasion of growth suppressors

Cancer cells evade some powerful programmes that negatively regulate cell proliferation. Many of these programmes depend on the action of tumour suppressor genes such as p53 and RB (retinoblastoma gene), which

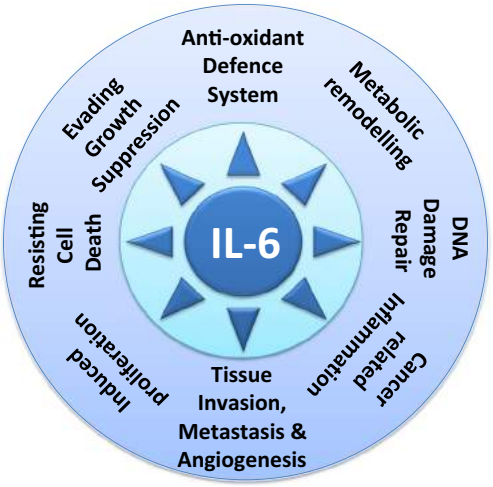

Fig. 2 IL-6 and cancer hallmarks: IL-6 plays an important role in cancer growth and progression by influencing nearly all hallmarks of cancer. The picture illustrates the contribution of IL-6 in some major characteristics of cancer, which are known as cancer hallmarks

undergo either loss or gain of function, respectively, to limit cell growth and proliferation. Rb (retinoblastoma-associated) and TP53 proteins are the essential regulatory nodes within two key complementary cellular regulatory circuits that govern the decisions of cells to proliferate or activate senescence and apoptotic programmes [87]. The hypermethylation of CpG islands in the promoter regions of tumour suppressor genes has been found in many tumours, which allows cancer cells to bypass crucial checkpoints in cell cycle progression and evade apoptotic signals (Fig. 3) [88, 89]. IL-6 is known to increase both the expression of DNA methyltransferase (DNMT-1) [90] and its translocation to the nucleus by DNMT-1 nuclear localizing signal's phosphorylation via PI-3K/AKT signalling [91], thereby increasing the activity of DNMT-1, resulting in CpG island methylation of the promoter region of the p53 gene (Fig. 3) [89]. Contrary to the hypermethylation of tumour suppressor genes, IL-6 is also involved in causing global hypomethylation of retrotransposon long interspersed nuclear element-1 in oral squamous cell carcinoma cell lines, which promotes tumorigenesis in the oral cavity [92]. These epigenetic alterations in tumour cells contribute to the epigenetic silencing of tumour suppressor genes and lead to enhanced tumorigenesis.

Mutations in the RB gene contribute to cellular transformation in various types of malignancies [93]. Normal retinoblastoma protein suppresses the transition from the G1 to the S phase of the cell cycle, which is regulated by the phosphorylation of Rb protein. The active, hypo- or dephosphorylated form of Rb binds with E2F and induces G1 growth arrest. On the contrary, the phosphorylated Rb, which is inactive, cannot bind E2F and activates CDK, thereby facilitating entry of cells into the S phase [94]. In multiple myeloma (MM) cells, IL-6

Author's personal copy

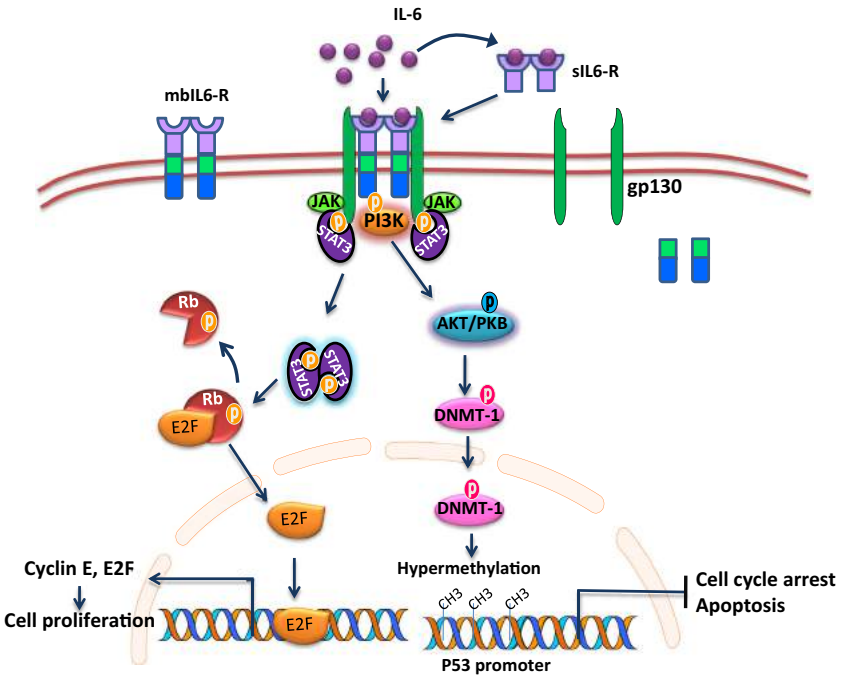

Fig. 3 Role of IL-6 in evading growth suppressors: Normally, E2F remains bound with Rb and localized to the cytosol. IL-6 signalling either induced by mbIL-6R or sIL-6R activates JAK/STAT-3 phosphorylation, which then phosphorylates Rb, resulting in the dissociation of E2F from Rb. The free E2F translocates to the nucleus, where it induces the expression of genes (cyclin E and E2F itself) responsible for the proliferation of cells. Similarly, IL-6 via PI3K/AKT signalling causes the activation of DNMT-1 by its phosphorylation. After phosphorylation, DNMT-1 translocates to the nucleus and hypermethylates the p53 promoter, resulting in silencing of tumour suppressor, pro-apoptotic and other p53 target genes

facilitates the phosphorylation of Rb and, thus, promotes cell growth (Fig. 3). Furthermore, Rb phosphorylation also upregulates IL-6 secretion by MM cells and IL-6-mediated autocrine tumour cell growth [95].

Resistance against cell death

Cancer cells evolve a variety of cytoprotective approaches to limit or circumvent cell death programmes, mainly apoptosis. Besides evading growth suppression signalling, by loss of TP53 function, tumours are also associated with an increase in the expression of anti-apoptotic regulators (Bcl-2, Bcl-xL and Mcl-1) and survival signals (Igf1/2) or downregulated pro-apoptotic factors (Bax, Bim and Puma) [96, 97]. IL-6 regulates the process of apoptosis by activating STAT-3 and NF-kB signalling (Fig. 4), which transactivates the expression of many anti-apoptotic proteins such as Bcl-2, Bcl-xL, Mcl-1, etc., in cholangiocarcinoma cells [98], cervical cancer [99], gastric cancer cells [81], myeloma cells [82], basal cell carcinoma cells [100] and esophageal carcinoma [101]. In addition, these pro-survival proteins, mainly Bcl-2, promote cell proliferation [102]. As the balance between pro-apoptotic and anti-apoptotic proteins is important for apoptotic decision, the ratio of pro-apoptotic to anti-apoptotic factors is increased with oxidative stress, but the increased levels of IL-6 may alter this ratio in favour of anti-apoptotic signalling, leading to cell survival, both in IL-6-treated cells and IL-6-expressing transgenic mice [103]. Besides this, IL-6-induced Bcl-2 regulates Bak interactions with mitofusins via inhibition of Bak dissociation from Mfn2 and also inhibits the interaction of Bak with Mfn1. These two mitochondrial events are the major determinants of cell death pathways as they prevent mitochondrial fragmentation during apoptosis [103, 104]. Therefore, Bcl-2 appears to be an essential mediator of IL-6-induced cytoprotection (Fig. 4).

Besides Bcl-2 and Bcl-xL, IL-6 also supports tumour cell survival by inducing the expression of survivin through direct binding of STAT-3 to the survivin promoter [105]. Furthermore, downregulation of survivin at the gene expression level by inhibiting STAT-3 induces apoptosis in tumour cells [105]. IL-6 triggers PI3K/Akt, NF-kB and MAPK/ERK signalling in prostate cancer cells and results in the upregulation of cyclin A1 expression that promotes tumour cell proliferation in hepatoma, prostate cancer, bladder cancer and in multiple myeloma. IL-6-induced activation of PI3K/Akt signalling further activates IkB kinase (IKK), which initiates NF-kB signalling, leading to transactivation of pro-survival and proliferation-inducing proteins (Fig. 4) [83, 106–109]. IL-6/STAT-3 signalling is also required for the survival of intestinal epithelial cells in colitis-associated cancer, where IL-6 produced from lamina propria myeloid cells protects normal and pre-malignant epithelial cells from cell death [75].

Author's personal copy

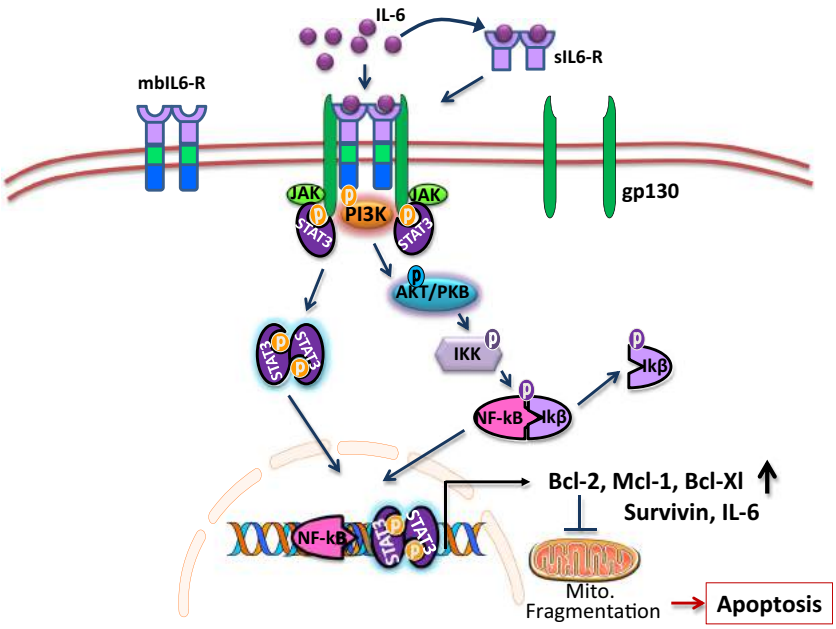

Fig. 4 IL-6 in resisting cell death: IL-6-induced JAK/STAT-3 and NF-kB signalling facilitates the translocation of STAT-3 and NF-kB in the nucleus. Activation of these signalling pathways results in the expression of anti-apoptotic genes (*Bcl-2*, *Bcl-xL*, *Mcl-1*, *survivin*, etc.) and IL-6 for the constitutive activation of IL-6-dependent signalling in cancer cells. IL-6-induced Bcl-2 expression inhibits stress (endogenous and therapeutic)-induced mitochondrial fragmentation and protects the cells from apoptosis

Collectively, it appears that IL-6 facilitates tumour growth primarily by inhibiting apoptosis and enhancing cell proliferation. Besides deriving the growth potential, cancer cells exploit IL-6 for inducing resistance towards anticancer therapy-induced death pathways. For example, IL-6 confers protection from dexamethasone-induced apoptosis by activating PI3K/AKT signalling and inactivating casapase-9, thereby inhibiting apoptosis in multiple myeloma cells [109]. It is also known to induce resistance in cisplatin-mediated cytotoxicity in prostate cancer cell lines and esophageal squamous cell carcinoma [110, 111]. Furthermore, IL-6-induced Bcl-2 confers protection against hyperoxic damage and oxidant (H_2O_2) injury [103]. Thus, enhanced IL-6 levels appear to confer resistance against chemotherapy in cancer by downregulating cell death pathways.

Induction of proliferation/replicative immortality

The potential growth stimulatory effect of IL-6 in tumour cells is due to the activation of several signalling pathways. IL-6 stimulates tumour cell proliferation and survival by activating the Ras/Raf/MEK/MAPK, PI3K/AKT and JAK/STAT pathways via gp130 tyrosine phosphorylation [83, 101, 108]. In colitis-associated cancer, IL-6 produced by myeloid cells stimulates the proliferation of malignant epithelial cells via NF-kB/IL-6/STAT-3 cascade [75]. These signalling pathways help tumours in the acquisition of unlimited replication potential, which is essentially required to generate large tumours.

Majority of the genes that regulate cell survival and proliferation, such as Bcl-2, Bcl-xL, Mcl-1, Fas, cyclin D1, cyclin E1 and p21, are direct targets of STAT-3. In addition, other transcription factors which promote proliferation, including c-Myc, c-Jun and c-Fos, are also targets of STAT-3 [112]. In tumour cells, STAT-3 activation is mediated through autocrine production and paracrine secretion of IL-6 from stroma and infiltrating inflammatory cells [58–62]. IL-6/STAT-3 signalling also functions as a transcriptional repressor of p53 expression, whilst blocking STAT-3 upregulates the expression of p53, leading to p53-mediated apoptosis [113].

IL-6 has also been found to mediate its multi-lineage haematopoietic effects by shifting stem cells from the G0 to the G1 stage of the cell cycle, thereby inducing the proliferation and making stem cells more responsive to additional haematopoietic growth factors such as IL-3, IL-4, G-CSF, M-CSF or GM-CSF [114]. The autocrine production of IL-6 by non-stem cells activates the JAK1/STAT-3 signal transduction pathway which plays an important role in the conversion of non-stem cells into stem-like cells through the upregulation of Oct-4 (a stem cell marker) [115]. Therefore, IL-6 not only induces the proliferation of cancer cells but also maintains the population of cancer stem cells that induce the reoccurrence of tumours. Since only the cancer stem cells have tumorigenic potential amongst the heterogeneous mass of tumours [116], IL-6 seems to play an important role in the maintenance of equilibrium between non-cancer and cancer stem cells, as observed in breast and prostate cancers

Author's personal copy

[44]. Thus, IL-6 has been suggested as a potential regulator of normal and tumour stem cell self-renewal.

Cancer-related inflammation

Accumulating evidences suggest that chronic inflammation predisposes cells and tissues to different forms of cancer [117]. Thus, cancer and inflammation have a strong connection, which prompted the use of anti-inflammatory drugs for cancer prevention. Cancer-related inflammation involves the infiltration of TAMs, white blood cells and inflammatory messengers like cytokines, such as TNF, IL-1 and IL-6, and chemokines (CCL2 and CXCL8), which facilitate tissue remodelling and angiogenesis [118]. IL-6 is one of the most highly expressed mediators of inflammation in the tumour microenvironment, and STAT-3-dependent tumorigenesis has been associated with the local secretion of IL-6 and its related trans-signalling within the tumour microenvironment in inflammation-induced colorectal cancer [75]. In addition, production of IL-6 by M2-type macrophages in ulcerative colitis supports the development of colon tumours [119]. These studies have identified a link between IL-6 and tumour-associated inflammation. The primary players in inflammation include transcription factors such as NF-kB, STAT-3 and primary inflammatory cytokines (IL-1b, IL-6 and TNFα) [1, 120]. NF-kB is the major regulator of inflammation which is deregulated in many cancers [120]. As a major effector molecule of NF-kB activation through the STAT-3 pathway, IL-6 appears to be an important component of the NF-kB/IL-6/STAT-3 cascade involved in tumorigenesis [75]. STAT-3 is required for the maintenance of NF-kB activation in tumours [121], whilst IL-6 promotes carcinogenesis through inflammation and cell proliferation [35, 44, 106]. Since inflammation enhances the growth and progression of gastrointestinal tumours via the activation of IL-6-mediated STAT-3 signalling, it appears that there is a strong link between IL-6, inflammation and tumour promotion [1, 117, 118].

Metabolic remodelling

Enhanced aerobic glycolysis is one of the prominent phenotypes of a majority of cancer cells which facilitate proliferation and confer protection against death, besides energy production [122, 123]. This induced glycolysis is one of the major factors that contribute to IL-6-induced therapeutic resistance in cancer. IL-6-mediated stimulation of glucose metabolism is dependent on the signal transduction involving the PI-3 kinase and JAK/STAT pathways through the enhanced expression of major glycolytic enzymes hexokinase 2 and PFKFB-3 [124]. It also enhances glucose transport by inducing the expression of glucose transporters GLUT-1 and GLUT-4, which further translocate to the plasma membrane, resulting in a higher glucose influx in cells (Fig. 5) [124]. In addition, it also increases fatty acid oxidation (Fig. 5) [85]. Furthermore, IL-6-induced p53 regulates glycolytic metabolism through NF-kB-mediated mechanism, which also increases GLUT-2 and GLUT-4 receptors on the cells to enhance glycolysis [125].

IL-6 also causes 5′ AMP-activated protein kinase (AMPK) phosphorylation, which is important for IL-6-mediated glucose uptake and lipid oxidation (Fig. 5) [126] and is known to be involved in obesity-associated cancers [127]. In sickle cell disease, elevated plasma IL-6 levels are correlated with increased rates of glycolysis in red blood cells, as evidenced by the increase in lactic acid and higher 2,3-bisphosphoglycerate levels [128]. More recently, treatment of IL-6$^{-/-}$ mice with diethylnitrosamine (a carcinogenic agent) after a high-fat diet has been shown not to support faster development of hepatocellular carcinoma (HCC) as compared to a low-fat diet, suggesting that IL-6 preferentially may render obese individuals susceptible to HCC [106]. In cachectic tumour-bearing mice, a high level of IL-6 has been found to suppress mTORC1 activity by AMPK activation, thereby rendering the mice irresponsive to glucose administration [86]. p62 is a scaffold protein that binds to the nutrient-sensing component of mTOR, crucial for metabolic reprogramming during cell transformation. Loss of p62 has been found to reduce mTOR activity, resulting in impaired metabolism and higher IL-6 release, causing tumorigenesis [129].

Maintenance of redox potential

Oxidative stress induced either by therapeutic agents or metabolic alterations induces damage to macromolecules, viz. proteins, lipids, membranes and DNA, that play a key role in the development of cancer. NF-kB is a critical transcription factor that senses redox imbalance and facilitates cytokine gene induction during cellular stress [130]. Endogenous or induced oxidative stress activates transcription factor NF-kB, which regulates the expression of IL-6 by binding to the promoter region of the IL-6 gene [131, 132]. IL-6, which is the major effector molecule of NF-kB, itself causes NF-kB activation in cancer cells, which results in more IL-6 production. Furthermore, this enhanced IL-6 concentration in the tumour microenvironment constitutively activates NF-kB signalling in the same or neighbouring cells (autocrine/paracrine) [131, 133]. Aberrant NF-kB regulation has been observed in many cancers, whose sustained activation requires STAT-3. Since NF-kB and STAT-3 are regulated by IL-6, it appears that the NF-kB/STAT-3/IL-6 signalling cascade plays an important role in oncogenesis [134]. IL-6 is known to protect cardiac myocytes from oxidative stress-induced apoptosis through STAT-3 signalling and gastric cancer cells by upregulating Mcl-1 expression [81]. In multiple myeloma cells, IL-6 causes radio-resistance by activating NF-kB in an autocrine manner, which results in the activation of antioxidant defence system

Author's personal copy

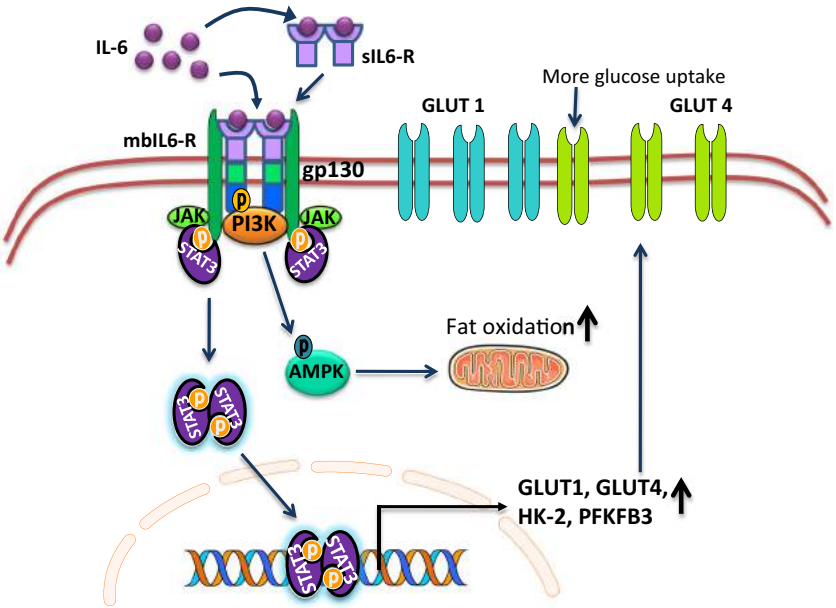

Fig. 5 IL-6 in metabolic remodelling: IL-6-induced JAK/STAT-3 signalling (both classical and trans) induces the expression of major glycolytic enzymes (*HK2* and *PFKB3*) and glucose transporters (*GLUT-1* and *GLUT-4*). The expression of these glycolytic genes ensures aerobic glycolysis in tumour cells. IL-6 also induces fatty acid oxidation in the mitochondria by activating the AMPK pathway

enzymes such as glutathione peroxidase (GPx), superoxide dismutase II (MnSOD) and catalase (Fig. 6) [135].

Apoptosis plays a very crucial role in maintaining genomic integrity by selectively removing the population of heavily damaged cells. Reactive oxygen species (ROS) and pro-inflammatory cytokines are generally elevated following exposure to ionizing radiation and during human carcinogenic processes [136]. Hydrogen peroxide (H_2O_2) is a potent reactive oxygen species that causes mitochondrial dysfunction and cell death. Preconditioning cells with IL-6 decreases H_2O_2-induced cell death by increasing the expression of prohibitin, which is involved in mitochondrial biogenesis and metabolism, apoptosis and replicative senescence [137]. In addition to signalling through STAT-3, the stress-induced activation

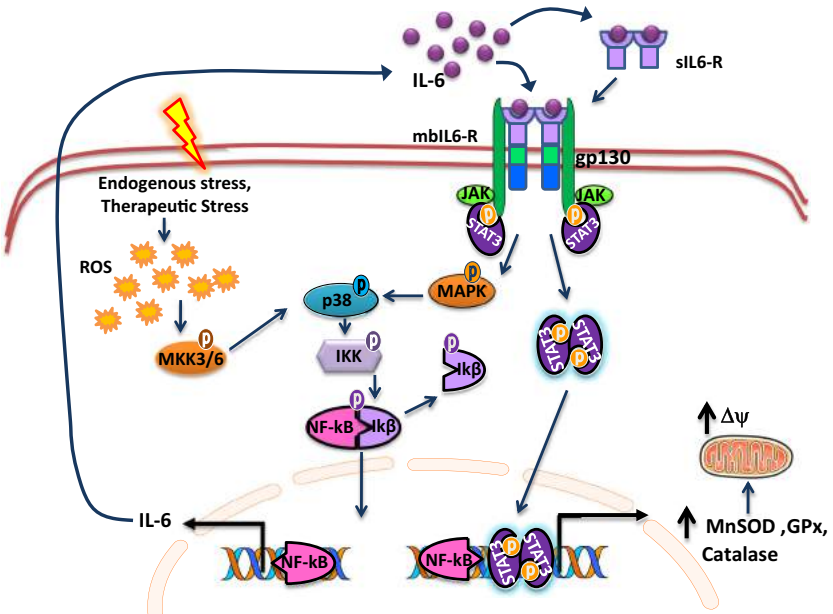

Fig. 6 IL-6 maintains redox balance: p38 senses oxidative stress through ROS-induced phosphorylation of MKK3/6. p38 activation (phosphorylation) induces NF-kB signalling, leading to the enhanced expression and secretion of IL-6 from affected cells. IL-6 (in classical/trans-signalling fashion) further activates JAK/STAT-3 signalling in both paracrine and autocrine manner, resulting in the overexpression of the antioxidant enzymes MnSOD, glutathione peroxidase (*GPx*) and catalase. Altered favourable redox balance also enhances the mitochondrial membrane potential

Author's personal copy

(phosphorylation) of p38 also induces IL-6 release from cells via the activation of NF-kB (Fig. 6) [138]. All these studies showed the antioxidant potential of IL-6.

Invasion, metastasis and angiogenesis

During tumour metastasis, cancer cells invade surrounding local tissues to migrate to distant organs by acquiring a mesenchymal phenotype that allows the metastatic cancer cells to migrate from the site of the primary tumour. Upon lodging into the new organ, tumour cells lodge themselves by switching back to an epithelial phenotype and proliferate to form metastatic tumours. The processes by which cells switch between epithelial and mesenchymal phenotypes are widely known as the epithelial-to-mesenchymal transition (EMT) and its counterpart, the mesenchymal-to-epithelial transition [139]. It is well established that inflammation promotes EMT [139, 140]. Elevated levels of IL-6 in the serum have been associated with EMT and invasion along with increased size of tumours, metastasis and decreased survival of colorectal cancer patients [60]. Available evidences suggest that IL-6 facilitates the metastasis of many tumours (e.g. breast, lung, prostate, renal carcinomas, neuroblastoma, melanoma and multiple myeloma) to the bone [141] by increasing CXCR4 expression via STAT-3 and c-Jun [142]. Furthermore, IL-6-activated STAT-3 plays a role in EMT, invasiveness and angiogenesis in bladder cancer by increasing VEGF, MMP9 and DNMT1 expressions [107]. Autocrine production of IL-6 has also been shown to enhance the capacity to invade the extracellular matrix in breast cancer [143].

Supply of nutrients and oxygen as well as the clearance of metabolic by-products required for tumour sustenance are provided by tumour-associated neovasculature. The formation and maintenance of this neovasculature remains always activated as an 'angiogenic switch' and helps tumour development [144]. STAT-3 activation by IL-6 facilitates angiogenesis in many cancers by inducing the expressions of VEGF, bFGF and MMP9 in tumour-associated endothelial cells, TAMs and MDSCs [60, 84, 143, 145]. In addition, the Notch ligand, JAG-2, has been reported to be overexpressed in malignant plasma cells from MM patients, which induces the secretion of IL-6 and VEGF [146], whilst in breast cancer, Notch-3-dependent ERK activation via IL-6 appears to activate JAG-1 (Notch ligand) and CA-IX (a hypoxia survival gene). Furthermore, this CA-IX upregulated by IL-6 has also been found to maintain the invasive potential of breast cancer cells and mammospheres [143].

DNA damage and repair

DNA is the primary target of majority of the established anticancer therapies which induce cell death processes in tumour cells. DNA damage has been shown to induce the expression and secretion of IL-6 from cancer cells, resulting in the activation of the JAK1/STAT-3 signalling pathway. STAT-3 activation not only protects tumour cells against DNA damage but also facilitates the growth of damaged cells by inhibiting induced senescence [147, 148]. Furthermore, inhibition of the IL-6/STAT-3 signalling pathway by the STAT-3 inhibitors, knockdown of gp130, or the neutralization of IL-6 impairs the growth of tumour cells exposed to DNA damage [147]. IL-6 secreted by tumour-associated endothelial cells in the tumour microenvironment has been suggested to protect lymphoma cells from genotoxic chemotherapy [149], whilst persistent DNA damage response has been shown to induce IL-6 secretion in stromal cells such as fibroblasts [148]. The ATM/NEMO/ELKS complex formed by DNA damage-induced phosphorylation of ATM promotes IKK-mediated IkBα degradation, leading to NF-kB activation, which further induces the expression of IL-6 (Fig. 7) [150]. In the partial hepatectomy (PH) model of DNA repair, wild-type mice were found to express some of the key DNA repair enzymes such as OGG-1, 8-oxo-GTP, Neil-1 and PARP, whereas these enzymes were absent in IL-6 knockout mice, suggesting a direct role of IL-6 in the repair of DNA damage [151]. Thus, in PH, it appears that IL-6 facilitates the restoration of hepatic mass by activating DNA repair enzymes, followed by accurate replication in proliferating hepatic cells [151]. Loss of Rrm2b function (a key enzyme in de novo deoxyribonucleotide synthesis) is known to cause severe numerical and structural chromosomal abnormalities, which leads to the activation of NF-kB through ATM phosphorylation and IKK activation, leading to enhanced IL-6 expression and constitutive activation of STAT-3 [152]. Since IL-6 signalling functions by the activation of transcription factors such as STAT-3 and NF-kB, inhibition of these transactivators or neutralizing the IL-6 may enhance the efficacy of DNA damage-causing chemotherapeutic drugs [153].

IL-6 induces therapeutic resistance in cancer

Accumulating evidences suggest that inflammatory signals from tumour cells and surrounding microenvironment facilitate tumour growth [63, 117]. Furthermore, most anticancer therapies induce inflammation by killing tumour cells and normal tissues [154]. Several inflammatory cytokines are believed to play key roles in therapeutic resistance and lead to tumour regrowth, invasion and angiogenesis. Anticancer therapies induce upregulation of the levels of a variety of inflammatory cytokines, including IL-6, IL-8 and TNFα [8, 12, 13]. Amongst these, IL-6 is known to contribute to poor therapeutic gain, tumour relapse and aggressive tumour growth [2, 8, 12]. IL-6 is also recognised as a key regulator of immunosuppression in patients with advanced cancer [1, 154]. Elevated IL-6 serum levels have been correlated with metastasis and

Author's personal copy

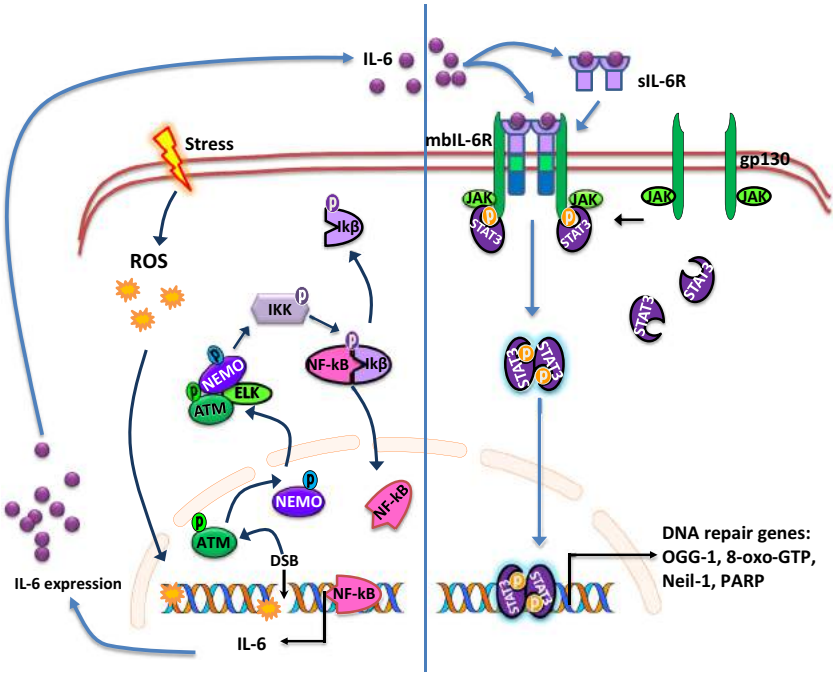

Fig. 7 Role of IL-6 in DNA repair: IL-6 facilitates DNA repair by inducing the expression of DNA repair enzymes in cancer cells. The induction of DNA damage phosphorylates the ATM, leading to the phosphorylation of IKK through the phosphorylation of various downstream kinases. IKK phosphorylation activates NF-kB signalling, resulting in sustained IL-6 expression and constitutive activation of STAT-3 signalling, which induces the expression of DNA repair enzymes

morbidity in prostate cancer and therapeutic resistance in ovarian cancer, whilst patients with reduced levels of IL-6 respond better to therapy [14, 15]. It appears that tumour cells produce IL-6 as a protective mechanism against drug-induced death, as in the case of prostate cancer where inhibition of IL-6 secretion increases the sensitivity of prostate cancer cells to anticancer drugs [12, 110]. Clinical studies on combinations of docetaxel and zolendronic acid in prostate cancer patients with bone metastasis have shown interesting data in relation to IL-6. Patients who responded to therapy had a 35 % decrease in overall serum IL-6 levels, whilst patients who did not respond had a 76 % increase in serum IL-6 levels [155], lending support to the notion that IL-6 confers therapeutic resistance in prostate cancer [5, 12]. The autocrine secretion of IL-6 by breast cancer cells is also shown to confer therapeutic resistance; however, it does not affect their growth. Further studies showed that drug-sensitive breast cancer cells do not express IL-6, whereas multidrug-resistant breast cancer cells produced high levels of IL-6 [156]. IL-6-mediated STAT3 activation has been reported to cause therapeutic resistance in tumours by inducing several pro-survival pathways [12, 105, 110]. However, IL-6-induced drug resistance is associated with increased expression of the multidrug resistance gene, *mdr1*, and upregulation of C/EBPβ and C/EBPδ (CCAAT enhancer-binding protein family of transcription factors) [156]. Moreover, in colorectal cancer, IL-6 secreted from stromal cells induces CYP2E1 and CYP1B1 expression (CYP450 enzymes have a significant role in xenobiotic activation) through the JAK/STAT and PI3K/AKT pathways, which causes tumour initiation and promotion via the activation of chemical carcinogens [157].

IL-6-induced modifications of the stromal cell function appear to be important for tumour growth and angiogenesis as an anti-IL-6 receptor antibody has been found to inhibit tumour angiogenesis and growth by blocking tumour–stroma interaction [60]. Cancer-associated adipocytes can also promote radio-resistance by secreting IL-6 [158], whilst IL-6 and IL-8 secreted by mesenchymal stem cells activate macrophages in the microenvironment of human colorectal and ovarian cancers, causing chemoresistance [159, 160]. Besides causing resistance to chemo- and radiotherapy, autocrine secretion of IL-6 (induced by therapy) also confers resistance to some targeted therapies; for example, aflibercept (anti-VEGF, inhibitor)-resistant epidermoid carcinoma cells and herceptin (trastuzumab, anti-HER2)-resistant breast cancer cells secrete a large amount of IL-6 and show hyperactivation of STAT-3 signalling, causing resistance to therapy [161, 162].

Besides therapeutic resistance, IL-6 also minimizes clinical outcome by promoting the maintenance of a highly therapeutic-resistant cancer stem cell population which is mainly responsible for tumour reoccurrence [116]. IL-6 secreted from either cancer cells or tumour microenvironment (immune cells and tumour stromal cells) not only facilitates tumour growth but also acts as a major obstacle in obtaining

Author's personal copy

therapeutic gain and tumour-free survival [163]. Therefore, targeting IL-6 and its associated signalling may hold greater promise in minimizing therapeutic resistance in cancer. IL-6 inhibition could sensitize tumour cells to anticancer drugs and radiation by increasing DNA damage and cell death, and mitigate tumour regrowth by inhibiting subsequent angiogenesis and reducing cancer stem cell population.

Targeting IL-6 for therapeutic gain

IL-6 plays an important role in tumour progression and therapeutic resistance through inhibition of cancer cell apoptosis and stimulation of tumour-promoting factors such as proliferation, angiogenesis, etc. These effects are mediated by several signalling pathways; however, STAT-3 plays a central and major role [1, 112]. Targeting the IL-6/JAK/STAT-3 pathway has shown promising results in many types of cancer and various inflammation-related diseases. The clinical correlation of increased serum IL-6 concentrations and advanced tumour stages in various malignancies, as discussed earlier in the review, makes a strong case of blocking IL-6 signalling for therapeutic gain. Therefore, inhibiting IL-6 signalling or minimizing the level of IL-6 can be a potential therapeutic strategy for those cancers which are characterized by overproduction of IL-6. IL-6 signalling can be targeted in multiple ways, such as the use of specific monoclonal antibodies against IL-6 or IL-6R [15, 19, 31], by using synthetic/semi-synthetic compounds as specific inhibitors of IL-6 downstream signalling molecules or by kinase inhibitors (like JAK inhibitor) [164]. All these approaches evaluated in experimental models and reached clinical trials are summarized in Table 1.

Table 1 Multiple therapeutic approaches for targeting IL-6, IL-6R and IL-6-associated signalling

S. no.	Target molecule	Type of cancer	Therapeutic approach	References
1	IL-6	Prostate cancer	IL-6 siRNA	[12]
			Siltuximab (CNTO328)—anti-IL-6 antibody	[165]
		Colorectal cancer	Siltuximab (CNTO328)	[3, 166]
		Ovarian cancer	Siltuximab (CNTO328)	[166]
			Lysophosphatidic acid	[167]
		Renal cancer	Siltuximab (CNTO328)	[166]
		Lung cancer	Siltuximab (CNTO328)	[166, 168]
		Multiple myeloma	Siltuximab (CNTO328)	[166, 169]
		Lymphoma	BE-8 (monoclonal antibody)	[170]
		Prostate cancer	Siltuximab, zoledronic acid	[15, 171]
		Breast cancer	Siltuximab, zoledronic acid, PMA (medroxyprogesterone acetate)	[15, 172, 173]
2	IL-6R	Colon cancer	MR16-1, tocilizumab (anti-IL-6R antibody)	[3, 60]
		Oral squamous cell carcinoma	Tocilizumab	[174]
		Lung cancer	Tocilizumab	[175]
		Multiple myeloma	Tocilizumab	[176, 177]
		Ovarian cancer	Tocilizumab	[178]
		Breast cancer	Tocilizumab	[179]
3	JAKs	Lung cancer	TG101209 (JAK inhibitor)	[180]
		Multiple myeloma	TG101209	[181]
		Ovarian cancer	AG490	[182]
		Acute myeloid leukaemia	Ruxolitinib (JAK1/JAK2 inhibitor)	[183]
		Colitis-associated cancer	CEP-33779 (JAK inhibitor)	[184]
		Acute myeloid leukaemia	SB1518 (JAK2)	[185]
4	STAT-3	Glioblastoma	Sorafenib (multiple kinase inhibitor)	[186]
		Breast cancer	SD-1029	[187]
		Ovarian cancer	SD-1029	[187]
		Lymphoma	JSI-124	[188]
		Glioblastoma	JSI-124	[189]
		Breast cancer	JSI-124	[190]
		Hepatocellular carcinoma	Sorafenib (Nexavar)	[191]
		Breast cancer	Sorafenib	[192]
		Advanced renal cell carcinoma	Sorafenib	[193]
		Colorectal cancer	Sorafenib	[194]

Author's personal copy

Antibodies targeting IL-6 or IL-6 signalling have been extensively investigated in experimental tumour models and clinical trials for a variety of cancers. Elsilimomab (BE-8), a murine monoclonal antibody, and siltuximab (CNTO 328), a chimeric antibody with strong affinity to IL-6 and licenced for the treatment of Castleman's disease, are used for the treatment of prostate cancer, ovarian cancer, renal cell carcinoma and colorectal cancer in combination with other chemotherapeutics [3, 6, 166]. In prostate cancer, siltuximab has been shown to downregulate the genes downstream of IL-6 signalling along with decreased STAT-3 expression [165]. Tocilizumab, a FDA-approved drug for rheumatoid arthritis and Crohn's disease, is the humanized antibody specific for IL-6R that recognises both soluble and membrane-bound receptors and blocks its signalling [195]. BE-8, a murine anti-IL-6 monoclonal antibody, has also been used in the treatment of lymphoma and multiple myeloma [196]. Sequestering the enhanced IL-6 showed a significant increase in the therapeutic efficacy of paclitaxel in mouse models of epithelial ovarian cancer by reducing tumour angiogenesis [197]. Tocilizumab has also been used in the treatment of oral cell carcinoma, prostate cancer, renal cancer, multiple myeloma and breast cancer [15]. It inhibits the growth of prostate and breast cancer cells by reducing STAT-3-induced VEGF expression. In addition, it reduces bone metastasis of breast cancer cells [142]. Tocilizumab has been shown to improve cachexia developed by IL-6 overexpression in lung cancer patients [175]. The combination of anti-IL-6R with herceptin and aflibercept enhances therapeutic gain, also in targeted therapy-resistant breast cancer and epidermoid carcinoma, respectively [161, 162]. However, blocking IL-6 signalling can be harmful and may result in some adverse effects, such as gastrointestinal, nasopharyngeal and upper respiratory tract infections, gastrointestinal haemorrhage, thrombocytopenia and neutropenia [198]. Therefore, selective blocking of trans-signalling (the major pathway involved in inflammation and related diseases like cancer) using sgp130Fc (a recombinant fusion protein of soluble gp130 and human IgG_1 Fc) may be useful in achieving therapeutic gain in cancer [76].

Besides antibodies, a number of other compounds are currently available that inhibit IL-6 signalling. Zoledronic acid (ZA) is the most potent nitrogen-containing bisphosphonate compound which has been used in adjuvant therapies to inhibit bone metastasis caused by multiple cancers [172]. It inhibits growth, besides inducing apoptosis by reducing IL-6 secretion in prostate cancer cell lines, which is suggestive of its use in the treatment of prostate cancer either alone or in combination with chemotherapy [171]. Radiation activates IL-6/STAT-3 signalling, which stimulates tumour invasion and EMT changes and promotes the survival of tumour cells after therapy, thereby conferring resistance to therapy [12, 84, 156]. However, use of siRNA against IL-6 inhibits tumour regrowth after radiotherapy in prostate cancer and sensitizes tumour cells to radiation by increasing cell death and DNA damage [12]. Its inhibition also mitigates tumour regrowth by eliminating radiotherapy-triggered MDSC and subsequent angiogenesis after radiation exposure [199]. Therefore, inhibition of IL-6 could be a potential therapeutic strategy for increasing the radiation response of tumours. Similarly, medroxyprogesterone acetate (MPA) is a synthetic compound used as an endocrine therapeutic agent for patients with breast cancer which is known to reduce serum IL-6 levels [173]. Several studies have shown that the use of an inhibitor for downstream targets of IL-6 signalling can also be a good approach for enhancing therapeutic gain. For example, the use of JAK inhibitor (TG101209) enhances the efficacy of radiotherapy in lung cancer [180]. Similarly, WP1066 and CEP3379, other JAK2 inhibitors, suppress the growth of gastric cancer and colorectal tumours by inhibiting IL-6/JAK2/STAT-3 signalling [184, 200]. Sorafenib, which is a multiple kinase inhibitor, causes dephosphorylation of STAT-3 and prevents AKT signalling in glioblastoma cells and prostate cancer, respectively [186]. AG490, a potent JAK inhibitor, targets STAT-3 signalling, reduces the invasion of human pancreatic cancer cells in vitro and induces apoptosis in gastric cancer cells [201, 202]. Moreover, AG490 is also effective in murine ovarian cancer, where it induces the expression of anti-tumour cytokines [182]. Another JAK inhibitor, ruxolitinib, is currently in clinical trials for leukaemia [183].

Inhibition of STAT-3 phosphorylation by the use of STAT-3 inhibitors can also be a good approach to block IL-6 signalling. JSI-124 (STAT-3 inhibitor) inhibits STAT-3 phosphorylation at serine 727 and sensitizes B-leukaemia cells to apoptosis [203]. JSI-124 suppresses breast cancer cell growth by downregulating STAT-3 activation in tumour-associated B cells. Stattic and Eriocalyxin B (a diterpenoid) also inhibit STAT-3 phosphorylation and induce apoptosis in MDA-MB-231 and HepG2 cells [204, 205]. Besides inhibiting STAT-3 phosphorylation and transcriptional activation, Decoy oligodeoxynucleotides target the DNA-binding domain of STAT-3 by competing against endogenous DNA *cis* element, which results in reduced cell growth and increased apoptosis [206]. G-quartet oligodeoxynucleotides can also be used as a STAT-3 inhibitor which suppresses the growth of prostate, breast, and head and neck cancers in nude mice [206, 207]. Instead of inhibiting STAT-3 phosphorylation, these oligodeoxynucleotides inhibit the binding of STAT-3 dimer on DNA. Moreover, small-molecule inhibitors can also be used to inhibit STAT-3. A small-molecule non-peptide STAT-3 inhibitor named S3I-201 (a.k.a. NSC74859) selectively inhibits STAT-3 DNA-binding activity in vitro and blocks the formation of STAT-3:STAT-3 dimer, which leads to the inhibition of STAT-3-dependent gene transcription and the blockade of the proliferation and survival of human breast carcinoma cells [208]. STA-21 also selectively inhibits STAT-3 DNA-binding activity in vitro, disrupts STAT-3:STAT-3

Author's personal copy

dimerization and suppresses STAT-3-mediated gene transcription along with cell growth inhibition and apoptosis through the caspase pathway in a human breast carcinoma and rhabdomyosarcoma model [209, 210]. Catechol-containing compounds, IS3 295, galiellalactone and peptide aptamers have been found to inhibit the DNA-binding ability of STAT-3 and further signalling [208, 211].

Conclusion

IL-6, which is produced by tumours and many other cells in the tumour microenvironment, facilitates tumour growth and sustenance by influencing and regulating nearly all hallmarks of cancer, besides contributing to therapeutic resistance. Recent studies have enhanced our knowledge regarding the potential role of IL-6 in the cross talk between tumour and its microenvironment. IL-6/JAK/STAT-3 appears to be the primary pathway through which IL-6 regulates majority of the tumour-promoting functions. Therefore, neutralizing IL-6 or the IL-6 receptor to prevent the initiation of signalling or inhibiting the activity of two other members, JAK and STAT-3, to prevent the execution in the end has established therapeutic efficacy in cellular and systemic models of cancer. Blocking IL-6 using monoclonal antibodies against either IL-6 or IL-6R has shown promising results in preclinical studies and clinical trials. Phase I and II clinical trials have established the efficacy of monoclonal antibodies either as a single agent or in combination with other chemotherapeutic drugs, radiation and targeted therapies in various types of cancer. Subsequently, certain synthetic molecules, such as ZA, MPA, polyphenols, etc., have also shown promising results in various cancers by regulating IL-6 levels. The use of small-molecule inhibitors of JAK and STAT-3 alone or in combination with radiation or anticancer agents has also resulted in promising anti-tumour effects in various cancers. However, undesirable effects (such as infections, gastrointestinal haemorrhage, thrombocytopenia and neutropenia) of anti-IL-6 therapy have also been reported in patients with various inflammatory diseases. Therefore, selective inhibition of IL-6 trans-signalling using molecules such as sgp130Fc in the future may result in better therapeutic gain without the side effects associated with anti-IL-6 therapy currently under evaluation.

Acknowledgments NK thanks the Defence Research and Development Organization, Government of India, for fellowship support. We acknowledge Director INMAS for constant support and encouragement.

References

1. Bromberg J, Wang TC. Inflammation and cancer: IL-6 and STAT3 complete the link. Cancer Cell. 2009;15:79–80.
2. Grivennikov S, Karin M. Autocrine IL-6 signaling: a key event in tumorigenesis? Cancer Cell. 2008;13:7–9.
3. Waldner MJ, Foersch S, Neurath MF. Interleukin-6—a key regulator of colorectal cancer development. Int J Biol Sci. 2012;8(9):1248–53.
4. Dethlefsen C, Højfeldt G, Hojman P. The role of intratumoral and systemic IL-6 in breast cancer. Breast Cancer Res Treat. 2013;138(3):657–64.
5. Culig Z, Puhr M. Interleukin-6: a multifunctional targetable cytokine in human prostate cancer. Mol Cell Endocrinol. 2012;360(1–2):52–8.
6. Macciò A, Madeddu C. The role of interleukin-6 in the evolution of ovarian cancer: clinical and prognostic implications—a review. J Mol Med. 2013;91:1355–68.
7. Miura T, Mitsunaga S, Ikeda M, Shimizu S, Ohno I, Takahashi H, et al. Characterization of patients with advanced pancreatic cancer and high serum interleukin-6 levels. Pancreas. 2015;44(5):756–63.
8. Chang CH, Hsiao CF, Yeh YM, Chang GC, Tsai YH, Chen YM, et al. Circulating interleukin-6 level is a prognostic marker for survival in advanced nonsmall cell lung cancer patients treated with chemotherapy. Int J Cancer. 2013;132(9):1977–85.
9. Altundag O, Altundag K, Gunduz E. Interleukin-6 and C-reactive protein in metastatic renal cell carcinoma. J Clin Oncol. 2005;23:1044.
10. Wei LH, Kuo ML, Chen CA, Chou CH, Lai KB, Lee CN, et al. Interleukin-6 promotes cervical tumor growth by VEGF-dependent angiogenesis via a STAT3 pathway. Oncogene. 2003;22:1517–27.
11. Singh U, Shevra CR, Singh S, Singh N, Kumar S, Rai M. Interleukin-6 and interleukin-4 levels in multiple myeloma and correlation of interleukin-6 with β2 microglobulin and serum creatinine. Clin Cancer Investig J. 2015;4:211–5.
12. Wu CT, Chen MF, Chen WC, Hsieh CC. The role of IL-6 in the radiation response of prostate cancer. Radiat Oncol. 2013;8:159.
13. Chen MF, Chen PT, Lu MS, Lin PY, Chen WC, Lee KD. IL-6 expression predicts treatment response and outcome in squamous cell carcinoma of the esophagus. Mol Cancer. 2013;12:26.
14. Shibayama O, Yoshiuchi K, Inagaki M, Matsuoka Y, Yoshikawa E, Sugawara Y, et al. Association between adjuvant regional radiotherapy and cognitive function in breast cancer patients treated with conservation therapy. Cancer Med. 2014;3(3):702–9.
15. Guo Y, Xu F, Lu T, Duan Z, Zhang Z. Interleukin-6 signaling pathway in targeted therapy for cancer. Cancer Treat Rev. 2012;38(7):904–10.
16. Veuger SJ, Hunter JE, Durkacz BW. Ionizing radiation-induced NF-kappaB activation requires PARP-1 function to confer radioresistance. Oncogene. 2009;28:832–42.
17. Kozakai N, Kikuchi E, Hasegawa M, Suzuki E, Ide H, Miyajima A, et al. Enhancement of radiosensitivity by a unique novel NF-kB inhibitor, DHMEQ, in prostate cancer. Br J Cancer. 2012;107:652–7.
18. Naugler WE, Karin M. NF-kappaB and cancer-identifying targets and mechanisms. Curr Opin Genet Dev. 2008;18(1):19–26.
19. Wolf J, Rose-John S, Garbers C. Interleukin-6 and its receptors: a highly regulated and dynamic system. Cytokine. 2014;70(1):11–20.
20. Yoon S, Woo SU, Kang JH, Kim K, Shin HJ, Gwak HS, et al. NF-kB and STAT3 cooperatively induce IL6 in starved cancer cells. Oncogene. 2012;31(29):3467–81.

Author's personal copy

21. Scheller J, Chalaris A, Schmidt-Arras D, Rose-John S. The pro- and anti-inflammatory properties of the cytokine interleukin-6. Biochim Biophys Acta. 2011;1813(5):878–88.
22. Hirano T, Taga T, Nakano N, Yasukawa K, Kashiwamura S, Shimizu K, et al. Purification to homogeneity and characterization of human B-cell differentiation factor (BCDF or BSFp-2). Proc Natl Acad Sci U S A. 1985;82(16):5490–4.
23. Kishimoto T, Akira S, Narazaki M, Taga T. Interleukin-6 family of cytokines and gp130. Blood. 1995;86:1243–54.
24. Mihara M, Hashizume M, Yoshida H, Suzuki M, Shiina M. IL-6/IL-6 receptor system and its role in physiological and pathological conditions. Clin Sci (Lond). 2012;122(4):143–59.
25. Wunderlich FT, Ströhle P, Könner AC, Gruber S, Tovar S, Brönneke HS, et al. Interleukin-6 signaling in liver-parenchymal cells suppresses hepatic inflammation and improves systemic insulin action. Cell Metab. 2010;12(3):237–49.
26. Taga T, Kishimoto T. Gp130 and the interleukin-6 family of cytokines. Annu Rev Immunol. 1997;15:797–819.
27. Hibi M, Murakami M, Saito M, Hirano T, Taga T, Kishimoto T. Molecular cloning and expression of an IL-6 signal transducer, gp130. Cell. 1990;63:1149–57.
28. Yawata H, Yasukawa K, Natsuka S, Murakami M, Yamasaki K, Hibi M, et al. Structure–function analysis of human IL-6 receptor: dissociation of amino acid residues required for IL-6-binding and for IL-6 signal transduction through gp130. EMBO J. 1993;12(4):1705–12.
29. Jones SA, Horiuchi S, Topley N, Yamamoto N, Fuller GM. The soluble interleukin 6 receptor: mechanisms of production and implications in disease. FASEB J. 2001;15(1):43–58.
30. Yoshida K, Taga T, Saito M, Suematsu S, Kumanogoh A, Tanaka T, et al. Targeted disruption of gp130, a common signal transducer for the interleukin 6 family of cytokines, leads to myocardial and hematological disorders. Proc Natl Acad Sci U S A. 1996;93(1):407–11.
31. Jones SA, Scheller J, Rose-John S. Therapeutic strategies for the clinical blockade of IL-6/gp130 signaling. J Clin Invest. 2011;121:3375–83.
32. Chalaris A, Garbers C, Rabe B, Rose-John S, Scheller J. The soluble interleukin 6 receptor: generation and role in inflammation and cancer. Eur J Cell Biol. 2011;90(6–7):484–94.
33. Islam O, Gong X, Rose-John S, Heese K. Interleukin-6 and neural stem cells: more than gliogenesis. Mol Biol Cell. 2009;20(1):188–99.
34. Peters M, Solem F, Goldschmidt J, Schirmacher P, Rose-John S. Interleukin-6 and the soluble interleukin-6 receptor induce stem cell factor and Flt-3L expression in vivo and in vitro. Exp Hematol. 2001;29(2):146–55.
35. Yeoh GC, Ernst M, Rose-John S, Akhurst B, Payne C, Long S, et al. Opposing roles of gp130-mediated STAT-3 and ERK-1/2 signaling in liver progenitor cell migration and proliferation. Hepatology. 2007;45(2):486–94.
36. Humphrey RK, Beattie GM, Lopez AD, Bucay N, King CC, Firpo MT, et al. Maintenance of pluripotency in human embryonic stem cells is STAT3 independent. Stem Cells. 2004;22(4):522–30.
37. Rose-John S. IL-6 trans-signaling via the soluble IL-6 receptor: importance for the pro-inflammatory activities of IL-6. Int J Biol Sci. 2012;8(9):1237–47.
38. McFarland-Mancini MM, Funk HM, Paluch AM, Zhou M, Giridhar PV, Mercer CA, et al. Differences in wound healing in mice with deficiency of IL-6 versus IL-6 receptor. J Immunol. 2010;184(12):7219–28.
39. Kovacs E. Investigation of interleukin-6 (IL-6), soluble IL-6 receptor (sIL-6R) and soluble gp130 (sgp130) in sera of cancer patients. Biomed Pharmacother. 2001;55(7):391–6.
40. Jostock T, Müllberg J, Ozbek S, Atreya R, Blinn G, Voltz N, et al. Soluble gp130 is the natural inhibitor of soluble interleukin-6 receptor transsignaling responses. Eur J Biochem. 2001;268(1):160–7.
41. Akira S, Kishimoto T. IL-6 and NF-IL6 in acute-phase response and viral infection. Immunol Rev. 1992;127:25–50.
42. Yang R, Lin Q, Gao HB, Zhang P. Stress-related hormone norepinephrine induces interleukin-6 expression in GES-1 cells. Braz J Med Biol Res. 2014;47(2):101–9.
43. Zhao W, Liu M, Kirkwood KL. p38alpha stabilizes interleukin-6 mRNA via multiple AU-rich elements. J Biol Chem. 2008;283(4):1778–85.
44. Iliopoulos D, Hirsch HA, Struhl K. An epigenetic switch involving NF-kappaB, Lin28, Let-7 microRNA, and IL6 links inflammation to cell transformation. Cell. 2009;139(4):693–706.
45. Narbutt J, Lukamowicz J, Bogaczewicz J, Sysa-Jedrzejowska A, Torzecka JD, Lesiak A. Serum concentration of interleukin-6 is increased both in active and remission stages of pemphigus vulgaris. Mediat Inflamm. 2008;2008:875394.
46. D'Auria L, Bonifati C, Mussi A, D'Agosto G, De Simone C, Giacalone B, et al. Cytokines in the sera of patients with pemphigus vulgaris: interleukin-6 and tumour necrosis factor-alpha levels are significantly increased as compared with healthy subjects and correlate with disease activity. Eur Cytokine Netw. 1997;8(4):383–7.
47. Devaraj S, Venugopal SK, Singh U, Jialal I. Hyperglycemia induces monocytic release of interleukin-6 via induction of protein kinase c-{alpha} and -{beta}. Diabetes. 2005;54(1):85–91.
48. Blackburn P, Després JP, Lamarche B, Tremblay A, Bergeron J, Lemieux I, et al. Postprandial variations of plasma inflammatory markers in abdominally obese men. Obesity (Silver Spring). 2006;14(10):1747–54.
49. Angstwurm MW, Gartner R, Ziegler-Heitbrock HW. Cyclic plasma IL-6 levels during normal menstrual cycle. Cytokine. 1997;9:370–4.
50. Reihmane D, Dela F. Interleukin-6: possible biological roles during exercise. Eur J Sport Sci. 2014;14(3):242–50.
51. Sakamoto K, Arakawa H, Mita S, Ishiko T, Ikei S, Egami H, et al. Elevation of circulating interleukin 6 after surgery: factors influencing the serum level. Cytokine. 1994;6:181–6.
52. Keski-Nisula L, Hirvonen MR, Roponen M, Heinonen S, Pekkanen J. Spontaneous and stimulated interleukin-6 and tumor necrosis factor-alpha production at delivery and three months after birth. Eur Cytokine Netw. 2004;15:67–72.
53. Naffaa M, Makhoul BF, Tobia A, Kaplan M, Aronson D, Saliba W, et al. Interleukin-6 at discharge predicts all-cause mortality in patients with sepsis. Am J Emerg Med. 2013;31(9):1361–4.
54. Muñoz-Cánoves P, Scheele C, Pedersen BK, Serrano AL. Interleukin-6 myokine signaling in skeletal muscle: a double-edged sword? FEBS. 2013;280(17):4131–48.
55. Steensberg A, Febbraio MA, Osada T, Schjerling P, van Hall G, Saltin B, et al. Interleukin-6 production in contracting human skeletal muscle is influenced by pre-exercise muscle glycogen content. J Physiol. 2001;537:633–9.
56. Bastard JP, Maachi M, Van Nhieu JT, Jardel C, Bruckert E, Grimaldi A, et al. Adipose tissue IL-6 content correlates with resistance to insulin activation of glucose uptake both in vivo and in vitro. J Clin Endocrinol Metab. 2002;87(5):2084–9.
57. Krishnamoorthy N, Oriss T, Pagila M, Ray A, Ray P. A critical role for IL-6 secretion by dendritic cells promoting Th2 and limiting Th1 response. J Immunol. 2007;178:S181.
58. Mitchem JB, Brennan DJ, Knolhoff BL, Belt BA, Zhu Y, Sanford DE, et al. Targeting tumor-infiltrating macrophages decreases tumor-initiating cells, relieves immunosuppression, and improves chemotherapeutic responses. Cancer Res. 2013;73(3):1128–4.
59. Bode JG, Nimmesgern A, Schmitz J, Schaper F, Schmitt M, Frisch W, et al. LPS and TNFalpha induce SOCS3 mRNA and inhibit IL-

Author's personal copy

6-induced activation of STAT3 in macrophages. FEBS Lett. 1999;463:365–70.
60. Nagasaki T, Hara M, Nakanishi H, Takahashi H, Sato M, Takeyama H. Interleukin-6 released by colon cancer-associated fibroblasts is critical for tumour angiogenesis: anti-interleukin-6 receptor antibody suppressed angiogenesis and inhibited tumour–stroma interaction. Br J Cancer. 2014;110(2):469–78.
61. Nolen BM, Marks JR, Ta'san S, Rand A, Luong TM, Wang Y, et al. Serum biomarker profiles and response to neoadjuvant chemotherapy for locally advanced breast cancer. Breast Cancer Res. 2008;10(3):R45.
62. Oh K, Lee OY, Shon SY, Nam O, Ryu PM, Seo MW, et al. A mutual activation loop between breast cancer cells and myeloid-derived suppressor cells facilitates spontaneous metastasis through IL-6 trans-signaling in a murine model. Breast Cancer Res. 2013;15(5):R79.
63. Fisher DT, Appenheimer MM, Evans SS. The two faces of IL-6 in the tumor microenvironment. Semin Immunol. 2014;26(1):38–47.
64. Lederle W, Depner S, Schnur S, Obermueller E, Catone N, Just A, et al. IL-6 promotes malignant growth of skin SCCs by regulating a network of autocrine and paracrine cytokines. Int J Cancer. 2011;128(12):2803–14.
65. Gruys E, Toussaint MJM, Niewold TA, Koopmans SJ. Acute phase reaction and acute phase proteins. J Zhejiang Univ Sci B. 2005;6(11):1045–56.
66. Tilg H, Trehu E, Atkins MB, Dinarello CA, Mier JW. Interleukin-6 (IL-6) as an anti-inflammatory cytokine: induction of circulating IL-1 receptor antagonist and soluble tumor necrosis factor receptor p55. Blood. 1994;83(1):113–8.
67. Aderka D, Le JM, Vilcek J. IL-6 inhibits lipopolysaccharide induced tumor necrosis factor production in cultured human monocytes, U937 cells and in mice. J Immunol. 1989;143:3517–23.
68. Xing Z, Gauldie J, Cox G, Baumann H, Jordana M, Lei XF, et al. IL-6 is an antiinflammatory cytokine required for controlling local or systemic acute inflammatory responses. J Clin Invest. 1998;101(2):311–20.
69. Croker BA, Krebs DL, Zhang JG, Wormald S, Willson TA, Stanley EG, et al. SOCS3 negatively regulates IL-6 signaling in vivo. Nat Immunol. 2003;4:540–5.
70. Radtke S, Wüller S, Yang XP, Lippok BE, Mütze B, Mais C, et al. Cross-regulation of cytokine signalling: pro-inflammatory cytokines restrict IL-6 signalling through receptor internalisation and degradation. J Cell Sci. 2010;123(6):947–59.
71. Ahmed ST, Mayer A, Ji JD, Ivashkiv LB. Inhibition of IL-6 signaling by a p38-dependent pathway occurs in the absence of new protein synthesis. J Leukoc Biol. 2002;72:154–62.
72. McLoughlin RM, Jenkins BJ, Grail D, Williams AS, Fielding CA, Parker CR, et al. IL-6 trans-signaling via STAT3 directs T cell infiltration in acute inflammation. Proc Natl Acad Sci U S A. 2005;102(27):9589–94.
73. Curnow SJ, Scheel-Toellner D, Jenkinson W, Raza K, Durrani OM, Faint JM, et al. Inhibition of T cell apoptosis in the aqueous humor of patients with uveitis by IL-6/soluble IL-6 receptor trans-signaling. J Immunol. 2004;173(8):5290–7.
74. Atreya R, Mudter J, Finotto S, Müllberg J, Jostock T, Wirtz S, et al. Blockade of IL-6 transsignaling abrogates established experimental colitis in mice by suppression of the antiapoptotic resistance of lamina propria T cells. Nat Med. 2000;6(5):583–8.
75. Grivennikov S, Karin E, Terzic J, Mucida D, Yu G-Y, Vallabhapurapu S, et al. IL-6 and STAT3 signaling is required for survival of intestinal epithelial cells and colitis associated cancer. Cancer Cell. 2009;16:103–13.
76. Barkhausen T, Tschernig T, Rosenstiel P, van Griensven M, Vonberg RP, Dorsch M, et al. Selective blockade of interleukin-6 trans-signaling improves survival in a murine polymicrobial sepsis model. Crit Care Med. 2011;39(6):1407–13.
77. Grivennikov SI, Karin M. Inflammatory cytokines in cancer: tumour necrosis factor and interleukin 6 take the stage. Ann Rheum Dis. 2011;70 Suppl 1:i104–8.
78. Cozen W, Gill PS, Ingles SA, Masood R, Martinez-Maza O, Cockburn MG, et al. IL-6 levels and genotype are associated with risk of young adult Hodgkin lymphoma. Blood. 2004;103:3216–21.
79. Naugler WE, Sakurai T, Kim S, Maeda S, Kim K, Elsharkawy AM, et al. Gender disparity in liver cancer due to sex differences in MyD88-dependent IL-6 production. Science. 2007;317(5834):121–4.
80. Wei Q, Guo P, Mu K, Zhang Y, Zhao W, Huai W, et al. Estrogen suppresses hepatocellular carcinoma cells through ERβ-mediated upregulation of the NLRP3 inflammasome. Lab Investig. 2015;95(7):804–16.
81. Lin MT, Juan CY, Chang KJ, Chen WJ, Kuo ML. IL-6 inhibits apoptosis and retains oxidative DNA lesions in human gastric cancer AGS cells through up-regulation of anti-apoptotic gene mcl-1. Carcinogenesis. 2001;22(12):1947–53.
82. Jourdan M, Veyrune JL, Vos JD, Redal N, Couderc G, Klein B. A major role for Mcl-1 antiapoptotic protein in the IL-6-induced survival of human myeloma cells. Oncogene. 2003;22(19):2950–9.
83. Wegiel B, Bjartell A, Culig Z, Persson JL. Interleukin-6 activates PI3K/Akt pathway and regulates cyclin A1 to promote prostate cancer cell survival. Int J Cancer. 2008;122(7):1521–9.
84. Zou M, Zhang X, Xu C. IL6-induced metastasis modulators p-STAT3, MMP-2 and MMP-9 are targets of 3,3′-diindolylmethane in ovarian cancer cells. Cell Oncol (Dordr). 2015;39:47–57.
85. Mauer J, Denson JL, Brüning JC. Versatile functions for IL-6 in metabolism and cancer. Trends Immunol. 2015;36(2):92–101.
86. White JP, Puppa MJ, Gao S, Sato S, Welle SL, Carson JA. Muscle mTORC1 suppression by IL-6 during cancer cachexia: a role for AMPK. Am J Physiol Endocrinol Metab. 2013;304(10):E1042–52.
87. Hanahan D, Weinberg RA. Hallmarks of cancer: the next generation. Cell. 2011;144(5):646–74.
88. Herman JG. Hypermethylation of tumor suppressor genes in cancer. Semin Cancer Biol. 1999;9:359–67.
89. Hodge DR, Peng B, Cherry JC, Hurt EM, Fox SD, Kelley JA, et al. Interleukin 6 supports the maintenance of p53 tumor suppressor gene promoter methylation. Cancer Res. 2005;65(11):4673–82.
90. Liu CC, Lin JH, Hsu TW, Su K, Li AF, Hsu HS, et al. IL-6 enriched lung cancer stem-like cell population by inhibition of cell cycle regulators via DNMT1 upregulation. Int J Cancer. 2015;136(3):547–59.
91. Hodge DR, Cho E, Copeland TD, Guszczynski T, Yang E, Seth AK, et al. IL-6 enhances the nuclear translocation of DNA cytosine-5-methyltransferase 1 (DNMT1) via phosphorylation of the nuclear localization sequence by the AKT kinase. Cancer Genomics Proteomics. 2007;4(6):387–98.
92. Gasche JA, Hoffmann J, Boland CR, Goel A. Interleukin-6 promotes tumorigenesis by altering DNA methylation in oral cancer cells. Int J Cancer. 2011;129(5):1053–63.
93. Nevins JR. The Rb/E2F pathway and cancer. Hum Mol Genet. 2001;10(7):699–703.
94. Giacinti C, Giordano A. RB and cell cycle progression. Oncogene. 2006;25(38):5220–7.
95. Urashima M, Ogata A, Chauhan D, Vidriales MB, Teoh G, Hoshi Y, et al. Interleukin-6 promotes multiple myeloma cell growth via phosphorylation of retinoblastoma protein. Blood. 1996;88(6):2219–27.
96. Zhuang L, Lee CS, Scolyer RA, McCarthy SW, Zhang XD, Thompson JF, et al. Mcl-1, Bcl-XL and Stat3 expression are associated with progression of melanoma whereas Bcl-2, AP-2 and

Author's personal copy

MITF levels decrease during progression of melanoma. Mod Pathol. 2007;20(4):416–26.
97. Borhani N, Manoochehri M, Saleh-Gargari S, Ghaffari Novin M, Mansouri A, Omrani MD. Decreased expression of proapoptotic genes caspase-8- and BCL2-associated agonist of cell death (BAD) in ovarian cancer. Clin Ovarian Other Gynecol Cancer. 2014;7:8–23.
98. Isomoto H, Kobayashi S, Werneburg NW, Bronk SF, Guicciardi ME, Frank DA, et al. Interleukin 6 upregulates myeloid cell leukemia-1 expression through a STAT3 pathway in cholangiocarcinoma cells. Hepatology. 2005;42:1329–38.
99. Wei LH, Kuo ML, Chen CA, Chou CH, Cheng WF, Chang MC, et al. The anti-apoptotic role of interleukin-6 in human cervical cancer is mediated by up-regulation of Mcl-1 through a PI 3-K/Akt pathway. Oncogene. 2001;20(41):5799–809.
100. Jee SH, Chiu HC, Tsai TF, Tsai WL, Liao YH, Chu CY, et al. The phosphotidyl inositol 3-kinase/Akt signal pathway is involved in interleukin-6-mediated Mcl-1 upregulation and anti-apoptosis activity in basal cell carcinoma cells. J Investig Dermatol. 2002;119(5):1121–7.
101. Leu CM, Wong FH, Chang C, Huang SF, Hu CP. Interleukin-6 acts as an antiapoptotic factor in human esophageal carcinoma cells through the activation of both STAT3 and mitogen-activated protein kinase pathways. Oncogene. 2003;22(49): 7809–18.
102. Garcia-Tuñón I, Ricote M, Ruiz A, Fraile B, Paniagua R, Royuela M. IL-6, its receptors and its relationship with bcl-2 and bax proteins in infiltrating and in situ human breast carcinoma. Histopathology. 2005;47(1):82–9.
103. Waxman AB, Kolliputi N. IL-6 protects against hyperoxia-induced mitochondrial damage via Bcl-2-induced Bak interactions with mitofusions. Am J Respir Cell Mol Biol. 2009;41(4): 385–96.
104. Brooks C, Wei Q, Feng L, Dong G, Tao Y, Mei L, et al. Bak regulates mitochondrial morphology and pathology during apoptosis by interacting with mitofusins. Proc Natl Acad Sci U S A. 2007;104:11649–54.
105. Gritsko T, Williams A, Turkson J, Kaneko S, Bowman T, Huang M, et al. Persistent activation of stat3 signaling induces survivin gene expression and confers resistance to apoptosis in human breast cancer cells. Clin Cancer Res. 2006;12(1):11–9.
106. Johnson C, Han YY, Nathan H, McCarra J, Alpini G, Meng F. Interleukin-6 and its receptor, key players in hepatobiliary inflammation and cancer. Transl Gastrointest Cancer. 2012;1:58–70.
107. Chen M-F, Lin P-Y, Wu C-F, Chen W-C, Wu C-T. IL-6 expression regulates tumorigenicity and correlates with prognosis in bladder cancer. PLoS ONE. 2013;8(4):e61901.
108. Hsu JH, Shi Y, Frost P, Yan H, Hoang B, Sharma S, et al. Interleukin-6 activates phosphoinositol-3′ kinase in multiple myeloma tumor cells by signaling through RAS-dependent, and separately, through p85-dependent pathways. Oncogene. 2004;23(19):3368–75.
109. Hideshima T, Nakamura N, Chauhan D, Anderson KC. Biologic sequelae of interleukin-6 induced PI3-K/Akt signaling in multiple myeloma. Oncogene. 2001;20(42):5991–6000.
110. Borsellino N, Belldegrun A, Bonavida B. Endogenous interleukin 6 is a resistance factor for *cis*-diamminedichloroplatinum and etoposide-mediated cytotoxicity of human prostate carcinoma cell lines. Cancer Res. 1995;55:4633–9.
111. Suchi K, Fujiwara H, Okamura S, Okamura H, Umehara S, Todo M, et al. Overexpression of interleukin-6 suppresses cisplatin-induced cytotoxicity in esophageal squamous cell carcinoma cells. Anticancer Res. 2011;31(1):67–75.
112. Hirano T, Ishihara K, Hibi M. Roles of STAT3 in mediating the cell growth, differentiation and survival signals relayed through the IL-6 family of cytokine receptors. Oncogene. 2000;19:2548–56.
113. Niu G, Wright KL, Ma Y, Wright GM, Huang M, Irby R, et al. Role of Stat3 in regulating p53 expression and function. Mol Cell Biol. 2005;25(17):7432–40.
114. Patchen ML, MacVittie TJ, Williams JL, Schwartz GN, Souza LM. Administration of interleukin-6 stimulates multilineage hematopoiesis and accelerates recovery from radiation-induced hematopoietic depression. Blood. 1991;77(3):472–80.
115. Kim SY, Kang JW, Song X, Kim BK, Yoo YD, Kwon YT, et al. Role of the IL-6–JAK1–STAT3–Oct-4 pathway in the conversion of non-stem cancer cells into cancer stem-like cells. Cell Signal. 2013;25(4):961–9.
116. Gupta PB, Fillmore CM, Jiang G, Shapira SD, Tao K, Kuperwasser C, et al. Stochastic state transitions give rise to phenotypic equilibrium in populations of cancer cells. Cell. 2011;146(4):633–44.
117. Landskron G, De la Fuente M, Thuwajit P, Thuwajit C, Hermoso MA. Chronic inflammation and cytokines in the tumor microenvironment. J Immunol Res. 2014;2014:149185.
118. Colotta F, Allavena P, Sica A, Garlanda C, Mantovani A. Cancer-related inflammation, the seventh hallmark of cancer: links to genetic instability. Carcinogenesis. 2009;30(7):1073–81.
119. Schiechl G, Bauer B, Fuss I, Lang SA, Moser C, Ruemmele P, et al. Tumor development in murine ulcerative colitis depends on MyD88 signaling of colonic F4/80^{+}CD11b^{high}Gr1^{low} macrophages. J Clin Invest. 2011;121(5):1692–708.
120. Karin M. Nuclear factor-kappaB in cancer development and progression. Nature. 2006;441(7092):431–6.
121. Kesanakurti D, Chetty C, Maddirela DR, Gujrati M, Rao JS. Essential role of cooperative NF-kB and Stat3 recruitment to ICAM-1 intronic consensus elements in the regulation of radiation-induced invasion and migration in glioma. Oncogene. 2013;32(43):10.
122. Warburg O. On the origin of cancer cells. Science. 1956;123:309–14.
123. Bhatt AN, Chauhan A, Khanna S, Rai Y, Singh S, Soni R, et al. Transient elevation of glycolysis confers radio-resistance by facilitating DNA repair in cells. BMC Cancer. 2015;15:335.
124. Ando M, Uehara I, Kogure K, Asano Y, Nakajima W, Abe Y, et al. Interleukin 6 enhances glycolysis through expression of the glycolytic enzymes hexokinase 2 and 6-phosphofructo-2-kinase/fructose-2,6-bisphosphatase-3. J Nippon Med Sch. 2010;77(2):97–105.
125. Kawauchi K, Araki K, Tobiume K, Tanaka N. p53 regulates glucose metabolism through an IKK–NF-kappaB pathway and inhibits cell transformation. Nat Cell Biol. 2008;10:611–8.
126. Carey AL, Steinberg GR, Macaulay SL, Thomas WG, Holmes AG, Ramm G, et al. IL-6 increases insulin-stimulated glucose disposal in humans and glucose uptake and fatty acid oxidation in vitro via AMP activated protein kinase. Diabetes. 2006;55: 2688–97.
127. Ghosh S, Ashcraft K. An IL-6 link between obesity and cancer. Front Biosci. 2013;5:461–78.
128. Sarkar PD, Gopinath A, Skaria LK. Association of serum interleukin-6 and glycolysis in sickle cell disease patients. Med J DPU. 2014;7(3):317–20.
129. Valencia T, Kim JY, Abu-Baker S, Moscat-Pardos J, Ahn CS, Reina-Campos M, et al. Metabolic reprogramming of stromal fibroblasts through p62-mTORC1 signaling promotes inflammation and tumorigenesis. Cancer Cell. 2014;26(1):121–35.
130. Mercurio F, Manning AM. NF-kappaB as a primary regulator of the stress response. Oncogene. 1999;18(45):6163–71.
131. Kratsovnik E, Bromberg Y, Sperling O, Zoref-Shani E. Oxidative stress activates transcription factor NF-kB-mediated protective

Author's personal copy

signaling in primary rat neuronal cultures. J Mol Neurosci. 2005;26(1):27–32.
132. Libermann TA, Baltimore D. Activation of interleukin-6 gene expression through the NF-kappa B transcription factor. Mol Cell Biol. 1990;10(5):2327–34.
133. Wang L, Walia B, Evans J, Gewirtz AT, Merlin D, Sitaraman SV. IL-6 induces NF-kappa B activation in the intestinal epithelia. J Immunol. 2003;171(6):3194–201.
134. Grivennikov S, Karin M. Dangerous liaisons: STAT3 and NF-kB collaboration and crosstalk in cancer. Cytokine Growth Factor Rev. 2010;21(1):11–9.
135. Brown CO, Salem K, Wagner BA, Bera S, Singh N, Tiwari A, et al. Interleukin-6 counteracts therapy-induced cellular oxidative stress in multiple myeloma by up-regulating manganese superoxide dismutase. Biochem J. 2012;444(3):515–27.
136. Reuter S, Gupta SC, Chaturvedi MM, Aggarwal BB. Oxidative stress, inflammation, and cancer: how are they linked? Free Radic Biol Med. 2010;49(11):1603–16.
137. Jia Y, Zhou F, Deng P, Fan Q, Li C, Liu Y, et al. Interleukin 6 protects H(2)O(2)-induced cardiomyocytes injury through upregulation of prohibitin via STAT3 phosphorylation. Cell Biochem Funct. 2012;30(5):426–31.
138. Craig R, Larkin A, Mingo AM, Thuerauf DJ, Andrews C, McDonough PM, et al. p38 MAPK and NF-kappa B collaborate to induce interleukin-6 gene expression and release. Evidence for a cytoprotective autocrine signaling pathway in a cardiac myocyte model system. J Biol Chem. 2000;275(31):23814–24.
139. Kalluri R, Weinberg RA. The basics of epithelial–mesenchymal transition. J Clin Invest. 2009;119(6):1420–8.
140. Ricciardi M, Zanotto M, Malpeli G, Bassi G, Perbellini O, Chilosi M, et al. Epithelial-to-mesenchymal transition (EMT) induced by inflammatory priming elicits mesenchymal stromal cell-like immune-modulatory properties in cancer cells. Br J Cancer. 2015;112(6):1067–75.
141. Tawara K, Oxford JT, Jorcyk CL. Clinical significance of interleukin (IL)-6 in cancer metastasis to bone: potential of anti-IL-6 therapies. Cancer Manag Res. 2011;3:177–89.
142. Helbig G, Christopherson 2nd KW, Bhat-Nakshatri P, Kumar S, Kishimoto H, Miller KD, et al. NF-kappaB promotes breast cancer cell migration and metastasis by inducing the expression of the chemokine receptor CXCR4. J Biol Chem. 2003;278(24):21631–8.
143. Sansone P, Storci G, Tavolari S, Guarnieri T, Giovannini C, Taffurelli M, et al. IL-6 triggers malignant features in mammospheres from human ductal breast carcinoma and normal mammary gland. J Clin Invest. 2007;117(12):3988–4002.
144. Hanahan D, Folkman J. Patterns and emerging mechanisms of the angiogenic switch during tumorigenesis. Cell. 1996;86(3):353–64.
145. Kujawski M, Kortylewski M, Lee H, Herrmann A, Kay H, Yu H. Stat3 mediates myeloid cell dependent tumor angiogenesis in mice. J Clin Invest. 2008;118(10):3367–77.
146. Houde C, Li Y, Song L, Barton K, Zhang Q, Godwin J, et al. Overexpression of the NOTCH ligand JAG2 in malignant plasma cells from multiple myeloma patients and cell lines. Blood. 2004;104(12):3697–704.
147. Yun UJ, Park SE, Jo YS, Kim J, Shin DY. DNA damage induces the IL-6/STAT3 signaling pathway, which has anti-senescence and growth-promoting functions in human tumors. Cancer Lett. 2012;323(2):155–60.
148. Rodier F, Coppé JP, Patil CK, Hoeijmakers WA, Muñoz DP, Raza SR, et al. Persistent DNA damage signalling triggers senescence-associated inflammatory cytokine secretion. Nat Cell Biol. 2009;11:973–9.
149. Gilbert LA, Hemann MT. DNA damage-mediated induction of a chemoresistant niche. Cell. 2010;143:355–66.
150. Wu ZH, Wong ET, Shi Y, Niu J, Chen Z, Miyamoto S, et al. ATM- and NEMO-dependent ELKS ubiquitination coordinates TAK1-mediated IKK activation in response to genotoxic stress. Mol Cell. 2010;40:75–86.
151. Tachibana S, Zhang X, Ito K, Ota Y, Cameron AM, Williams GM, et al. Interleukin-6 is required for cell cycle arrest and activation of DNA repair enzymes after partial hepatectomy in mice. Cell Biosci. 2014;4(1):6.
152. Chang L, Guo R, Huang Q, Yen Y. Chromosomal instability triggered by Rrm2b loss leads to IL-6 secretion and plasmacytic neoplasms. Cell Rep. 2013;3(5):1389–97.
153. Deorukhkar A, Krishnan S. Targeting inflammatory pathways for tumor radiosensitization. Biochem Pharmacol. 2010;80(12):1904–14.
154. Grivennikov SI, Greten FR, Karin M. Immunity, inflammation, and cancer. Cell. 2010;140(6):883–99.
155. Woods Ignatoski KM, Friedman J, Escara-Wilke J, Zhang X, Daignault S, Dunn RL, et al. Change in markers of bone metabolism with chemotherapy for advanced prostate cancer: interleukin-6 response is a potential early indicator of response to therapy. J Interferon Cytokine Res. 2008;29(2):105–12.
156. Conze D, Weiss L, Regen PS, Bhushan A, Weaver D, Johnson P, et al. Autocrine production of interleukin 6 causes multidrug resistance in breast cancer cells. Cancer Res. 2001;61:8851–8.
157. Patel SAA, Bhambra U, Charalambous MP, David RM, Edwards RJ, Lightfoot T, et al. Interleukin-6 mediated upregulation of CYP1B1 and CYP2E1 in colorectal cancer involves DNA methylation, miR27b and STAT3. Br J Cancer. 2014;111(12):2287–96.
158. Bochet L, Meulle A, Imbert S, Salles B, Valet P, Muller C. Cancer-associated adipocytes promotes breast tumor radioresistance. Biochem Biophys Res Commun. 2011;1:102–6.
159. Xu H, Lai W, Zhang Y, Liu L, Luo X, Zeng Y, et al. Tumor-associated macrophage-derived IL-6 and IL-8 enhance invasive activity of LoVo cells induced by PRL-3 in a KCNN4 channel-dependent manner. BMC Cancer. 2014;14:330.
160. Touboul C, Lis R, Al Farsi H, Raynoud CM, Warfa M, Althawadi H, et al. Mesenchymal stem cells enhances ovarian cancer cell infiltration through IL-6 secretion in an amniochorionic membrane based 3D model. J Transl Med. 2013;11:28.
161. Eicthen A, Su J, Adler A, Zhang L, Loffe E, Parveen AA, et al. Resistance to anti-VEGF therapy mediated by autocrine IL-6/STAT3 signaling and overcome by IL-6 blockade. Cancer Res. 2016;76:2327–39.
162. Korkaya H, Kim GI, Davis A, Malik F, Henry NL, Ithimakin S, et al. Activation of IL-6 inflammatory loop mediates transtuzumab resistance in HER2+ breast cancer by expanding the cancer stem cell population. Mol Cell. 2012;47(4):570–84.
163. Chen F, Zhuang X, Lin L, Yu P, Wang Y, Shi Y, et al. New horizons in tumor microenvironment biology: challenges and opportunities. BMC Med. 2015;13:45.
164. Kontzias A, Kotlyar A, Laurence A, Changelian P, O'Shea JJ. Jakinibs: a new class of kinase inhibitors in cancer and autoimmune disease. Curr Opin Pharmacol. 2012;12(4):464–70.
165. Karkera J, Steiner H, Li W, Skradski V, Moser PL, Riethdorf S, et al. The anti-interleukin-6 antibody siltuximab down-regulates genes implicated in tumorigenesis in prostate cancer patients from a phase I study. Prostate. 2011;71(13):1455–65.
166. Chen R, Chen B. Siltuximab (CNTO 328): a promising option for human malignancies. Drug Des Devel Ther. 2015;9:3455–8.
167. Chou CH, Wei LH, Kuo ML, Huang YJ, Lai KP, Chen CA, et al. Up-regulation of interleukin-6 in human ovarian cancer cell via a Gi/PI3K-Akt/NF-kappaB pathway by lysophosphatidic acid, an ovarian cancer-activating factor. Carcinogenesis. 2005;26(1):45–52.
168. Song L, Smith MA, Doshi P, Sasser K, Fulp W, Altiok S, et al. Antitumor efficacy of the anti-interleukin-6 (IL-6) antibody

Author's personal copy

siltuximab in mouse xenograft models of lung cancer. J Thorac Oncol. 2014;9(7):974–82.
169. Bagcchi S. Siltuximab in transplant-ineligible patients with myeloma. Lancet Oncol. 2014;15(8):e309.
170. Emilie D, Wijdenes J, Gisselbrecht C, Jarrousse B, Billaud E, Blay JY, et al. Administration of an anti-interleukin-6 monoclonal antibody to patients with acquired immunodeficiency syndrome and lymphoma: effect on lymphoma growth and on B clinical symptoms. Blood. 1994;84:2472–9.
171. Asbagh LA, Uzunoglu S, Cal C. Zoledronic acid effects interleukin-6 expression in hormone findependent prostate cancer cell lines. Int Braz J Urol. 2008;34(3):355–64.
172. Gnant M. Zoledronic acid in breast cancer: latest findings and interpretations. Ther Adv Med Oncol. 2011;3(6):293–301.
173. Kurebayashi J, Yamamoto S, Otsuki T, Sonoo H. Medroxyprogesterone acetate inhibits interleukin 6 secretion from KPL-4 human breast cancer cells both in vitro and in vivo: a possible mechanism of the anticachectic effect. Br J Cancer. 1999;79(3/4):631–6.
174. Shinriki S, Jono H, Ota K, Ueda M, Kudo M, Ota T, et al. Humanized anti-interleukin-6 receptor antibody suppresses tumor angiogenesis and in vivo growth of human oral squamous cell carcinoma. Clin Cancer Res. 2009;15(17):5426–34.
175. Ando K, Takahashi F, Kato M, Kaneko N, Doi T, Ohe Y, et al. Tocilizumab, a proposed therapy for the cachexia of interleukin6-expressing lung cancer. PLoS One. 2014;9(7):e102436.
176. Moreau P, Harousseau JL, Wijdenes J, Morineau N, Milpied N, Bataille R. A combination of anti-interleukin 6 murine monoclonal antibody with dexamethasone and high-dose melphalan induces high complete response rates in advanced multiple myeloma. Br J Haematol. 2000;109:661–4.
177. Tai YT, Anderson KC. Antibody-based therapies in multiple myeloma. Bone Marrow Res. 2011;2011:924058.
178. Isobe A, Sawada K, Kinose Y, Ohyagi-Hara C, Nakatsuka E, Makino H, et al. Interleukin 6 receptor is an independent prognostic factor and a potential therapeutic target of ovarian cancer. PLoS ONE. 2015;10(2):e0118080.
179. Jiang XP, Yang DC, Elliott RL, Head JF. Down-regulation of expression of interleukin-6 and its receptor results in growth inhibition of MCF-7 breast cancer cells. Anticancer Res. 2011;31:2899–906.
180. Sun Y, Moretti L, Giacalone NJ, Schleicher S, Speirs CK, Carbone DP, et al. Inhibition of JAK2 signaling by TG101209 enhances radiotherapy in lung cancer models. J Thorac Oncol. 2011;6(4):699–706.
181. Ramakrishnan V, Kimlinger T, Haug J, Timm M, Wellik L, Halling T, et al. TG101209, a novel JAK2 inhibitor, has significant in-vitro activity in multiple myeloma and displays preferential cytotoxicity for CD45+ myeloma cells. Am J Hematol. 2010;85(9):675–86.
182. Kobayashi A, Tanizaki Y, Kimura A, Ishida Y, Nosaka M, Toujima S, et al. AG490, a Jak2 inhibitor, suppressed the progression of murine ovarian cancer. Eur J Pharmacol. 2015;766:63–75.
183. Eghtedar A, Verstovsek S, Estrov Z, Burger J, Cortes J, Bivins C, et al. Phase II study of the JAK kinase inhibitor ruxolitinib in patients with refractory leukemias, including post myeloproliferative neoplasms (MPN) acute myeloid leukemia (AML). Blood. 2012;119(20):4614–8.
184. Seavey MM, Lu LD, Stump KL, Wallace NH, Hockeimer W, O'Kane TM, et al. Therapeutic efficacy of CEP-33779, a novel selective JAK2 inhibitor, in a mouse model of colitis-induced colorectal cancer. Mol Cancer Ther. 2012;11(4):984–93.
185. Hart S, Goh KC, Novotny-Diermayr V, Tan YC, Madan B, Amalini C, et al. Pacritinib (SB1518), a JAK2/FLT3 inhibitor for the treatment of acute myeloid leukemia. Blood Cancer J. 2011;1(11):e44.
186. Yang F, Brown C, Buettner R, Hedvat M, Starr R, Scuto A, et al. Sorafenib induces growth arrest and apoptosis of human glioblastoma cells through the dephosphorylation of signal transducers and activators of transcription 3. Mol Cancer Ther. 2010;9(4):953–62.
187. Duan Z, Bradner JE, Greenberg E, Levine R, Foster R, Mahoney J, et al. SD-1029 inhibits signal transducer and activator of transcription 3 nuclear translocation. Clin Cancer Res. 2006;12(22):6844–52.
188. Shi X, Franko B, Frantz C, Amin HM, Lai R, et al. JSI-124 (cucurbitacin I) inhibits Janus kinase-3/signal transducer and activator of transcription-3 signalling, downregulates nucleophosmin-anaplastic lymphoma kinase (ALK), and induces apoptosis in ALK-positive anaplastic large cell lymphoma cells. Br J Haematol. 2006;135(1):26–32.
189. Su Y, Li G, Zhang X, Gu J, Zhang C, Tian Z, et al. JSI-124 inhibits glioblastoma multiforme cell proliferation through G2/M cell cycle arrest and apoptosis augment. Cancer Biol Ther. 2008;7(8):1243–9.
190. Blaskovich MA, Sun J, Cantor A, Turkson J, Jove R, Sebti SM. Discovery of JSI-124 (cucurbitacin I), a selective Janus kinase/signal transducer and activator of transcription 3 signaling pathway inhibitor with potent antitumor activity against human and murine cancer cells in mice. Cancer Res. 2003;63(6):1270–9.
191. Gholam P. The role of sorafenib in hepatocellular carcinoma. Clin Adv Hematol Oncol. 2015;13(4):232–4.
192. Moreno-Aspitia A. Clinical overview of sorafenib in breast cancer. Future Oncol. 2010;6(5):655–63.
193. Jäger D, Ma JH, Mardiak J, Ye DW, Korbenfeld E, Zemanova M, et al. Sorafenib treatment of advanced renal cell carcinoma patients in daily practice: the large international PREDICT Study. Clin Genitourin Cancer. 2015;13(2):156–64.e1.
194. Moreira RB, Peixoto RD, de Sousa Cruz MR. Clinical response to sorafenib in a patient with metastatic colorectal cancer and FLT3 amplification. Case Rep Oncol. 2015;8(1):83–7.
195. Tanaka T, Narazaki M, Kishimoto T. Anti-interleukin-6 receptor antibody, tocilizumab, for the treatment of autoimmune diseases. FEBS Lett. 2011;585(23):3699–709.
196. Trikha M, Corringham R, Klein B, Rossi J-F. Targeted anti-interleukin-6 monoclonal antibody therapy for cancer: a review of the rationale and clinical evidence. Clin Cancer Res. 2003;9(13):4653–65.
197. Coward J, Kulbe H, Chakravarty P, Leader D, Vassileva V, Leinster DA, et al. Interleukin-6 as a therapeutic target in human ovarian cancer. Clin Cancer Res. 2011;17(18):6083–96.
198. Guan M, Zhou YP, Sun JL, Chen SC. Adverse events of monoclonal antibodies used for cancer therapy. Biomed Res Int. 2015;2015:428169.
199. Chen MF, Hsieh CC, Chen WC, Lai CH. Role of interleukin-6 in the radiation response of liver tumors. Int J Radiat Oncol Biol Phys. 2012;84(5):e621–30.
200. Judd LM, Menheniott TR, Ling H, Jackson CB, Howlett M, Kalantzis A, et al. Inhibition of the JAK2/STAT3 pathway reduces gastric cancer growth in vitro and in vivo. PLoS One. 2014;9(5):e95993.
201. Huang C, Yang G, Jiang T, Huang K, Cao J, Qiu Z. Effects of IL-6 and AG490 on regulation of Stat3 signaling pathway and invasion of human pancreatic cancer cells in vitro. J Exp Clin Cancer Res. 2010;29(1):51.
202. Xiong A, Yang Z, Shen Y, Zhou J, Shen Q. Transcription factor STAT3 as a novel molecular target for cancer prevention. Cancers. 2014;6(2):926–57.
203. Ishdorj G, Johnston JB, Gibson SB. Inhibition of constitutive activation of STAT3 by curcurbitacin-I (JSI-124) sensitized human B-leukemia cells to apoptosis. Mol Cancer Ther. 2010;9(12):3302–14.
204. Schust J, Sperl B, Hollis A, Mayer TU, Berg T. Stattic: a small-molecule inhibitor of STAT3 activation and dimerization. Chem Biol. 2006;13(11):1235–42.

Author's personal copy

205. Yu X, He L, Cao P, Yu Q. Eriocalyxin B inhibits STAT3 signaling by covalently targeting STAT3 and blocking phosphorylation and activation of STAT3. PLoS ONE. 2015;10(5):e0128406.
206. Jing N, Li Y, Xiong W, Sha W, Jing L, Tweardy DJ. G-quartet oligonucleotides: a new class of signal transducer and activator of transcription 3 inhibitors that suppresses growth of prostate and breast tumors through induction of apoptosis. Cancer Res. 2004;64(18):6603–9.
207. Jing N, Zhu Q, Yuan P, Li Y, Mao L, Tweardy DJ. Targeting signal transducer and activator of transcription 3 with G-quartet oligonucleotides: a potential novel therapy for head and neck cancer. Mol Cancer Ther. 2006;5(2):279–86.
208. Yue P, Turkson J. Targeting STAT3 in cancer: how successful are we? Expert Opin Investig Drugs. 2009;18(1):45–56.
209. Chen CL, Loy A, Cen L, Chan C, Hsieh FC, Cheng G, et al. Signal transducer and activator of transcription 3 is involved in cell growth and survival of human rhabdomyosarcoma and osteosarcoma cells. BMC Cancer. 2007;7:111.
210. Song H, Wang R, Wang S, Lin J. A low-molecular-weight compound discovered through virtual database screening inhibits Stat3 function in breast cancer cells. Proc Natl Acad Sci U S A. 2005;102(13):4700–5.
211. Weidler M, Rether J, Anke T, Erkel G. Inhibition of interleukin-6 signaling by galiellalactone. FEBS Lett. 2000;484(1):1–6.

J. Biochem. 2020;167(3):303–314 doi:10.1093/jb/mvz091

JB THE JOURNAL OF BIOCHEMISTRY

Interleukin-6 confers radio-resistance by inducing Akt-mediated glycolysis and reducing mitochondrial damage in cells

Received August 21, 2019; accepted October 22, 2019; published online October 31, 2019

Neeraj Kumari[1,2], Asmita Das[2] and Anant Narayan Bhatt[1,*]

[1]Division of Radiation Biosciences, Institute of Nuclear Medicine and Allied Sciences, Brig. S K Mazumdar Marg, Delhi 110054, India and [2]Department of Biotechnology, Delhi Technological University, Main Bawana Road, Delhi 110 042, India

*Anant Narayan Bhatt, Division of Radiation Biosciences, Institute of Nuclear Medicine and Allied Sciences, Brig. S K Mazumdar Marg, Delhi 110054, India. Tel: +91-11-2390-5138, Fax: +91-11-2391-9509, email: anant@inmas.drdo.in anbhatt@yahoo.com

Interleukin-6 (IL-6)-induced glycolysis and therapeutic resistance is reported in some cell systems; however, the mechanism of IL-6-induced glycolysis in radio-resistance is unexplored. Therefore, to investigate, we treated Raw264.7 cells with IL-6 (1 h prior to irradiation) and examined the glycolytic flux. Increased expression of mRNA and protein levels of key glycolytic enzymes was observed after IL-6 treatment, which conferred glycolysis dependent resistance from radiation-induced cell death. We further established that IL-6-induced glycolysis is activated by Akt signalling and knocking down Akt or inhibition of pan Akt phosphorylation significantly abrogated the IL-6-induced radio-resistance. Moreover, reduction of IL-6-induced pAkt level suppressed the expression of Hexokinase-2 and its translocation to the mitochondria, thereby inhibiting the glycolysis-induced resistance to radiation. IL-6-induced glycolysis also minimized the radiation-induced mitochondrial damage. These results suggest that IL-6-induced glycolysis observed in cells may be responsible for IL-6-mediated therapeutic radio-resistance in cancer cells, partly by activation of Akt signalling.

Keywords: Akt signalling; glycolysis; hexokinase-2; IL-6; radio-resistance.

Abbreviations: 2-DG, 2-dexoy-D-glucose; 3-BP, 3-bromo pyruvate; ANOVA, analysis of variance; DMSO, dimethyl sulfoxide; HGD, high glucose Dulbecco's; HK-2, hexokinase-2; IL-6, interleukin-6; IR, ionizing radiation; MMP, mitochondrial membrane potential; PBS, phosphate-buffered saline; PFK-1, phosphofructokinase 1; PFKFB3, 6-phosphofructo-2-kinase/fructose-2,6-bisphosphatase 3; PKM2, pyruvate kinase M2; SF, surviving fraction; SRB, sulforhodamine B.

Introduction

Interleukin-6 (IL-6) is a cytokine synthesized and secreted by various types of human body cells like monocytes, adipocytes, fibroblasts, vascular endothelial cells and tumour cells of different types of cancers (*1*). It was primarily known as pro-inflammatory cytokine for decades, however, many recent evidences demonstrated its role in tissue remodelling and as anti-inflammatory cytokine (*1*, *2*). IL-6 is also known as myokine as it is secreted by muscle cells during exercise and acts on skeletal muscles to promote myogenesis, regulate energy metabolism and protect them from physical exercise-induced ischaemic–reperfusion injury (*3*). It also protects cardiomyocytes and lung cells from ischaemic–reperfusion injury and oxidative stress-induced cell death (*4*, *5*). Besides this, IL-6 plays an important role during differentiation and tumour progression in majority of cancers. Increased IL-6 secretion in serum and tumour tissues is one of the key factors that promote rapid growth rate and resulted in aggressive phenotypes of cancer (*1*, *6*). An adaptive consequence of chemotherapy and radiotherapy resulted in elevated levels of IL-6 in tumour microenvironment through NF-kB signalling that impose the major limitation to therapies (*7–9*). The cytoprotective role of IL-6 is beneficial in normal physiological conditions; however, it brings in an additional challenge in therapeutic management of tumours with high IL-6 levels.

The cancer cells and also the normal cells during various types of stress primarily depends on glycolysis for energy production even in the presence of oxygen, due to faster rate of ATP synthesis, this phenomenon is known as Warburg effect (*10*). Moreover, glycolysis over the oxidative phosphorylation is predominant pathway of energy metabolism in all the cells involved in inflammatory response (*11*). Hence, it is clear that this phenomenon of aerobic glycolysis, which was originally discovered in cancer cells, is not restricted to cancer cells only (*12*). It has been recently reported that pro-inflammatory cytokine IL-6 increases the availability of substrates such as glucose and lipids by promoting glycogenolysis and lipolysis in skeletal muscles in an autocrine manner and its deficiency suppresses the key genes of glycolysis pathway (*6*, *13*). These studies suggest that aerobic glycolysis is a common phenomenon among many proliferating cells, which provides advantage during proliferation in terms of faster ATP production to meet the high demand of rapidly dividing cells and cells recovering from injury.

It has been demonstrated earlier that IL-6 can induce glycolysis in various types of cell-like mouse embryonic fibroblasts, human skeletal muscles, etc. (*14*, *15*). However, the molecular mechanism of IL-6-induced glycolysis is poorly understood. Recent studies have demonstrated that the IL-6-mediated activation of cellular antioxidant pathway is implicated in the radio-resistance of cancer cells (*16–18*). Accumulating evidences indicate that induced

Downloaded from https://academic.oup.com/jb/article-abstract/167/3/303/5610530 by guest on 03 May 2020

© The Author(s) 2019. Published by Oxford University Press on behalf of the Japanese Biochemical Society. All rights reserved

glycolysis confers radio-resistance in various cancers (*6*, *7*, *19*, *20*). Although, various mechanisms of IL-6-induced radio-resistance is known but the role of IL-6-induced glycolysis in radio-resistance remains unclear. In the present study, we, therefore, investigated the mechanism of IL-6-induced glycolysis in Raw 264.7 cells and tested the hypothesis, if IL-6 can protect normal cells from ionizing radiation (IR) by inducing glycolysis-mediated radio-resistance. In this study, we have shown that IL-6 treatment induces glycolysis in relatively radio-sensitive Raw 264.7 (murine monocytic) cells (*21*, *22*), which protects it from IR-induced cell death. Results obtained clearly showed that IL-6-induced Akt signalling plays an important role in stimulating glycolysis and protect the cells by conferring glycolysis-mediated radio-resistance.

Materials and methods

Materials

High glucose Dulbecco's Minimum Essential Medium (HGD), Penicillin G, streptomycin, nystatin, dimethyl sulfoxide (DMSO), Sulforhodamine B (SRB) and 3-(4,5-dimethylthiazol-2-yl)-2,5-diphenyltetrazolium bromide (MTT) were purchased from Sigma Chemicals Co. (St Louis, MO, USA), whereas mouse IL-6 was purchased from Merck Millipore (Burlington, VT, USA). MK2206 (Akt inhibitor) and Akt1/2 siRNA was purchased from selleckchem (Houston, TX, USA) and Santacruz Biotechnology (Dallas, TX, USA), respectively.

Sources of cell line

The mouse normal monocyte macrophage (Raw 264.7) was obtained from NCCS, Pune, India and cultured in their respective media containing 10% heat inactivated foetal bovine serum and antibiotics. Stock culture was maintained in the exponential growth phase by passaging them every 3 days with their respective growth medium supplemented with 10% foetal bovine serum and antibiotics in 60 mm tissue culture petri dish (BD Falcon, USA).

Radiation treatment

All the experiments were carried out using 96, 24 and 6 well plates, 35 and 60 mm tissue culture dishes. Exponentially growing cells were treated with 1 ng/ml IL-6 followed by γ-radiation (2 Gy) and kept for overnight incubation at 37°C in 5% CO_2 incubator. All experiments were carried out at a single dose of gamma radiation (2 Gy), cells were irradiated using ^{60}Cobalt-Teletherapy Unit (Bhabhatron-II, Panacea Medical Technologies, Bangalore, India) at a source to sample distance of 80 cm and a field size of 35×35 cm^2 with dose rate of 1.05 Gy/min. The treatment schedule and concentration of other drug/inhibitors are mention in respective figure legends.

Glucose uptake and lactate production assay

Raw264.7 cells were incubated in HGD before IL-6 treatment and irradiation. Cells were treated with IL-6, 1 h prior to irradiation. Subsequently cell medium was removed and cells were incubated with 2NBDG (50 μM, 2-(*N*-(7-Nitrobenz-2-oxa-1,3-diazol-4-yl)Amino)-2-Deoxyglucose) prepared in phosphate-buffered saline (PBS) for 30 min (Fig. 1A). Further the cells were harvested and washed twice with cold PBS to analyse on flow cytometer. Lactate production was estimated in the growth medium using enzymatic assays (Fig. 1B). Lactate was estimated using lactate oxidase method using kit (Randox; Cat. No.-LC2389). Glucose uptake and lactate production were normalized with number of viable cells in respected wells.

Immunoblot for protein levels

The protein level of hexokinase 2, phosphofructokinase 1 (PFK-1), PKM2, GLUT4, phospho Akt, Akt and loading control β-Actin were determined in control and irradiated cells (Raw264.7) by immunoblot analysis (Fig. 1C and 4A). Cells were cultured in PD60 incubated in CO_2 incubator before treatment. Further cells were harvested post-irradiation at various time points and lysed in ice-cold RIPA lysis buffer (Tris-HCl: 50 mM, pH 7.4, NP-40: 1%, NaCl: 150 mM, EDTA: 1 mM, PMSF: 2 mM, protease inhibitor cocktail, Na3VO4: 1 mM, NaF: 1 mM) containing protease inhibitors. The protein concentration in cell lysates was determined using BCA protein assay kit. Protein (40 μg) was resolved on 10–12% SDS–PAGE (depending on the molecular weight) and electroblotted onto PVDF membrane (MDI). The membrane was then incubated in 4% body surface area for 2 h followed by primary antibody incubation HK-2 (1:1000), PKM2 (1:500), PFK-1 (1:500), GLUT4 (1:500) and β-Actin (1:3000) from Santa Cruz Biotechnology and pAkt (1:1000), Akt (1:1000) and SDH (1:1000) from Cell Signalling Technology. Membrane was washed followed by incubation with the appropriate HRP conjugated secondary antibody (1:5000, Santa Cruz Biotechnology) for 2 h. After washing, the blots were developed using Luminata Forte western HRP substarte (Millipore) The signal was captured by Chemidoc system (Bio-Rad, CA, USA) and band intensities for each individual protein were quantified by densitometry, corrected for background staining, and normalized to the signal for β-Actin.

Quantitative PCR for mRNA levels

Total RNA was isolated from cells by Qiagen RNA isolation kit according to the manufacturer's instructions (Qiagen RNeasy mini kit). Further RNA was dissolved in nuclease-free water (Thermo Scientific, USA) and quantified with Nanodrop (Thermo Scientific, USA). About 1 μg of RNA was used for cDNA synthesis via First-strand cDNA synthesis kit (Thermo Scientific, USA) in thermal cycler (Applied Biosystems, CA, USA). Kick start ready to use primers were purchased from Sigma Aldrich (St Louis, MO, USA). For real-time PCR, 25 ng of cDNA was added to 100 nM gene-specific primers and 1× Sybr Green supermix (Bio-Rad, CA, USA). The amplification programme consisted of a hot start at 95°C for 3 min, followed by 40 cycles of denaturation at 95°C for 15 s, annealing at 60°C for 30 s, and extension at 72°C for 15 s. The amount of target gene was normalized by β-Actin (Fig. 1D).

Growth kinetics/cell number

Cells were seeded in PD35. After IL-6 and radiation treatment cells were kept at 37°C in 5% CO_2 incubator for doublings (Fig. 2A). At respective time points cell numbers were counted with a Neubauer-improved counting chamber (Paul Marienfeld GmbH & Co. KG, Germany) under 10 X objective, and 10× eyepiece magnification with compound light microscope (Olympus CH30, Japan).

Clonogenic cell survival assay

Macro-colony assay was performed using pre-plating method of macro-colony assay. Cells were plated at a low density of 100–3200 cells in triplicates in 60 mm Petri dishes. After IL-6 and radiation treatment (0–8 Gy), cells were incubated at 37°C in a humidified CO_2 (5%) incubator for 7–10 days. Colonies of at least 50 cells (5–6 generations of proliferation) were scored as survivors. Colonies were washed once with PBS to remove media, fixed with methanol and then stained with 1% crystal violet (dissolved in 7% methanol in PBS). Plating efficiency was calculated as PE = (Number of colonies counted/Number of cells plated) × 100. The surviving fraction (SF) was calculated as $SF = PE_T/PE_C$, where PE_T is the plating efficiency of the treated group and PE_C is the value of the control.

ATP measurement

ATP was measured using ATP bioluminescent assay kit (Sigma Aldrich, St Louis, MO, USA) following manufacturer's protocol. Briefly, cells were treated with IL-6 followed by irradiation at 1 h. At 4 and 24 h, post-irradiation cells were washed and scraped in cold PBS and pelleted at 1000 rpm for 10 min. Cells were lysed in 350 μl of lysis buffer (4 mM EDTA and 0.2% Triton X-100). About 100 μl of this lysate was loaded per well in triplicates with 100 μl of ATP mix in a 96-well white luminescence measuring plate. Luminescence of samples along with standards was read at 562 nm and normalized with the cell number (Fig. 3D). ATP concentration is depicted as pg/cell.

Acridine orange-ethidium bromide staining

Raw 264.7 cells were seeded in 96 well and stained with acridine orange-ethidium bromide according to Deborah Ribble protocol (*23*) with minimal modifications (Fig. 3G). Images were captured

Downloaded from https://academic.oup.com/jb/article-abstract/167/3/303/5610530 by guest on 03 May 2020

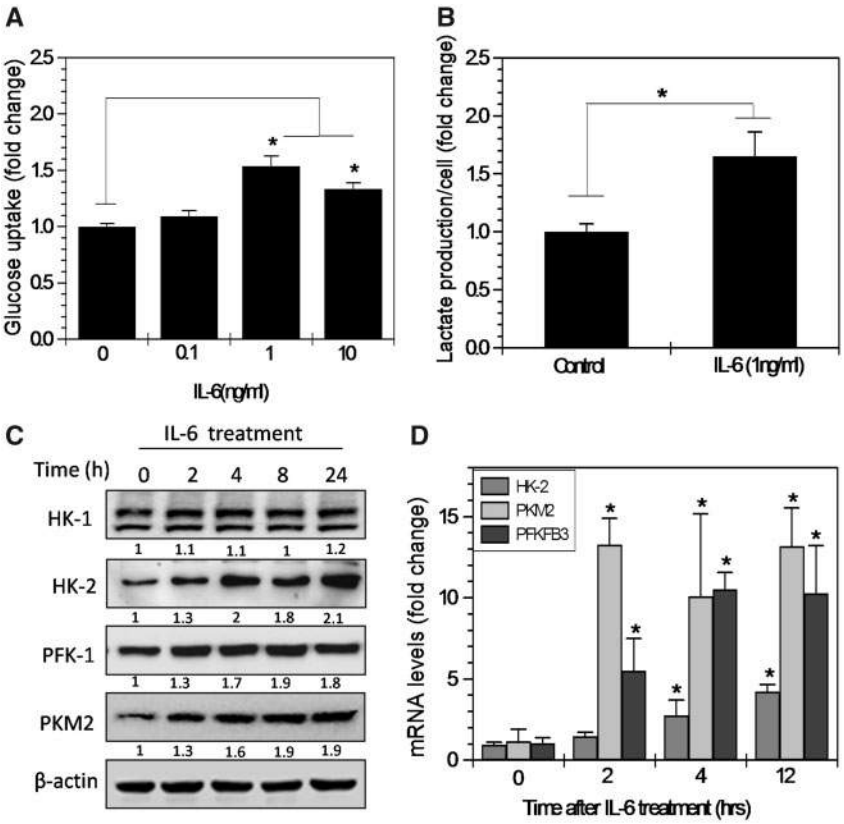

Fig. 1 IL-6 induced rate of glycolysis was measured by observing glucose uptake and lactate production in cells after IL-6 treatment. Glucose uptake (**A**) and lactate production (**B**) was measured in culture media, 2 h after IL-6 treatment. (**C**) Protein levels of various glycolytic regulatory enzymes (indicated in figure) were measured in untreated and IL-6 (1 ng/ml) treated cells at given time points. β-Actin was used as loading control. Values shown in between the blots are the average fold change value of densitometric analysis of three blots, normalized with respective β-Actin. (**D**) The mRNA levels of HK-2, PKM2 and PFKFB3 genes at indicated time points after IL-6 (1 ng/ml) treatment. Statistical significance calculated by one-way ANOVA and the Student's *t*-test between the groups. Data are expressed as mean ± SD ($n = 4$). $^*P < 0.05$.

under fluorescence microscope using 10× objective, and 10× eyepiece magnification with fluorescence microscope (Olympus IX51 Fluorescence Microscope, Japan).

Formazan quantification

The cells were plated in 24 well culture plates (40,000 cells/well) and incubated in CO_2 incubator. Next day, treatment was given according to the experimental requirement. Further, at respective time points, 50 µl MTT solutions from the stock (5 mg/ml) was added and cells were incubated in CO_2 incubator in the dark for 2 h. The medium was removed and formazan crystals formed by the cells were dissolved using 500 µl of DMSO followed by transfer in 96-well plate. The absorbance was read at 570 nm using 630 nm as reference wavelength on a Multiwell plate reader (Biotech Instruments, USA). Reduced formazan quantification was done with formazan standard. At each respective time points, cell numbers were counted with a Neubauer-improved counting chamber (Paul Marienfeld GmbH & Co. KG, Germany) under 10× objective, and 10× eyepiece magnification with compound light microscope (Olympus CH30, Japan).

Measurement of mitochondrial mass and mitochondrial calcium

Quantitative analysis of mitochondrial content was carried out using Mitotracker Green (at respective time points, post-irradiation), Cells were incubated with mitotracker green (100 nM; 15 min; 37°C), in PBS, then washed with PBS and resuspended in PBS before analysis. The signals were recorded using BD FACSAria^{TM} III cell sorter. (BD Biosciences, USA). Images of calcium-loaded mitochondria were captured by staining cells with A23187 (6 µM, 20 min). Briefly, Raw264.7 cells were grown in PD-35 having cover slip. At 4 h post-irradiation medium was removed and stained for 20 min in dark. Stain was removed and cells washed with cold PBS. Images were captured under fluorescence microscope with 40× objective.

Mitochondrial membrane potential

Quantitative and qualitative analysis of mitochondrial membrane potential (MMP) was carried out using TMRM and JC-1 dyes respectively, Cells were incubated with TMRM (50 nM; 30 min; 37°C) in PBS, then washed and resuspended in PBS for analysis. Fluorescence signals were measured by flow cytometer (BD FACSAria^{TM} III cell sorter). For microscopy, cells were stained with JC-1 dye (10 µg/ml; 30 min; 37°C). After staining, cells were washed with PBS and observed at 40× magnification under fluorescence microscope (Olympus IX51 Fluorescence Microscope, Japan). JC-1 accumulates in mitochondria as monomer or J-aggregates depending on the membrane potential. The monomeric form is predominately present in depolarized mitochondria and emits green fluorescence (~530 nm), whereas the oligomeric (J-aggregate) form in mitochondria with more potentials and emits red fluorescence (~590 nm).

siRNA transfection

The control siRNA and Mouse Akt1/2 siRNA pool were purchased from Santacruz Biotechnology (Dallas, TX, USA) to knock down gene expression. siRNA transfection was performed using Lipofectamine 2000 (Invitrogen, Carlsbad, CA, USA), according to the manufacturer's instructions, briefly, 0.1 ×106 cells were seeded in 6-well plate a day before transfection. Next day, transfection was done in Opti-MEM (serum and antibiotic-free medium) for 4 h followed by 24 h recovery in 2× serum-containing medium. Pilot experiments were performed to optimize the amount and time of maximal protein knockdown.

Statistical analysis

All the experiments were carried out in triplicates or quadruplicates. Means and standard errors were computed. The Student's *t*-test and one-way analysis of variance (ANOVA) test were performed for

Downloaded from https://academic.oup.com/jb/article-abstract/167/3/303/5610530 by guest on 03 May 2020

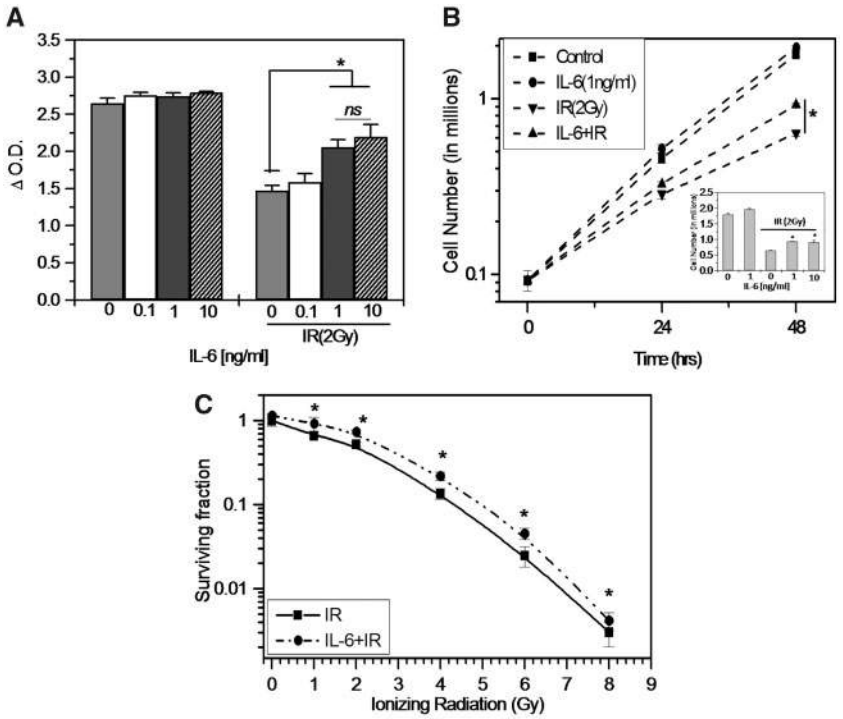

Fig. 2 IL-6 confers radio-resistance (**A**) SRB assay carried out at 48 h post-irradiation using different concentrations of IL-6 (0.1–10 ng/ml). Graph (ΔOD 340 nm) plotted and treatment groups were compared with their respective control. (**B**) The cell number in control and treatment group was quantified at 0–48 h post-irradiation and graph presented on log scale against time at single concentration of IL-6 (1 ng/ml). Inset graph presents the cell number at 48 h on two different concentrations of IL-6. (**C**) Dose-response curve of Raw264.7 cells with or without IL-6 treatment. Surviving fraction was plotted against increasing radiation doses (0–8 Gy). Star shows the statistical significance of change between the groups calculated by one-way ANOVA and the Student's *t*-test. Data are expressed as mean ± SD ($n = 4$). $^*P < 0.05$.

comparisons between two groups and multiple groups, respectively. *P*-values of <0.05 were considered statistically significant.

Results

IL-6 induces glycolysis

We first tested if IL-6 can induce glycolysis in Raw 264.7 cells. Thus, we measured glucose uptake using non-metabolizing, fluorescent glucose analogue 2-NBDG (2-(*N*-(7-Nitrobenz-2-oxa-1,3-diazol-4-yl)Amino)-2-Deoxyglucose) in Raw264.7 cells. IL-6 treatment showed significant increase in glucose consumption at both 1 and 10 ng/ml IL-6 with highest 1.5-fold consumption at 1 ng/ml (Fig. 1A). Therefore, we used 1 ng/ml concentration of IL-6 for all the further experiments. Consequently, lactate production, which is the end product of glycolysis was also increased by 1.65-fold after IL-6 treatment (Fig. 1B). Further to understand if the high rate of glycolysis is achieved by IL-6-induced enhanced levels of glycolytic enzymes, we checked the levels of key glycolytic enzymes HK-1, HK-2, PFK-1 and PKM2 after IL-6 treatment. We found nearly 1.3–2-fold time-dependent increase in the protein levels of HK-2, PFK-1, and PKM2, while the protein level of HK-1 was found unchanged (Fig. 1C). Enhanced levels of HK-2 and PKM2 protein was further supported by the time-dependent increase in HK-2 and PKM2 mRNA levels (Fig. 1D). We also checked the IL-6-induced gene expression of PFKFB3 gene, which produces Glucose 2,6 bis phosphate for allosteric activation of PFK-1 enzyme (*24*) We found, IL-6 induced the mRNA levels of PFKFB3 gene also, suggesting it regulates the flow of glucose through glycolysis (Fig. 1D). These findings suggest that IL-6 induces glycolysis by inducing the expression of glycolytic regulatory enzymes in Raw264.7 cells.

IL-6 protects Raw264.7 cells from radiation-induced cell death

Our previous studies suggest that transient elevation of glycolysis confers radio-resistance (*20*). Therefore, in order to check the correlation between IL-6-induced glycolysis and radio-resistance, we further carried out SRB assay and growth kinetics in Raw264.7 cells to test the effects of IL-6 on radiation-induced cell death. SRB assay was performed at same concentration range of IL-6 0.1 to 10 ng/ml as used in glucose uptake and we found significant protection of 45–50% at 1 and 10 ng/ml (Fig. 2A). Growth kinetic assay was also performed under similar experimental conditions and nearly 45% reduction in radiation-induced cell death was observed in IL-6 treated cells as compared to irradiated cells (Fig. 2B). The marginal increase in protection, observed at 10 ng/ml with respect to 1 ng/ml IL-6 in SRB assay (Fig. 2A) and marginally low cell count at 10 ng/ml (Fig. 2B inset) was statistically insignificant; Since significant and nearly equal increase in glucose consumption and radioprotection were observed at both 1 and 10 ng/ml doses of IL-6, therefore, we

Downloaded from https://academic.oup.com/jb/article-abstract/167/3/303/5610530 by guest on 03 May 2020

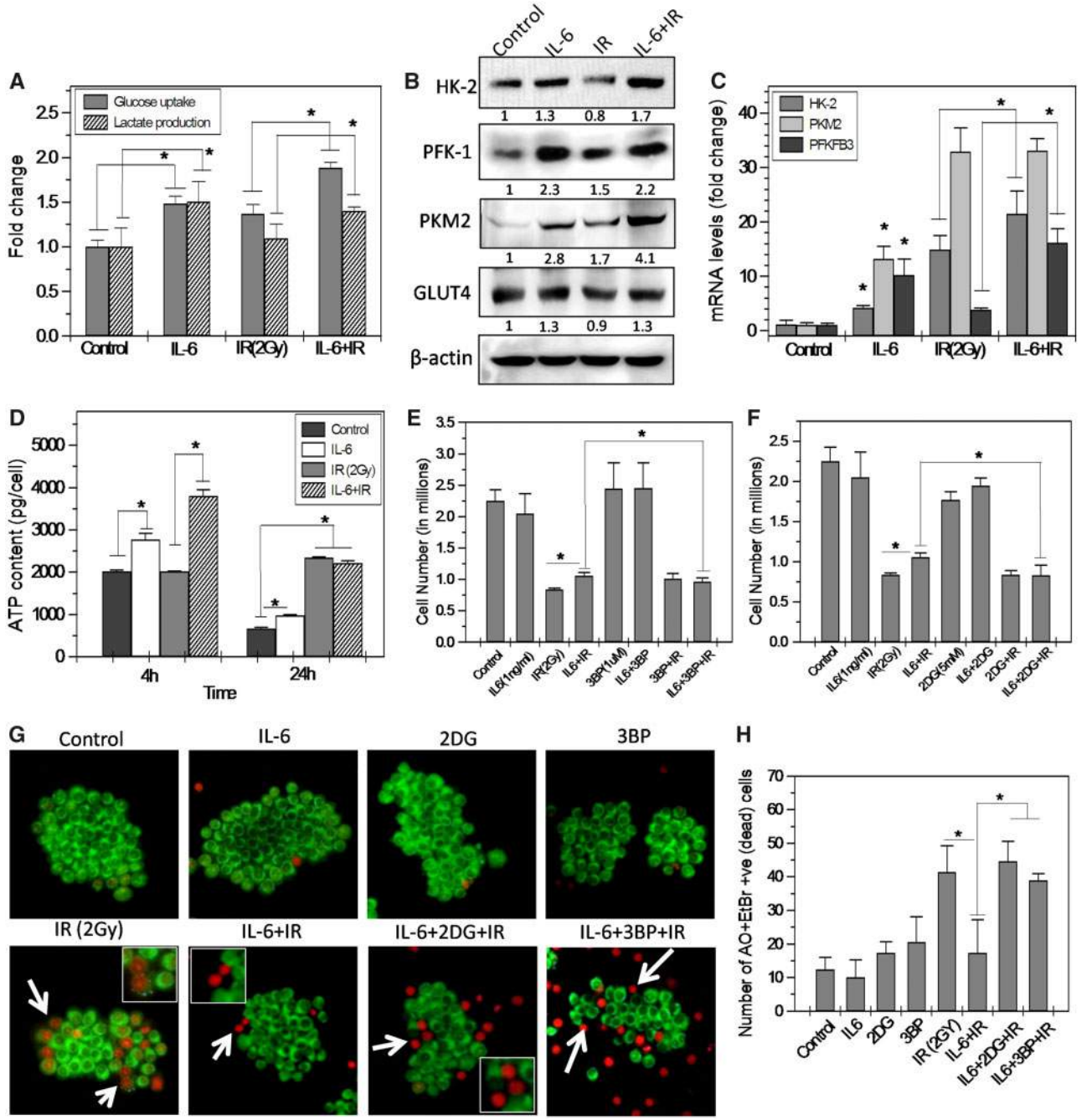

Fig. 3 IL-6-induced radio-resistance is glycolysis dependent. (**A**) Glucose uptake and lactate production measured 2 h post-irradiation, as described (**B**) Immuno-blotting of key regulatory glycolytic enzymes was performed at 24 h post-irradiation. β-Actin was used as loading control. Values shown in between the blots are the average fold change value of densitometric analysis of three blots, normalized with respective β-Actin. (**C**) The mRNA levels of HK-2, PKM2 and PFKFB3 with respect to control were observed after 12 h post-irradiation (**D**) ATP levels in cells was measured by bioluminescence ATP assay kit at indicated time points and represented as ATP concentration per cell calculated from standard. (**E** and **F**) Cell number was quantified at 48 h post-irradiation in various treatment groups and plotted as bar graph with cell number on *Y*-axis. (**G** and **H**) Cells were stained with AO/EtBr 24 h post-irradiation and examined under a fluorescent microscope at 10× magnification. Zoomed images of dying cells are shown in inset for improved view. Dead cells (EtBr stained and marked with arrow) were counted from multiple images and the mean of dead cells per group was plotted as bar graph. Star shows the statistical significance of change between the groups calculated by the Student's *t*-test. Data are expressed as mean ± SD ($n = 4$). $^*P < 0.05$.

used 1 ng/ml concentration for all further experiments. Further, to validate IL-6 treatment-induced radio-resistance; we irradiated the IL-6 pre-treated cells and then analysed the clonogenicity using macro-colony assay. Indeed, a significant increase in survival was evident in IL-6 pre-treated cells as compared to radiation alone on all radiation doses between 0 and 8 Gy (Fig. 2C). Together, these findings suggest that IL-6-induced glycolysis confers radio-resistance in monocytic Raw264.7 cells.

Downloaded from https://academic.oup.com/jb/article-abstract/167/3/303/5610530 by guest on 03 May 2020

IL-6-induced radio-resistance is glycolysis dependent

Further, to validate the correlation between IL-6-induced glycolysis and radio-resistance; we analysed the levels of glucose uptake and lactate production after radiation exposure in IL-6 pre-treated samples. Radiation alone group also showed increase in glucose uptake, however, it was significantly less (~1.5 fold) as compared to IL-6 alone and combined (IL-6 pre-treatment followed by irradiation) treatment groups (~2 fold) (Fig. 3A). Similarly, the lactate production was also found significantly higher in IL-6 and radiation combined treatment as compared to radiation-exposed cells (Fig. 3A). This result is substantiated by several fold increased protein levels of glycolytic enzymes (HK-2, PFK-1 and PKM2), glucose transporter GLUT4 (Fig. 3B) and mRNA expression of HK-2, PKM2 and PFKFB3 gene (Fig. 3C) in cells co-treated with IL-6 and radiation as compared to radiation alone. We also found about 1.9-fold increased ATP level at 4 h post-irradiation in IL-6 pre-treated cells with respect to control and radiation alone (Fig. 3D).

We further inhibited the glycolysis using non-toxic concentrations of 2-dexoy-D-Glucose (2-DG) and 3-bromo pyruvate (3-BP) in IL-6 pre-treated cells before exposing to radiation and performed growth kinetics. Both the glycolytic inhibitors 2-DG and 3-BP reversed the IL-6-induced protection from radiation-induced cell death (Fig. 3E and F). This observation from growth kinetics assay was correlated with qualitative imaging of ethidium bromide and acridine orange (apoptosis assay) at 24 h. Radiation alone and in combination with glycolytic inhibitors (2-DG and 3-BP) in IL-6 pre-treated group showed nearly similar number of apoptotic and necrotic cell population, which was significantly higher as compared to the IL-6 pre-treated and radiation-exposed treatment group (Fig. 3G and H). Therefore, these findings evidently validate our earlier observation that induced glycolysis confers radio-resistance. It also suggests that IL-6-induced radio-resistance in Raw264.7 cells is glycolysis dependent.

IL-6 protects from radiation-induced mitochondrial damage

Ionizing radiation is known to damage mitochondria and affect its energy metabolism (*25*, *26*). Therefore, we tested if IL-6 protects from radiation-induced mitochondrial damage also. To test the mitochondrial energy metabolism, we analysed complex II activity of mitochondrial respiratory chain by monitoring formazan formation. We found, radiation induces nearly 2.5-fold increased formazan formation in IL-6 untreated and treated cells at early time point (4 h), which comes down to normal at later time point (24 h, Fig. 4A). Mitochondrial enzymatic activity depends on the mitochondrial mass in cells, and we have shown in our earlier study that radiation-induced mitochondrial damage can induce mitochondrial biogenesis, thereby increases the mitochondrial mass and formazan formation in cells (*25*). Interestingly, we noted nearly similar formazan formation in IL-6 untreated and treated cells after radiation exposure from 1.8- to 1.25-fold increased mitochondrial mass, respectively (Fig. 4B). This observation shows that radiation-exposed cells have 80% more mitochondrial mass but all may not be contributing to enhanced complex II activity. However, similar formazan formation from only 25% increased mitochondrial mass and nearly similar SDH level (Fig. 4C and D) after radiation exposures in IL-6 pre-treated cells as compared to radiation alone exposed cells suggest reduced mitochondrial damage and higher efficiency of mitochondrial respiration in IL-6 pre-treated cells. Subsequently, we also analysed the MMP under similar experimental conditions to analyse the mitochondrial status in radiation-exposed cells using fluorescent potentiometric dyes JC-1 and TMRM (Fig. 4E and F). We observed radiation induced increased MMP in IL-6 and radiation treated cells (Fig. 4E), however, radiation-induced hyperpolarized mitochondria and increased mitochondrial mass (Fig. 4B) can also show higher dyes uptake in cells giving false information of higher MMP (*25*). Therefore, we normalized the MMP values with mitochondrial mass of the respective sample to obtain the accurate MMP of the cells. When radiation induced increased MMP was normalized with enhanced mitochondrial mass, it showed significant 30% decrease in MMP, which was restored in IL-6 pre-treated and radiation-exposed samples both at 4 and 24 h (Fig. 4F). This was further validated by microscopic observation of radiation induced damaged mitochondria using A23187 dye (*26*). We found highly reduced numbers of A23187 puncta positive cells and much smaller intracellular bodies (showing damaged mitochondria) in IL-6 pre-treated cells as compared to radiation alone (Fig. 4G and H). Interestingly, glycolysis inhibition using 2-DG in IL-6 pre-treated cells reverses the protective effects of IL-6 from radiation-induced mitochondrial damage (Fig. 4G and H). These observations suggest that IL-6 protects from radiation-induced mitochondrial damage and this protective effect is also linked with IL-6-induced glycolysis.

IL-6-induced Akt signalling promotes glycolysis and confers radio-resistance

Enhanced glycolytic metabolism is known to be regulated by two main signalling pathways in normal cells namely, HIF1α and Akt. IL-6 activates both HIF1α and Akt signalling pathway (*1*, *27*). Whereas, we found that IL-6 at 1 ng/ml concentration does not induce detectable levels HIF1α in Raw264.7 cells. Therefore, we tested Akt pathway by estimating the time-dependent protein levels of pAkt (active form) in IL-6 treated cells. We found more than 2-fold increase in pAkt levels as early as 1 h of IL-6 treatment (Fig. 5A). Further, to authenticate if IL-6-induced radio-resistance is dependent on Akt signalling and enhanced glycolysis mediated by it; we inhibited Akt signalling using pan Akt inhibitor MK2206 (*28*) and also knock down the Akt expression (53% depletion in Akt1/2 level) using Akt1/2 siRNA. Down-regulation of Akt signalling not only reduced the IL-6-induced pAkt levels to un-induced basal level (Fig. 5B) but also significantly brought down the level of IL-6-

Downloaded from https://academic.oup.com/jb/article-abstract/167/3/303/5610530 by guest on 03 May 2020

induced glucose uptake, and lactate production to the basal level (Fig. 5C). Further, low pAkt level reduced the IL-6 induced total and mitochondrial bound fraction of HK-2 (Fig. 5D and F) and reversed the IL-6-induced radio-resistance, indicated by significant reduction in cell number of IL-6 pre-treatment combined with Akt1/2 siRNA and MK2206 in irradiated cells nearly to the level of radiation control (Fig. 5E). These results suggest that IL-6-induced Akt signalling up-regulate the levels of glycolytic enzymes, which leads to enhanced glycolysis and radio-resistance in Raw264.7 cells.

Discussion

IL-6, which is known to be a cytoprotective cytokine in normal physiological conditions, also protects tumour cells from radiotherapy and chemotherapeutic agents posing major limitation in therapeutic gain in cancer treatment (*1*). IL-6 protects the cells from therapeutic stress-induced cell death by inducing various pro-survival signalling namely inhibition of apoptosis, induce survival and proliferation (*1*, *6*, *14*). Therefore, IL-6-induced cellular defense to therapeutic stress causes therapeutic resistance (*1*, *6*, *16–19*). It is known that

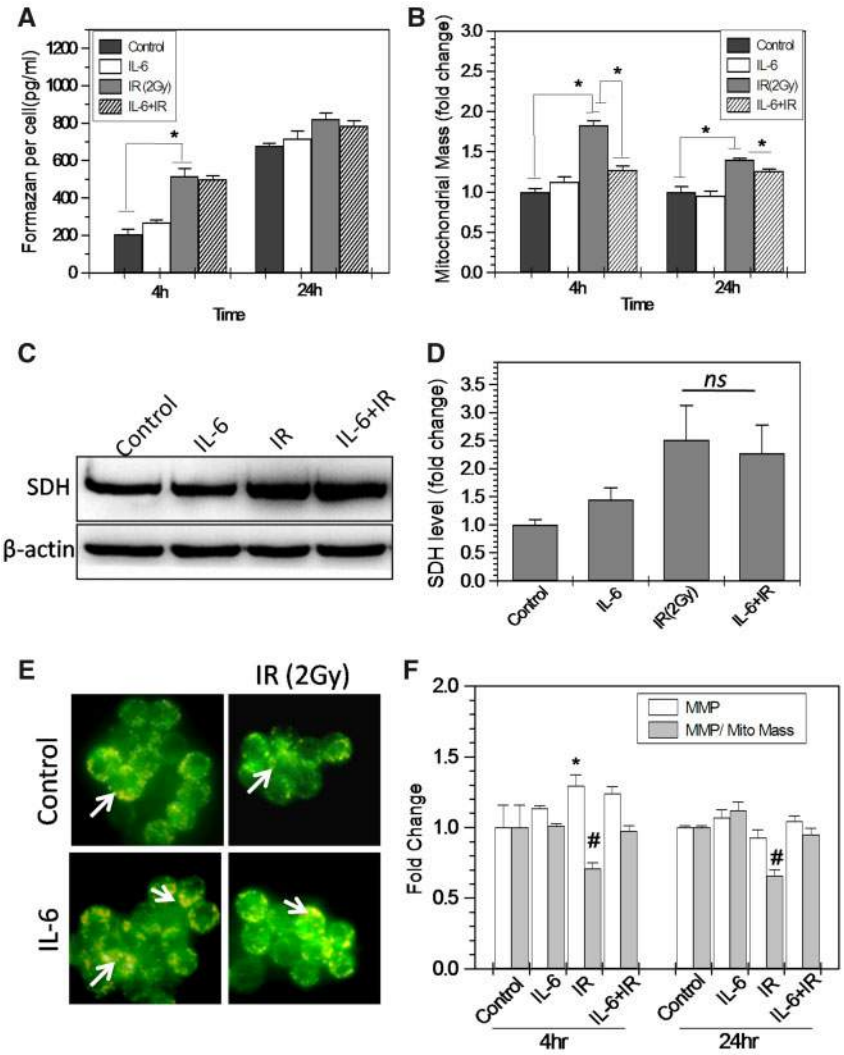

Fig. 4 IL-6 prevents mitochondrial damage from radiation. (**A**) The formazan formed per cell was quantified spectro-photometrically and presented as bar graph at indicated time points. (**B**) The mitochondrial mass was analysed by staining cells with MitoTracker Green FM (100 nM; 20 min) at indicated time points. Graph showing mean fluorescence intensity, presented as fold change with respect to control. (**C** and **D**) Immunoblot showing protein expression of mitochondrial complex-II subunit SDH-A presented in Raw264.7 cells. The bar graph represents the fold increase in SDH levels quantified by densitometry and normalized with β-Actin. (**E**) Microscopic evaluation of mitochondrial membrane potential shown by distribution of JC-1-loaded mitochondria in response to radiation, the retention of monomer and aggregates (marked with arrow) represents the shift in mitochondrial membrane potential. Images were captured at 40× (objective) and 10× (eyepiece) magnification. (**F**) Quantitative estimation of MMP by TMRM and normalized with respective mitochondrial content (data obtained from mitotracker green, Fig. 4B) at 4 and 24 h post-irradiation. (**G**) Photomicrograph shows the radiation induced changes (marked with arrow) in mitochondrial calcium by staining the cells with A23187 (6 μM, 30 min). Images were captured under fluorescence microscope with 40× objective. (**H**) Graph representing quantification of I-bodies formation per cell in different treatment groups. Data were obtained from $n = 10$ fields per group. Star shows the statistical significance of change between the groups calculated by the Student's *t*-test. Data are expressed as mean ± SD ($n = 4$). *$P < 0.05$, # represents the significance with respect to the MMP/mitochondrial mass of control group.

Downloaded from https://academic.oup.com/jb/article-abstract/167/3/303/5610530 by guest on 03 May 2020

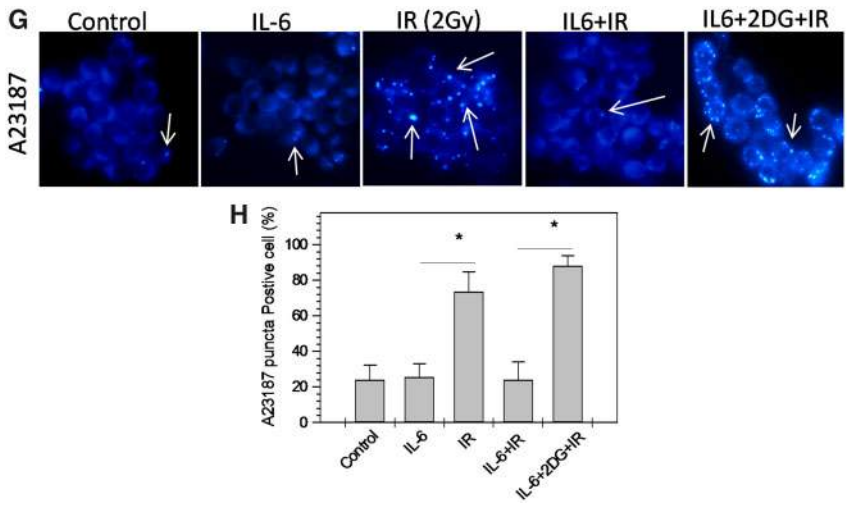

Fig. 4 Continued

IL-6 can induce aerobic glycolysis in cells (*12*, *15*), and we have demonstrated earlier that induced glycolysis caused radio-resistance in cells (*20*). IL-6-mediated radio-resistance in cells has been attributed to IL-6-induced anti-oxidant defense system and STAT-3-mediated pro-survival signalling (*14*, *18*); however, the role of IL-6-induced energy metabolism mainly glycolysis in radio-resistance is not known. Therefore, we tested the hypothesis, if IL-6-induced glycolysis plays any role in cellular radio-resistance, which may be diminishing the therapeutic gain in cancer treatment. IL-6-induced radio-resistance can also be exploited in protecting the normal tissues from radiation hazards. We selected murine monocytic cell line Raw264.7 to test the IL-6-induced radio-resistance because haematopoietic cells are relatively more sensitive to radiation (*21*, *22*).

The data presented above demonstrate the potential of IL-6 to induce glycolysis in haematopoietic Raw264.7 cells. It induced the glycolysis by increasing the levels of many regulatory glycolytic enzymes viz. HK-2, PFK-1 and PKM2 (Fig. 1C and D). Enhanced expression of HK-2 and its association with mitochondria ensures rapid phosphorylation of glucose using mitochondrial ATP (*29*). The PFK-1 is the first critical and irreversible step of glycolysis which diverts the glucose through glycolysis (catabolic pathway) and ensures that glucose should not enter to pentose phosphate pathway or gluconeogenesis, both anabolic pathways. At the time of stress or cellular injury, ATP generated from catabolic pathways is required for macromolecular repair and cell survival, therefore, diverting glucose towards glycolysis for more ATP production is vital and decisive for cell survival (*24*). We found higher ATP levels in IL-6 treated cells (Fig. 3D), which acts as inhibitor of PFK-1, however, increased expression of PFKFB3 (Fig. 1D) produces fructose 2,6bisphosphate, which acts as allosteric activator of PFK-1 and ensures the continuous activation of PFK-1, even in the presence of high ATP (*15*, *24*). Further, IL-6 induced higher protein levels of PKM2 (Fig. 1C and D) maintains the smooth running of glucose through glycolysis by reducing the level of its substrate phosphoenolpyruvate, which can inhibit the PFK-1 and stop the flow of glucose towards glycolysis. These results suggest that IL-6 induces the glycolysis by elevating the levels of all the crucial regulatory enzymes of this pathway.

Interestingly, IL-6 pre-treatment to induce glycolysis could protect the radio-sensitive Raw264.7 cells from radiation-induced cell death (Fig. 2). The protein levels of glucose transporter and glycolytic enzymes, which was decreased after radiation exposure was found high in IL-6 alone and combined treatment group, suggesting that IL-6 induced the glycolysis in radiation-exposed cells also. Radiation is also known to induce the glycolysis (*30*), which can be observed by enhanced glucose uptake, lactate production and higher levels of glycolytic enzymes, HK-2, PFK-1 and PKM2 in radiation-exposed sample as compared to control (Fig. 3A–C). However, these levels were found further increased in IL-6 pre-treated and radiation-exposed (combined treatment) sample. These findings suggest that radiation-induced glycolysis, which is marginally higher than the control cannot meet the requirement of energy to rescue the cells from radiation-induced cell death, however, IL-6 can induce the glycolysis at sufficiently higher level to accomplish the requirement of energy for repair and survival of cells battling with radiation-induced damage. This proposition is further confirmed by significantly higher levels of ATP in radiation-exposed cells pre-treated with IL-6 as compared to control and radiation alone (Fig. 3D). The IL-6 induced high levels of ATP in IL-6 alone and combined treatment was noted at early time point (4 h), when it was obligatory to rescue the cells, as ATP is essentially required for energy-consuming processes like macromolecular repair, mainly DNA (*20*). The reversal of IL-6-induced radio-resistance by glycolytic inhibitors 3-BP and 2-DG (Fig. 3E–H) authenticated the role of glycolysis in IL-6-induced radio-resistance. Radiation-induced mitochondrial damage also contributes in radiation-induced cell death; we observed that IL-6 reduced the

Downloaded from https://academic.oup.com/jb/article-abstract/167/3/303/5610530 by guest on 03 May 2020

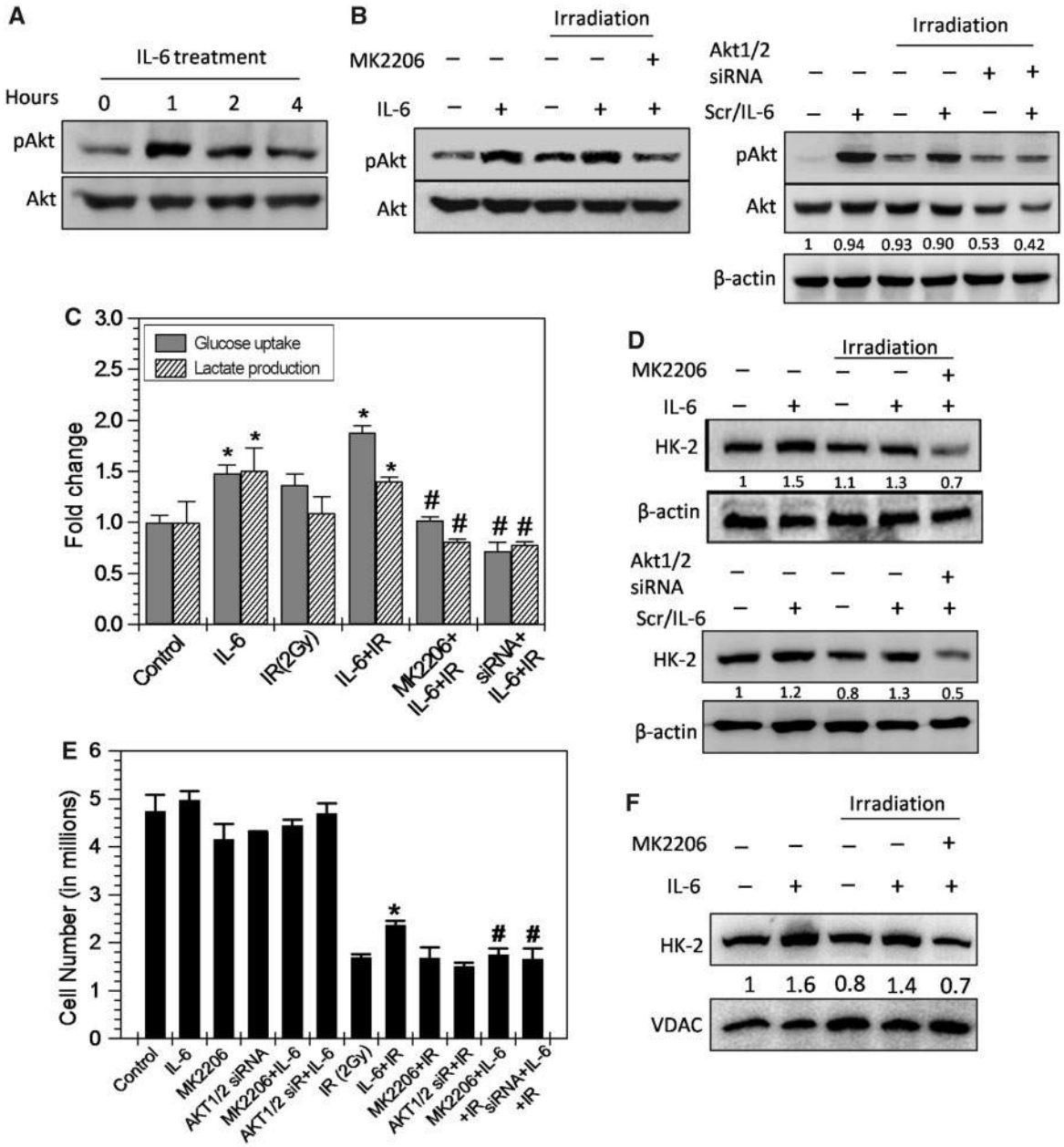

Fig. 5 IL-6-induced glycolysis is Akt dependent. (**A**) Phosphorylation of Akt at ser473 was detected at indicated time points after IL-6 treatment. (**B**) Cells treated with MK2206 (2.5 μM) 15 min prior to IL-6 treatment followed by irradiation were harvested 1 h post-irradiation for western blotting. Akt1/2 siRNA (100 nM) and Control (scramble) siRNA transfected cells were also treated with IL-6 followed by irradiation and harvested for western blotting of pAkt and Akt levels. Total Akt levels were normalized with the values of beta-actin (loading control). (**C**) Graph represents fold change in glucose uptake and lactate production per cell respectively in various treatment groups at 2 h post-irradiation. (**D**) Immunoblot of total HK-2 protein with MK2206 and Akt siRNA. β-Actin used as loading control and (**E**) Cell number quantified at 48 h post-irradiation in various treatment groups is presented as bar diagram. (**F**) Showing immunoblot of mitochondrial bound fraction of HK-2 where VDAC used as loading control. Values shown in between the blots are the average fold change value of densitometric analysis of three blots, normalized with respective β-Actin. Star shows the statistical significance of change between the groups calculated by one-way ANOVA and the Student's *t*-test. # represents the statistical significance between siRNA or MK2206 group with respect to IL-6 pre-treated irradiated group. Data are expressed as mean ± SD ($n = 4$). *$P < 0.05$.

mitochondrial damage in IL-6 pre-treated cells. Interestingly, inhibition of IL-6-induced glycolysis also reverses the protective effect of IL-6 from radiation-induced mitochondrial damage (Fig. 4).

IL-6 after binding to its receptor on the cell surface induces the phosphorylation of STAT-3 and PI3K (Phosphoinositol-3-kinase), which further phosphorylates the Akt (*1*). Increased Akt phosphorylation is found to be associated with increased rates of glucose metabolism in cells (*31*). Akt signalling influence the glycolysis directly by regulating the localization of the GLUT to the plasma membrane (*32*), HK-2 expression and mitochondrial interaction (*33*), and expression of PFK-1 and PFKFB3 (*34*). Since we found the expression levels of all these genes were increased by IL-6 treatment in Raw264.7 cells; we envisaged that IL-6-

Downloaded from https://academic.oup.com/jb/article-abstract/167/3/303/5610530 by guest on 03 May 2020

induced glycolysis in Raw264.7 cells could be mediated by Akt pathway. IL-6-induced Akt phosphorylation suggested the involvement of Akt signalling in IL-6 induced enhanced glycolysis, which was further verified by knocking down the Akt expression and inhibition of Akt signalling under similar experimental settings (Fig. 5). Down-regulation of Akt signalling in IL-6 pre-treated samples not only reduced the glycolysis (glucose uptake and lactate production) but also the expression level of key glycolytic enzyme HK-2 and its association with mitochondria, which resulted in reversal of IL-6-induced radio-resistance (Fig. 5). HK-2 association with mitochondrial outer membrane not only facilitates the quick phosphorylation of glucose using mitochondrial ATP but also prevents the cytochrome C release from mitochondria thereby inhibiting the apoptosis (*35*). Therefore, IL-6-induced and Akt-mediated translocation of HK-2 to mitochondrial membrane may cause radio-resistance besides glycolysis also. Moreover, besides the direct role of PKM2 in glucose catabolism, it was demonstrated to facilitate the homologous recombination of DNA repair in nucleus (*36*). Hence, we can assume that IL-6 induced high levels of PKM2 and HK-2 may be causing radio-resistance through glycolysis as well as other moonlighting functions. It will be pertinent to see the role of IL-6-induced glycolytic enzymes in DNA repair and other moonlighting functions. Pending this insight to be unravelled, results of the present studies lend support to our hypothesis that IL-6-induced glycolysis is a favourable metabolic change partly responsible for radio-resistance. This study adds induced glycolysis also as one of the factors among the list of various causes responsible for IL-6-induced radio-resistance.

Conclusion

In conclusion, the results of this study suggest that IL-6 induced the glycolysis in Raw264.7 cells by activating Akt signalling, which further induced the expression of key regulatory glycolytic enzymes and glucose transporters. The IL-6-induced aerobic glycolysis and reduced mitochondrial damage at the time of radiation exposure ensures continuous and sufficient supply of energy for repair of radiation-induced macro-molecular and cellular damages, thereby causing radio-resistance (Fig. 6). The moonlighting functions of IL-6-induced glycolytic enzymes also need to be understood to know their role in IL-6-induced radio-resistance. Further, understanding the mechanisms underlying IL-6 induced Glycolysis may help in unravelling critical molecular targets responsible for therapeutic resistance and facilitate the design and/or identification of molecules/agents that specifically overcome resistance linked to enhanced glycolysis, thereby enhancing the efficacy of radio- and chemotherapies. Clinical use of costly anti-IL-6 or anti IL-6 receptor antibodies in combination with therapies in IL-6 over-expressing tumours is challenging. Instead, use of metabolic inhibitors will

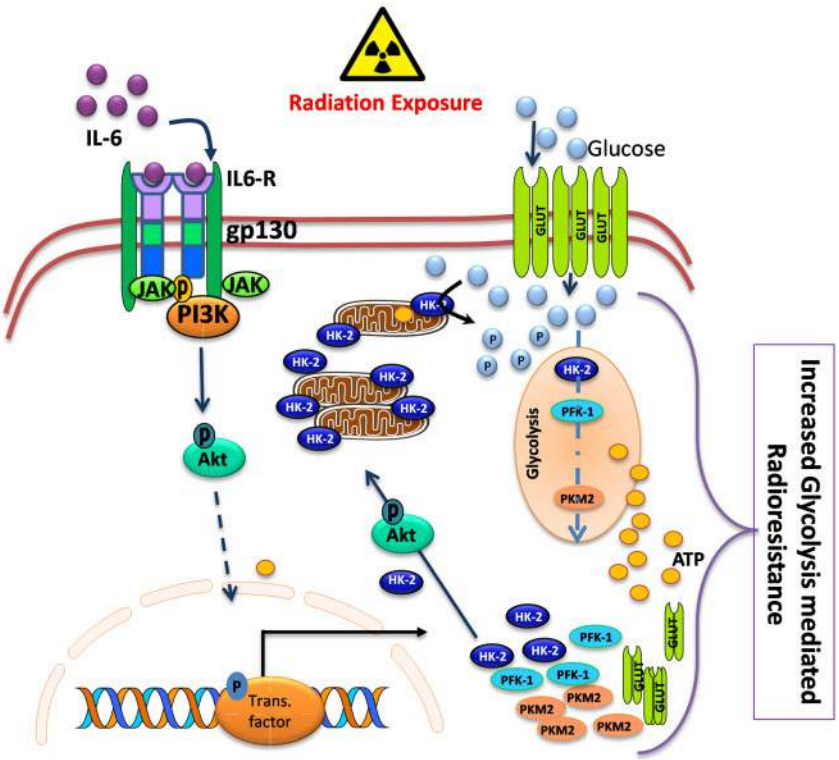

Fig. 6 The picture illustrates that IL-6 treatment before irradiation activates PI3K-Akt pathway which resulted in the up-regulation of important regulatory genes of glycolysis. Akt also phosphorylates HK-2, which allows its binding to outer membrane of mitochondria where it facilitates efficient glucose phoshphorylation using mitochondrial ATP and ensures rapid rate of glycolysis. Efficient supply of energy (ATP) for repair of radiation-induced macro-molecular and cellular damages and moonlighting functions of glycolytic enzymes like prevention of cytochrome C release from mitochondria by HK-2 resulted in IL-6-induced radio-resistance.

Downloaded from https://academic.oup.com/jb/article-abstract/167/3/303/5610530 by guest on 03 May 2020

be economical in achieving a similar level of therapeutic gain; however, more research is required to validate this proposition. This study also throws the light that IL-6 can protect the normal cells from radiation-induced cell death and it has potential to be developed as radio-protector.

Acknowledgements

N.K. thanks the Defence Research and Development Organisation, Government of India, for fellowship support. The authors acknowledge Director INMAS for constant support and encouragement. They also acknowledge Yogesh Rai, Dhananjay Sah and Ankit Chauhan for support during experiments. They extend sincere thanks to Dr Ravi Soni and the staff of the institutional Central Instrumentation Facility.

Author contributions

A.N.B.: Conceptualization, writing-reviewing and editing, supervision. N.K.: Data curation, investigation and writing-original draft. A.D.: Writing-reviewing and editing. All authors reviewed and approved the final version of the manuscript for submission.

Funding

This work was supported by grant (INM 311/1.4) funded by Defence Research and Development Organisation, Government of India.

Conflict of Interest
None declared.

References

1. Kumari, N., Dwarakanath, B.S., Das, A., and Bhatt, A.N. (2016) Role of interleukin-6 in cancer progression and therapeutic resistance. *Tumor Biol.* **37**, 11553–11572
2. Scheller, J., Chalaris, A., Schmidt-Arras, D., and Rose-John, S. (2011) The pro- and anti-inflammatory properties of the cytokine interleukin-6. *Biochim. Biophys. Acta* **1813**, 878–888
3. Muñoz-Cánoves, P., Scheele, C., Pedersen, B.K., and Serrano, A.L. (2013) Interleukin-6 myokine signaling in skeletal muscle: a double-edged sword? *FEBS J.* **280**, 4131–4148
4. Smart, N., Mojet, M.H., Latchman, D.S., Marber, M.S., Duchen, M.R., and Heads, R.J. (2006) IL-6 induces PI 3-kinase and nitric oxide-dependent protection and preserves mitochondrial function in cardiomyocytes. *Cardiovasc. Res.* **69**, 164–177
5. Kolliputi, N. and Waxman, A.B. (2009) IL-6 cytoprotection in hyperoxic acute lung injury occurs via suppressor of cytokine signaling-1-induced apoptosis signal-regulating kinase-1 degradation. *Am. J. Respir. Cell Mol. Biol.* **40**, 314–324
6. Mauer, J., Denson, J.L., and Brüning, J.C. (2015) Versatile functions for IL-6 in metabolism and cancer. *Trends Immunol.* **36**, 92–101
7. Ishibashi, K., Koguchi, T., Matsuoka, K., Onagi, A., Tanji, R., Takinami-Honda, R., Hoshi, S., Onoda, M., Kurimura, Y., Hata, J., Sato, Y., Kataoka, M., Ogawsa, S., Haga, N., and Kojima, Y. (2018) Interleukin-6 induces drug resistance in renal cell carcinoma. *Fukushima J. Med. Sci.* **64**, 103–110
8. Ahmed, K.M. and Li, J.J. (2008) NF-kappa B-mediated adaptive resistance to ionizing radiation. *Free Radic. Biol. Med.* **44**, 1–13
9. Yoon, S., Woo, S.U., Kang, J.H., Kim, K., Shin, H.-J., Gwak, H.-S., Park, S., and Chwae, Y.-J. (2012) NF-κB and STAT3 cooperatively induce IL6 in starved cancer cells. *Oncogene* **31**, 3467–3481
10. Warburg, O. (1956) On the origin of cancer cells. *Science* **123**, 309–314
11. Wang, T., Liu, H., Lian, G., Zhang, S.-Y., Wang, X., and Jiang, C. (2017) HIF1α-induced glycolysis metabolism is essential to the activation of inflammatory macrophages. *Mediators Inflamm.* **2017**, 9029327
12. Wang, T., Marquardt, C., and Foker, J. (1976) Aerobic glycolysis during lymphocyte proliferation. *Nature* **261**, 702–705
13. Inoue, H., Ogawa, W., Asakawa, A., Okamoto, Y., Nishizawa, A., Matsumoto, M., Teshigawara, K., Matsuki, Y., Watanabe, E., Hiramatsu, R., Notohara, K., Katayose, K., Okamura, H., Kahn, C.R., Noda, T., Takeda, K., Akira, S., Inui, A., and Kasuga, M. (2006) Role of hepatic STAT3 in brain-insulin action on hepatic glucose production. *Cell Metab.* **3**, 267–275
14. Chen, X., Wei, J., Li, C., Pierson, C.R., Finlay, J.L., and Lin, J. (2018) Blocking interleukin-6 signaling inhibits cell viability/proliferation, glycolysis, and colony forming activity of human medulloblastoma cells. *Int. J. Oncol.* **52**, 571–578
15. Ando, M., Uehara, I., Kogure, K., Asano, Y., Nakajima, W., Abe, Y., Kawauchi, K., and Tanaka, N. (2010) Interleukin 6 enhances glycolysis through expression of the glycolytic enzymes hexokinase 2 and 6-phospho-fructo-2-kinase/fructose-2,6-bisphosphatase-3. *J. Nippon Med. Sch.* **77**, 97–105
16. Matsuoka, Y., Nakayama, H., Yoshida, R., Hirosue, A., Nagata, M., Tanaka, T., Kawahara, K., Sakata, J., Arita, H., Nakashima, H., Shinriki, S., Fukuma, D., Ogi, H., Hiraki, A., Shinohara, M., Toya, R., and Murakami, R. (2016) IL-6 controls resistance to radiation by suppressing oxidative stress via the Nrf2-antioxidant pathway in oral squamous cell carcinoma. *Br. J. Cancer* **115**, 1234–1244
17. Tamari, Y., Kashino, G., and Mori, H. (2017) Acquisition of radioresistance by IL-6 treatment is caused by suppression of oxidative stress derived from mitochondria after γ-irradiation. *J. Radiat. Res.* **58**, 412–420
18. Brown, C.O., Salem, K., Wagner, B.A., Bera, S., Singh, N., Tiwari, A., Choudhury, A., Buettner, G.R., and Goel, A. (2012) Interleukin-6 counteracts therapy-induced cellular oxidative stress in multiple myeloma by up-regulating manganese superoxide dismutase. *Biochem. J.* **444**, 515–527
19. Wang, T., Ning, K., Sun, X., Zhang, C., Jin, L.F., and Hua, D. (2018) Glycolysis is essential for chemoresistance induced by transient receptor potential channel C5 in colorectal cancer. *BMC Cancer* **18**, 207
20. Bhatt, A.N., Chauhan, A., Khanna, S., Rai, Y., Singh, S., Soni, R., Kalra, N., and Dwarakanath, B.S. (2015) Transient elevation of glycolysis confers radio-resistance by facilitating DNA repair in cells. *BMC Cancer* **15**, 335
21. Huang, B., Zhang, Q., Yuan, Y., Xin, N., He, K., Huang, Y., Tang, H., and Gong, P. (2018) Sema3a inhibits the differentiation of Raw264.7 cells to osteoclasts

Downloaded from https://academic.oup.com/jb/article-abstract/167/3/303/5610530 by guest on 03 May 2020

under 2Gy radiation by reducing inflammation. *PLoS One* **13**, e0200000

22. Kato, K., Omori, A., and Kashiwakura, I. (2013) Radiosensitivity of human haematopoietic stem/progenitor cells. *J. Radiol. Prot.* **33**, 71–80
23. Ribble, D., Nathaniel B Goldstein, D.A.N., and Shellman, Y.G. (2005) A simple technique for quantifying apoptosis in 96-well plates. *BMC Biotechnol.* **5**, 12
24. Berg, J.M., Tymoczko, J.L., and Stryer, L. (2002) The glycolytic pathway is tightly controlled in *Biochemistry*, 5th edn. W H Freeman, New York. https://www.ncbi.nlm.nih.gov/books/NBK22395/
25. Rai, Y., Pathak, R., Kumari, N., Sah, D.K., Pandey, S., Kalra, N., Soni, R., Dwarakanath, B.S., and Bhatt, A.N. (2018) Mitochondrial biogenesis and metabolic hyperactivation limits the application of MTT assay in the estimation of radiation induced growth inhibition. *Sci. Rep.* **8**, 1531
26. Verma, A., Bhatt, A.N., Farooque, A., Khanna, S., Singh, S., and Dwarakanath, B.S. (2011) Calcium ionophore A23187 reveals calcium related cellular stress as "I-Bodies": an old actor in a new role. *Cell Calcium* **50**, 510–522
27. Zhang, F., Duan, S., Tsai, Y., Keng, P.C., Chen, Y., Lee, S.O., and Chen, Y. (2016) Cisplatin treatment increases stemness through upregulation of hypoxia-inducible factors by interleukin-6 in non-small cell lung cancer. *Cancer Sci.* **107**, 746–754
28. Oki, Y., Fanale, M., Romaguera, J., Fayad, L., Fowler, N., Copeland, A., Samaniego, F., Kwak, L.W., Neelapu, S., Wang, M., Feng, L., and Younes, A. (2015) Phase II study of an AKT inhibitor MK2206 in patients with relapsed or refractory lymphoma. *Br. J. Haematol.* **171**, 463–470
29. Chen, Z., Zhang, H., Lu, W., and Huang, P. (2009) Role of mitochondria-associated hexokinase II in cancer cell death induced by 3-bromopyruvate. *Biochim. Biophys. Acta* **1787**, 553–560
30. Zhong, J., Rajaram, N., Brizel, D.M., Frees, A.E., Ramanujam, N., Batinic-Haberle, I., and Dewhirst, M.W. (2013) Radiation induces aerobic glycolysis through reactive oxygen species. *Radiother. Oncol.* **106**, 390–396
31. Elstrom, R.L., Bauer, D.E., Buzzai, M., Karnauskas, R., Harris, M.H., Plas, D.R., Zhuang, H., Cinalli, R.M., Alavi, A., Rudin, C.M., and Thompson, C.B. (2004) Akt stimulates aerobic glycolysis in cancer cells. *Cancer Res.* **64**, 3892–3899
32. Barthel, A., Okino, S.T., Liao, J., Nakatani, K., Li, J., Whitlock, J.P., and Roth, R.A. (1999) Regulation of GLUT1 gene transcription by the serine/threonine kinase Akt1. *J. Biol. Chem.* **274**, 20281–20286
33. Miyamoto, S., Murphy, A.N., and Brown, J.H. (2008) Akt mediates mitochondrial protection in cardiomyocytes through phosphorylation of mitochondrial hexokinase-II. *Cell Death Differ.* **15**, 521–529
34. Deprez, J., Vertommen, D., Alessi, D.R., Hue, L., and Rider, M.H. (1997) Phosphorylation and activation of heart 6-phosphofructo-2-kinase by protein kinase B and other protein kinases of the insulin signaling cascades. *J. Biol. Chem.* **272**, 17269–17275
35. Pastorino, J.G., Shulga, N., and Hoek, J.B. (2002) Mitochondrial binding of hexokinase II inhibits Bax-induced cytochrome c release and apoptosis. *J. Biol. Chem.* **277**, 7610–7618
36. Sizemore, S.T., Zhang, M., Cho, J.H., Sizemore, G.M., Hurwitz, B., Kaur, B., Lehman, N.L., Ostrowski, M.C., Robe, P.A., Miao, W., Wang, Y., Chakravarti, A., and Xia, F. (2018) Pyruvate kinase M2 regulates homologous recombination-mediated DNA double-strand break repair. *Cell Res.* **28**, 1090–1102

Downloaded from https://academic.oup.com/jb/article-abstract/167/3/303/5610530 by guest on 03 May 2020